Université de Strasbourg

UNIVERSITÉ DE STRASBOURG

École doctorale Sciences de la vie et de la santé | ED 414 Université de Strasbourg

ÉCOLE DOCTORALE SCIENCES DE LA VIE ET SANTÉ

UPR 3212 CNRS

THÈSE présentée par / DISSERTATION presented by :

Varen EERSAPAH

soutenue le /defended on : **Avril 2021**

pour obtenir le grade de / to obtain the grade of :
Docteur de l'Université de Strasbourg / Strasbourg University Doctor

Discipline/Spécialité / Discipline/Specialty : [Neuroscience]

DÉTECTION ET QUANTIFICATION DE LA LIBÉRATION D'ATP À PARTIR DES CELLULES GLIALES DE LA CORNE DORSALE DE MOELLE ÉPINIÈRE DE SOURIS : EFFET DE LA NORADRÉNALINE ET DES IMIDAZOLINES

THÈSE dirigée par / DISSERTATION supervisor :

M. SCHLICHTER Rémy	Professeur, Université de Strasbourg

RAPPORTEURS :

Mme ULMANN Lauriane M	Maitre de conférences, Universté de Montpellier
CHARPAK Serge	Directeur de recherches INSERM, Paris

AUTRES MEMBRES DU JURY / OTHER MEMBERS OF THE JURY :

M. GALZI Jean-Luc	**Directeur de recherches CNRS, Strasbourg**

Acknowledgement

First, I would like to thank Dr. Lauriane Ulmann, Dr. Serge Charpak and Dr. Jean-Luc Galzi for accepting to be a part of the jury and taking your time to evaluate my manuscript.

I would like to start to thank Dr. Sylvain Hugel for teaching me all the methods when I started in the lab and for sharing so much scientific knowledge and supporting me through all those years, both at a professional and personal level. I am profoundly grateful for all the time that you have spent with me during the last five years and that you have always taken your time to provide me with solutions and ideas whenever I needed.

Also, I would like to thank Dr. Perrine Inquimbert for providing much practical advice and great scientific discussions during the Monday meetings. I would especially like to thank you for helping me to take care of my personal health during my years at the INCI.

Dhanasak (Taddy) Dhanasobhon. I would like to thank you for taking your time to help me with so many things when I just arrived in France and also for being a great friend who supported me a lot during the years we spent together in Strasbourg. I wish you all the best in the future.

I would also like to thank my father for always encouraging me to pursue academical studies and for all the support that I have received.

I also want to thank my Swedish friends Måns, Adrian, Jonathan, Martin, Philip, Erik, Scott, Rebecka for their great friendship and support.

I would also want to thank my former supervisor in Lund University, Marcus Granmo, for introducing me to neurophysiology and being a great mentor during my 3 years at the Neuronano Research Center (Medicon Village, Lund, Sweden).

Dr. Jean-Luc Rodeaue, I want to thank you for taking your time to teach me statistics during my first years and providing computational tools that have been of essential value for my progress with the statistical analysis of my calcium imaging data. And I am very grateful that you were always available to provide the best and simplest solutions whenever I needed.

I am hugely appreciative to Mme. Catherine Moreau and Mme. Chantal Fitterer for their excellent assistance in the lab which ensured that my experiments ran smoothly. I also want to thank you both for all help I received to navigate through the French administration and the kindness that you showed me since my first day in the lab.

I also want to thank my best friend, Gunnþórunn Gísladóttir, for always being there for me and supporting me during my last years in France. Our conversations and many adventures have been a great motivation for me throughout my time as a PhD student. Your encouragement has been invaluable to me during this journey and I wish you and Nadia all the best in the future.

I am very grateful for having had the opportunity to meet my current and past lab-mates, whom all has become good personal friends; Dr. Maria-Carmen Medrano and Dr. Yunuen Moreno-Lopez, Dr. Benjamin Leonardon, Dr. Charlotte Bichara, Lou Cathenaut, Sehrazat Kavraal, Louise Vial, Lucien Ruelle-Le Glaunec, thank you all for the good times in and outside the lab.

I would also like to thank my mother, Grace Kamala, for the encouragement that you have provided me and for always supporting me both personally and professionally. I am grateful for the time that we have spent together during my last year in Strasbourg and all the valuable help that I have received. Thank you very much Mum.

My profound gratitude goes to my supervisor, Prof. Rémy Schlichter, for accepting me into your lab and supervising me throughout my entire time in France. You have been a brilliant supervisor and teacher from the first day I started to the very end. Under your guidance, you have made me appreciate science at so many levels more than I could ever imagine. Most importantly, I want you to know that I am amazed by you, as a person and as a mentor, the patients and kindness that you have shown me both during the good times but also the hard times has been of incredible value. Your level of scientific knowledge is truly fascinating, and I feel lucky that I have been able to take part of that during our discussions. I want to thank you for spending much of your time to keep motivating me and providing me with extraordinary support both professionally and personally. Without your constant dedication, this thesis would not have been possible. Thank you so much Rémy, I hope that we will keep continuing to be in contact and I wish you the very best in the future.

List of Contents

List of Tables

List of Figures

Abbreviation list

Abbreviation	Full name
2-azido-dUTP+	2-Azido-Deoxyuridine-5′-Triphosphate
2-MeCCPA	2-Chloro-N-Cyclopentyl-2′-Methyladenosine
2-Cl-IB-MECA	2-Chloro-N6-(3-Iodobenzyl)-9-[5-(Methylcarbamoyl) -B-D-Ribofuranosyl] Adenine
2-MeSADP	2-Methylthio-Adp
2-MeSAMP	2-Methylthio-Amp
2-MeSATP	2-Methylthio-Atp
2-thio-UTP	2-Thio-Uridine 5′-Triphosphate
5-AMPS	5′-O Thiomnophosphate
5-HT	Serotonin
5-OMe-UDP αB	5-Methoxyuridine-5′-Diphosphate-Aβ
AR	Adenosine Receptor
A3P5P	Adenosine-3′-5′-Bisphosphate
ABC	Atp Binding-Cassette
ACC	Anterior Cingulate Cortex
Ach	Acetylcholine
ADP	Adenosine 5′-Diphosphte
ADPKD	Autosomal Dominant Polycystic Kidney Disease
ADP-β-S	Adenosine-5′-(B-Thio)-Diphosphate
AMP	Adenosinemonophospate
AMPA	A-Amino-3-Hydroxy-5-Methyl-4-Isoxazolepropionic Acid Receptor
ANP	Atrial Natriuretic Peptide,
Ap4A	Diadenosine Tetraphosphate
Ap5(γB)	Adenosine Pentaphosphate (Bγ)
AR	Adrenoceptors
ARC	Arachidonic Acid-Regulated Calcium
ATP	Adenosine 5’-Triphosphate
ATPγS	Adenosine 5′-(Γ-Thio)-Triphosphate
AUC	Area Under The Curve
BBB	Blood Brain Barrier
BBG	Brilliant Blue Green

BDNF	Brain-Derived Neurotrophic Factor,
BEST	Bestrophine (Chloride Channel)
BFA	Brefeldin A,
BzATP	2′(3′)-O-(4-Benzoylbenzoyl) Adenosine 5′-Triphosphate
CALHM	Calcium Homeostasis Modulator
cAMP	Cyclic Amp, Dbxrm
CCPA	Chlorocyclopentyl Adenosine
CFA	Complete Freund'S Adjuvant
CGPR	Calcitonin Gene-Related Peptide
CL	Centrolateral
CLO	Clonidine
CLORG	Clorgyline
CNS	Central Nervous System
COMT	Catechol-O-Methyltransferase
CORM 2	Carbon Monoxide Donor 2
CRAC	Calcium-Release Activated Calcium Channels
CTP	Cytosine Triphosphate
CX3CL1	Fraktalkine
DA	Dopamine
DAG	Diacylglycerol
DBH	Dopamine-B-Hydroxylase
DBXRM	1,3-Dibutylxanthine 7-Riboside 5′-N-Methylcarboxamide
DCN	Dorsal Column Nuclei
DCV	Dense-Core Vesicles
DDC	Dopa-Decarboxylase
DEX	Dexmedetomidine
DF	Dorsal Funiculus
DH	Dorsal Horn
DHPG	3,5-Dihydroxyphenylglycine
DLF	Dorsolateral Funiculus
DMSO	Dimethyl Sulfoxide
DOPA	3,4-dihydroxyphenylalanine
DPCPX	1,3-Dipropyl-8-Cyclopentylxanthine
DRG	Dorsal Root Ganglia
DRN	Dorsal Raphe Nuclei

EGF	Epidermal Growth Factor
EGFP	Enhance Green Fluorescent Protein
ENBA	(2S)-N6-[2-Endo-Norbornyl] Adenosine
EPSC	Excitatory Post-Synaptic Current
FDA	Food And Drug Administration
GABA	Gamma-Aminobutyric Acid
GAD	Glutamate Decarboxylase
GAT-1/-3	Gaba Transporters 1-3 (Operating In Reverse Mode)
GFAP	Glial Fibrillary Acidic Protein
GLUT	Glutamate Transporters
GlyT1	Glycine Transporter 1 (Operating In Reverse Mode)
GPN	Glycyl-L-Phenylalanine 2-Naphthylamide
GTP	Guanosine-5'-triphosphate
HDL	High Density Lipoprotein
HEK	Human Embryonic Kidney
HEMADO	2-(1-Hexynyl)-N-Methyl Adenosine
HENECA	2-Hexynyladenosine-59-N-Ethylcarboxamide
IAA-RP	Imidazole-4-Acetic Acid-Ribotide
IASP	International Association for the Study of Pain
IDAZ	Idazoxan
IP_3	Inositol Triphosphate
IP_3R	Inositol Triphosphate Receptors
IP5I	Di-Inosinepentaphosphate
IPSC	Inhibitory Postsynaptic Currents
ISO	Isoproterenol
isoPPADS	Iso-Pyridoxalphosphate-6-Azophenyl-2′,4′-Disulfonic Acid
KA	Kainate
LAMP1	Lysosomal-Associated Membrane Protein 1
LCN	Lateral Cervical Nucleus
LPS	Lipopolysaccharide
LRN	Lateral Reticular Nucleus
LSN	Lateral Spinal Nucleus
LTD	Long-Term Depression
LTP	Long Term Potentiation
MAC	Maxi Ion Channel

MAO	Mono-Amino-Oxidase
MCP	Monocyte Chemoattractant Protein
mGluR	Muscarinic Glutamate Receptors
ML	Median Lemniscus
NA	Noradrenaline
NAADP	Nicotinic Acid Adenine Dinucleotide Phosphate
NAD	Nicotinamide Adenine Dinucleotide
NANC	Non-Adrenergic, Non-Cholinergic
NCF	Nucleus Cuneiformus
NECA	5′-Nethylcarboxamido-Adenosine
NET	Noradrenaline Transporter
NK1	Neurokinin Type 1
NMDA	N-Methyl-D-Aspartate
NMDAR	N-Methyl-D-Aspartate Receptor
NO	Nitric Oxide
NPGC/NGC	Nucleus (Paro) Gigantocellularis
NPY	Neuropeptide Y
NS	Nociceptive-Specific
NTS	Nucleus Tractus Solitarius
OAT	Organic Anion Transporter
OCT	Organic Cation Transporter
PAG	Periaquaductal Grey
PAN	Pannexin
PAPET	2-[2-(4-Aminophenyl) Ethylthio]Adenosine-5′-Triphosphate
PAR	Protease Activated Receptors
PBN	Parabrachial Nucleus
PHE	Phenylephrine
PIT	2,2′-Pyridylisatogen Tosylate
PKA	Protein Kinase A
PKC	Protein Kinase C
PLC-β	Phospholipase
PO	Posterior Group Of Thalamic Nuclei
PPADS	Pyridoxal-5-Phosphate-6-Azophenyl-2′,4′-Disulfonic Acid
PPTN	4-((Piperidin-4-Yl) Phenyl)-7-(4-(Trifluoromethyl) -Phenyl)-2-Napthoic Acid
RB2	Reactive Blue 2

REST	Re-1-Silencing Transcription Factor.
RF	Reticular Formation
RNA	Ribonucleic Acid
mRNA	messenger Ribonucleic Acid
R-PIA	R-Phenylisopropyl-Adenosine
SARAF	The Store-Operated Calcium Entry-Associated Regulatory Factor Proteins
SCAMP	Secretory Carrier Membrane Proteins
SCL	Superior Colliculus
SLMV	Synaptic-Like Microvesicle
SNI	Spared Nerve Injury
SNL	Spinal Nerve Ligation
SOC	Store-Operated Calcium
SOCE	Store-Operated Calcium Entry
SOM	Somatostatin
SP	Substance P
STIM	Stromal Interaction Molecule
THL	Tyrosine Hydroxylase
TIRF	Total Internal Reflection Fluorescence
TI-VAMP	Tetanus Neurotoxin-Insensitive Vesicle Associated Membrane Protein,
TNF	Tumour Necrosis Factor
tPA	Tissue Plasminogen Activator,
TTX	Tetrodotoxin
UDP	Uridine Di-Phosphate
UDP-βS	Uridine-5′-(B-Thio)-Diphosphate Uridine-5'-(B-Thio)-Diphosphate
Up3U	Diuridine Triphosphate
Up4-phenyl ester	Uridine Tetraphosphate Phenyl Ester
Up4U	Diuridine Tetraphosphate
UTP	Uridine Tri-Phosphate
UTPγS	Uridine-5′-(Γ-Thio)-Triphosphate
VAMP	Vesicle Associated Membrane Protein
VEAT	Vesicular Aspartate Transporter
VGAT	Vesicular GABA/Glycine Transporter
VGUT	Vesicular Glutamate Transporter
VSerT	Vesicular D-serine Transporter
VIP	Vasoactive Polypeptid

VLF	Ventrolateral Funiculus
VMAT	Vesicular Monoamine Transporter
VMH	Ventromedial Hypothalamus
VMPo	Ventromedial Posterior Thalamus
VNT	Vesicular Neurotransmitter Transporters
VNUT	Vesicular Nucleotide Transporter
VPI	Ventroposterioinferior Thalamus
VPL	Ventroposteromedial Thalamus
VPM	Ventroposteromedial Thalamus
VRAC	Volume Regulated Channel
WDR	Wide-Dynamic Range
YOH	Yohimbine
α,β-meATP	L-A,B-Methylene Atp
α,β-meUDP	A,B-Methylene-Udp
γ-CF2ATP	A,B-Difluoromethylene-Atp
BAPTA	1,2-Bis(2-Aminophenoxy)Ethane-N,N,N′,N′-Tetraacetic Acid
LC	Locus Coeruleus
IL	Interleukin
CK_B	Creatine Kinase Brain

Summary of the thesis

Introduction

Pain is an individual and subjective sensory experience with an unpleasant emotional component that has been developed by the organism to inform and protect it from tissue injury or potential future insult. Therefore, during tissue insult, acute pain and the associated pain memories are essential for the survival of a species. Normally, pain disappears after the injury has been resolved, but unfortunately, in some cases, it persists in the absence of any physiological protective role and becomes chronic. It is therefore obviously important to understand the nociceptive system and its regulation. One of the supraspinal structures involved in pain control is the *Locus Coeruleus* (LC) that is located in the brain stem. The axons of LC neurons that project to the dorsal horn (DH) of the spinal cord release NA that modulates synaptic transmission and integration in the DH where nociceptive signals first enter the central nervous system. The neurons and astrocytes in the dorsal horn express different types of adrenoceptors (α_1-ARs, α_2-ARs, and β-ARs) that might be activated by spinally released NA. In the DH of the spinal cord, NA has a potent analgesic effect in different pain models in rodents, which has mostly been attributed to the activation of α_2-ARs present on neurons. Indeed, intrathecal injection of α_2-AR agonists such as clonidine (CLO) and dexmedetomidine induce analgesia in rodents as well as in humans. Direct experimental evidence showing that NA can directly modulate purinergic signalling in neurons or glial cells of the dorsal horn of the spinal cord is lacking. Therefore, the main aim of this thesis was to study the effect of NA on astrocytes located in the DH of the spinal cord. And our main focus was to study the effect of noradrenaline on primary mouse dorsal horn glial cells. Our objectives were: **1)** to characterize the effects of NA and adrenergic receptor agonists on the free intracellular calcium concentration ($[Ca^{2+}]_i$) DH glial cells **2)** to develop a method for detecting ATP release from cultured DH glia, **3)** to use this technique in order to characterize the effect of noradrenaline on ATP release from DH spinal glia, **4)** to investigate the presence of functional α_2-ARs on cultured DH glial cells and **5)** to evaluate the consequences of α_2-ARs activation on ATP release.

Methods:

To obtain primary DH glial cells we carefully dissected and harvested DH-tissue from 3-6 days old mouse pups. The tissue samples were then mechanically dissociated until obtaining a suspension of individual glial cells (N.B. this dissociation protocol did not allow the survival of DH neurons). The dissociated glial cells were seeded on glass-coverslips and placed to grow in an incubator (37 ° C with 5% CO_2) for 10-14 days prior to experiments. Changes in $[Ca^{2+}]_i$ were studied through ratiometric calcium imaging measurements on fura-2-loaded cell cultures. Cells were alternately excited at wavelengths of 350 and 380 nm by a filter wheel and emitted light wavelengths above 520 nm were collected and quantified. To study ATP release we used human embryonic kidney 293 (HEK293) cells stably transfected with rat P2X2 receptors as sniffer/detector cells (see result 2 and 3 below). The P2X2 transfected HEK293 (HEK293-P2X2) cells were maintained in an incubator (37 ° C with 5% CO_2) prior to experiments.

Results:

Result 1) Our calcium imaging experiment showed that application of noradrenaline (20 μM) increased $[Ca^{2+}]_i$ in 85 % of the DH cells tested Activation of α_1-AR with phenylephrine (PHE, 20μM) closely mimicked the effect of NA and increased $[Ca^{2+}]_i$ in 95 % of the astrocytes while application of the β-AR agonist isoproterenol (ISO, 20 μM) and the α_2-AR agonist clonidine (CLO, 10 μM) increased $[Ca^{2+}]_i$ in only 24% and 6 % of the astrocytes, respectively. The $[Ca^{2+}]_i$ responses induced by NA and PHE could be classified into three types. The first type of response was characterized by a sharp initial peak-like increase, that lasted for a few seconds, followed by a sustained $[Ca^{2+}]_i$ plateau during the presence of the agonist. The second type of response was made of $[Ca^{2+}]_i$ oscillations that persisted during the presence of the agonist. For both the first and second response $[Ca^{2+}]_i$ patterns, $[Ca^{2+}]_i$ values rapidly returned to baseline within seconds after removal of the agonist. The third type of response was characterized by an early single transient peak in $[Ca^{2+}]_i$ that appeared after 5-20 seconds after the onset of agonist application and then rapidly returned to baseline.

Result 2) To characterize the effect of noradrenaline on ATP release from astrocytes at a single cell level and with high temporal and spatial resolutions we developed a cell-based ATP-detection system. We used HEK293 cells stably transfected with rat P2X2 receptors (HEK293-P2X2) as an ATP detector/sniffer cells system. The HEK293-P2X2 cells were seeded on top of our astrocyte culture after having loaded them with the fluorescent calcium indicator fura-2. To improve the ATP sensitivity of the P2X2 receptors we pre-incubated the HEK293-P2X2 with progesterone (PROG), a positive allosteric modulator of the P2X2 receptor. In the presence of PROG the ATP sensitivity of our detection system increased more than 7 fold, with an EC_{50} of 100 nM compared to 750 nM in the untreated cells.

Result 3) To investigate if NA induced astrocytic ATP release, we placed fura-2 loaded HEK293-P2X2-PROG cells on top of the astrocyte cultures as ATP detector cells and monitored changes in $[Ca^{2+}]_i$ in these cells. Application of NA (20 μM) or of the α_1-AR agonist PHE (20 μM), but not of the α_2-AR agonist CLO (10 μM) or the β-ARs agonist ISO (20 μM), induced an increase $[Ca^{2+}]_i$ in the detector cells. These effects of NA or PHE were abolished in the presence of the P2X-receptor antagonist PPADS (50 μM), indicating that DH astrocytes released ATP following the activation of α_1-ARs. We then investigated the mechanism(s) underlying the PHE-induced ATP release. ATP release was blocked when astrocytes were loaded with calcium chelator BAPTA, indicating that the ATP release was dependent on the increase in $[Ca^{2+}]_i$. We also noticed that lowering the external potassium concentration to 0.2 mM increased $[Ca^{2+}]_i$ in DH astrocytes. ATP release induced by adrenoceptor stimulation was blocked by pre-treatments of glial cells with GPN (-L-phenylalanine 2-naphtylamide) that selectively disrupts the integrity of secretory lysosomes, or with bafilomycin A1 that prevents ATP transport into acidic vesicles due to its inhibitory effect on the vesicular H^+-pump. By contrast, ATP release induced by application of a low potassium solution was abolished by bafilomycin A1 but not by GPN. This indicated that spinal DH astrocytes released ATP through at least two distinct vesicular calcium-dependent mechanisms and that adrenoceptor stimulation activated only the secretory lysosomes pathway whereas low external K^+ induced the ATP release from both lysosomes and from an additional pool of acidic vesicles. Moreover, when the general perfusion system was stopped, we observed a low level of tonic spontaneous ATP release from the astrocytes that was dependent on $[Ca^{2+}]_i$ (blocked by BAPTA) but was resistant to bafilomycin A1 and GPN treatment, indicating that astrocytes can also release ATP through a calcium-dependent but non-vesicular pathway/mechanism.

Result 4) So far we demonstrated that NA and activation of α_1-ARs increase $[Ca^{2+}]_i$ and induce ATP release from DH astrocytes, whereas the α_2-AR agonist CLO (10 μM) did not. However, most of the analgesic properties of NA in the spinal cord has been attributed to α_2-ARs. Therefore we studied in more detail the role of α_2-ARs in DH astrocytes by exploring potential interactions between α_1-ARs and α_2-ARs and considered the possibility of an inhibitory action of α_2-ARs on PHE evoked $[Ca^{2+}]_i$. To address this point we applied CLO (10 μM) on top of a PHE-(20 μM) induced increase in $[Ca^{2+}]_i$ and found that CLO reversibly inhibited the plateau phase of PHE- responses in virtually all cells (98%). To check if this the inhibition was dependent on α_2-AR activation, we tested the effect of yohimbine (2 μM) (a selective α_2-AR antagonist). We found that the CLO response was not affected in the presence of yohimbine, indicating that it was not mediated by α_2-AR. Interestingly, CLO did not show any effect on increases in $[Ca^{2+}]_i$ triggered by the application of a low potassium solution (see above Result 3). This result indicated that CLO did not induce a general non-specific inhibition of $[Ca^{2+}]_i$. We next tested the effect of α-me-NA (α-methyl-noradrenaline, a selective α_2-ARs agonist at sub-micromolar concentrations). Application of α-me-NA (0.5 μM) induced an increase in $[Ca^{2+}]_i$ in 72 % of the cells and in the presence of yohimbine (2 μM) the effect of α-me-NA on $[Ca^{2+}]_i$ was completely abolished, indicating that the increase in $[Ca^{2+}]_i$ triggered by α-me-NA was due to the activation of α_2-ARs. We also found that a low concentration of CLO (0.3 μM) replicated the effect of α-me-NA (0.5 μM) on $[Ca^{2+}]_i$. Application of increasing concentrations (0.1 μM – 10 μM) of CLO on top of the PHE evoked $[Ca^{2+}]_i$ plateau response revealed that CLO concentrations below 1 μM increased, whereas CLO concentrations ≥ 1 μM decreased the amplitude of the calcium plateau. Our finding that CLO induced either increases or decreases on the PHE evoked $[Ca^{2+}]_i$ plateau lead us to investigate a possible role of imidazoline receptors/sites in the inhibition of the $[Ca^{2+}]_i$ plateau. Among the three types (I1, I2 and I3) of imidazoline receptors/binding sites that have been identified, I1 and I2 are expressed in the central nervous system. We first tested the effect of the selective I1 agonist cimetidine and the selective I2 agonist 2-BFI (2-(2-Benzofuranyl)-2-imidazoline hydrochloride) on the PHE induced $[Ca^{2+}]_i$ plateau. Cimetidine (10 μM) had no modulatory effect on the calcium plateau while 2-BFI (10 μM) reduced the plateau in 98 % of the astrocytes from which we recorded. The effect of 2-BFIwas significantly reduced by

idazoxan (IDAZ, 2 μM), an antagonist of both α_2-ARs and I2 receptors/sites. However IDAZ failed to completely block the inhibitory effect of 2-BFI on the PHE-induced $[Ca^{2+}]_i$ plateau.

Result 5) Using our ATP detector cell system, we then examined the effect of α2-AR activation on the release of ATP from DH astrocytes in culture. Application of α-me-NA (0.5 μM) induced a significant increase in $[Ca^{2+}]_i$ in HEK293-P2X2-PROG cells seeded on top of DH astrocytes. 2-BFI (10 μM) and CLO (10 μM) blocked ATP release by the astrocytes as well as the increase in $[Ca^{2+}]_i$ normally induced by PHE in the astrocytes. These inhibitory phenomena were rapidly reversible. Our data indicate that, at a concentration of 10 μM, 2-BFI and CLO probably directly blocked the Ca^{2+} channels responsible for calcium influx following the activation of α1-ARs.

Summary

Human embryonic kidney (HEK293) cells transfected with P2X2 receptors were pre-incubated with fura-2 and progesterone and seeded on top of cultured mouse DH astrocyte cultures in order to detect release of ATP via changes in $[Ca^{2+}]_i$ in these sensor cells. By using progesterone, a potent positive allosteric modulator of homomeric P2X2 receptors, we were able to increase the sensitivity of P2X2 receptors for their agonist 7 fold. This allowed us to detect low concentrations of ATP (in the nanomolar range) from single astrocytes. We show for the first time that NA induced the release of ATP from DH astrocytes by inducing calcium-dependent exocytosis of secretory lysosomes. In addition to lysosomes, ATP can be released in a calcium-dependent manner from a population of vesicles distinct from secretory lysosomes as well as by a non-vesicular mechanism. These two types of ATP release were not modulated by NA. In addition, our results also showed that a majority (70%) of DH astrocytes co-expressed α_1-ARs and α_2-ARs that, when activated, increased $[Ca^{2+}]_i$. Moreover, virtually all DH glial cells also posessed funtional imidazoline I2 receptors/sites, the activation of which inhibited the elevation of $[Ca^{2+}]_i$ induced by PHE as well as the release of ATP.

In summary, our results demonstrate an effect of NA on mouse DH glial cells via α_1 and α_2 adrenoceptors. Activation of these receptors leads to the release of ATP which may participate in the modulation of synaptic transmission in the DH of the spinal cord and contribute significantly to he analgesic effect of NA at the spinal level.

Résumé de la thèse

Introduction

La douleur est une expérience sensorielle individuelle et subjective avec une composante émotionnelle désagréable qui a été développée par l'organisme pour l'informer et le protéger contre des lésions tissulaires réelles, potentielles ou futures. Par conséquent, lors d'une agression tissulaire, la douleur aiguë et les souvenirs de douleur associés sont essentiels pour la survie d'une espèce. Normalement, la douleur disparaît une fois que la lésion a guéri, mais malheureusement, dans certains cas, elle persiste en l'absence de tout rôle protecteur physiologique et peut devenir chronique. Il est donc important de comprendre le fonctionnement et la régulation du système nociceptif. L'une des structures centrales qui contrôle de la douleur est le *Locus Coeruleus* (LC) situé dans le tronc cérébral. Les projections axonales du LC vers la corne dorsale (CD) de la moelle épinière libèrent de la noradrénaline (NA) qui module la transmission et l'intégration synaptique dans la CD où les nocicepteurs primaires périphériques établissent des synapses avec des neurones/interneurones du système nerveux central. Les neurones et les astrocytes de la CD expriment différents récepteurs adrénergiques (α1-AR, α_2-AR et β-AR) qui pourraient être activés par la noradrénaline suite à sa libération au niveau spinal. Dans la CD, la NA a un puissant effet analgésique qui a été observé dans différents modèles de douleur chez les rongeurs. Cet effet a été principalement attribué à l'activation des α_2-ARs neuronaux. En effet, des injections intrathécales d'agonistes des α_2-ARs tels que la clonidine (CLO) ou la dexmedetomidine induisent une analgésie chez les rongeurs et chez l'homme. Cependant, il existe peu de données expérimentales indiquant que la NA pourrait directement moduler la signalisation purinergique (mettant en jeu l'adénosine triphosphate (ATP)) dans les neurones ou les cellules gliales de la CD.

L'objectif principal de cette thèse était donc d'étudier l'effet de la NA sur les astrocytes de la CD de souris en culture primaire. Dans ce contexte, il s'agissait: 1) de caractériser les effets de la NA et des agonistes des récepteurs adrénergiques sur la concentration de calcium libre intracellulaire ($[Ca^{2+}]_i$) des cellules gliales de la CD, 2) de développer une méthode pour détecter la libération d'ATP à partir de ces cellules, 3) d'utiliser cette méthode dans le but de caractériser l'effet de la noradrénaline sur la libération d'ATP par la glie, 4) de rechercher la présence d'α_2-ARs fonctionnels sur les cellules gliales de la CD et 5) d'évaluer les conséquences de l'activation des α_2-ARs sur la libération d'ATP.

Méthodes:

Pour obtenir des cultures de cellules gliales primaires, nous avons prélevées les CD de moelle épinire chez des souris âgées de 3 à 6 jours. Le tissu prélevé a ensuite été dissocié mécaniquement jusqu'à obtention de cellules gliales individuelles (N.B. Cette dissociation mécanique détruit les neurones présents dans les échantillons tissulaires prélevés). Les cellules gliales dissociées ont été ensemencées sur des lamelles de verre et les boites de culture ont été placées dans un incubateur à 37 ° C dans une atmosphère contenant 5% de CO_2 pendant 10 à 14 jours avant les expériences. Les changements de ($[Ca^{2+}]_i$ ont été enregistrés et quantifiés par une technique d'imagerie ratiométrique du calcium en utilisant la sonde fura-2. Les cellules chargées avec la sonde fura-2 ont été excitées en alternance avec des longueurs d'onde de 350 et 380 nm grâce à une roue porte-filtres et les ondes lumineuses émises ayant une longueur d'onde > 520 nm ont été quantifiées. Pour étudier la libération d'ATP, nous avons utilisé une lignée tumorale de cellules embryonnaires rénales humaines (HEK293) qui exprimaient de manière stable des récepteurs P2X2 de rat (HEK293-P2X2). Nous avons utilisé ces cellules comme éléments de détection de la libération d'ATP par les cellules gliales (voir les résultats 2 et 3 ci-dessous). Les cellules HEK293-P2X2 ont été maintenues dans un incubateur (à 37 °C avec 5% de CO2) avant les expériences.

Résultats:

Résultat 1) Nos expériences d'imagerie de la concentration de calcium libre intracellulaire ($[Ca^{2+}]_i$) ont montré que l'application de NA (20 μM) augmentait la $[Ca^{2+}]_i$ dans 85% des cellules gliales de la CD. L'activation des α_1-ARs avec la phényléphrine (PHE, 20 μM) a reproduit l'effet de la NA et a augmenté la $[Ca^{2+}]_i$ dans 95% des astrocytes tandis que des applications d'isoprotérénol (ISO, 20 μM) un agoniste des β-ARs, ou de clonidine (CLO, 10 μM), un agoniste des α_2-ARs, n'ont augmenté la $[Ca^{2+}]_i$ que dans 24% et 6% des astrocytes, respectivement. Les réponses induites par la NA et la PHE pouvaient être classées en trois types. Le premier type de réponse était caractérisé par une forte augmentation initiale en forme de pic, qui dure en moyenne quelques secondes, suivie d'une phase en plateau soutenue de la $[Ca^{2+}]_i$ qui persiste pendant toute la durée de

l'application de l'agoniste. Le deuxième type de réponse était constitué d'oscillations de la $[Ca^{2+}]_i$ qui persistaient pendant toute la durée d'application de l'agoniste. Les réponses de types 1 et 2 se terminaient rapidement quelques secondes après la fin de l'application de l'agoniste, la valeur de la $[Ca^{2+}]_i$ revenant à la valeur basale observée avant l'application d'agoniste. Le troisième type de réponse était constitué d'un pic transitoire unique et précoce (apparaissant 5 à 20 secondes après le début de l'application de l'agoniste) après lequel la $[Ca^{2+}]_i$ revenait à la valeur basale malgré le maintien de l'application de l'agoniste.

Résultat 2) Afin de caractériser l'effet de la noradrénaline sur la libération d'ATP par les astrocytes à au niveau d'une seule cellule avec des résolutions temporelles et spatiales élevées, nous avons développé un système utilisant des cellules HEK293 transfectées de manière stable avec des récepteurs P2X2 de rat (HEK293-P2X2). Les cellules HEK293-P2X2 ont été déposées sur les astrocytes en culture après les avoir chargées avec l'indicateur de calcium fluorescent fura-2. Pour augmenter l'affinité des récepteurs P2X2 pour l'ATP, nous avons pré-incubées les HEK293-P2X2 avec de la progestérone (PROG), un modulateur allostérique positif du récepteur P2X2. En présence de PROG, la sensibilité pour l'ATP de notre système de détection a augmenté de d'un facteur 7, avec une CE_{50} pour l'ATP de 100 nM après PROG contre 750 nM dans les cellules non traitées.

Résultat 3) Pour déterminer si la NA induisait la libération d'ATP partir des astrocytes, nous avons mesuré les variations de la $[Ca^{2+}]_i$ dans les cellules HEK293-P2X2-PROG chargées en fura-2 et déposées sur les astrocytes en culture. Des applications de NA (20 µM) ou de PHE (20 µM), mais pas celles de CLO (10 µM) ou d'ISO (20 µM), ont induit une augmentation de $[Ca^{2+}]_i$ dans les cellules détectrices d'ATP. Ces réponses à la NA ou à la PHE ont été abolie par le PPADS (50 µM), un antagoniste des récepteurs P2X2, indiquant ainsi que les astrocytes e la DH libéraient de l'ATP suite à la stimulation des α_1-ARs. Nous avons ensuite caractérisé plus en détail le(les) mécanisme(s) de libération d'ATP stimulée par l'application de PHE. Cette libération d'ATP induite par la PHE a été bloquée lorsque les astrocytes ont été pré-incubés avec du BAPTA-AM afin de chélater le calcium libre intracellulaire, indiquant que la libération d'ATP était dépendante de l'augmentation de la $[Ca^{2+}]_i$. Nous avons également constaté qu'en abaissant les concentrations externes de potassium à 0,2 mM, les astrocytes de la CD présentaient une élévation de la $[Ca^{2+}]_i$ qui augmentait la libération d'ATP. La libération d'ATP induite par l'activation des α_1-ARs a été bloquée par un prétraitement des cellules gliales avec du GPN (-L-phénylalanine 2-naphtylamide) qui perturbe l'intégrité des lysosomes sécrétoires, ou avec de la bafilomycine A1 qui empêche le transport d'ATP dans les vésicules de sécrétion à contenu acide en raison de son inhibiteur effet sur la pompe H^+ vésiculaire. En revanche, la libération d'ATP induite par l'application d'une solution à faible concentration en potassium a été abolie par la bafilomycine A1 mais pas par le GPN. Ces données indiquent l'existence d'au moins deux mécanismes distincts de libération vésiculaire et calcium-dépendante d'ATP à partir des astrocytes de la CD en culture. De plus l'activation des α_1-ARs par la PHE induisait spécifiquement la libération d'ATP par exocytose de lysosomes sécrétoires tandis qu'un baissement de la concentration extracellulaire en ions K^+ stimulaità la fois la libération d'ATP à partir de lysosomes sécrétoires et d'un autre ensemble de vésicules à contenu acide. De plus, lorsque nous avons arrêté la perfusion générale continue du milieu extracellulaire, nous avons pu détecter une faible libération basale et continue d'ATP à partir des astrocytes. Cette libération basale spontanée dépendait de la $[Ca^{2+}]_i$ (car bloqué par le BAPTA intracelllaire) mais persistait après traitement des astrocytes par la bafilomycine A1 (et le GPN). Ces résultats indiquent que les astrocytes peuvent également libérer de l'ATP par un mécanisme non vésiculaire mais calcium-dépendant.

Résultat 4) Les résultats présentés ci-dessus ont montré que la l'activation des α_1-ARs augmentait la $[Ca^{2+}]_i$ dans les astrocytes et induisait la libération d'ATP alors que l'application de CLO (10 µM), un agoniste en général considéré comme sélectif des α_2-AR n'avait pas d'effet. Cependant, la plupart des propriétés analgésiques de la noradrénaline dans la moelle épinière sont dues à l'activation de α_2-ARs. Par conséquent, nous avons cherché à aborder le rôle des α_2-ARs dans les astrocytes de la CD en explorant les interactions potentielles entre α1-ARs et α_2-ARs et en considérant la possibilité d'une action inhibitrice des α_2-ARs sur l'élévation de la $[Ca^{2+}]_i$ induite par la PHE. Ainsi, nous avons appliqué de la CLO (10 µM) durant la phase en plateau de la l'augmentation de la $[Ca^{2+}]_i$ induite par la PHE (20 µM). Nous avons observé que la CLO inhibait de manière rapide et réversible la phase en plateau des réponses à la PHE dans pratiquement toutes les cellules enregistrées (98%). Pour vérifier si l'inhibition dépendait de l'activation de α_2-ARs, nous avons testé l'effet de la yohimbine (2 µM), un antagoniste sélectif des α_2-ARs. L'effet de la CLO n'était pas affecté en présence de yohimbine, indiquant qu'il n'était pas dû à l'activation de α_2-ARs. Il est intéressant de noter que la CLO (10 µM) n'a eu aucun effet sur l'élévation de $[Ca^{2+}]_i$ induite par l'application d'une solution extracellulaire à faible

concentration en K^+, indiquant que la CLO n'inhibait pas de façon non spécifique les élévations de $[Ca^{2+}]_i$ dans les astrocytes. Nous avons ensuite testé l'effet de l'α-me-NA (α-méthyl-noradrénaline), un agoniste sélectif de α_2-ARs à des concentrations submicromolaires. L'application d'α-me-NA (0,5 µM) a induit une augmentation de la $[Ca^{2+}]_i$ dans 72% des cellules testées et cet effet était bloqué en présence de yohimbine (2 µM), indiquant que les effets de l'α-me-NA étaient dus à l'activation de α_2-ARs. Nous avons également constaté qu'une faible concentration de CLO (0,3 µM) induisait une réponse comparable à celle de l'α-me-NA (0,5 µM). L'étude de la dose-dépendance des effets de la CLO (entre 0,1 µM et 10 µM) appliquée durant le plateau de la réponse calcium induite par la PHE a révélé que des concentrations de CLO inférieures à 1 µM induisaient une augmentation de la $[Ca^{2+}]_i$ alors que des concentrations de CLO supérieures à 1 µM avaient un effet inhibiteur sur le plateau de $[Ca^{2+}]_i$. La CLO étant une molécule de la famille des imidazolines, nous avons ensuite recherché l'implication potentielle de récepteurs/sites des imidazolines dans l'inhibition du plateau de $[Ca^{2+}]_i$ induit par la PHE. Parmi les trois types (I1, I2 et I3) des récepteurs/sites de liaison des imidazolines qui ont été identifiés, I1 et I2 sont exprimés dans le système nerveux central. Nous avons testés les effets de la cimétidine, un agoniste sélectif des récepteurs/sites I1 cimétidine, et du 2-BFI (chlorhydrate de 2- (2-benzofuranyl) -2-imidazoline), un agoniste sélectif des récepteurs/sites I2 sur le plateau de $[Ca^{2+}]_i$ induit par la PHE. La cimétidine (10 µM) n'a eu aucun effet modulateur sur le plateau calcium tandis que le 2-BFI (10 µM) a inhibé le plateau dans 98% des astrocytes. L'effet du 2-BFI a été réduit significativement par l'idazoxan (IDAZ, 2 µM), un antagoniste des récepteurs α_2 et I2. Cependant l'IDAZ n'a pas complètement bloqué l'inhibition du plateau calcium par le 2-BFI.

Résultat 5) En utilisant notre système de cellules détectrices d'ATP, nous avons ensuite voulu examiner l'effet de l'activation des α_2-ARs sur la libération d'ATP partir des astrocytes de la CD en culture. L'application d'α-me-NA (0,5 µM) a induit une augmentation significative de $[Ca^{2+}]_i$ dans les cellules HEK293-P2X2-PROG ensemencées sur les astrocytes la CD en culture. Par contre le 2-BFI (10 µM) et la CLO (10 µM) ont bloqué la libération ATP par les astrocytes ainsi que l'élévation de la $[Ca^{2+}]_i$ normalement induite par la PHE dans les astrocytes. Ces phénomènes inhibiteurs étaient rapidement réversibles. Nos données indiquent, qu'à une concentration de 10 µM, le 2-BFI et la CLO bloquent probablement directement les canaux Ca^{2+} responsable de l'influx de calcium suite à l'activation des α_1-ARs.

Conclusion

Des cellules de rein embryonnaire humain (HEK293) transfectées avec des récepteurs P2X2 ont été pré-incubées avec du fura-2 et de la progestérone et ensemencées sur des cultures d'astrocytes de CD de souris en culture pour détecter la libération d'ATP sous forme de changements de la $[Ca^{2+}]_i$ dans ces cellules détectrices. En utilisant la progestérone, un puissant modulateur allostérique positif des récepteurs homomériques P2X2, nous avons pu multiplié par un facteur 7 la sensibilité des récepteurs P2X2 pour leur agoniste. Ceci nous a permis de détecter même de faibles concentrations d'ATP (de l'ordre du nanomolaire) à partir d'astrocytes individuels. Nous montrons ainsi pour la première fois que la NA induit la libération d'ATP a partir des astrocytes de la DH en provoquant l'exocytose calcium-dépendante de lysosomes sécrétoires. De plus, l'ATP peut être libérée de manière calcium-dépendante à partir d'une population de vésicules distinctes des lysosomes sécrétoires ainsi que par un mécanisme non vésiculaire. Cependant, ces deux types de libération d'ATP ne sont pas modulés par la NA. Nos résultats montrent également qu'environ 70% des astrocytes de la DH co-expriment des α_1-ARs et des α_2-ARs dont l'activation augmente la $[Ca^{2+}]_i$. Par ailleurs, toutes les cellules gliales DH expriment également des récepteurs/sites de type I2 des imidazolines fonctionnels dont l'activation inhibe l'élévation de la $[Ca^{2+}]_i$ induite par la PHE et la libération d'ATP.

En résumé, nos données mettent en évidence un effet de la NA sur les cellules gliales de la CD de souris par l'intermédiaire de récepteurs α_1 et α_2. L'activation de ces récepteurs conduit à la libération d'ATP qui pourrait participer à la modulation de la transmission synaptique dans la CD et à l'effet analgésique de la NA au niveau spinal.

1 Introduction

1.1 Introduction: An overview

The ability to accurately detect and react to the environment is key for the survival for all species. The means by which the nervous system can differentiate and interpret the various forms of somatosensory experiences, including pain, has always been a central topic in neurophysiology. In its simplest form, pain is a consequence of the transmission, modulation, and interpretation of noxious information within different structures of the nervous system. The importance of a correct functioning sensory system can easily be appreciated in children born without the ability to detect and perceive pain due to genetic mutations linked to the transmission of noxious information within the nervous system (Goldberg et al., 2007). These children, with congenital insensibility to pain, experience numerous harmful and potentially life-threatening injuries throughout their life due to malfunctioning conveyance of noxious information between the periphery and the spinal cord (Cox et al., 2006).

In the spinal cord, noxious somatosensory signals are subjected to facilitatory and inhibitory modulation by local spinal interneurons and by the descending controls from higher brain centers including the brainstem (Garraway and Hochman, 2001; Polgár et al., 2003). One key player in the modulation of somatosensory information is noradrenaline from the brainstem (Jasmin et al., 2003). Noradrenaline is released, by neurons having their cell bodies located in the brainstem at the point. These neurons project their axons to the dorsal horn of the spinal cord where noxious information enters the central nervous system (Llorca-Torralba et al., 2016). This modulatory effect in the dorsal horn by noradrenaline may be one of the mechanisms that contribute to the phenomenon that the same stimuli may give rise to different pain-experiences in different subjects or even in the same subject under different conditions. Although noradrenaline is essential for the processing of pain-related information and has been shown to have an analgesic effect by its action in the dorsal horn, the mechanism by which noradrenaline modulates the spinal somatosensory network is not well understood. Yet, some studies have suggested that non-neuronal cells (glia) might have a key role in the action of noradrenaline (Fuxe et al., 2015; Seibt and Schlichter, 2015).

Therefore, the general aim of this thesis was to study the effect of noradrenaline on non-neuronal cells (glia) in the dorsal horn of the spinal cord and to investigate possible mechanisms by which noradrenaline, through its action on glia, could modulate neuronal communication in the dorsal horn. The spinal noradrenergic system appears to be important in pain regulation and selective manipulation of the noradrenergic could have great therapeutic potential. Therefore, the work of this thesis has been put into the context of pain. This introduction will be divided into three major parts. The first part is an overview of pain and of how pain is generated by different cellular and anatomical elements of the somatosensory nervous system, with an emphasis on the spinal cord. The second part of the introduction focusses on (1) the description of the physiology of noradrenaline (2) the basic anatomical aspects of noradrenergic projections within the CNS and (3) the noradrenergic regulation of the nociceptive information through its action in the spinal cord. The third part of the introduction is devoted to the fundamental biology of glial cells and calcium signaling in glial cells for communication within the glial network. We will also discuss how glial cells can modulate cellular activity by releasing active molecules into the extracellular space, in a process called gliotransmission, and what mechanisms govern the release of gliotransmitters.

1.2 Pain and Organization of the Nociceptive System

Pain is an essential survival mechanism that evolutionarily has been developed as a warning system of ongoing or "recent" tissue injury in humans as well as in many other species. However, once the initial damage or insult has been resolved, the maintenance of pain serves no future protection for an individual and should therefore normally disappear. In cases where the pain is persistent in the absence of any physiological protective role, pain can often become a burden rather than a benefit for the individual. Some studies have reported that countries like Canada, Spain and Sweden have an estimated prevalence of chronic pain of over 50% and that the social and financial burden of chronic pain should be taken into account (Watkins et al., 2008). In Europe, as well as in America, about 30% of the general adult population has been estimated to suffer from some form of persistent or chronic pain (Cohen and Mao, 2014). Pain is an individual and subjective experience with a high level of complexity, as each individual will exhibit a unique behavioral and emotional response-pattern following a given noxious stimulus. Remarkably, a single individual can be subjected to different pain-experiences from the same noxious stimulation if presented under different conditions (McGrath, 1994). Those differences are a consequence of a person's genetic background, psychological and social factors, expectations, past experiences, etc. In its simplest form, pain is a sensation/perception that arises from the processing of noxious information (nociception) within different structures of the nervous system (DeLeo, 2006). The International Association for the Study of Pain (IASP) defines pain as:

"An unpleasant sensory and emotional experience associated with actual or potential tissue damage or described in terms of such damage".

This definition highlights the complexity of pain and differentiates pain from nociception.

The differential diagnosis between acute physiological "protective" pain and pathological chronic pain has traditionally relied on a single time continuum with some arbitrary time interval such as 3 or 6 months after the primary pain onset. A fixed time point for separating acute pain and pathological pain is problematic for several reasons. First, it suggests that we know that after a certain time point, 3 months, for example, there will be no further protective function that justifies the presence of pain (Colloca et al., 2017). Second, some pain conditions such as migraine, trigeminal neuralgia and rheumatoid arthritis are episodic and occur "spontaneously" and most subjects suffering from those conditions do not experience continuous pain (J. D. Loeser and Turk, 2000).

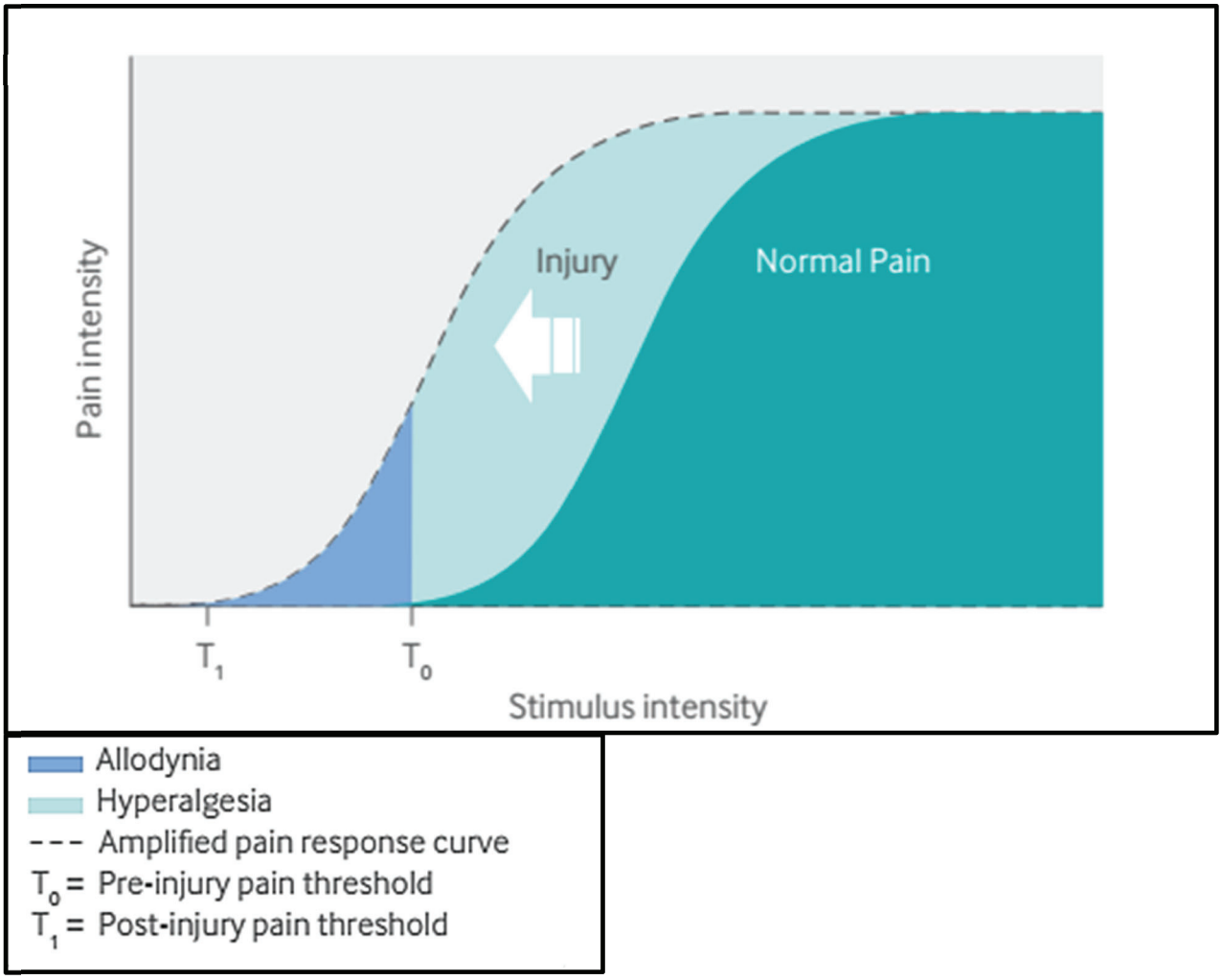

Figure 1. Relationship between stimulation intensity and pain.. During normal physiological conditions, pain experience displays a sigmoidal relationship to the stimulation intensity (turquoise panel on the most right-hand side). During injury, the intensity threshold (T0) for pain shifts towards a lower threshold (T1) leading to allodynia (non-noxious stimulations are experienced as painful). The shift of the curve to the left consequently makes noxious stimulations more painful, a state termed hyperalgesia. Both allodynia and hyperalgesia are hallmarks of many chronic pain states. [Modified from: Cohen and Mao, 2014].

Table 1. Clinically observed differences between neuropathic and nociceptive pain.

Clinical characteristic	Neuropathic pain	Nociceptive pain
Cause	Injury to the nervous system, often accompanied by maladaptive changes in the nervous system	Damage or potential damage to tissues
Descriptors	Lancinating, shooting, electric-like, stabbing pain	Throbbing, aching, pressure-like pain
Sensory deficits	Common—for example, numbness, tingling, pricking	Uncommon; if present they have a non-dermatomal or non-nerve distribution
Motor deficits	Neurological weakness may be present if a motor nerve is affected; dystonia or spasticity may be associated with central nervous system lesions and sometimes peripheral lesions (such as complex regional pain syndrome)	May have pain induced weakness
Hypersensitivity	Pain often evoked by non-painful (allodynia) or painful (exaggerated response) stimuli	Uncommon except for hypersensitivity in the immediate area of an acute injury
Character	Distal radiation common	Distal radiation less common; proximal radiation more common
Paroxysms	Exacerbations common and unpredictable	Exacerbations less common and often associated with activity
Autonomic signs	Colour changes, temperature changes, swelling, or sudomotor (sweating) activity occur in a third to half of the patients	Uncommon

Modified from: Cohen and Mao, 2014

Instead, diagnosis of chronic pain should be individualized with respect to the underlying pathology, if such exist, while investigating functional plastic changes in the nervous system that occur when the pain is becoming chronic or pathologic. Such changes in the nervous system will be described further below. Therefore, it is important not to oversimplify and not to consider pain as a single homogeneous condition but instead recognize that there are different types of pain. Today, the most common subdivision of pain pathologies classifies pain as either neuropathic or nociceptive pain based on neurobiological and clinical manifestations. For a more extensive and complete list of classification of different pain pathologies please see reviews by Nicholas, 2019 and Treede, 2019 (Nicholas et al., 2019; Treede et al., 2019) Table 1 highlights some of the common clinically observed differences between neuropathic and nociceptive pain. A hallmark of many pain conditions (chronic and non-chronic) is a leftward shift in the "stimulus intensity" – "pain intensity" curve meaning that stimulation intensities that are normally perceived as non-painful become painful and that a noxious stimulus is described as more painful than normal. These phenomena are termed allodynia and hyperalgesia, respectively, see Fig. 1

While pain can only be experienced by a conscious individual, nociception which is the transduction and processing of noxious stimuli can occur independently of pain (Julius and Basbaum, 2001). Pain is the conscious interpretation of nociceptive messages and requires communication between several cortical areas. Nociceptors are a family of somatosensory neurons that can detect damaging or potentially harmful stimuli (see Section 1.3.2 and 1.3.3). Detection of noxious stimuli occurs through the activation of specific receptors expressed by the peripheral terminals of the primary somatosensory neurons (Julius and Basbaum, 2001) The primary or first-order neurons have their cell bodies organized in ganglia positioned just lateral along the spinal cord (dorsal root ganglia; DRG). The primary sensory neurons are characterized by their pseudo-unipolar morphology, meaning that they do not have dendrites like classical neurons. Instead, they possess a single axon that gives rise to a branch that projects to the periphery of the body and a branch that projects to the dorsal horn of the spinal cord. At the peripheral branch of the axon, the terminals are associated with different sensory receptors that can be activated by different modalities such as thermal, mechanical and chemical (Julius and Basbaum, 2001). By contrast, the central axonal branch extends into the central nervous system where it forms chemical synapses with DH neurons, in different layers of the dorsal horn of the spinal cord depending on modality and fiber type (see Section 1.3). Therefore, the primary afferents connect the peripheral body to the

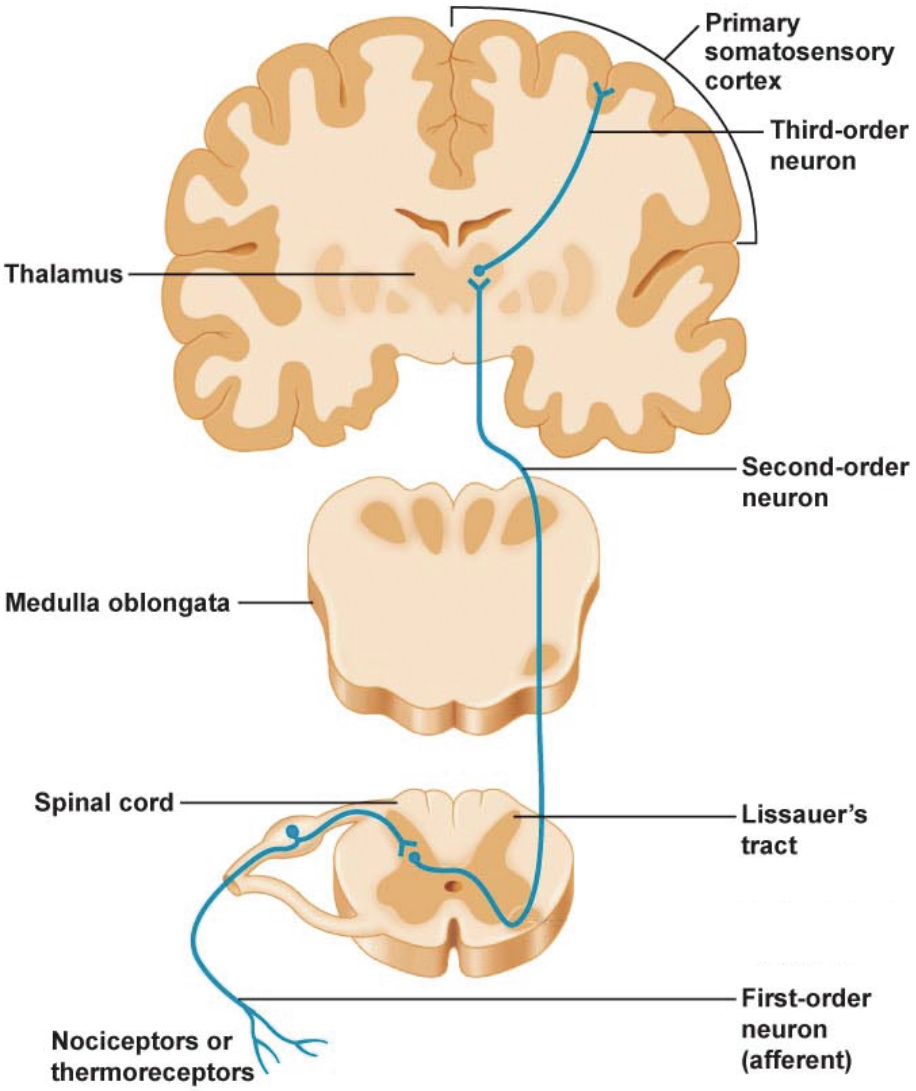

Figure 2. **Simplified anatomical illustration of the ascending nociceptive pathway**. Incoming nociceptive sensory information reaches the central nervous system by entering the dorsal horn of the spinal cord through first order sensory neurons with cell bodies located in the dorsal root ganglion. In the dorsal horn of the spinal cord information is transmitted to supra spinal centers by second order neurons. The primary target for projection neurons carrying nociceptive information from the dorsal horn is the thalamus. From the thalamus, the information reaches several brain regions, by third order neurons, where it is/can be interpreted as pain. [Illustration modified from: Marieb and Hoehn, 2010].

central nervous system and provide sensory information to the CNS through the dorsal horn of the spinal cord, see Fig. 2. In the dorsal horn, before being relayed to supraspinal centers, nociceptive information is subjected to modulation by local interneurons and by descending projections from higher center neurons.

1.2.1 Excitatory vs inhibitory neurotransmission within the dorsal horn circuits

Within the dorsal horn of the spinal cord, information is processed by local spinal interneurons, projection neurons and glial cells. Both the local excitatory interneurons and the primary afferents utilize L-glutamate as the main excitatory neurotransmitter.Glutamatergic neurons can be identified by immunohistochemical methods through labelling of the vesicular glutamate transporters (vGLUT-1/-2/-3). The vGLUT-1 and vGLUT-2 are the most prevalent vesicular glutamate transporters in the dorsal horn and vGLUT-1/2 mRNAs have been detected throughout the dorsal horn (Todd et al., 2003). vGLUT-3 is present in C-fiber terminals in the superficial laminae and transient vGLUT-3 expression has been described in the context of the development of mechanical allodynia (Peirs et al., 2015). However, vGLUT-1 is generally found in higher densities in intermediate laminae (laminae III-IV) whereas vGLUT-2 has been reported to be highly localized within the superficial laminae (lamina I-II) of the dorsal horn (Alvarez et al., 2004; Seal et al., 2009; Todd et al., 2003).

In opposition to glutamate, GABA and glycine serve as the main inhibitory neurotransmitters in the dorsal horn spinal cord. GABAergic neurons are commonly identified based on the presence of the enzyme glutamate decarboxylase (GAD) that produces GABA from glutamate (through decarboxylation) and GAD mRNA expression has been described both in deep and superficial laminae of the dorsal horn (Castro-Lopes et al., 1994). Glycinergic neurons are predominantly identified by detection of the plasma membrane glycine transporter type 2 (GlyT-2). GlyT-2 can be detected throughout the dorsal horn and GABA and glycine co-localization has been documented in the spinal cord (Mackie et al., 2003; Todd and Sullivan, 1990; Todd et al., 1996).

During neuropathic pain, the electrical properties of sensory neurons and the balance between excitatory and inhibitory components of synaptic transmission within dorsal horn circuits are altered and the nociceptive system becomes hyperexcitable (Colloca et al., 2017).

The increase in glutamate release that follows repetitive C-fiber stimulation and the subsequent NMDA (N-methyl-D-aspartate) receptor activation in the dorsal horn can recruit intracellular signaling events, such as

activation of protein kinase C, and result in long-lasting neuroplastic changes in the spinal cord that can contribute to the development of a pathological pain state (Malmberg et al., 1997). For example, damage to peripheral nerves leads to an increased glutamate release in the spinal cord that is accompanied by a down-regulation of spinal glutamate transporters. Such a reduction in the clearance of extracellular glutamate will lead to a prolonged dwell-time of glutamate in the extracellular space and therefore a prolonged activation of excitatory glutamate receptors (Guo et al., 2002). This will, in turn, facilitate the activation of projection neurons or local interneurons and induce functional synaptic plasticity such as LTP (long term potentiation) (Miller et al., 2011; Sung et al., 2003).

In addition to changes in the nociceptive transmission that is seen in many chronic pain situations, modulatory descending control systems are also dysfunctional in chronic neuropathic pain (Colloca et al., 2017). The major components of descending control system originate from the brain stem and involve monoaminergic neurons that project to the dorsal horn of the spinal cord. Noradrenaline, that is released from a subpopulation of *locus coeruleus* neurons, plays a key role in the modulation of nociceptive information in the dorsal horn, see Fig. 3 (Vanegas and Schaible, 2004).

1.2.2 **Ascending pathways and descending control**

After the modulation and integration by the neuro-glial networks in the dorsal horn, sensory information is relayed to supraspinal structures by projection neurons, the axons of which ascend in various tracts of the spinal cord white matter, see Table 2. The axons of the second-order neurons carrying nociceptive information mostly decussate to the contralateral side, within the same spinal segment, before ascending to supraspinal structures.

The target supraspinal structures of spinal projection neurons include subcortical and cortical areas such as:

- the bulbar and mesencephalic reticular formations, that play a key role in the modulatory descending control of pain through their anatomical connection to PAG
- the parabrachial nucleus, that is likely to be involved in emotional (including aversive) and autonomic components of pain
- the nucleus of the solitary tract, that also receives cardio and respiratory inputs and has a role in the increase of heart rate that is usually induced by a painful stimulation
- the periaqueductal grey matter (PAG), which is implicated in the formation of strategies for coping with stressors such as pain and is one of the supraspinal sites that are important for analgesia. Through its projections to other brainstem areas (including the rostral ventromedial medulla), it has a vital role in the descending control systems in the dorsal horn

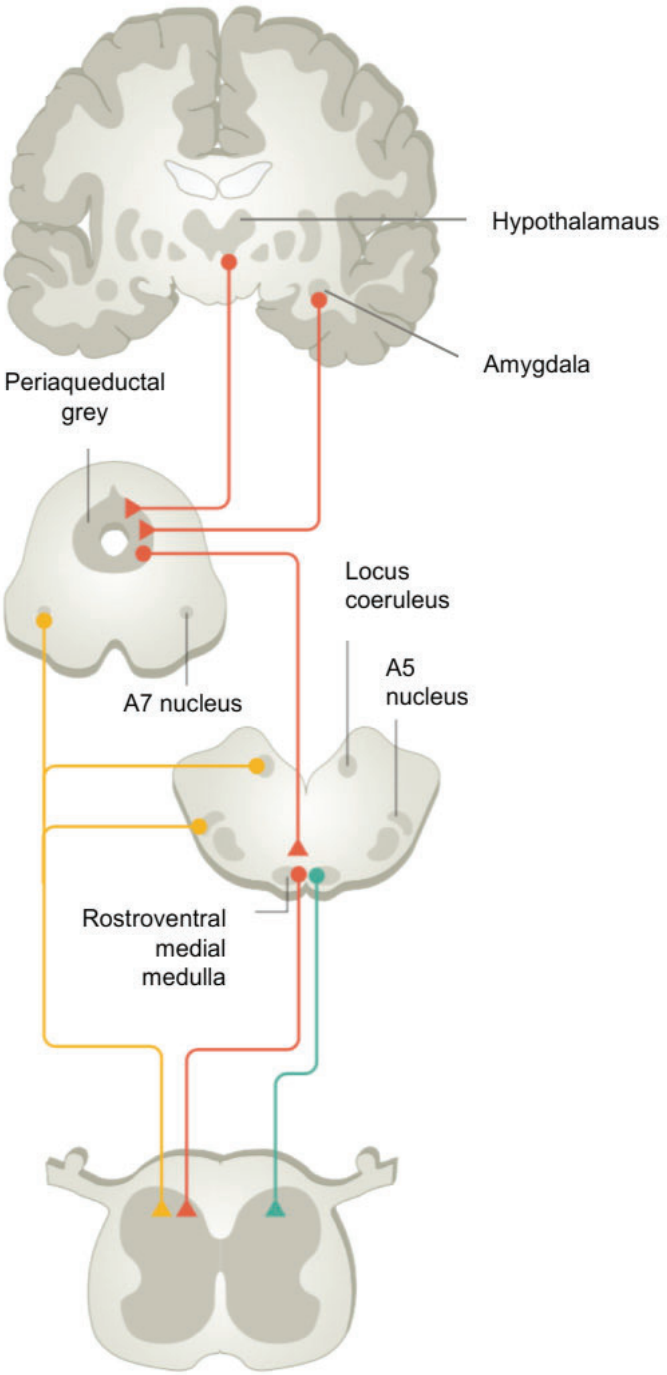

Figure 3. **Simplified anatomical illustration of descending control of nociception to the dorsal horn of the spinal cord**. The dorsal horn of the spinal cord receives multiple inputs through descending pathways originating in the brain stem, these pathways include pain suppression pathways (**red**), pain faciliatory pathways (**green**) and are partially regulated by inputs from brain structures such as hypothalamus and amygdala. The noradrenergic descending system is of special importance in descending regulation of pain with most of the fibers originating from the brain stem nucleus Locus Coeruleus. [Illustration modified from: Colloca et al., 2017]

- the hypothalamus (ventromedial), that involved the generation of affective components during pain perception as well as execution of defensive behavior
- the cuneiformis nucleus, which is involved in the descending pain modulatory system
- the posterior raphe nuclei, that project to both deeper and superficial laminae of the dorsal horn and play a key role in the descending control system.
- the thalamus (ventral posterior and medial), that receive inputs from the superficial dorsal horn and have reciprocal connections with the somatosensory cortex the anterior cingulate cortex (ACC). The ACC that involves the anticipation and attention to pain as well as anxiety and motor responses associated with pain
- the insular cortex, that plays a role in the affective and sensory discriminative aspects associated with painful experiences
- the prefrontal cortex that is involved in attention processing and sensory integration
- the limbic system areas, such as the amygdala and the hippocampus that are associated with emotional events such as fear that is strongly associated with painful experiences
- the primary and secondary sensory cortices that are involved in the interpretation of the intensity and the localization of noxious inputs.

(Bornhövd et al., 2002; Chen et al., 2002; Giesecke et al., 2004; Jaggi and Singh, 2011; Millan, 1999; Zubieta and Stohler, 2009).

To reach supraspinal structures nociceptive information can ascend through several pathways, for a full list see Table 2. The lateral spinothalamic pathway has been traditionally viewed to be the major ascending "pain/nociceptive pathway". However, it is important to remember that spinal projection neurons project to multiple brain targets and are not exclusively synapsing in the thalamus (Hylden et al., 1989; Millan, 1999). For example, a subpopulation of projection neurons from lamina I seem to primarily project to the parabrachial nucleus and neurons from lamina I and deeper laminae project to periaqueductal grey matter (PAG) and several other supraspinal structures including the cerebellum, the mesencephalon and the reticular formation, (Hylden et al., 1989; Lu and Willis, 1999). The projections providing nociceptive input to the PAG are of special interest since the PAG exerts a tight control over supraspinal descending projections that modulate nociceptive information at the spinal level.

The main regulatory neurotransmitter/modulator which is involved in these descending pathways are noradrenaline and serotonin (Cohen and Mao, 2014). During neuropathy, several processes appear to take place that reduce the efficacy of physiological pain attenuating pathways. These include a loss or reduction of tonic inhibition by noradrenaline and a switch from a mainly inhibitory to a predominantly facilitatory role of

Table 2. Overview of ascending spinal pathways transmitting nociceptive information to supraspinal structure.

Tract	Spino-thalamic	Spino-reticular	Spino-mesencephalic	Spino-parabrachio amygdaloid	Spino-parabrachio hypothalamic	Spino-hypothalamic (-telencephalic)	Spino-cervical	Dorsal column (ML) pathway
Laminae of origin	I II (few) IV V/VI VII/VIII LSN	I V/VI VII/VIII X (few)	I–II IV/V VII X LSN	I II (few)	I II (few)	IVX LSN	I (few) III/IV(most) V	III-V (most) VI VII
Ascending pathways	Mainly VLF DLF (I, LSN) Mainly contralateral	Mainly VLF Mainly contralateral But ipsilateral (I–V) via dorsal columns to DRN	Mainly VLF DLF (I, LSN) Mainly contralateral	DLF-LF Mainly contralateral	DLF-LF Mainly contralateral	VLF Mainly contralateral	DLF Ipsilateral-then contralateral (from LCN)	DF (and DLF) Ispsilateral-then contralateral (from DCN)
Principal sub-cortical targets	Thalamus: VLF → VPL/VPM DLF→ VMPo/ VPI/MDvc Also PAG and collaterals →Reticular structures	RF of brainstem →LRN (NPGC/NGC), medial thalamus and DRN (few)	Midbrain and PAG Deep SCL, NCF and PBN Thalamus (few)	PBN→ amygdala and striaterminalis	PBN→ hypo-thalamus (VMH)	Hypothalamus and thalamus. Also pons, amygdala, striatum (bilateral	Relay LCN (C1–C3 level) →Contralateral thalamus (VPL/VMPo) and midbrain (PAG and SCL) Some LCN cells →spinal cord	Relay DCN of caudate medulla: via ML → contralateral thalamus (VPL/VMPo) Also SCL and spinal cord
Possible roles	Discriminative -sensory (VLF) Motivation-affective (DLF) Descending inhibition	Motivational-affective? Descending inhibition	Motivational-affective. Autonomic, motor	Motivational-affective. Autonomic	Motivational-affective. Endocrine	Sleep, autonomic and endocrine function Thermo-regulation	Discriminative -sensory Motivational affective Autonomic ?	Discriminative -sensory (VPL) Motivational-affective (VMPo)

Abbrevations: WDR, wide-dynamic range; NS, nociceptive-specific; Non-N, non-nociceptive; CL, centrolateral; DCN, dorsal column nuclei; DF, dorsal funiculus; DLF, dorsolateral funiculus; DRN, dorsal raphe nuclei; LCN, lateral cervical nucleus; LRN, lateral reticular nucleus; LSN, lateral spinal nucleus; ML, median lemniscus; NCF, nucleus cuneiformus; MDvc, medial dorsal thalamus, ventral aspect; NPGC/NGC, nucleus (paro) gigantocellularis; PAG, periaquaductal grey; PBN, parabrachial nucleus; PO: posterior group of thalamic nuclei; RF, reticular formation; SCL, superior colliculus; VLF,ventrolateral funiculus; VMPo, ventromedial posterior thalamus; VPL/VPM, ventroposterolateral/ventroposteromedial thalamus; VPI, ventroposterioinferior thalamus and VMH, ventromedial hypothalamus. Symbolizes subsequent, second order projection. [Modified from Millan, 1999]

serotonergic modulation within the nociceptive network in the dorsal horn of the spinal cord (Wei et al., 2010).Under normal physiological conditions, noradrenaline exerts a strong inhibition on nociception/pain, through its action on the α2 receptors of the dorsal horn neurons, but during neuropathy, there is a decrease in the efficiency of this inhibitory noradrenergic control (Ossipov et al., 2014). Importantly, the descending noradrenergic control is likely to act also on dorsal horn glial cells which play a key role in the integration and modulation of afferent information in the dorsal horn of the spinal cord. This point will be discussed in more detail in Sections 1.4 and 1.5. In short, both microglia and astrocytes are activated within 24 hours after injury and can maintain an activated state for up to 12 weeks (Cohen and Mao, 2014). Activated dorsal horn glial cells are essential for the development and maintenance of many neuropathies, with astrocytes releasing a variety of pro-nociceptive molecules such as prostaglandins, cytokines, chemokines, and excitatory amino acids (Mika et al., 2013). The pro-inflammatory environment induces neuroplastic adaptations in the dorsal horn, such as upregulations of glucocorticoid and glutamate receptors which tilt the balance towards spinal excitation and hyperexcitability (Wang et al., 2005).

1.2.2 Summary

During pathological (chronic) pain, neurons and glial cells in several regions of the nervous system undergo plastic changes that will result in a facilitation of nociceptive transmission and pain experiences. A common alteration in the dorsal horn of the spinal cord includes a shift in the inhibitory to excitatory balance. The shift from a prominently inhibitory to an excitatory state of the dorsal horn network can occur through multiple mechanisms, in which glutamate dysregulation appears to play a major role, together with an alteration in the descending control systems, among which the noradrenergic system. Most noradrenergic neurons in the descending control system have their cell bodies located in the *Locus Coeruleus*, and the axons of these neurons target neurons and possibly glial cells in the dorsal horn of the spinal cord, see Fig. 3. Although the mechanisms by which the noradrenergic descending control system modulates spinal nociceptive networks are not fully understood, it is well established that alterations in the descending systems are involved in various pathological pain conditions (Colloca et al., 2017).

1.3 Anatomy and physiology of the dorsal horn of the spinal cord and the primary sensory afferents

Sensory information is conveyed from the periphery to the dorsal horn of the spinal cord through the three different types of sensory nerve fibers termed Aβ, Aδ and C-fibers. The distinction of the Aβ, Aδ and C-fibers are based on the diameters of the axon, degree of myelination of axons and conduction velocity of action potentials (Basbaum et al., 2009). Aα-fibers are associated with muscle spindle and golgi tendon organ to regulate muscle tension and position; it will not be covered in more detail in this thesis.

1.3.1 Primary afferents encoding non-noxious information

Aβ fibers are large sensory fibers with a diameter 5-10 μm and are heavily myelinated, these fibers originate from large (> 50μm) cell bodies (measured in cats). They are fast conducting fibers with a conduction velocity of approximately 30-120 ms^{-1} (measured in different mammalian sensory afferent) (Smith and Lewin, 2009). Aβ fibers are classical responding and transmitting non-noxious information such as vibrations, touch, and proprioception. However, it has been proposed that the Aβ fibers have a role in the sharpness of the first sensation/response of mechanically induced pain (Djouhri, 2016; Djouhri and Lawson, 2004; Dubin and Patapoutian, 2010). About 20% of the sensory primary afferents have the characteristics of Aβ neurons which mostly establish synapses in the deeper laminae of the dorsal horn (Djouhri, 2016).

1.3.2 Primary afferents encoding noxious information

Aδ fibers are smaller than Aβ fibers with an axon diameter of 2-6μm (measured in cats). The conduction velocity of Aδ fibers generally ranges from 3 – 30 $m.s^{-1}$ (measured in different mammalian) (Coggeshall et al., 1978; Smith and Lewin, 2009). Nociceptive information coded by Aδ -fibers is commonly perceived as a brief but intense and well-localized pain experience after exposure to noxious stimulation. Fibers with characteristics of Aδ transmit different nociceptive modalities including heat, cold, mechanical (Basbaum et al., 2009). It has been estimated that around 20 % of the cutaneous sensory fibers have properties similar to Aδ fibers (Smith and Lewin, 2009). Aδ fibers terminate prominently in lamina I, outer lamina II and lamina V in the dorsal horn of the spinal cord (Basbaum et al., 2009).

Compared to other fiber types, the C-fibers conduct information, from the periphery to the dorsal horn of the spinal cord, at a very slow velocity at around 0,5 – 2 $m.s^{-1}$ (Smith and Lewin, 2009). The C-fiber axons emerge

from neurons with small cell bodies and the most prominent characteristic of C-fibers is that their axons have a small diameter (0,2 – 2 μm) and are devoid of myelin, which explains the slow conduction velocity (Smith and Lewin, 2009). C-fibers are classically associated with the slow transmission of nociceptive information and C-fiber driven pain is usually expressed as dull and poorly localized non-sharp pain, in opposition to Aδ-fiber mediated pain (Dubin and Patapoutian, 2010; Smith and Lewin, 2009). Most C-fibers are polymodal, meaning that they can respond to more than a single stimulus type (heat/cold, chemical, mechanical). Most of the cells displaying C-fiber features terminate and synapse superficially in lamina I and lamina II in the dorsal horn of the spinal cord. In the periphery, the C-fiber cells terminate as free nerve ending throughout the skin at various densities. Approximately 50-70 % of cutaneous fibers appear to have the characteristic of C-fibers (Smith and Lewin, 2009). In acute pain, both Aδ- and C-fibers cooperate to ensure appropriate pain behaviours. Interestingly, a small fraction of C-fiber cells are silent during normal physiological conditions and will be only recruited during different pathological states such as during inflammation (Prato et al., 2017).

1.3.3 Functional and neurochemical classification of nociceptors

One common system for classifying primary neurons is based on the modality of the nociceptive information conveyed by the sensory fiber i.e. heat (H); mechanical (M) and cold (C). Electrophysiological recordings have shown the existence of both polymodal (e.g. C-MH; interpreted as mechano- and heat-sensitive C-fiber), single modal (e.g. C-M and C-H) as well as polymodal "silent" (e.g. C-M_iH_i, i.e. C-Mechano-insensitive and Heat-insensitive) C-fibers (Dubin and Patapoutian, 2010). A similar classification has been achieved for Aδ fibers, however, in humans, A-MH fibers have been further divided into type I and type II (A-MH I and A-MH II). The A-MH II fibers are rapidly activated and respond to a slightly lower temperature than the type I and therefore mediate the first nociceptive heat (Dubin and Patapoutian, 2010). A-MH I require a longer duration of exposure to reach maximal firing rate and are together with the C-fibers responsible for the secondary pain experience during noxious heat exposure (Dubin and Patapoutian, 2010; Smith and Lewin, 2009).

The primary afferents have also been further distinguished on the basis of their activation threshold following electrical and on nociceptive stimulation, thus separating high- and low threshold fibers (Cordero-Erausquin et al., 2016). In addition, nociceptors have been classified by their neurochemical markers, for example by dividing Aδ and C-fibers into peptidergic or non-peptidergic fibers (also substance P and calcitonin gene-related peptide

positive/negative). For further details concerning the neurochemical classification of spinal cell-population readers are referred to the comprehensive summary by (Ribeiro-da-Silva and De Koninck, 2008) which also covers differences among species.

Once the stimuli have been detected by the primary afferents, the information is conveyed to the spinal cord and relayed to the central nervous system in the dorsal horn of the spinal cord. The dorsal horn of the spinal cord is also a key site where sensory information can be modulated by both neuronal- and glia networks before being relayed to higher supraspinal structures. The spinal cord, therefore, is a crucial structure by bridging the peripheral body with the brain

1.3.4 Anatomy and cytoarchitecture of the spinal cord

The spinal cord is a crucial part of the central nervous system and is located inside the vertebral canal and protected by the vertebrae. The spinal cord is usually divided into; centrally located grey matter and surrounded by white matter, see Fig. 4. The white matter appears white due to a large number of myelinated axons while the grey matter mostly contains the cell bodies of neurons and glia. The grey matter of the spinal cord has commonly been divided into 10 different regions known as Rexed's laminae. The dorsal horn is a structure that is especially important for integration, processing and transmission of peripheral nociceptive information. The dorsal horn of the spinal cord comprises laminae I to VI. The Rexed lamination is defined based on the cell density, cell morphology, dendritic arborization and axonal connections (Wall, 1967). The functional classification of dorsal horn cells is determined through electrophysiological properties and primary afferent inputs properties.

1.3.5 Anatomy and characteristics of the dorsal horn laminae

Lamina I in the dorsal horn of the spinal cord is located at the most dorsal part of the grey matter thus forming a thin border (marginal zone) between the white and grey matter (Fig. 5). In lamina I, three different morphologic types of cells have been described: pyramidal cells, fusiform cells and multipolar cells (Lima and Coimbra, 1986; Zhang and Craig, 1997). A small fraction of the lamina I cells have dendrites that are spreading to lamina II and deeper laminae while most of the cells keep their dendritic arborization localized in lamina I. Lamina I also possesses interneurons that show axonal branches stretching deep into the dorsal horn while also extending over several spinal segments (Szucs et al., 2013) Some larger cell body (diameter >200 µm) projection

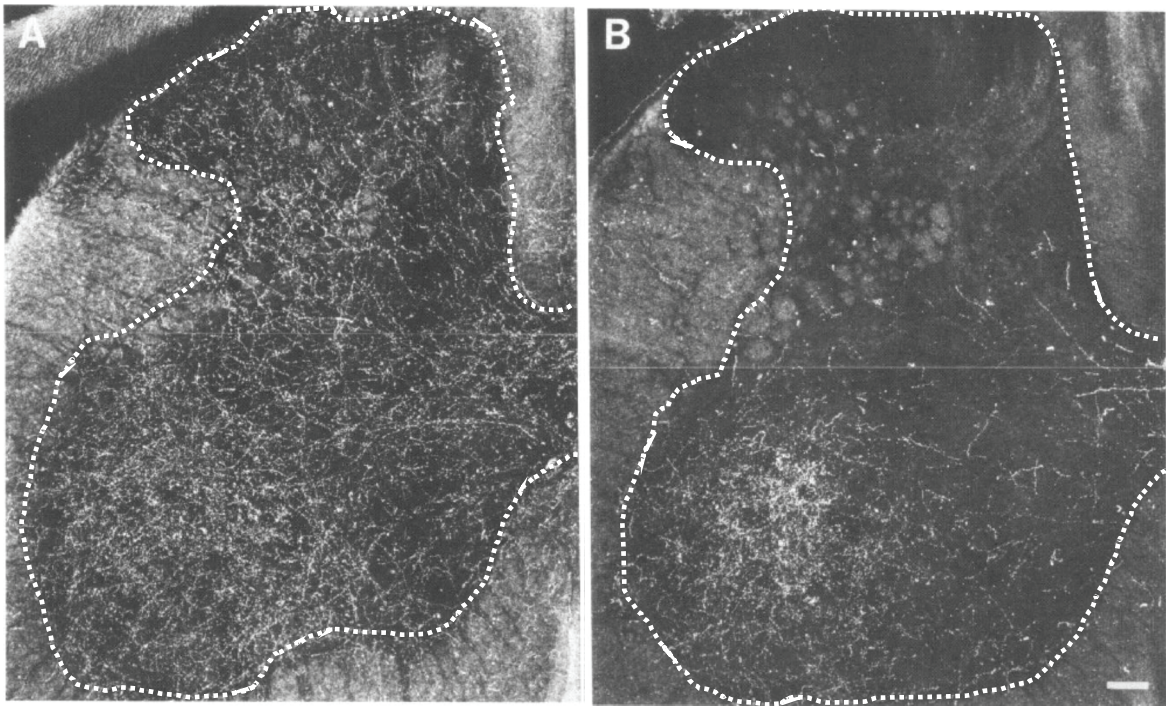

Figure 4. Noradrenergic fibers in the grey and white matter the spinal cord. Dotted white line indicate the separation betweem the, soma dense, central grey matter from the outer, myeline dense, white matter in the lumbar part of rat spinal cord Dark-field micrographs of spinal cord slices stained with anti-dopamine-beta-hydroxylase. **A** Control animal, **B** Slice from animal treated with DSP-4 (LC-axon toxin) during two weeks. In B, note the significant losses of noradrenergic axons in the dorsal and intermediate regions after drug treatment. DSP-4 has little effect on NA-axon staining in the ventral regions of the spinal cord. Scale bar 100µm. [Illustration modified from: Lyons et al., 1989]

neurons are situated in lamina I. The projection neurons project to several supraspinal regions; including the thalamus and part of the brain stem such as parabrachial complex and periaqueductal grey (PAG) (Al Ghamdi et al., 2009; Todd, 2010).

Lamina II also called *Substantia Gelatinosa* can be seen as a more "gelatinous" region located in the dorsal horn ventral to lamina I (Fig. 5). Compared to other parts of the dorsal horn its more translucent aspect is due to the presence of neurons with small cell bodies arranged/packed at a high density and having non-myelinated axons. Furthermore, the cells in lamina II are divided into four different morphological subtypes; the vertical cells, central cells, radial cells and islet cells (Grudt and Perl, 2002; Yasaka et al., 2007). Classically *Substantia Gelatinosa* is divided into two regions; the outer part (LII_o) and the inner part (LII_i) which correspond to the most dorsal and ventral regions of lamina II, respectively. Most vertical cells are excitatory meaning that they release glutamate as a primary neurotransmitter. In contrast, most of the islet cells are thought to release GABA as its main neurotransmitter, meaning that they are inhibitory cells (Todd and McKenzie, 1989). Central cells, on the other hand, have no major dominant neurotransmitter and include subpopulations that are either inhibitory or excitatory (Hughes et al., 2012).

Laminae III-IV are located ventral of lamina II and are recognized by their higher density of myelin and lower cell soma density (Fig. 5). The neurons in laminae III-IV are considered to consist of a heterogeneous population expressing inhibitory and excitatory markers, GAD and vGLUT2 respectively (Polgár et al., 1999; Schneider and Walker, 2007). Based on morphology, interneurons in lamina III-IV are divided into local interneurons with local axons and interneurons with deep axonal branches. The local interneurons have their axons within laminae III-IV and are usually oriented through the rostro-caudal axis. In comparison to the local interneurons, interneurons with deep axonal spread have large dendritic trees that project along the dorso-ventral as well as the mediolateral axis and extend their axons rostro-caudally through the bifurcation of the axon, crossing several spinal segments.

Laminae V-VI are located at the most ventral part of the dorsal horn (Fig. 5). Together they form the ventral border (the end/start) of the dorsal horn. Cells in lamina VI are involved in locomotion and the primary afferents which are mainly large-diameter fibers that originate from muscle spindles and joints (Hochman, 2007; MacKinnon, 2018). Interestingly, cells in lamina V respond to both nociceptive input as well as innocuous

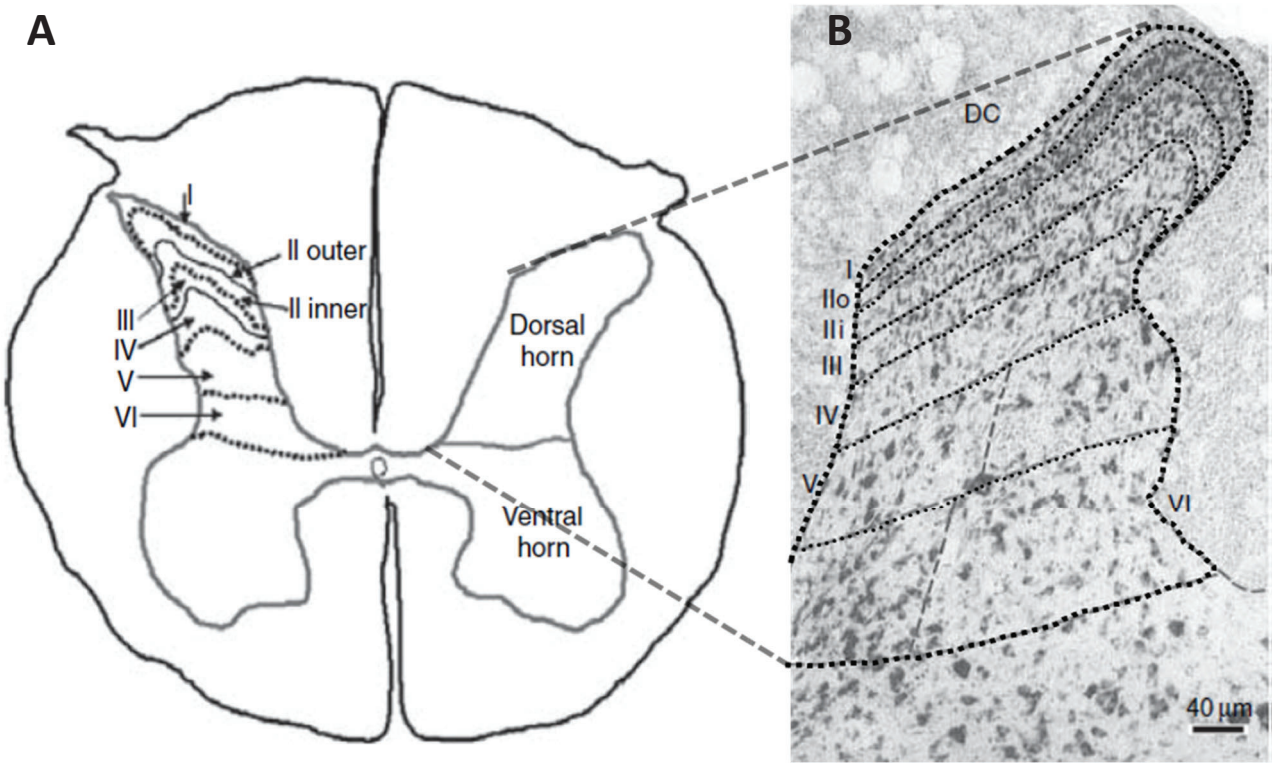

Figure 5. **Illustration of gross anatomical features of the spinal cord** and organization of the dorsal horn laminae. **A** Schematic illustration of a transversal section of spinal cord with Rexed's laminae in the dorsal horn of the spinal cord .**B** Micrograph of the doral horn from frozen cross section (50 mm thickness) at the cervical level (C4) of the adult rat spinal cord stained with toluidine blue. Different laminas, according to Rexed's classification, can be identified by ultrastructural differences within the dorsal horn. Lamina I has relatively few cell bodies compared to Lamina II. Lamina II is commonly divided in to two separate segments, the inner (LII_i) and the outer part (LII_o) of LII. Both LII_o and LII_i have many small neurons, of rather uniform size. The LII_o is characterized by the clustering of small cells which distinguish it from the LIIi. The occurrence of slightly larger neurons separates LIII from LII_i, while lamina IV can easily be identified from lamina III by the lower occurrence of cell bodies and the presence of some large neurons. [Illustration modified from: Ribeiro-da-Silva and De Koninck, 2008]

stimuli (Ritz and Greenspan, 1985). These multi-receptive cells are referred to as Wide Dynamic Range (WDR) neurons. The axons of WDR neurons do not seem to make any collaterals before they decussate with the spinal cord and their axons ascend in the white matter of the contralateral side spinal cord (Ritz and Greenspan, 1985).

1.3.6 Innervation of superficial laminae of the dorsal horn by primary afferent

Electrophysiological recording in the spinal cord combined with peripheral electrical stimulation have allowed addressing the issue of afferent primary sensory neurons projections to the different subpopulation. Many studies have concluded that the cells in superficial laminae (I-II) do not receive monosynaptic input from Aβ primary afferents under basal physiological condition (Nakatsuka et al., 1999; Yoshimura and Jessell, 1989). This goes well along with the classical notion that the superficial laminae only process nociceptive information. However, by looking specifically at certain identified sub-populations Duan and colleagues found that about 50 % of SOM^+ (in LIIi) and 13 -27 % $dynorphine^+$ interneurons in the superficial laminae receive direct monosynaptic input from peripheral Aβ afferents (Duan et al., 2014).

1.3.7 Synaptic Aδ-fiber input to the dorsal horn

The majority of studies concerning monosynaptic input have been focusing on the superficial laminae and in particular on lamina II. During electrical stimulation of the dorsal root ganglia (DRG) about half (47%) of the radial cells in the lamina II receive excitatory monosynaptic Aδ input (and 12 % excitatory polysynaptic) and approximately three fourth (81%) of the vertical neurons in lamina II receive Aδ input. Among the vertical cells that displaying Aδ input, 76% was excitatory monosynaptic connections (Lu and Perl, 2003; Yasaka et al., 2007). Apparently, neither central nor islet cell in lamina II receive monosynaptic Aδ input (Yasaka et al., 2007).

1.3.8 Synaptic C-fiber input in the dorsal horn

In opposite to the Aδ input, approximately two-third of all cells found in lamina II receive monosynaptic C-fiber input (evoked, by electrical stimulation). Synaptic C-fiber input is almost equally distributed among the four different cell types found in lamina II. In quantitative terms; 64 % of radial cells, 67 % of central cells, 76 % of vertical cells and 73 % of islet cells received direct monosynaptic input from C-fibers during electrical DRG stimulation (Lu and Perl, 2003; Yasaka et al., 2007). Cells in lamina I have also been described to have synaptic C-fiber input, however, no quantitative or cell-specific data have been provided (Lu and Perl, 2003).

1.3.9 Synaptic innervation of the deep laminae of the dorsal horn

Although rather few studies have addressed synaptic input to deeper layers, two studies conducted on unidentified cells in hamster showed that within Laminae III-IV almost all (95 %) cells received synaptic input from large Aβ fibers whereas almost none (0-1%) of the cells received monosynaptic input from C-fibers (Schneider, 1992; Schneider, 2005). Although at first sight, this gives the impression that nociceptive (Aδ and C-fibers) and low threshold fibers (Aβ) are directly connected to distinct pools of cells that are divided into superficial and deep lamina respectively, interpretation of related data must be done carefully. While it is still partially true that nociceptive and non-nociceptive fibers have synaptic connections to cells that are segregated in the spinal cord, this applies only to the cell bodies. As mentioned above, certain cells in lamina III have dendritic arborizations that extend into the superficial layers and these lamina III cells may receive synaptic input directly from primary nociceptive fibers (Cordero-Erausquin et al., 2016; Giesler et al., 1976; Giesler et al., 1981).

1.3.10 Communication to and within the dorsal horn - summary and conclusion

In addition to receiving direct primary afferent input, dorsal horn neurons display a high degree of intrinsic connectivity that forms microcircuits that are essential for its function to modulate incoming sensory response properties. The dense micro-circuitry formed by inter-neuronal connections can be appreciated through the great number of polysynaptic inputs that are evoked by electrical stimulation of the dorsal roots (Torsney and MacDermott, 2006; Yasaka et al., 2007; Yoshimura and Nishi, 1992).

The neuronal network of the dorsal horn is composed of a local circuit of neurons synapsing within the same lamina. In addition, many neurons within each segment have large dendritic arborizations that stretch over several laminae. In addition to neurons projecting across laminae and establishing *inter*-laminar connections, glial cells in the dorsal horn of the spinal cord work in parallel to neurons to process and transfer information across the spinal cord (Cordero-Erausquin et al., 2016). To fully comprehend the complexity of the dorsal horn circuitry, it is important to simultaneously consider the glial network that works in concert with the neuronal network to carry information within the dorsal horn. The importance of the functional glial network in inter-laminar communication in the dorsal horn was elegantly shown by Seibt and Schlichter in 2015. By a series of an electrophysiological experiment, they showed that the increase in the frequency of neuronal inhibitory post-

synaptic currents induced by noradrenaline in lamina III-IV could be disrupted by pharmacologically interfering the glial network in the dorsal horn and also by physically suppressing inputs from lamina V to more superficial laminae in the dorsal horn (Seibt and Schlichter, 2015). This highlights the complexity of information processing in the dorsal horn as well as the importance of the inter-laminar communications and the glial network.

1.4 Noradrenaline and the modulation of nociceptive synaptic processing

1.4.1 Noradrenaline – structure, synthesis, storage and degradation

Noradrenaline, also known as norepinephrine, is a neurotransmitter and a hormone and acts as a ligand on the adrenergic receptor family. Here we will limit our study discussion to the role of noradrenaline as a neurotransmitter. Chemically noradrenaline is a monoamine, and it belongs to the catecholamine family, meaning that it contains an amine-group attached to a catechol-group. Noradrenaline synthesis starts with the non-essential amino acid tyrosine being converted by tyrosine hydroxylase (THL) to levodopa, see Fig. 6. Levodopa is then further converted, by DOPA-decarboxylase (DDC), to dopamine that is further metabolised to noradrenaline by the enzyme dopamine-β-hydroxylase (DBH). Therefore, DBH is commonly used as a marker to identify noradrenaline producing neurons (Llorca-Torralba et al., 2016). (In neurons containing phenyl-ethanolamine N-methyltransferase noradrenaline can be further converted to adrenaline). The first step of the biosynthesis noradrenaline, namely the production of dopamine, takes place in the cytoplasm. However, the conversion of dopamine into noradrenaline occurs inside the secretory vesicles due to the subcellular localization of dopamine-β-hydroxylase, see Fig. 6 (Gonzalez-Lopez and Vrana, 2020). Therefore, dopamine is translocated, by the vesicular monoamine transporter (VMAT) from the cytoplasm to the luminal side of secretory vesicles (Gasnier, 2000). Two isoforms of the vesicular monoamine transporters, VMAT-1 and VMAT-2, with individual pharmacological properties and tissue distributions have been identified and characterized in humans (Erickson et al., 1996). VMAT-1 is commonly expressed in large dense-core vesicles of various neuroendocrine cells in the peripheral body (Weihe et al., 1994). In contrast, VMAT-2 is primarily localized in monoaminergic cells in the central nervous system but can also be found in peripheral immune cells and histamine-positive cells in the gastrointestinal system (Erickson et al., 1996; Weihe et al., 1994). Once released into the extracellular environment, noradrenaline can be taken up pre-synaptically by the plasma membrane noradrenaline transporter (NET) and metabolized by the enzymes monoamine oxidase (MAO) or catechol-O-methyltransferase (COMT), see Fig. 6 (Llorca-Torralba et al., 2016; Torres et al., 2003).

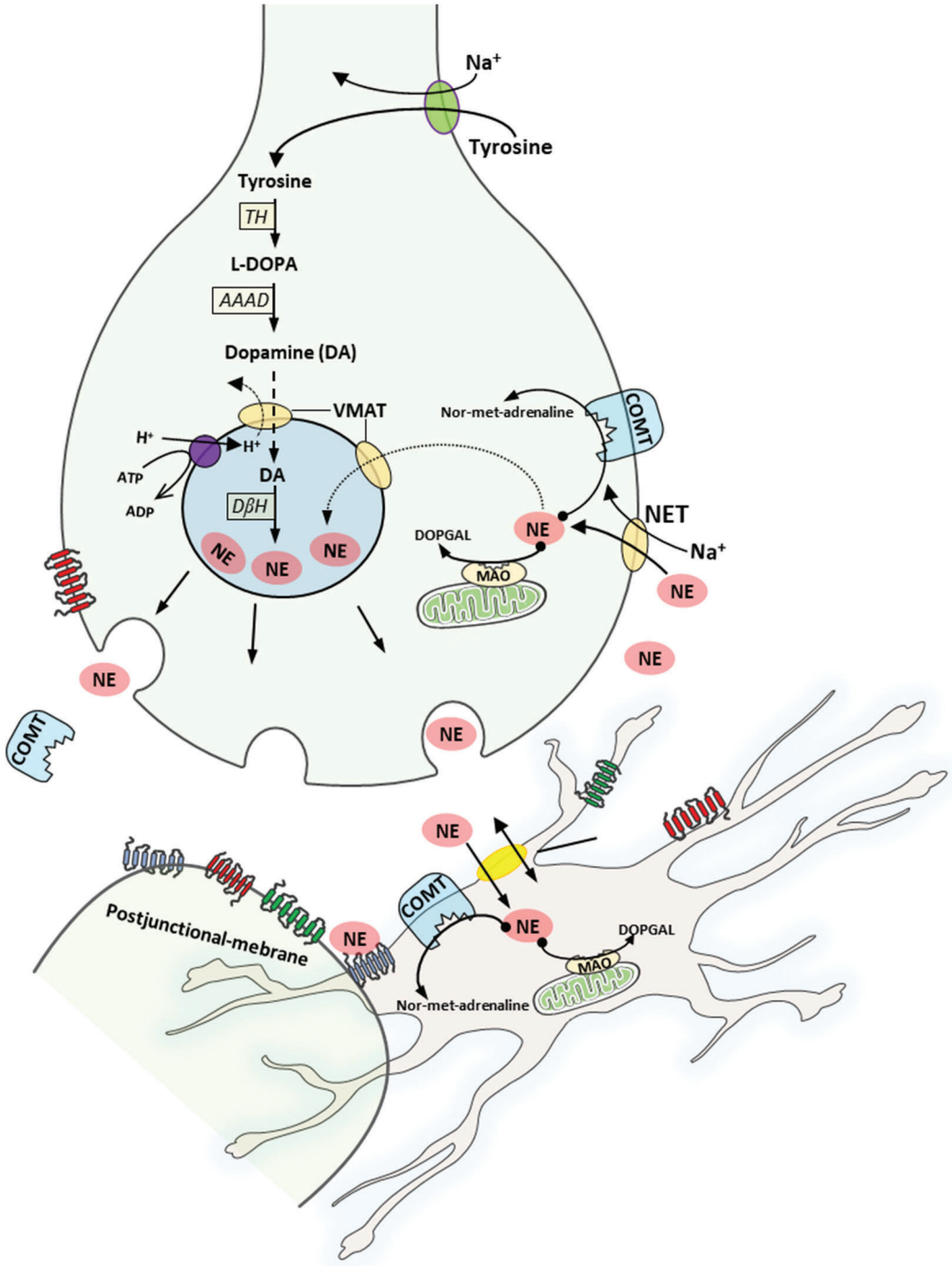

Figure 6. **Simplified illustration of the biosynthesis and the clearance/degradation of noradrenaline (NA)**. NA is synthesized by a series of enzymatic steps starting from the non-essential amino acid tyrosine. Tyrosine is converted to L-DOPA (levodopa, l-3,4-dihydroxyphenylalanine) by TH (tyrosine hydroxylase) which is the rate limiting step in the synthesis of NA. L-DOPA is further converted to dopamine by AAAD (aromatic L-amino acid decarboxylase). The conversion of dopamine to NA take place inside the small synaptic vesicles, and dopamine is therefore transported from the cytoplasm into synaptic vesicles by the VMAT (vesicular monoamine transporter). On the luminal side of the vesicles dopamine is catalyzed to NA by DβH (dopamine-β-hydroxylase). After NA is released it diffuses to reach its target receptors while also being transported back into either the releasing neuron or by neighboring glial cells. Reuptake by the NA-releasing is mediated through NETs (norepinephrine transporters) while glial cells utilize ESMP (extra-synaptic-monoamine-transporters). Inside the cells, NA can be metabolized to by MAO (monoamine oxidase) or COMT (catechol-O-methyltransferase) to DOPGAL or nor-met-adrenaline, respectively. Alternatively, NA can also be recycled back in to synaptic vesicles through VMATs. Freely circulating COMT has been in the identified, in the extracellular space, but is thought to contribute only marginally to NA clearance

1.4.2 Adrenergic receptor – structure, subtypes and distribution

Adrenergic receptors (adrenoceptor) are part of the seven-transmembrane receptor family and their action is mediated by guanine nucleotide-binding regulatory proteins also called G-proteins (Pertovaara, 2013). Adrenoceptors are divided into two classes: the α- and β-adrenoceptor Furthermore, α-adrenergic receptors are classified into subtypes α_{1A}, α_{1B}, α_{1D} α_{2A}, α_{2B}, and α_{2C}, and β-adrenoceptors have been classified into 3 different subtypes β_1, β_2, and β_3 (Bylund et al., 1994; Llorca-Torralba et al., 2016). Among the adrenoceptors (abbreviation: AR) both α- and β-AR adrenoceptor have been identified to have a strong mRNA expression in the spinal cord.

In rats, using in-situ hybridization techniques mRNA signals for the α_{1A}-AR have been observed throughout the spinal cord but are more densely expressed in laminae VII and IX. In laminae V-VII the α_{1A}-AR mRNA is also expressed but at a lower level (Day et al., 1997). α_{1B}-AR mRNA are weakly expressed in the spinal cord compared to those for the α_{1A}-AR and α_{1D}-AR, however, mRNA for α_{1B}-AR can be seen weakly in laminae I-VIII with a slightly higher density in laminae IX (Day et al., 1997). α_{1D}-AR mRNA is also expressed throughout the spinal cord but with very week levels in the superficial dorsal horn of the spinal cord (laminae I-VI). Slightly higher (but still low/moderate) mRNA levels were detected in lamina VII, VIII and X. However, the most ventral part of the spinal cord (~lamina IX) has been found to express moderately strong levels of α_{1D}-AR. (Day et al., 1997). By co-expressing α_1-AR with EGFP (enhance green fluorescent protein) α_1-AR receptors had successfully been identified in the spinal cord of mice. Both the α_{1a}-AR and the α_{1B}-AR subtypes had been found to be moderately expressed in the ventral and the dorsal horn in mice with similar density, for more details please see (Papay et al., 2006; Papay et al., 2004). Common features for all α_1-adrenoceptors are that they will be activated by noradrenaline (and adrenaline) and are sensitive to the antagonist prazosin. All of them show a low affinity for α_2-AR antagonists such as yohimbine and rauwolscine, see Table 3-4 (Bylund et al., 1994). In the prenatal rat, α_{2A}-AR and α_{2B}-AR can be detected in the spinal cord, however, after birth α_{2A}-AR expression persists while α_{2B}-AR disappears and expression of α_{2C}-AR increases (Huang et al., 2002). Immunohistochemical studies in postnatal rats found that α_{2A}-AR and α_{2C}-AR are found predominantly, but not exclusively in the most superficial dorsal horn (laminae I-II) (Stone et al., 1997). Among the α_2-AR in the deeper dorsal horn, the α_{2C}-AR is more prevalent and densely distributed than the α_{2A}-AR subtype. However, expression of α_2-AR is not restricted to the dorsal horn since α_{2A}-AR have been observed surrounding the central

Table 3 Affinity variability among α1-AR subtypes

Compound	**Mean K_i (nM)**			
α_2-AR- antagonist/ agonist	**α_{1A}**	**α_{1B}**	**α_{1C}**	**α_{1D}**
WB 4101[(1)]	0.08 ± 0.02	8.0 ± 2.8	0.65 ± 0.20	1.6 ± 0.3
5-Methylurapidil[(1)]	0.70 ± 0.1	96 ± 26	7.6 ± 2.8	15 ± 0.4
Prazosin1	0.13 ± 0.02	0.32 ± 0.09	0.54 ± 0.14	0.32 ± 0.01
Oxymethazoline[(2)]	3.7 ± 0.83	280 ± 56	46 ± 20	2140
Spiperone[(1)]	7.2	1.3 ± 0.72	22	-

[Modified from: Bylund et al., 1994]

Table 4. Affinity variability among α_2-AR subtypes.

	Mean K_i (nM)			
α_2-AR antagonist	**α_{2A}**	α_{2D}	α_{2B}	α_{2C}
Rauwlsocine	3.7 ± 1.6	33 ± 10	1.2 ± 0.5	0.18 ± 0.03
Prazosin	1034 ± 403	1127 ± 337	30 ± 7	61 ± 17
ARC-239	256 ± 86	285 ± 135	4.6 ± 2.0	51 ± 28
BAM-1303	3.6 ± 1.9	16	174 ± 30	187
BRL 44408	5.6 ± 1.9	34 ± 14	350 ± 91	72 ± 23
Imiloxan	1750 ± 1250	79	50 ± 6	-

[Modified from: Bylund et al., 1994]

canal of the spinal cord (Stone et al., 1997). All known α_2-AR bind both noradrenaline and adrenaline with similar affinity across all subtypes, which can be blocked by antagonists such as yohimbine and rauwolscine ($K_B < 40$ nM) (see Table 3-4) (Bylund et al., 1994). Both α_{2A}-AR and α_{2C}-AR have been identified in the spinal cord of the mice. Radiolabelling shows that both subtypes are widely distributed throughout the spinal cord (and brain) but are more prevalent in α_{2A}-AR and that α_{2C}-AR expression is low, with the exception in the superficial dorsal horn (laminae I-II) as well as the in central canal (lamina X) where α_{2C}-AR is indicated to be strongly expressed. β_2-AR has been observed to be highly expressed in the superficial dorsal horn. In particular, β_2-AR are most densely expressed in lamina I and II. Moderate expression of β_2-AR has been identified in the ventral horn as well as around the central canal (Mizukami, 2004).

1.4.3 Signalling mechanisms and pharmacology of adrenoceptors

As mentioned above, noradrenaline exerts its effect by binding to adrenergic receptors that are coupled to different G-proteins. The β-adrenergic receptor is coupled to a stimulatory G-protein (G_s), and when activated it stimulates the conversion of ATP to cyclic AMP (cAMP) by activating adenylyl cyclase. Activation of β-adrenergic receptors by application of the specific β-AR agonist isoproterenol will activate β_1 and β_2 in cultured mouse astrocytes. However, pharmacological studies have shown that β_1AR has a much higher affinity for isoproterenol and can be activated at very "low" concentration, in the nanomolar range (~ 100nM), while β_2 activation of usually requires micromolar concentrations of isoproterenol (Du et al., 2010). Therefore, isoproterenol can be a tool for differentiating between β_1 and β_2 signalling pathways. Application of 100 nM of isoproterenol to cultured mouse astrocytes leads to activation of β-arrestin-2 (through β_2-AR) which in turn activates Src, a cytoplasmic tyrosine kinase. Src activates pathways that stimulate phosphorylation of $ERK_{1/2}$ as well as directly phosphorylates EGF-receptors. However, "high" concentration of isoproterenol (>1μM) activates the β_1-AR which promotes the conversion of ATP to cAMP which in turn activates protein kinase A (PKA). Intriguingly, it has been observed in cultured astrocytes, that the increase in PKA activation, induced by β_1AR stimulation, leads to a "G_s/G_i switch" followed by an increase in $[Ca^{2+}]_i$ that is released from intracellular stores. For a more detailed description please see Daaka et al. 1997 (Baillie et al., 2003; Daaka et al., 1997; Du et al., 2010).

The α1 adrenergic receptors are associated with Gq heterotrimeric G-proteins and upon agonist binding, they activate phospholipase C (PLC) that in turn converts the lipid phosphatidylinositol into both inositol triphosphate (IP_3) and diacylglycerol (DAG). IP_3 can diffuse in the cytoplasm to the endoplasmic reticulum where it acts as an agonist of the IP_3-receptor, that when stimulated, causes a release of Ca^{2+} from intracellular stores and a subsequent increase in $[Ca^{2+}]_i$ (Graham et al., 1996). For a more detailed description of α_1-AR pharmacology and signalling pathways please see the extensive review from Graham and colleagues, 1996 (Graham et al., 1996).

α_2-AR are coupled to an inhibitory G-proteins (Go/i) and works an in opposite to the Gs-proteins. Upon ligand binding and Gi - activation the G-proteins α-subunit associate with adenylyl cyclase which leads to an inactivation of adenylyl cyclase and consequently a decrease in the production of cAMP. Decreased intracellular cAMP levels lead to a lower level of protein kinase A activation and all the following downstream events described above. Unexpectedly, it has been observed that the α_2-AR agonist dexmedetomidine induces an increase in free cytoplasmic calcium. Interestingly, this only applies to astrocytes but not to neurons. This effect is unlikely to be attributed to a cross-activation of the α_1-AR since dexmedetomidine has an α2/α1 selectivity ratio of 1600:1, so at low concentrations of dexmedetomidine, virtually no α1-AR will be activated (Chen et al., 2000). Additionally, the increase in $[Ca^{2+}]_i$ induced by nanomolar levels of dexmedetomidine is abolished by the α_2-AR antagonists yohimbine and rauwolscine. Pre-treatment of astrocytes with pertussis-toxin also abolished the $[Ca^{2+}]_i$ increased, strongly suggesting that it is an α2-AR – Go/i based mechanism (Chen et al., 2000; Enkvist et al., 1996).

1.4.4 Origin of noradrenaline in the central nervous system

In the central nervous system, the noradrenergic neurons have their cell bodies confined to small nuclei termed A1 to A7 situated in the brainstem. Although few in number the noradrenaline-positive (noradrenaline+) neurons send projections to virtually all major parts of the central nervous system (Fuxe et al., 2015). Among the noradrenergic neurons, the A6 nucleus, termed Locus Coeruleus (LC), is by far the most important source of noradrenaline both for the brain and for the spinal cord, see Fig. 4. The LC is situated in the posterior part of the rostral pons in the brainstem in the lateral floor of the fourth ventricle (Llorca-Torralba et al., 2016). The LC has approximately 1500 neurons in which two types of noradrenergic neurons have been observed, the

smaller (~ 20 µm) fusiform neurons and the larger (~ 35 µm) multipolar neurons (Grzanna and Molliver, 1980). Both the fusiform and the multipolar cells can be observed throughout the Locus Coeruleus but are however not equally distributed along the dorso-ventral axis. The fusiform cells are mostly found in the dorsal part of the LC whereas the multipolar cells are predominant in the ventral LC (Grzanna and Molliver, 1980; Swanson, 1976).

1.4.5 *Locus Coeruleus* projections and cytoarchitecture

It has previously been shown through radioisotope ([3H]-proline) injection directly into the LC that it has dense projections to the forebrain, cerebellum, brainstem, and the spinal cord (Fig. 4) (Pickel et al., 1974). The noradrenaline+ neurons projecting to the hippocampus, the septum and other forebrain regions are generally located in the dorsal LC while most of the afferents projecting to the cerebellum and the spinal cord, including the dorsal horn, have their soma situated in the more ventral regions (Loughlin et al., 1986; Mason and Fibiger, 1979; Schwarz et al., 2015). Interestingly, the LC receives nociceptive input directly from the dorsal horn of the spinal cord (and the trigeminal nucleus),. The LC represents a major subcortical structure that participates in the pain modulatory system (Fig. 3) (Craig, 1992).

1.4.6 *Locus Coeruleus*, noradrenaline and the modulation of acute and chronic pain

Today there is abundant evidence showing the involvement of spinally released noradrenaline in the modulation of nociception and pain. Most focus has been on manipulating the LC in different acute or chronic pain models while measuring the behavioural outcome (nocifensive behaviour). Interestingly, it has been difficult to come to a single conclusion since many laboratories have provided opposing results during similar experiments (see Table 5 and 6, also for references). However, in bilateral LC lesion experiments independently of lesion protocol used, it appears that nociceptive heat thresholds, measured tail-flick experiments, were not unchanged (Jasmin et al., 2003; Kudo et al., 2010; Ossipov et al., 1985; Sawynok and Reid, 1986; Tsuruoka et al., 2011). Interestingly, bilateral changes are frequently detected after unilateral pain stimulus exposure. For example, after acute painful stimulation of the right pulp of the tooth, c-Fos expression increased in the ipsi- and contra-lateral LC (Voisin et al., 2005). Similarly, in an inflammatory pain situation produced by unilateral paw injection of carrageenan, a bilateral increase of c-Fos could be observed in the LC (Tsuruoka et al., 2003). Furthermore, a substantial decrease in the expression of pERK1/2 has been observed bilaterally in neurons of the LC in an animal model of chronic constriction injury (unilateral) model of neuropathy (Borges et al., 2013).

Table 5. Behavioral effect on pain threshold after bilateral *Locus Coeruleus* lesions.

Model of Pain	Side of the injury/ Measurement	Effect on pain Threshold	References
Acute pain			
Cold-plate	Hindpaw (both)	=	Jasmin et al., 2003
Hot plate	Hindpaw (both)	=	Jasmin et al., 2003
Carregeenan	Hindpaw (left)	↓	Maeda et al., 2009
Hot plate	Hindpaw (both)	=	Ossipov et al., 1985
Stimulation	Hindpaw	↑	Sasa et al., 1977
Flinch-jump	Hindpaw (both)	↑	Bodnar et al., 1978
Formalin	Hindpaw (right)	↑	Martin et al., 1999 Taylor et al., 2000
Carregeenan	Hindpaw (left)	↓	Tsuruoka et al., 2004
Carregeenan	Hindpaw (left)	↓	Tsuruoka and Willis, 1996b
Carregeenan	Hindpaw (left)	↓	Tsuruoka and Willis, 1996a
Paw pressure	Hindpaw (both)	↓	Fukui et al., 2004
Paw pressure	Hindpaw (both)	=	Fukui et al., 2004
Hot plate	Hindpaw	↓	Kudo et al., 2010
Hot plate	Hindpaw	↓	Kudo et al., 2011
Chronic pain			
SNI (2 W)	Spared nerve (left)	↑	Brightwell and Taylor, 2009
SNL (2 W)	L5 spinal nerve	↓	Jasmin et al., 2003
SNL (2 W)	L5 spinal nerve	=	Jasmin et al., 2003
SNL (1-2 W)	L5 and L6 spinal nerve (right)	↓	Hayashida et al., 2012

Abbreviations: SNI, spared nerve injury; SNL, spinal nerve ligation; W, week. [Modified from: Llorca-Torralba et al., 2016].

Table 6. Behavioural effect of electrical and optogenetic activation of LC.

Model of pain	Side of the injury/ measurement	Type and side of the manipulation	Effect on pain threshold	References
Heat stimulation (1)	Skin	Electrical stimulation (side lesioned)*	↑	Hodge et al., 1983
Tail flick (1)	Tail	Electrical stimulation (left and right)*	↑	Janss and Gebhart, 1988
Tail flick (1)	Tail	Electrical stimulation (left)*	↑	Jones and Gebhart, 1986
Heat stimulation (1)	Hindpaw (left)	Electrical stimulation (left)*	↑	Jones and Gebhart, 1988
Stimulation (1)	Hindpaw (left)	Electrical stimulation (left)*	↑	Liu and Zhao, 1992
Heat stimulation (1)*	Left hindpaw	Electrical stimulation (left)*	↑	Viisanen and Pertovaara, 2007
Heat stimulation (1)	Hindpaw (left)	Optoactivation (left or both)*	↑ (v.n.)/↓ (d.n)	Hickey et al., 2014
Tail flick (1)	Tail	Electrical stimulation (left and right)**	↑	Janss and Gebhart, 1988
Rhizotomy (1)	Skin	Electrical stimulation (side lesioned)*	↑/↓	Hodge et al., 1983
SNL (1-2 W) (2)	L5-L6 spinal nerve (left)	Electrical stimulation (left)*	↑	Viisanen and Pertovaara, 2007

Abbreviations: d.n, dorsal neurons, LC, Locus Coeruleus; SNL, spinal nerve ligation; v.n, ventral neurons; W, week; (1) Acute pain model; (2) Chronic pain models. * indicate bilateral manipulation of LC and unilateral manipulation of LC. [Modified from: Llorca-Torralba et al., 2016].

Most data from animal studies (mostly rodents) indicate that neurons in LC are not involved in the setting of the basal nociceptive thresholds. However, in cases when a more persistent injury appears (such as in acute inflammatory conditions – like during carrageenan injections), then the descending noradrenergic control system appears to be recruited to increase the nociceptive/pain thresholds (Llorca-Torralba et al., 2016). Moreover, electrical stimulations of the LC induce analgesia. More recent approaches using optogenetics, suggest that specific populations of the LC (dorsal vs ventral) are associated with either antinociceptive or pronociceptive functions and this dual role of LC activation on nociception will most likely be clarified in the near future (Llorca-Torralba et al., 2016).

As mentioned in Section 1.2, it is clear that during chronic pain conditions neuroplastic changes occur within the nervous system, including in the spinal cord and its noradrenergic innervation, which will trigger a change in the efficacy of the analgesia provided by the LC. A general idea would therefore be that in the earlier processes of pain, the descending noradrenergic-Locus Coeruleus system works as a part of an inhibitory control system, but as the pain persists over time, and more plastic changes occur, the inhibitory role of the descending LC fibres loses or reduces its analgesic properties (Llorca-Torralba et al., 2016).

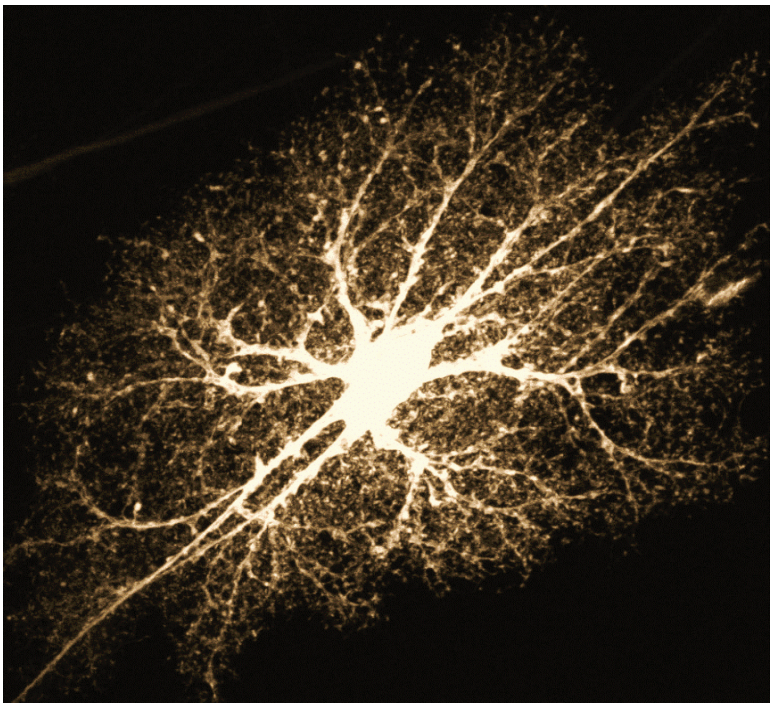

Figure 7. **Confocal image of a lucifer yellow-filled astrocyte.** Hippocampal (CA1)-tissue taken from 4 week old Sprague Dawley rat. Cell soma approx. 7–11µm. [Image modified from: Bushong et al., 2004].

1.5 Glial cells and Ca^{2+} -signalling

1.5.1 Glial cells in the central nervous system

Glial cells are non-neuronal cells in the nervous system that support neuronal activity. Although it has been hard to estimate the exact number of glial cells in the nervous system it is widely accepted that they most likely outnumber the neurons (Ji et al., 2006; von Bartheld et al., 2016). Historically, the role of glial cells has been largely unappreciated, and their importance neglected (Khakh and Sofroniew, 2015). However, the last decade of research has provided accumulating evidence that the glial cell network has a wide capacity and can with a high temporal and spatial precision release transmitters, called gliotransmitters. It, therefore, appears that glial cells can work together with neurons to ensure a proper brain and spinal cord function (Bazargani and Attwell, 2016). Glial cells can be categorized into at least 3 groups; Astrocytes, the most common and functionally diverse glial cells; microglia, classically known as the innate immune system of the central nervous system; and oligodendrocytes, primarily responsible for creating the myelin sheath around axons of neurons in the CNS (Peferoen et al., 2014).

Below, I will mainly centre this introductory section on astrocytes since these cells have been the main focus of my research work. For a more detailed and expanded view on glial cells including microglia and oligodendrocytes the reader is referred to the following reviews (Nayak et al., 2014; Philips and Rothstein, 2017; Simons and Nave, 2016; Wolf et al., 2017).

1.5.2 Astrocytes

Astrocytes constitute a relatively heterogeneous population of cells with different receptor profiles, levels of ion channel expression as well as morphological differences. In general, astrocytes are characterized by their star-like shape with large processes extending out from the cell body that branch out into very thin processes, see Fig. 7. Another very distinctive feature of a certain astrocytic population (discussed further below) is their endfeet which interact with the vascular capillaries of the central nervous system to create the outer layer of the blood-brain barrier (Oberheim et al., 2006; Ventura and Harris, 1999; Wilkin et al., 1990).

Astrocytes originate from the neuro-epithelial stem cells (which also give rise to neurons) and are probably the most common cell type in the central nervous system. Although the ratio of astrocytes to neurons might have

previously been slightly overestimated, more recent research has estimated that of astrocytes represent 20-40% of the cells in the central nervous system (Aldskogius and Kozlova, 1998; Herculano-Houzel, 2014; Khakh and Sofroniew, 2015). Astrocytes are implicated in most aspects of neuronal functioning, including extracellular ion homeostasis, transmitter reuptake, release of transmitters, metabolism, regulation of the integrity of blood-brain barrier, modulation of synaptic strength and control metabolic homeostasis, see Fig. 8 (Butt, 2011; Kimelberg, 2010; Svensson and Brodin, 2010). Three-dimensional reconstruction of astrocytes shows that astrocytic processes are tightly connected with several neuronal compartments including neuronal cell bodies, dendritic spines as well as synapses (Halassa et al., 2007). This morphological diversity among astrocytes can partially be explained by the fact that they express a broad range of receptors and consequently, they respond to a wide range of neurotransmitters and release gliotransmitters and a variety of neuromodulators, for instance, different cytokines (and chemokines) and growth factors, see Fig. 8 (Coco et al., 2003; Lee and Haydon, 2011; Mothet et al., 2005; Parpura et al., 1994).

In the case of a tissue/nerve damage, the associated astrocytes will transform and shift into an activated/reactive state which is morphologically characterized by an increase in cell size and particularly by an increased expression of the glial fibrillary acidic protein (GFAP) (Garrison et al., 1991; Svensson and Brodin, 2010; Watkins et al., 2001). GFAP is the most commonly used histological marker for identifying astrocytes, however as mentioned above, many astrocytes do not present a high amount of GFAP before they switch to an activated state. This is important to consider when trying to detect the presence of astrocytes in an experiment (Xu, 2018). Activated astrocytes are thought to have a significant role in nociceptive signaling and abnormal pain perception and thus the development of chronic pain (Gao and Ji, 2010b; Ren and Dubner, 2008). Activated astrocytes have been identified in most chronic pain models, including inflammatory and neuropathic pain, (for details, see Gao, 2010 and Ma, 2002 (Gao and Ji, 2010a; Gao and Ji, 2010b; Ma and Quirion, 2002). Also, after peripheral injury, the increase of GFAP in the dorsal horn has been shown to correlate with the level of measured hyperalgesia in rodents (Garrison et al., 1991).

Interestingly, in some instances in the dorsal horn of rodents, it has been reported that activated astrocytes can be found not only on the ipsilateral side but also on the contralateral side to the injury in the dorsal horn of the spinal cord (Choi et al., 2015). However, the mechanisms involved in the activation of astrocytes in the dorsal horn contralateral to the side of the injury remain to be established.

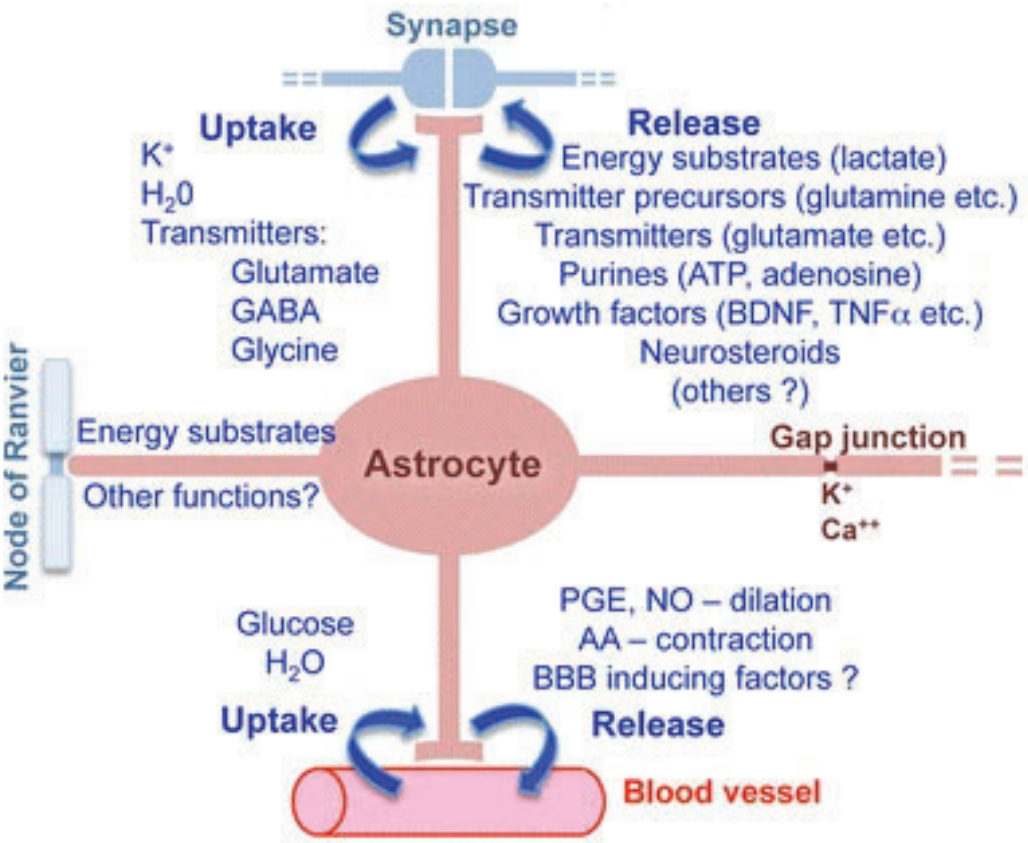

Figure 8. **Schematic representation of the multifaceted role of astrocytes in CNS**. Astrocytes are involved in regulation of the extracellular environment by release and uptake of gliotransmitters, cytokines, small ions, vaso-regulatory substances among others. By keeping intimate contact with the vasculature as well as synaptic and non-synaptic neuronal regions, astrocyte can direct energy substrates to various regions of the CNS depending on the metabolic demand. [Modified from: Sofroniew and Vinters, 2010]

Based on morphology and their location, astrocytes have been divided into two different classes: protoplasmic astrocytes and fibrous astrocytes, see Fig.9 (H Miller and C Raff, 1984). Protoplasmic astrocytes, in rodents, are most commonly found throughout the grey matter in the central nervous system, they can be identified by their vastly branched and "bushy" processes. Their processes are short (2-10 μm) and thin (100-200 nm) (Bushong et al., 2004; Liu et al., 2012). The protoplasmic astrocytes display endfeet that enwrap the vasculature to form a glial membrane that covers the blood vessels and thereby create the innermost layer of the blood-brain barrier (BBB). In addition to the role in the BBB, protoplasmic astrocytes simultaneously display close associations with neuronal synapses, which position them ideally to modulate and sense neuronal activity while bridging the energy supplying vasculature with the neurons. Astrocytes can, therefore, regulate local blood flow according to the synaptic activity and energy demand and thus ensure enough energy supply, in a given microdomain, to promote proper neuronal functioning (Simard et al., 2003; Takano et al., 2005). In mice, a single protoplasmic astrocyte is associated with around 100 000 synapses from 4-8 neurons, and those synapses can be regulated simultaneously by a single protoplasmic astrocyte (Bushong et al., 2002; Halassa et al., 2007). In opposition to the protoplasmic astrocytes, the fibrous astrocytes are located in the white matter and display long and straight processes. They contain a higher level of GFAP than the protoplasmic astrocytes and they also interact with local blood vessels, see Fig.9 (Oberheim et al., 2009). However not much is known about the fibrous astrocytes. A subpopulation of those astrocytes uses their endfeet to form an outer glial “membrane”, located slightly below the pia mater, that works in concert with the BBB to ensure structural support and metabolic control of neuronal tissue respectively.

Interestingly, the ratio between neurons and astrocytes differs among species; for example, in worms, the ratio is, 6:1 meaning that there are 6 neurons for each astrocyte, however, in rodents, this number is 3:1 while in humans 1:1.4 meaning that for each neuron, human has 1.4 astrocytes (Nedergaard et al., 2003). In this context, it, therefore, appears that the relative proportion of astrocytes to neuron increased through evolution. However, it is not only the number of astrocytes that increases but there is also a change their morphology and size. In addition to an increased soma size, human protoplasmic astrocytes display about 10 times more primary processes, compared to rodents, that extend out from the cell body, and create an exceptionally complex arborization network with a volume 16 times larger than in rat, and together cover ~ 2 000 000 synaptic contacts (compared to 20 000 – 120 000 in rodents) (Bushong et al., 2002; Oberheim et al., 2009). Similarly, the fibrous

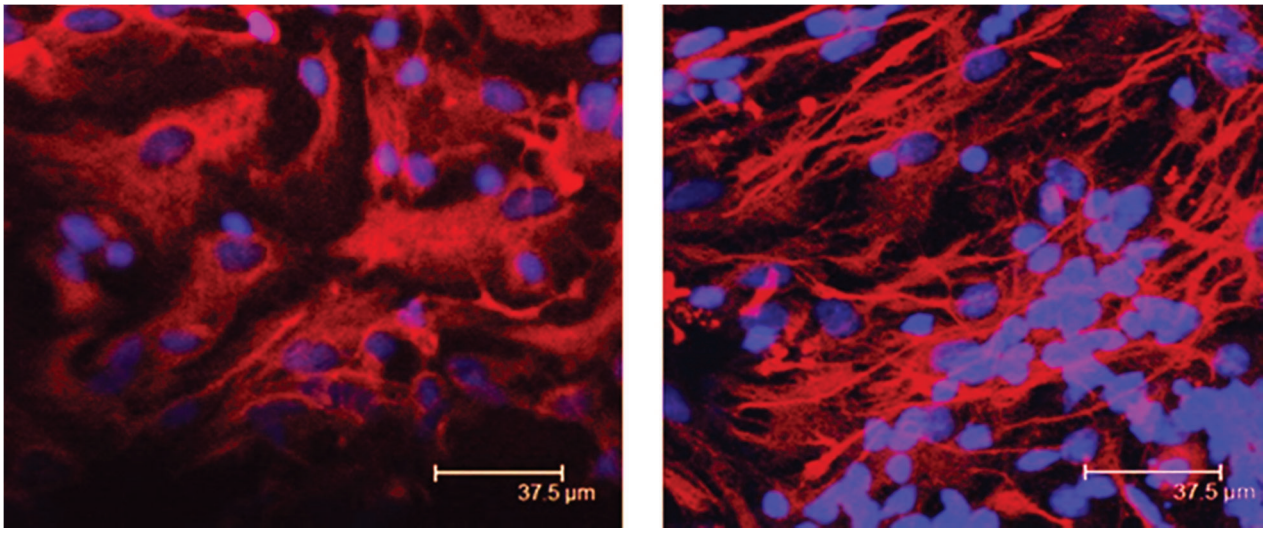

Figure 9. Morphological difference between protoplasmic and fibrous astrocytes. Cultured astrocytes visualized by immunocytochemical staining. Left: image of purified protoplasmic astrocytes. Right: image of purified fibrous astrocytes in culture. Red indicates labeling of the astrocyte specific marker GFAP. Blue indicates DAPI labeled cell nuclei (bar = 37.5 µm). [Modified from: Liu et al., 2012].

astrocytes situated in the white matter are also about 2 -3 times larger in humans than in rodents (Verkhratsky and Nedergaard, 2018).

Taken together, these data suggest that memory and cognitive capabilities appear to be correlated with the increased informational processing that involves astrocytes. This was investigated in an elegant study by M. Nedergaard's group in 2013 by grafting human glial progenitor cells into the brain of newborn mice (P1) (Han et al., 2013a). The cells integrated well into the mice's brains during development and expanded and replaced many of the mouse glial cells. Electrophysiological recordings in the hippocampus showed that animals that had received human grafts displayed a lower threshold for initiation of long-term potentiation (LTP) compared to sham animals. Interestingly, those mice showed an augmented memory as well as an increased ability to learn to perform cognitive tasks (Han et al., 2013a; Windrem et al., 2014).

This highlights the importance of astrocytes for developing a cognitive performance that is characteristic of higher species and especially humans. Indeed, this emphasizes the need to revise the old neuron-centric view where glial cells were merely considered to be the only structural and metabolic support to facilitate neuronal function. Instead, the neuronal- and the astrocytic-networks should be viewed as two entities that process information in parallel but have strong functional interactions. It should therefore be clear that both astrocytic and neuronal information processing is vital for a well-functioning nervous system and there is an obvious need to catch up and try to understand the molecular mechanisms involved in astrocytic signaling.

1.5.3 Intracellular signaling in astrocytes

Calcium has proven to be one of the most important ions for intracellular signaling in astrocytes, and, as described below, many astrocytic functions are partially or completely dependent on variations in free intracellular calcium concentration $[Ca^{2+}]_i$. Several mechanisms modulating the intracellular calcium dynamics in astrocytes have been described (see below).

1.5.3 Amplification of calcium signals

The most well-studied and understood way to stimulate an increased $[Ca^{2+}]_i$ in astrocyte is through the activation of G-protein coupled membrane receptors with an extracellular ligand that targets the PLC-IP_3 pathway to release calcium from intracellular stores (mostly endoplasmic reticulum). Increases in cytosolic calcium through IP_3 and IP_3-receptors naturally reduce calcium concentrations in calcium storage compartments such as the

endoplasmic reticulum (ER). Reduction of [Ca^{2+}] in the ER can activate pathways that allow extracellular calcium to enter the cytoplasm. Extracellular calcium influx due to emptying calcium storage compartments has been termed store-operated calcium entry (SOCE) which is mediated via calcium-release activated calcium channels (CRAC). However, at physiological agonist-concentrations, it is unlikely that enough calcium is released from the intracellular calcium storage compartments to fully activate the SOCE through CRAC channels - especially in cells with a high level of calcium storage compartments. This is because SOCE requires a rather profound and sustained depletion of the internal calcium stores (see Section 1.5.4.1) (Fierro and Parekh, 2000; Parekh et al., 1997). Therefore, in addition to SOCE, a non-store operated calcium entry pathway has been identified which relies on the arachidonic acid-regulated Ca^{2+} (ARC) channels. Although not identical, ARC channels display biophysical properties that closely resemble those of CRAC channels but their mechanism of activation is independent of Ca^{2+}-store depletion, (see Section 1.5.4.2) (Shuttleworth et al., 2007).

1.5.3.1 Store-operated calcium entry in astrocytes

The first SOC calcium current was identified in 1992 by Hoth and Penner who termed it I_CRAC, calcium release-activated calcium current (Hoth and Penner, 1992). Since then, the search for identifying specific CRAC channels and their associated signaling pathways has been extensive and is still under active investigation. The CRAC-channel architecture differs significantly from other ion channels and displays high selectivity for calcium as a permeant ion (Hou et al., 2012).

Using siRNA (small interfering-RNA) techniques, it was shown that the calcium-binding protein STIM1 (stromal interaction molecule 1) functions as calcium sensor at the endoplasmic reticulum (Trebak and Putney, 2017). STIM1 serves as the main intracellular CRAC regulator through its ability to sense calcium levels inside the endoplasmic reticulum (and other calcium storing organelles). When the concentration of calcium in the endoplasmic reticulum becomes low, the STIM1 proteins aggregate and interact with calcium release-activated calcium modulator 1 (Orai1) proteins on the plasma membrane to enable calcium influx, see Fig. 10 (Feske, 2010). The membrane channel protein Orai together with STIM protein function as obligatory elements for SOCE, see Fig. 11-12 (Putney et al., 2017). This has been confirmed in many laboratories by inducing and amplifying store-operated calcium entry and CRAC currents through co-transfection of STIM1 and Orai proteins (Putney et al., 2017; Vig et al., 2006; Zhang and De Koninck, 2006). Orai proteins (in humans Orai1

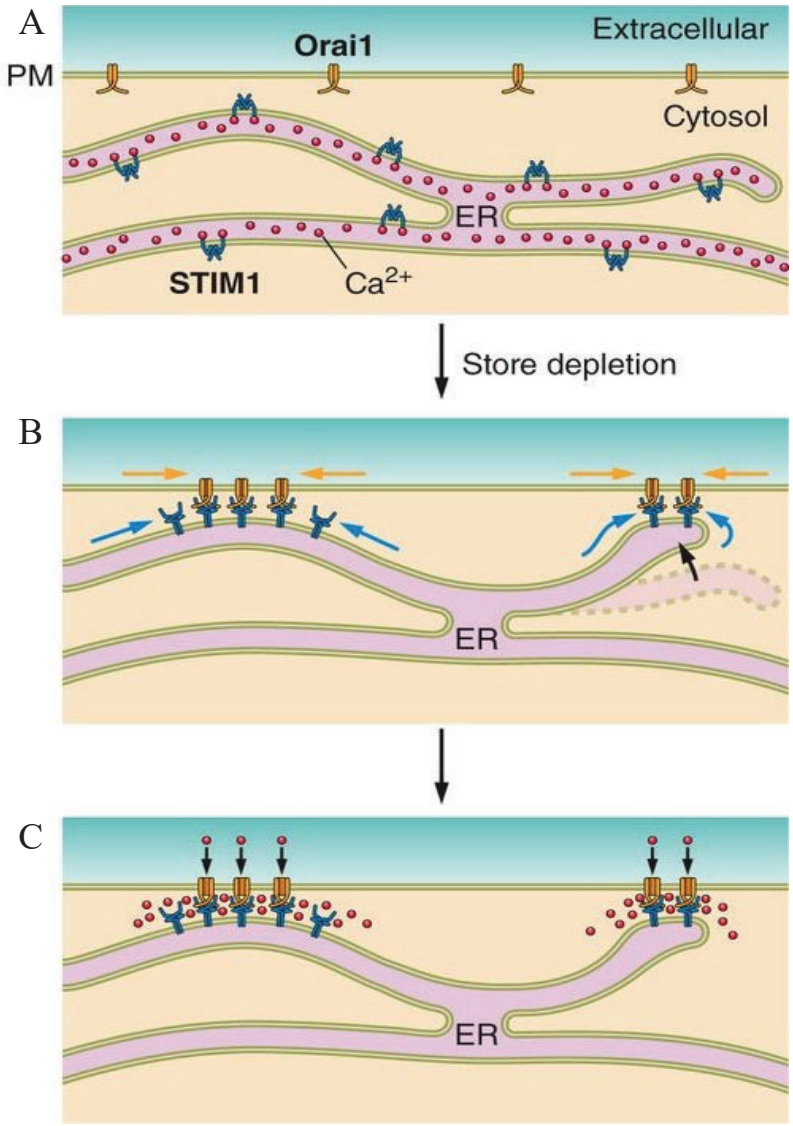

Figure 10. **Schematic illustration of the events leading from calcium-store depletion to clustering of STIM1 and Orai1**. A) When calcium-stores are full Orai1 proteins are distributed on the plasma membrane and STIM1 proteins are located on the endoplasmic reticulum. B) During calcium-store depletion, STIM1 senses a decrease in $[Ca^{2+}]_{ER}$ and induces translocation of STIM1 towards the plasma membrane. C) At the plasma membrane STIM1 proteins form complexes with Orai1 which activate the CRAC channels and allow calcium entry through the CRAC channel into the cytoplasm. [Modified from: Prakriya and Lewis, 2015].

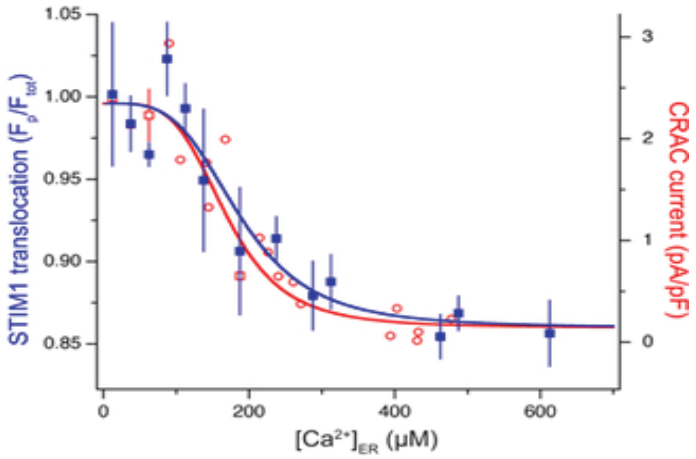

Figure11. **Relationship between calcium concentration in the endoplasmic reticulum ($[Ca^{2+}]_{ER}$) and translocation of STIM1 to the cell membrane, and $[Ca^{2+}]_{ER}$ and density of CRAC currents**. Blue curve illustrates the measured ratio (F_p/F_{tot}) of labeled STIM1 at the periphery to the total STIM1 in the cell, and CRAC channel current density is illustraded in red. Both (F_p/F_{tot}) and I_{CRAC} show a strong dependence on $[Ca^{2+}]_{ER}$. [Modified from: Lewis,

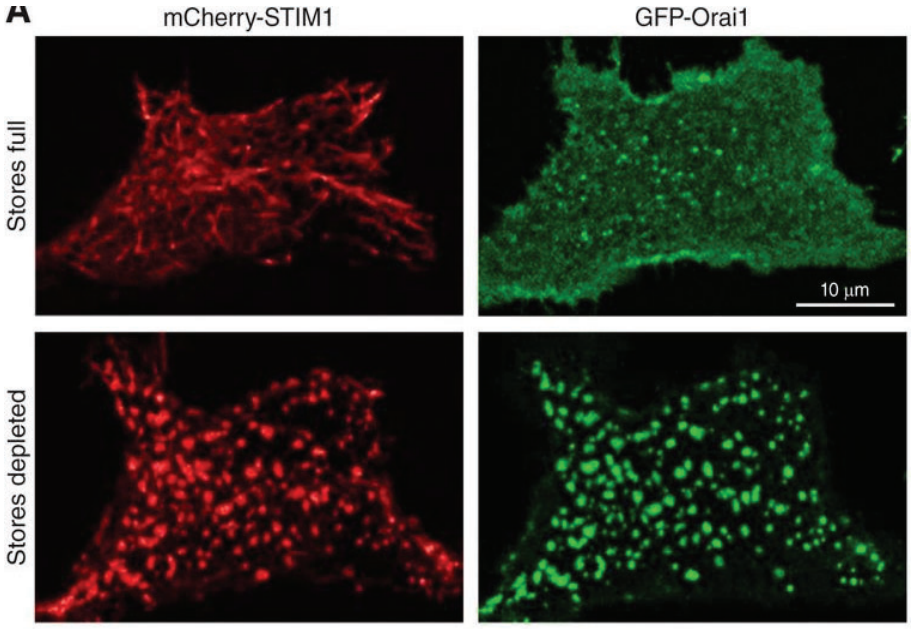

Figure 12. **STIM1 and Orai1 aggregation at the plasma membrane junction to form the basic unit of SOCE**. During full $[Ca^{2+}]_{ER}$, STIM1(red) and Orai1(green) are distributed relatively uniformly over ER and the plasma membrane, respectively (top figures). A few minutes after store depletion with tapsigargin, both proteins have redistributed and translocated to accumulate at the cell surface. This situation is visualized as co-localized in puncta at the cell surface in confocal microscopy images (bottom figures) [Modified from: Prakriya and Lewis, 2015].

and Orai2) form the pore of the CRAC channel and thereby act as a structural core component of the calcium release-activated calcium channel (Hou et al., 2012). The calcium channel is composed of a hexameric assembly of Orai subunits that are positioned around a central pore that crosses the plasma membrane and stretches into the cytoplasm of the cell (Hou et al., 2012).

As mentioned above, when the level of calcium in the endoplasmic reticulum approaches a lower limit, STIM1 proteins accumulate and move to interact with Orai1 located in the plasma membrane (Feske, 2010). On the contrary, when calcium level in the endoplasmic reticulum is high, the store-operated calcium entry-associated regulatory factor proteins SARAF (also called TMEM66) contacts STIM1 to inactivate the store-operated calcium channel. SARAF reduces or stops the activity of the store-operated calcium entry machinery to prevent excess calcium refilling in the cell (Palty et al., 2012). Multiple gene splice-forms of Orai and STIM have been identified. It appears that STIM1 and Orai1 are the most crucial subtypes for SOCE since mice lacking STIM1 and Orai1 do not show any sign of store-operated calcium influx. Humans born with malfunctioning Orai1/STIM proteins suffer from reoccurring and in many cases fatal infections as well as autoimmunity due to severe immunodeficiency (Lacruz and Feske, 2015).

1.5.3.2 Non-store-operated calcium entry in astrocytes

As described above, the role of CRAC channels and other types of similar store-dependent channels (SOCs) have been extensively studied compared to channels involved in calcium-independent calcium entry. Calcium entry via SOCs determines the level of sustained elevation of cytoplasmic calcium following stimulation with moderately high agonist concentrations (Fierro and Parekh, 2000; Parekh et al., 1997). Although the precise extent of endoplasmic reticulum calcium depletion required to induce a global activation of store-operated calcium channels in cells is still not well defined, it is agreed that it is a slow process that generally requires tens of seconds following a reduction/depletion of endoplasmic [Ca^{2+}] (Zweifach and Lewis, 1993). As mentioned in Section 1.5.4.2, an alternative mechanism to the store-operated calcium entry through CRAC channels has been identified. In the mid-'90s, Shuttleworth suggested that, under conditions with low concentrations of agonists and little receptor activity, when the endoplasmic reticulum calcium levels might not be substantially reduced, a second pathway, that is calcium store-independent is stimulated as a result of the production of arachidonic acid (Shuttleworth, 1996).

The identified arachidonic acid-regulated Ca2+ (ARC) channels demonstrate biophysical properties that closely resemble CRAC channels, but in contrast to the CRAC channels, calcium entry via ARC channels is particularly active at low agonist concentrations (Martin and Shuttleworth, 1994). Although ARCs share many similarities with SOCE, deeper pharmacological investigations show that they are two completely separate, but coexisting, entities. This has been shown by the observation that ARC currents (IARC) are not affected by the levels of calcium in the endoplasmic reticulum, which has been shown by emptying of calcium storing compartments (e.g. pre-treatment with thapsigargin) and that ARC and CRAC currents are additive in the same cell (Mignen and Shuttleworth, 2000). In similarity with the CRAC channels, the ARC channels are also structurally build-up of clustered Orai-proteins. However, electrophysiological studies in cells expressing different ratios of Oria1/Orai3 show that while the CRAC are homomeric structures build from four identical Orai-subunits the ARC channels are heteropentameric structures formed by assembling three Orai1 subunits with two Orai3 subunits, see Fig. 13 (Feske et al., 2006; Vig et al., 2006).

1.5.4 Intercellular Ca^{2+} -signaling through the astrocytic network and its modulation by ATP

Astrocytes have the capacity of interconnecting themselves to other nearby astrocytes and form large astrocytic networks that stretch and cover all parts of the brain and the spinal cord. The construction of astrocytic networks is achieved in part owing to the presence of membrane-anchored protein structures termed gap-junctions. Gap-junctions are formed through linking 2 connexons from 2 neighboring cells together. Each connexon is a result from the assembly of six connexin proteins. The connexons can either exist as free membrane hemichannels (half gap-junction channel) or as a part of a gap-junction when associated with a connexon of the neighboring cell. In an open state, the connexon hemichannels allow passage of small molecules and ions such as IP_3 and Ca^{2+} (Giaume et al., 2013). The connexins, therefore, provide a mean for physically and electrically connecting astrocytes by allowing an exchange of small cytoplasmic molecules (less than ~ 1K Dalton) (Yeager and Nicholson, 1996).

One of the key characteristics of astrocytes within the astrocytic networks is that calcium signals can be observed to spread from one cell to the neighboring cells. Therefore, a large fraction of astrocytes can rapidly display an increase in calcium following the stimulation of a single astrocyte. This phenomenon has been termed calcium wave propagation (Charles et al., 1991; Guthrie et al., 1999; Hassinger et al., 1996).

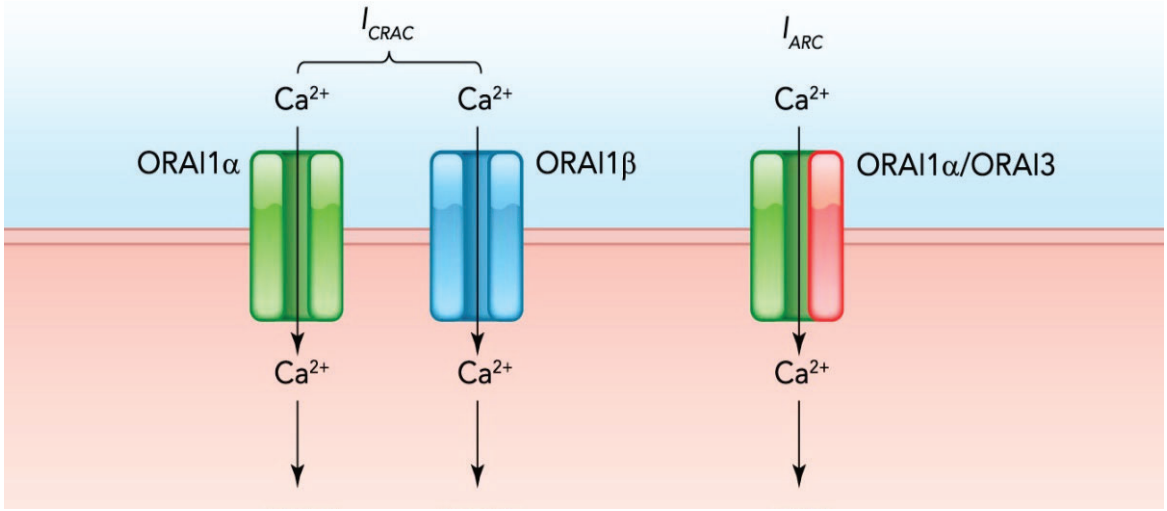

Figure 13. **Differences in subunit composition between CRAC channels and ARC channels**. Calcium release activated calcium (CRAC) channel currents are mediated by homomeric proteins of either Orai1α or Orai1β subunits whereas arachidoncic acid regulated calcium (ARC) channels are heteromeric proteins composed of Orai1α and Orai3 subunits. [Illustration modified from: Trebak and Putney, 2017]

Following stimulation of a single astrocyte, calcium waves can spread through the astrocytic network at the speed of 20 μm s^{-1} and can propagate to involve several hundreds of astrocytes, see Fig. 14 (Khakh and McCarthy, 2015). Some clues concerning the calcium wave propagation mechanisms were deduced from the following observation: Ca^{2+} waves can be terminated by gap-junction inhibitors, IP_3 receptor antagonists, and by blocking refilling of endoplasmic reticulum calcium through calcium ATPase inhibitors (Haydon, 2001; Leybaert et al., 1998). It was therefore plausible to speculate that the propagation of calcium waves was due to the diffusion of IP_3 through gap-junctions which induces a calcium increase through the IP_3 receptor in the neighbouring cells. However, modelling studies have shown that the diffusion of IP_3 alone would not be sufficient to sustain the propagation of calcium waves. This opened up the idea that calcium waves propagate through a mechanism that utilizes an extracellular component and this hypothesis was confirmed in the early '90s where it was shown that, in cultures of astrocytes, the calcium wave can 'jump' between cells spaced up to 120 μm apart (Hassinger et al., 1996) . Additionally, in experimental setups where an extracellular perfusion system was used to perfuse cultured astrocytes, calcium waves were observed to propagate in the same direction as the flow from the perfusion pipet, which further strengthened the hypothesis of the involvement of an extracellular component participating in the propagation of calcium through astrocytic networks (Charles, 1998; Guthrie et al., 1999; Hassinger et al., 1996). The main extracellular element involved in Ca^{2+} wave propagation and regeneration were later identified to be ATP (Haydon and Carmignoto, 2006). Taken together, there is today a generally well-accepted understanding of the mechanisms underlying the calcium waves in astrocytic networks, see Fig. 14. This phenomenon can be summarized as follows:

1. IP_3 induces Ca^{2+} release from the endoplasmic reticulum.
2. Free cytosolic Ca^{2+} induces ATP to be released from the astrocyte into the extracellular environment.
3. Both IP_3 and Ca^{2+} can diffuse to adjacent astrocyte through gap-junctions.
4. Extracellular ATP activates purinergic receptors on the neighbouring astrocyte that activate phospholipase C to generate IP_3 in the neighbouring astrocyte which elevates $[Ca^{2+}]_i$

1.5.5 Modulation of intracellular calcium by noradrenaline in astrocytes

Early studies by McCarty's group showed that noradrenaline induced a transient [Ca2+]i increase in approximately 80% of cerebral type 1 astrocytes (protoplasmic astrocytes)(Section 1.5.2). These calcium transients were characterized by a biphasic response pattern described as an initial sharp rise followed by a smaller sustained elevation that continued in the presence of agonist (Salm and McCarthy, 1990). The removal

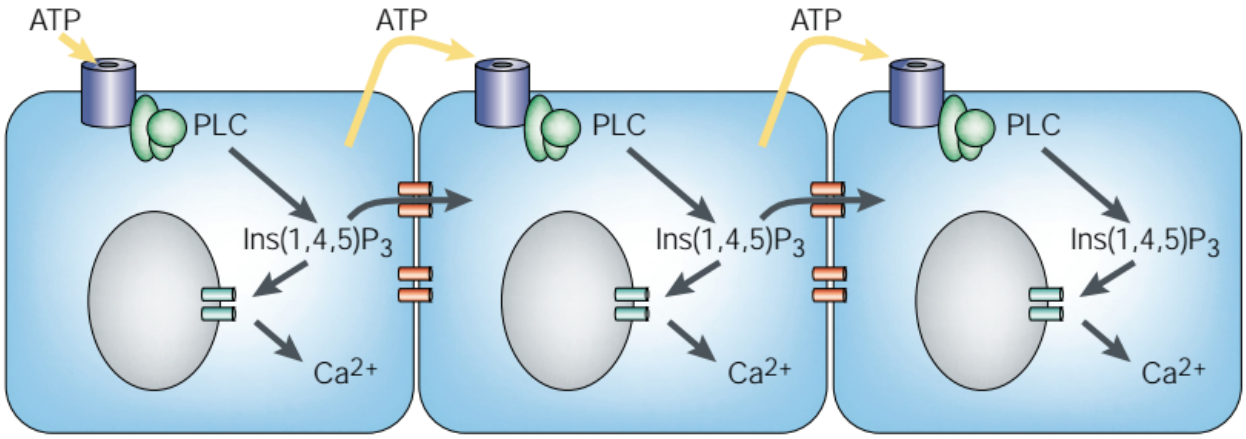

Figure 14. **Proposed mechanism for astrocytic calcium-wave propagation.** IP3 induces intracellular calcium elevation via calcium release from internal calcium storing organelles such as the endoplasmic reticulum. IP3 can diffuse to neighboring cells through gap junctions to cause short-range signaling. Longer-range calcium signaling requires the release of ATP, which causes the regenerative production of IP3 and further release of ATP from neighboring astrocytes. [Modified from: Haydon, 2001].

of extracellular calcium abolished the sustained calcium elevation but did not affect the initial component, implicating that the sharp initial calcium transient was due to Ca^{2+} released from internal calcium stores while the sustained secondary component was caused by Ca^{2+} influx from the extracellular space. Pharmacological work has concluded that, in cell culture, the latency shape of the calcium transients is strongly correlated with the dose. At lower noradrenaline concentrations (<1μM) the response pattern was characterized by long latency a single-phase calcium transit while during higher concentrations, the onset was fast and the response had a biphasic aspect (initial peak followed by a sustained plateau) (Salm and McCarthy, 1990). A more recent study noted that noradrenaline (50μM) induced slightly different calcium response patterns when astrocytes were cultured alone compared to astrocytes co-cultured with neurons. Indeed, astrocytes cultured with neurons displayed more frequently oscillation in $[Ca^{2+}]_i$ following noradrenaline application (Bar El et al., 2018). In fully awaken behaving mice optogenetical stimulation of LC-neurons with simultaneous recording of astrocyte $[Ca^{2+}]_i$ levels with two-photon calcium imaging, confirmed in vivo the initial observation made by the McCarty´s group on cultured astrocyte (Oe et al., 2020). The and physiology consequences of $[Ca^{2+}]_i$ signalling in astrocytes have been described in detail in Section 1.5.3-1.5.5, α_1 adrenergic receptors on astroglia are sensitive to activation by submicromolar concentrations of noradrenaline which trigger an elevation in $[Ca^{2+}]_i$ in the cell body and the processes in slice preparations (Pankratov and Lalo, 2015). The EC_{50} for noradrenaline-induced calcium elevation in cortical astroglia was of 370 nM and 19nM for the α_1-AR specific agonist A61603. Those noradrenaline-induced calcium elevations were blocked by the α_1-AR antagonist terazosin (Pankratov and Lalo, 2015). The α_1-AR, through their coupling and of Gq-proteins and activation of PKC and subsequent generation of IP_3, have a key role in modulating intracellular calcium levels in astrocytes following noradrenaline exposure. In vivo studies in behaving animals consistently show that LC-induced calcium elevations in cortical astrocytes can be significantly inhibited through pharmacological interventions with α_1-AR antagonist (but not by β-AR-antagonist) (Ding et al., 2013; Oe et al., 2020). However, pharmacological application of the β-AR-antagonist propranolol prevented noradrenaline-induced elevation of cAMP in astrocytes, suggesting that noradrenaline also acted on functional Gs-coupled β-AR in vivo (Oe et al., 2020). In addition to increased intracellular levels of calcium and cAMP, noradrenaline simultaneously induced a reduction in $[K^+]_i$ in astrocytes that have been described in detail by Muyderman and colleague (Muyderman et al., 1997).

1.6 Gliotransmission and purinergic signaling

The ability of astrocytes (and other glia) to *directly* modulate neuronal networks has historically been a subject of substantial controversy. However, nowadays, most literature positively supports the idea that astrocytes retain the capacity to release modulatory signals into their extracellular environment. The active release of signaling molecules from astrocytes (and other glial cells) that can modulate the cells in the local environment has been termed gliotransmission, and the extracellular messengers, such as ATP, involved in this type of communication are referred to as gliotransmitters. Since the discovery of gliotransmitters, efforts have been spent to investigate the mechanisms involved in gliotransmitter release and in determining the role of intracellular calcium in the regulation of gliotransmission (Section 1.6.2). Evidence from imaging studies has suggested a model in which an agonist stimulates an astrocytic increase in intracellular free calcium concentration ($[Ca^{2+}]_i$) through the PLC-IP_3 pathway which then propagates to the neighboring astrocytes via gap-junctions and underlies propagating waves of increased $[Ca^{2+}]_i$ (Section1.5.3-1.5.5 and see Fig 11). Moreover, the resulting increase in $[Ca^{2+}]_i$ is likely to induce the release of astrocytic gliotransmitters contained in intracellular vesicles by a mechanism of calcium-dependent exocytosis (Halassa et al., 2007; Khakh and Sofroniew, 2015; Oya et al., 2013).
Due to the advancement in cellular imaging techniques such as total internal reflection fluorescence (TIRF) microscopy, which enables tracking of fluorescent molecules close to the cell membrane, the connection between changes in $[Ca^{2+}]_i$ and vesicular trafficking has been revealed. Gliotransmission involving the release of vesicles will be further described below, in Section 1.6.3 (Bezzi et al., 2004). Although the precise mechanisms of gliotransmission and the release mechanisms of gliotransmitters are not fully understood, the modes of release for the most commonly studied gliotransmitters such as glutamate, glycine, GABA, ATP from astrocytes have been described. Those include release via channels such as hemichannels, transporters, as well as the exocytotic release of intracellular vesicles. These mechanisms operate at different time scales and are regulated by different mechanisms (see Table 7 and see Fig.15).

A major difference between neurotransmission and gliotransmission is the time scale at which transmitter release occurs in these two systems. Neurotransmission is a fast process that occurs in the low millisecond range,

Table 7. Commonly released gliotransmitters: functions and secretory mechanisms.

Substance	Function in CNS	Secretory Mechanism in Astrocyte	References
GLUTAMATE	Agonist for ionotropic glutamate receptors (AMPA, KA, and NMDA) and metabotropic receptors ($mGluR_{1-8}$) in neurons and glia	Exocytosis	Crippa et al., 2006; Hua et al., 2004; Marchaland et al., 2008; Montana et al., 2004; Parpura et al., 1994; Xu et al., 2007; Zhang et al., 2004b
		Connexons	Giaume et al., 2013; Ye et al., 2003
		P2X7-Rs	Duan et al., 2003; Fellin et al., 2006
		Best-1 channels	Woo et al., 2012
		VRAC	Basarsky et al., 1999; Feustel et al., 2004; Kimelberg et al., 1990; Krzan et al., 2003; Takano et al., 2005
ATP	The excitatory effect through ionotropic P2X receptors in neurons and glia. Also serves as an agonist to metabotropic P2Y receptors which sustains and amplify calcium waves. ATP rapidly degrades to adenosine that acts on metabotropic A1 A2A, A2B, and A3 receptors in glia and neurons.	Exocytosis	Florian et al., 2011; Halassa et al., 2009; Liu et al., 2011; Pascual et al., 2005; Vardjan et al., 2014
		Lysosomes	Jaiswal et al., 2002; Li et al., 2008; Zhang et al., 2007
		Connexons	Arcuino et al., 2002; Chever et al., 2014; Cotrina et al., 1998; Kang et al., 2008; Stehberg et al., 2012; Stout et al., 2002; Torres et al., 2012
		Panx-1	Suadicani et al., 2012
		P2X7R	Suadicani et al., 2006
GABA	Agonist of $GABA_A$- and $GABA_B$- receptor. Inhibitory neurotransmitter acting on neurons and on neuroglia.	GAT-1/-3	Héja et al., 2009; Unichenko et al., 2013; Unichenko et al., 2012
		Best-1	Lee et al., 2010
		VRAC	Kozlov et al., 2006
		GlyT1	Hawkins and Olszewski, 1957
Glycine	Coagonist for NMDA receptors and Inhibitory neurotransmitter in the spinal cord.	VRAC	Choe et al., 2012

Abbreviations: A1-3 receptor: Adenosine receptor, AMPA: α-amino-3-hydroxy-5-methyl-4-isoxazolepropionic acid receptor, ATP: Adenosine tri-phosphate, Best-1: Bestrophine 1 (Chloride channel), GAT-1/-3: GABA transporters 1-3 (operating in reverse mode), GlyT1: glycine transporter 1 (operating in reverse mode), KA: Kainate, mGluR: muscarinic glutamate receptors, NMDA: N-methyl-D-aspartate, Panx1: pannexin-1, VRAC: Volume regulated channel. [Data from: Verkhratsky and Nedergaard, 2018].

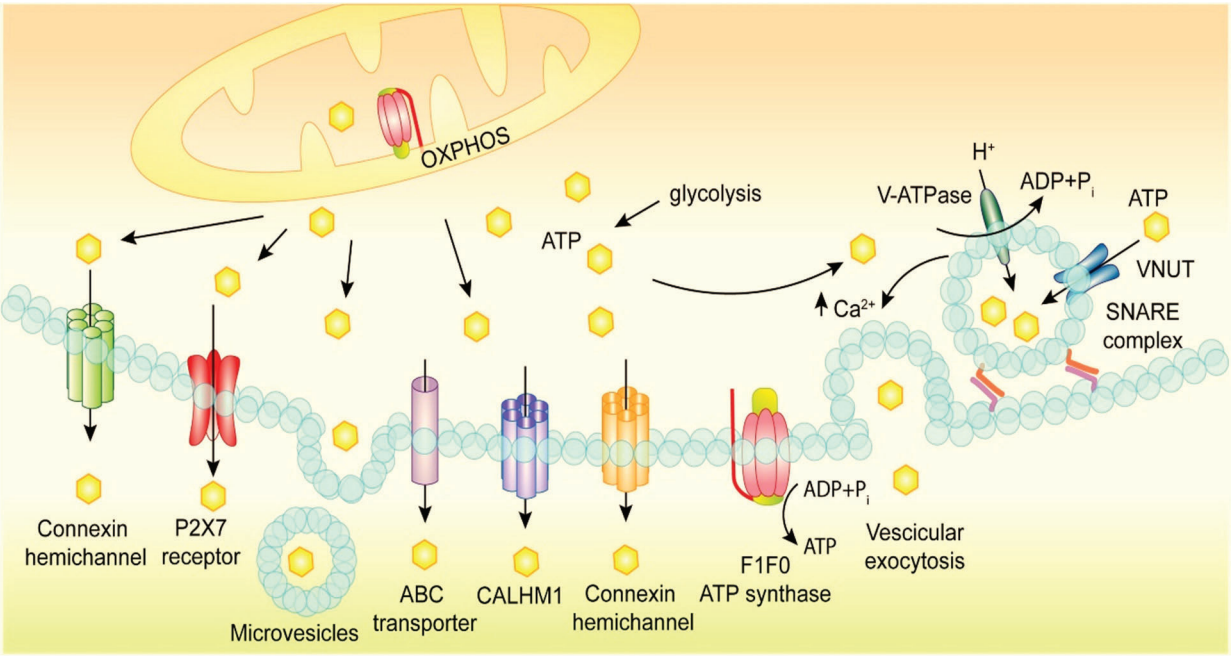

Figure 15. ATP is released through multiple pathways from astrocytes. ATP is produced inside astrocytes, primarily through oxidative phosphorylation in the mitochondria but also through glycolysis in the cytoplasm. Several different ATP release mechanisms have been suggested including receptor channels, transporters and regulated exocytosis by vesicular compartments. To accumulate ATP on the luminal side of the vesicles, astrocytes utilize a vesicular nucleotide transporter that transports ATP into the vesicular compartment by exploiting the proton gradient between the inside of the vesicle and the cytoplasm. It has been speculated that specific ATP binding cassette (ABC) transporters and a plasma membrane F1F0 ATP synthase also contribute to ATP release. [Modified from: Giuliani et al., 2019].

whereas gliotransmission is a much slower process operating in the seconds to minutes range (Table 8) (Araque et al., 2014; Hamilton and Attwell, 2010; Sahlender et al., 2014).

However, a fast gliotransmission mechanism was reported in 2012 by Lee and coworkers, who described glutamate release from astrocytes involving the potassium channel TREK-1 and occurring within a few milliseconds after stimulation, see Fig.16-18. (Woo et al., 2012). Gliotransmission through plasma membrane ion channels will be further described below (Section 1.6.6-1.6.8).

In summary, astrocytes can release a variety of signaling molecules, termed gliotransmitters, that can directly modulate the function of neuronal as well as glial networks. While most studies indicate that the release of gliotransmitters from astrocytes is a relatively slow process and operates within the timeframe of seconds to minutes, there is evidence demonstrating that gliotransmitters can be released within a few milliseconds, which indeed make them effective in modulating synaptic transmission at both short and long term levels. In addition, many gliotransmitters, such as ATP, can be released both through exocytotic and non-exocytotic mechanisms that can operate in parallel. As ATP is probably the most common and well-understood gliotransmitter and since the study of ATP release from dorsal horn astrocytes was the objective of my thesis work I will focus the following section of this introduction on the release of ATP and purinergic signaling.

1.6.1 ATP and purinergic signaling in the nervous system

ATP constitutes the primary source of metabolic energy in cells, including in astrocytes, but can also act as an extracellular messenger that exerts its effect by activating P2X and/or P2Y purinergic receptors, see Fig. 19. **P2X receptors** are transmembrane ion channels activated by ATP and permeable to cations (Giuliani et al., 2019). The P2X receptors are trimeric-protein receptors that are formed by the assembly of three subunits from the P2X receptor family. Today seven subunits (P2X1-7) have been identified that can form heteromeric and/or homomeric P2X receptor channels. The main characteristics of homomeric P2X receptors are summarized in Table 9. Functional expression of P2X1-5 and P2X7 homomeric receptors have been identified in astrocytes (Boue-Grabot and Pankratov, 2017; North, 2002).

P2Y receptors are G-protein coupled seven-transmembrane receptors for ATP that exert their effects by coupling to different intracellular effector proteins via different types of trimeric GTP binding proteins (G_q; G_i; G_s), (see Table 10). In the central nervous system, eight different metabotropic P2Y receptors have been

Table 8. Vesicular fusion kinetics for regulated vesicular exocytosis.

Cell type	Max rate regulated exocytosis	References
Endocrine cells		
Endocrine pituitary Melanotropes	25 s^{-1} 44 s^{-1}	Rupnik et al., 2000 Thomas et al., 1993
Endocrine pancreatic **β** cells	70 s^{-1}	Barg et al., 2001; Wan et al., 2004
Chromaffin cells	1,500 s^{-1}	Voets, 2000
Neurons		
Rod photoreceptors	300 s^{-1} 400 s^{-1}	Kreft et al., 2003 Thoreson et al., 2004
Retinal bipolar neurons	3,000 s^{-1}	Heidelberger et al., 1994
Inhibitory basket cell	5,000 s^{-1}	Sakaba, 2008
Calyx of Held neurons	6,000 s^{-1}	Bollmann et al., 2000; Schneggenburger and Neher, 2000
Glia		
Astrocytes	0.1-2 s^{-1}	Kreft et al., 2004

[Table modified from: Verkhratsky et al., 2016].

Table 9. Properties and distribution of homomeric P2X receptors.

Receptor	Main distribution	Agonists	Antagonists	Transduction mechanisms
P2X1	Smooth muscle, platelets, cerebellum, dorsal horn spinal neurons	BzATP > ATP = 2-MeSATP ⩾ α,β-meATP = L-β,γ-meATP (rapid desensitisation); PAPET-ATP	NF864 > NF449 > IP5I ⩾ TNP-ATP > RO 0437626 > NF279, NF023, RO1, MRS2159	Intrinsic cation channel (Ca^{2+} and Na^{+})
P2X2	Smooth muscle, CNS, retina, chromaffin cells, autonomic and sensory ganglia, pancreas	ATP ⩾ ATPγS ⩾ 2-MeSATP >> α,β-meATP (pH+zinc sensitive); β,γ-CF_2ATP	PSB-1011 > RB2, isoPPADS > PPADS > Suramin, NF770, NF778, Aminoglycoside	Intrinsic ion channel (particularly Ca^{2+})
P2X3	Sensory neurones, NTS, some sympathetic neurons	2-MeSATP ⩾ ATP ⩾ Ap_4A ⩾ α,β-meATP (rapid desensitisation); PAPET-ATP; BzATP	TNP-ATP, AF353, A317491, RO3, isoPPADS > NF110 > PPADS, Ip_5I, phenol red, RN-1838, Spinorphin	Intrinsic cation channel
P2X4	CNS, testis, colon, endothelial cells, microglia	ATP >> α,β-meATP >> CTP, 2-MeSATP Ivermectin potentiation	5-BDBD >> TNP-ATP, PPADS > BBG, Paroxetine, 5MTPT phenolphthalein,	Intrinsic ion channel (especially Ca^{2+})
P2X5	Proliferating cells in skin, gut, bladder, thymus, spinal cord, heart, adrenal medulla	ATP = 2-MeSATP = ATPγS >> α,β-meATP > AP_4A	BBG > PPADS, Suramin	Intrinsic ion channel
P2X6	CNS, motor neurons in spinal cord	Only functions as a heteromultimer	–	Intrinsic ion channel
P2X7	Immune cells including dendritic cells (mast cells, macrophages), microglia	BzATP > ATP ⩾ 2-MeSATP >> α,β-meATP (clemastine potentiates)	KN62, BBG, KN04, MRS2427, O-ATP, RN-6189, Perazine, AZ10606120, A740003, A-438079, A-804598, GSK-1370319,	Intrinsic cation channel and a large pore with prolonged activation

Abbreviations: 2′-azido-dUTP: 2′-azido-deoxyuridine-5′-triphosphate, 2-MeSADP: 2-methylthio-ADP, 2-MeSAMP: 2-methylthio-AMP, 2-MeSATP: 2-methylthio-ATP, 2-thio-UTP: 2-thio-uridine 5′-triphosphate, 5′-AMPS: 5′-O thiomnophosphate, 5-OMe-UDP αB: 5-methoxyuridine-5′-diphosphate-αβ, α,β-meATP: L-α,β-methylene ATP, α,β-meUDP: α,β-methylene-UDP, γ-CF2ATP: α,β-difluoromethylene-ATP,A3P5P: adenosine-3′-5′-bisphosphate, ADP: adenosine 5′-diphosphte, ADP-β-S: adenosine-5′-(β-thio)-diphosphate, AMP: adenosinemonophospate, Ap4A: diadenosine tetraphosphate, Ap5(γB): adenosine pentaphosphate (βγ), ATP: adenosine 5′-triphosphate, ATPγS: adenosine 5′-(γ-thio)-triphosphate, BBG: brilliant blue green, BzATP: 2′(3′)-O-(4-benzoylbenzoyl) adenosine 5′-triphosphate, CNS: central nervous system, CORM 2: carbon monoxide donor 2, CTP: cytosine triphosphate, IP5I: di-inosinepentaphosphate, isoPPADS: iso-pyridoxalphosphate-6-azophenyl-2′,4′-disulfonic acid, NAADP+: nicotinic acid adenine dinucleotide phosphate, NAD+: nicotinamide adenine dinucleotide, NTS: nucleus tractus solitarius, PAPET: 2-[2-(4-aminophenyl) ethylthio]adenosine-5′-triphosphate, PIT: 2,2′-pyridylisatogen tosylate, PLC-β: phospholipase C-β, PPADS: pyridoxal-5-phosphate-6-azophenyl-2′,4′-disulfonic acid, PPTN: 4-((piperidin-4-yl) phenyl)-7-(4-(trifluoromethyl) -phenyl)-2-napthoic acid, RB2: reactive blue 2, UDP: uridine 5′-diphosphate, UDP-βS: uridine-5′-(β-thio)-diphosphate Uridine-5'-(β-thio)-diphosphate, Up3U: diuridine triphosphate, Up4-phenyl ester: uridine tetraphosphate phenyl ester, Up4U: diuridine tetraphosphate, UTP: uridine 5′-triphosphate, UTPγS: uridine-5′-(γ-thio)-triphosphate. P2X receptor subtype agonist potencies are based on rat preparations, (=, equal potency; >, greater potency; ⩾, greater than or equal potency) [Data source: Burnstock, 2007].

Table 10. Properties and distribution of P2Y receptors.

Receptor	Main distribution	Agonists	Antagonists	Transduction mechanisms
$P2Y_1$	Epithelial and endothelial cells, platelets, immune cells, osteoclasts, brain	MRS2365 > 2-MeSADP = Ap5(γB) >> ADPβS > ATP > 2-MeSATP = ADP	MRS2500 > MRS2279 > MRS2179, PIT, A3P5P	G_q/G_{11}; PLC-β activation
$P2Y_2$	Immune cells, epithelial and endothelial cells, kidney tubules, osteoblasts	2-thio-UTP > UTP, MRS2698 ⩾ ATP, INS 365 > INS 37217, UTPγS > Ap4A > MRS 2768, Up_4-phenyl ester	AR-C126313 > Suramin > RB2, PSB-716, MRS2576, PSB-0402, AR-C118925	G_q/G_{11} and possibly G_i/G_o; PLC-β activation
$P2Y_4$	Endothelial cells, placenta, spleen, thymus	2′-azido-dUTP > UTPγS, UTP ⩾ ATP ⩾Ap_4A Up_4U MRS4062	ATP (human) > Reactive Blue 2 > Suramin, MRS2577, PPADS	G_q/G_{11} and possibly G_i; PLC-β activation
$P2Y_6$	Airway and intestinal epithelial cells, placenta, T cells, thymus, microglia (activated)	MRS2693 > UDPβS, PSB0474 > INS48823, Up3U, 3-phenacylUDP >> UDP > UTP >> ATP, α,β-meUDP, MRS2957, MRS4129, 5-OMe-UDP αB	MRS2578 > Reactive Blue 2, PPADS, MRS2567, MRS2575 (human)	G_q/G_{11}; PLC-β activation
$P2Y_{11}$	Spleen, intestine, granulocytes	ATPγS > AR-C67085MX > BzATP ⩾ ATP, NF546, NAD+, NAADP+, Sp-2-propylthio- ATP-α-B	NF157 > Suramin > RB2, 5′-AMPS, NF340, AMP-α-5	G_q/G_{11} and G_S; PLC-β activation
$P2Y_{12}$	Platelets, glial cells	2-MeSADP ⩾ ADP > ATP, ADP-β-S	AR-C69931MX > AZD6140 (Ticagrelor), INS50589 > RB2 > 2-MeSAMP AR-C66096, CT50547, PSB- 0413, Carba-nucleosides, MRS2395, AR-C67085,	$G\alpha_1$; inhibition of adenylate cyclase
$P2Y_{13}$	Spleen, brain, lymph nodes, bone marrow, erythrocytes	ADP = 2-MeSADP > 2-MeSATP, ATP	AR-C69931MX > AR-C67085 > MRS2211, 2-MeSAMP	G_i/G_o
$P2Y_{14}$	Placenta, adipose tissue, stomach	MRS2690>UDP>UDP glucose⩾UDP-galactose, UDP-glucosamine, MRS2905 Uracil nucleotides	PPTN PZB01415033	Gq/G11 Gi, adenylate cyclase inhibition

Abbreviations: A3P5P: adenosine-3′-5′-bisphosphate, ADP: adenosine 5′-diphosphte, ADP-β-S: adenosine-5′-(β-thio)-diphosphate, 5′-AMPS: 5′-O-thiomnophosphate, Ap4A: diadenosine tetraphosphate, Ap5(γB): adenosine pentaphosphate (βγ), ATP: adenosine 5′-triphosphate, ATPγS: adenosine 5′-(γ-thio)-triphosphate, BzATP: 2′(3′)-O-(4-benzoyl-benzoyl)-ATP, α,β-meUDP: α,β-methylene-UDP, 2-MeSADP: 2-methylthio-ADP, 2-MeSAMP: 2-methylthio-AMP, 2-MeSATP: 2-methylthio-ATP, 5-OMe-UDP αB: 5-methoxyuridine-5′-diphosphate-αB, NAADP+: nicotinic acid adenine dinucleotide phosphate, NAD+: nicotinamide adenine dinucleotide, PIT: 2,2′-pyridylisatogen tosylate, PLC-β: phospholipase C-β, PPADS: pyridoxal-5-phosphate-6-azophenyl-2′,4′-disulfonic acid, PPTN: 4-((piperidin-4-yl)phenyl)-7-(4-(trifluoromethyl)-phenyl)-2-napthoic acid, RB2: reactive blue 2, 2-thio-UTP: 2-thio-uridine 5′-triphosphate, UDP: uridine 5′-diphosphate, UDP-βS: uridine-5′-(β-thio) diphosphate, Up3U: diuridine triphosphate, Up4U: diuridine tetraphosphate, Up4-phenyl ester: uridine tetraphosphate phenyl ester, UTP: uridine 5′-triphosphate, UTPγS: uridine-5′-(γ-thio)-triphosphate.. P2Y receptor subtype agonist potencies are based on human preparations (=, equal potency; >, greater potency; ⩾, greater than or equal potency) [Data source: Burnstock, 2007].

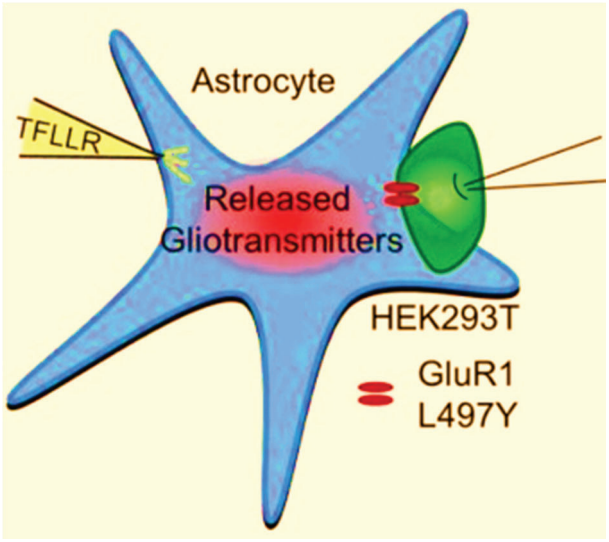

Figure16. Detection of glutamate release from astrocytes. Human embryonic kidney (HEK) cell 293, transfected with a mutated glutamate receptor 1 (GluR1) L497Y is used to detect glutamate release from astrocytes by a sniffer-cell approach. Astrocytes were stimulated by the Protease-activated-receptors-1 agonist TFLLR while simultaneously recording glutamate evoked currents in HEK293 cells with the patch-clamp technique. TFLLR has no direct effect on the HEK cells and can therefore be utilized as a glutamate detector/sniffer cell. [Figure modified from: Woo et al., 2012].

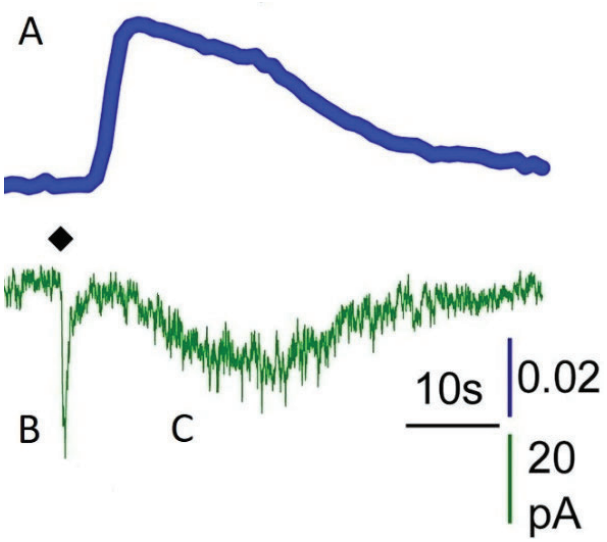

Figure 17. Calcium imaging performed on astrocyte while recording glutamate induced currents in transfected HEK293 cells (as in Fig 16). Black diamond indicates the time of TFLLR application. Blue line shows calcium signal monitored in the astrocyte and green line shows the recorded membrane current in the sniffer HEK293 cell. Approximately 5 sec after TFLLR application astrocytes start to display an increase in $[Ca^{2+}]_i$. B) Within milliseconds after application of TFLLR, glutamate induced a fast but short-lasting current in HEK293 cells. C) Several seconds after application of TFLLR a second current, that coincides with the calcium elevation in the astrocyte, is detected in HEK293 cells. [Figure modified from: Woo et al., 2012].

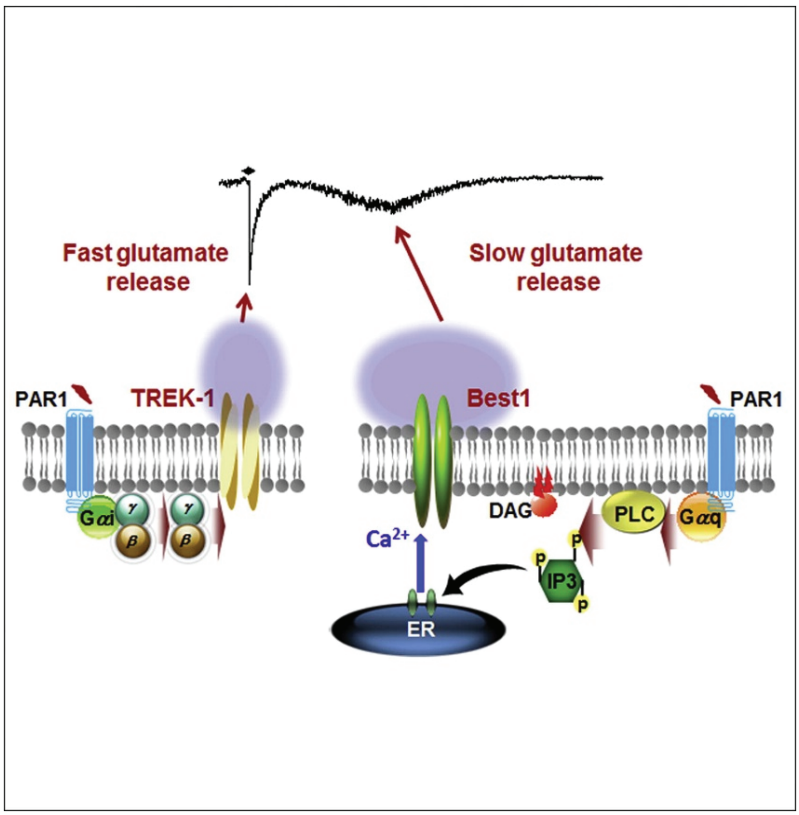

Figure 18. Activation of protease activated receptors 1 (PAR1).
Activation of PAR1 with TFLLR induces release of glutamate through two different types of channels with clearly separate mechanisms, kinetics, and pharmacological profiles in an astrocyte. The black trace represents an electrophysiological glutamatergic current in a sniffer cell (HEK293-cell transfected with GluR1-L497Y), recorded with patch-clamp while positioned on top of cultured astrocytes.
Activation of PARs associated inhibitory G-protein resulting in a fast (few ms. after stimulation) opening of the potassium channel TREK-1 causing glutamate release from the astrocyte which is recorded as the fast glutamatergic current in the HEK293 cell.
Simultaneously, agonist-binding to PAR1 receptor also activates Gq-proteins and consequently initiate the phospholipase C (PLC)/IP_3 signaling cascade resulting in glutamate release through Best-1 channels that is subsequently measured as a secondary glutamatergic current. [Modified from: Woo et al., 2012].

identified, among which P2Y1, P2Y12, and P2Y13 that are preferentially activated by ATP and its metabolite ADP (adenosine di-phosphate); P2Y4 by ATP and UTP (uridine tri-phosphate); P2Y6 by UDP; P2Y11 by ATP and P2Y14 by UDP-sugars (see Table 10) (Boue-Grabot and Pankratov, 2017; Burnstock, 2007).

In the extracellular environment, ATP is rapidly metabolized to ADP (Adenosine diphosphate), AMP (Adenosine monophosphate) and adenosine by hydrolysis of the phosphate groups through the action of extracellular ectonucleotidases, (Fig. 19) (Burnstock, 2006b). Together with ATP, ADP is an agonist at P2 receptors with different affinities depending on receptor type (see Table 9 - 11). In addition to the P2 family, adenosine primarily acts as an agonist at the P1 receptors (also called adenosine receptors), see Fig. 19. The P1 receptors are also G-protein coupled seven-transmembrane receptors and, like P2Y, their effects are mediated by coupling to intracellular effectors via different types of G-proteins (Gi/Gq/Gs). Four different adenosine receptors subtypes (A1, A2A, A2B and A3) have so far been cloned and A1, A2A, and A2B have been found in astrocytes (see Table 11).

Since ATP is synthesized primarily in the mitochondria and the cytoplasm through the action of glycolytic enzymes, it is necessary to transport ATP from the cytoplasm to the extracellular space (Fig. 15). In the extracellular space, ATP released from astrocytes induces/amplifies calcium waves (Section 1.5.5) in neighboring astrocytes and can modulate excitability and synaptic transmission in neuronal networks (Guthrie et al., 1999). The importance of ATP release and purinergic signaling in nociception has been addressed in several purinoceptor knock-out studies (see Table 12). For example, deletion of either adenosine receptors A1, A2A or P2 receptors such as P2Y12, P2Y14, P2X2, P2X4 or P2X7 is associated with dysfunction in the nociceptive circuits and consequently in pain sensation (Burnstock, 2007).

1.6.2 Mechanism of gliotransmission and the role of Ca^{2+} in gliotransmitter release

The change in the concentration of free intracellular calcium ions ($[Ca^{2+}]_i$) is involved in many intracellular cellular signalling events and biological processes. Understanding the biology of calcium regulation and clarifying its role in different physiological processes are therefore important points in gliobiology. Astrocytes display calcium “excitability” in response to a range of agonists. In contrast to the neuronal action potential, elevations in $[Ca^{2+}]_i$ are not an “all or none” signal in glial cells but display variable kinetics, amplitudes, frequencies, and patterns, such as single peak elevation, calcium oscillations or a maintained increase of

Table 11. Distribution, pharmacology and intracellular transduction pathways of adenosine receptors.

Receptor	Main distribution	Agonists	Antagonists	Transduction mechanisms
A_1	Brain, spinal cord, testis, heart, autonomic nerve terminals	CCPA > R-PIA = S-ENBA; CVT-510; GR79236 2′-MeCCPA, SDZ WAG 994, INO-8875, MRS 5474	DPCPX, N-0840, MRS1754, WRC-0571, PSB36, SLV320, CGS 16943, PQ-69	G_i/G_o ↓cAMP
A_{2A}	Brain, heart, lungs, spleen	HENECA > CGS 21680 = CVT-3146; ATL-146e; Regadenoson	KF17837, SCH58261, ZM241385, KW 6002	G_s ↑cAMP
A_{2B}	Large intestine, bladder	Bay60-6583, NECA	PSB603, MRE-2029-F20, MRS1754, PSB0788 MRS1706, PSB1115, Alloxazine, GS-6201	G_s ↑cAMP
A_3	Lung, liver, brain, testis, heart	IB-MECA > MRS5698 > MRS5168 > 2-Cl-IBMECA; DBXRM; VT160; HEMADO	MRS1220, L-268605, MRS1191, MRS1523(rat), VUF8504, VUF5574, MRS1334(human), PSB10	G_i/G_o, G_q/G_{11}, ↓cAMP, PLC-β activation

Abbrevations: 2-Cl-IB-MECA: 2-chloro-N6-(3-iodobenzyl)-9-[5-(methylcarbamoyl) -β-d-ribofuranosyl] adenine, CCPA: chlorocyclopentyl adenosine, 2′-MeCCPA: 2-chloro-N-cyclopentyl-2′-methyladenosine, DPCPX: 1,3-dipropyl-8-cyclopentylxanthine, cAMP: cyclic AMP, DBXRM: 1,3-dibutylxanthine 7-riboside 5′-N-methylcarboxamide, HEMADO: 2-(1-Hexynyl)-N-methyl adenosine, HENECA: 2-hexynyladenosine-59-N-ethylcarboxamide, IB-MECA: N6-(3-Iodobenzyl)-9-[5-(methylcarbamoyl)-β-d-ribofuranosyl]-adenine, NECA:5′-Nethylcarboxamido-adenosine, R-PIA:R-phenylisopropyl-adenosine, S-ENBA: (2S)-N6-[2-endo-Norbornyl] adenosine. P1 subtype agonist potencies are based on human preparations (=, equal potency; >, greater potency; ⩾, greater than or equal potency) [Data source: Burnstock, 2007].

Table 12. Phenotypes associated with genetic knock-out of purinoceptors.

Receptor	Selected Knock-out phenotypes
Ionotropic P2X	
$P2X_1$	Male infertility kidney function ↓, arterial thrombosis ↓
$P2X_2$	Inflammatory pain ↓, urinary bladder reflex ↓, taste sensing ↓, intestinal motility ↓
$P2X_3$	Hippocampal LTD pain ↓, bladder reflex ↓, taste sense ↓, temperature sense ↓, intestinal motility ↓
$P2X_4$	Hippocampal LTD ↓, inflammatory & neuropathic pain ↓, heart function and blood pressure ↑
$P2X_5$	-
$P2X_6$	-
$P2X_7$	Inflammation ↓, pain ↓, fluid secretion (pancreas, salivary gland) ↓, skeletal abnormalities
Metabotropic P2Y	
$P2Y_1$	Platelet aggregation ↓renal disease ↓
$P2Y_2$	salt resistant arterial hypertension ↑ monocyte and macrophage recruitment ↓
$P2Y_4$	cardiac angiogenic defect, exercise capacity ↓ effort-induced adaptive cardiac hypertrophy ↓
$P2Y_6$	Altered IP_3 and Ca^{2+} levels in rat proximal tubule, macrophages and glial cells
$P2Y_{11}$	Not found in mouse
$P2Y_{12}$	Allodynia after nerve injury ↓ platelet activation/adhesion ↓ microglial extension toward cortical damage ↓
$P2Y_{13}$	Hepatic HDL and cholesterol ↓, cholesterol uptake↓, biliary cholesterol output ↓ bone volume ↓
$P2Y_{14}$	Neuropathic pain ↓neutrophil/macrophage chemotaxis ↓
Metabotropic P1	
A_1	Hyperalgesia, blood pressure and plasma Renin activity ↑ Anxiety ↑
A_{2A}	Acute pain response ↓ Anxiety and aggression ↑ Damage by focal brain ischemia ↓ Neonatal brain ischemic damage ↑
A_{2B}	Leukocyte adhesion to vascular endothelium ↑ Inflammation ↑Vascular leakiness ↑
A_3	Airway responsiveness ↓Mast cell degranulation ↓Intraocular pressure ↓Resistance to cardiac ischemia-reperfusion injury

Abbreviations: HDL: high density lipoprotein, IP_3: inositol triphosphate, LTD: long-term depression. [Table modified from: Jacobson and Muller, 2016].

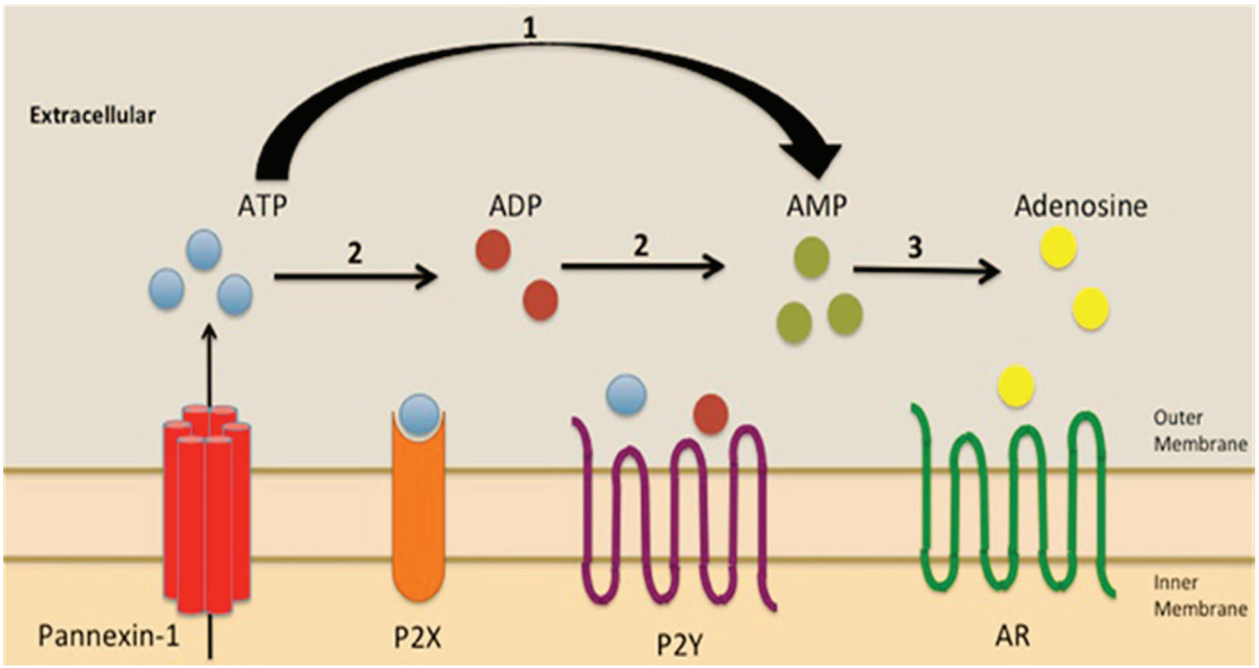

Figure 19. **Extracellular metabolism of ATP**. ATP released through astrocytic pannexin-1 rapidly degraded to ADP and AMP by the enzyme (2) Ectonucleoside triphosphate diphosphydrolase (E-NTPase). ATP, and ADP induce purinergic signaling by serving as agonists for the P2-receptors. (3) AMP is rapidly hydrolyzed to adenosine by Ecto-5´-nuclrotidaste (CD73). Adenosine can then activate metabotropic P1 receptors that are widely distributed in most cells in the central nervous system. (1) Alternatively, ATP can be directly hydrolyzed to AMP by the enzyme Ecto-nucleotide pyrophosphatase/phosphodiesterase (E-NPP). [Modified from: Morandini et al., 2014].

intracellular calcium levels (Bazargani and Attwell, 2016). In addition, variations in $[Ca^{2+}]_i$ are not restricted to a global increase that occurs in the cell bodies of astrocytes but have instead been described to mostly appear as local calcium transients in the narrow processes at various distances from the cell body of the astrocyte. Among the many agonists that have a modulatory capacity on astrocytic calcium levels, ATP and its metabolite ADP are among the most common. Due to its high prevalence in virtually all cells, it has historically been extensively debated whether ATP release mechanisms from astrocytes are calcium-dependent or calcium-independent (Bazargani and Attwell, 2016). It is clear that among the many mechanisms that induce astrocytic ATP release, some mechanisms require elevations in intracellular free calcium concentrations while others do not (see Table 7).

1.6.3 Exocytosis and vesicular release of gliotransmitters

The active storage of vesicular ATP is a key process in initiating the vesicular branch of purinergic signaling and ATP-mediated communication, and it has been known for many decades that ATP is a major constituent of secretory vesicular compartments (Johnson, 1988). However, until the last decade, it was unknown by which mechanism astrocytes accumulate ATP on the luminal side of intracellular vesicles for storage and future release (Moriyama et al., 2017). However, in 2008 Sawada K. et al. identified a nucleotide transporter present on intracellular vesicles (VNUT/SLC17A9), which serves as a vesicular ATPase by utilizing the acidic intra-vesicular environment to translocate ATP from the cytoplasm into vesicular compartments of astrocytes (Sawada et al., 2008). The vesicular nucleotide transporter is distributed throughout the brain and the spinal cord. In astrocytes, the vesicular nucleotide transporters have been identified on lysosomes, dense-core vesicles, and small secretory vesicles (Angelova et al., 2015; Kasymov et al., 2013; Moriyama et al., 2017; Oya et al., 2013).

The mechanism that concentrates ATP in vesicular compartments for later release requires two steps. In the first step, an ATP molecule serves as the energy supply to transport a proton via a proton pump and against its gradient into the lumen of a vesicle to create an acidic (high proton) intra-vesicular environment (Moriyama et al., 2017). During the second step, an ATP molecule is transported into the vesicle by the vesicular nucleotide transporter in exchange with a proton (Fig. 15) (Moriyama et al., 2017). Inside the vesicle, ATP can either be used to drive chemical reactions or be stored for future release and purinergic signaling

1.6.4 Astrocytic proteins controlling exocytosis and motility of vesicles.

Some 30 years ago, it was revealed that SNARE-complexes are not exclusive to neurons but are also present in astrocytes. Many proteins, such as VAMP-2 (vesicle-associated membrane protein 2), that are associated with neuronal vesicular movement and exocytosis are found in astrocytes as well (Parpura et al., 1995). Additionally, glial cells have proven to express protein complexes that have not been identified in neurons, such as SCAMP (secretory carrier membrane proteins) and VAMP-3 (Crippa et al., 2006; Maienschein et al., 1999; Mothet et al., 2005; Wilhelm et al., 2004). Furthermore, lysosomal proteins that are linked to the lysosomal secretory machinery, such as Q-SNARE proteins, SNAP-23 (homologue of the neuronal SNAP-25), and syntaxins 1, 2, 3, 4 and other SNARE proteins that are linked to the SNARE-complex such as Synaptotagmin 4 have been identified in astrocytes (Hepp et al., 1999; Paco et al., 2009; Zhang et al., 2004a; Zhang et al., 2004b). Accordingly, by monitoring amperometric spikes or by recording membrane capacitance in cultured astrocytes, it has been shown that calcium-dependent release of glutamate, D-serine and to a lesser extent ATP from astrocytes was reduced (but not fully blocked) when interfering with the SNARE-complex with tetanus toxin (Coco et al., 2003; Verderio et al., 1999). This indicates that to release gliotransmitters, astrocytes utilize a piece of complex machinery that includes both calcium and SNARE-dependent pathways as well as SNARE and calcium-independent mechanisms (Coco et al., 2003; Verderio et al., 1999). The toxin-resistant resistant component could involve larger vesicles with lysosomal features that are associated with VAMP7 (that is toxin-resistant) and calcium-independent release mechanisms could involve membrane transporters or channels (see below) (Verderio et al., 2012).

Quantitative measurements of the kinetics of astrocytic secretory vesicle movements have identified two types of movement patterns. The first types movement is associated with vesicles moving along defined cellular trajectories, including cytoskeletal structures such as actin- and intermediate filaments, and has been termed directional vesicular mobility (Verkhratsky et al., 2016). The second type, i.e. non-directional mobility, is associated with what appears to be a disorganized and unsystematic movement, with no clear trajectory, similar to particles following a Brownian motion (pedesis) (Verkhratsky et al., 2016).

Recent research has also identified a contrast in calcium physiology concerning vesicular movements, namely, that in the event of an increase in cytoplasmic calcium concentration, vesicles containing peptides as well as endolysosomes decrease their speed of motion whereas glutamatergic vesicles accelerate their motion (Potokar

et al., 2010; Potokar et al., 2008; Stenovec et al., 2007). Regulation of calcium-dependent changes in vesicular mobility, as described above, is a mechanism that is exclusively found in astrocytes and has not yet been described in neurons (Verkhratsky et al., 2016). The rationale behind these unique patterns of vesicular motility in astrocytes is unknown, but it has been speculated that it might represent an adaptive mechanism for astrocytes to redirect vesicles and vesicular content to the appropriate locations (Verkhratsky et al., 2016).

1.6.5 Release via different vesicular compartments in astrocytes

Electron-microscopy studies have identified several intracellular secretory organelles in astrocytes with differences in dimension and vesicular content, see Fig. 20. The synaptic-like micro vesicles (SLMV) are the smallest vesicles with a diameter of approximately 30-100 nm. Synaptic-like micro vesicles strongly resemble neuronal synaptic vesicles (1-3μm) and have been identified in astrocytes from acute hippocampal slices or hippocampal slice cultures (Fig. 20). SLMVs are transparent, appear in groups of 2-15 vesicles and are much fewer in number than vesicles in neuronal terminals which usually exist in pools of 100-1000 vesicles (Bergersen et al., 2012; Bezzi et al., 2004; Jourdain et al., 2007).

Six different vesicular neurotransmitter transporters (VNTs) have been identified on the SLMVs, including VSer (D-serin), VGUT1-3 (glutamate), VEAT (aspartate), VMAT1-2 (monoamines) and VGAT (GABA/Glycine), which in addition to astrocytic SLMVs also fill the neuronal synaptic vesicles with neurotransmitter (see Table 13). The latest vesicular membrane transporter that was recently identified is the vesicular nucleotide transporter – VNUT. The nucleotide transporter is responsible for transporting ATP from the cytoplasm into the lumen of the synaptic-like micro vesicles, see Fig. 15.

The SLMVs can be found in the astrocytic process that surrounds neuronal synapses as well as in the astrocyte soma. Most of the SLMVs in astrocytes are glutamate and D-serine positive, in comparison to neuronal synaptic-like micro vesicles which lack D-serine but instead contain glycine, GABA or glutamate (Bezzi et al., 2004; Montana et al., 2004; Ormel et al., 2012). In addition to the small synaptic-like micro vesicles, larger (~100–600 nm) ATP-containing dense-core vesicles (DCVs) that also contain neuropeptides have been identified in astrocytes (Fig. 20) (Burgoyne and Morgan, 2003). The dense core vesicles contain a higher amount of ATP than the SLMVs, and ATP is believed to enter these dense core vesicles via the vesicular nucleotide transporter (Kasymov et al., 2013; Moriyama et al., 2017; Oya et al., 2013). The proportion of dense-core vesicles among

Table 13. ATP co-localization and co-release with neurotransmitters.

Neuron type	Transmitters	References
Peripheral nervous system		
Sympathetic nerves	ATP + NA + NPY	Westfall et al., 1978
Parasympathetic nerves	ATP + ACh + VIP	Hoyle, 1996
Sensory-motor	ATP +CGPR + SP	Burnstock, 1993
NANC enteric nerves	ATP + NO + VIP	Belai and Burnstock, 1994
Motor nerves (in early development)	ATP + ACh	Silinsky and Hubbard, 1973
Central Nervous System		
Cortex, caudate nucleus	ATP + ACh	Richardson and Brown, 1987
Hypothalamus, *locus coeruleus*	ATP + NA	Sperlágh et al., 1998
Hypothalamus, dorsal horn	ATP + GABA	Jo and Role, 2002 Jo and Schlichter, 1999
Mesolimbic system	ATP + DA	Krugel et al., 2003
Hypothalamus, dorsal horn	ATP + glutamate	Mori et al., 2001

Abbreviations: ACh, acetylcholine; ATP, adenosine 5'-triphosphate; CGPR, calcitonin gene-related peptide; DA, dopamine ; GABA, y-aminobutyric acid; NA,noradrenaline; NANC, non-adrenergic, non-cholinergic; NO, nitric oxide; NPY, neuropeptide Y; SP, substance P; VIP, vasoactive polypeptide. C [Table modified from: Abbracchio et al., 2009].

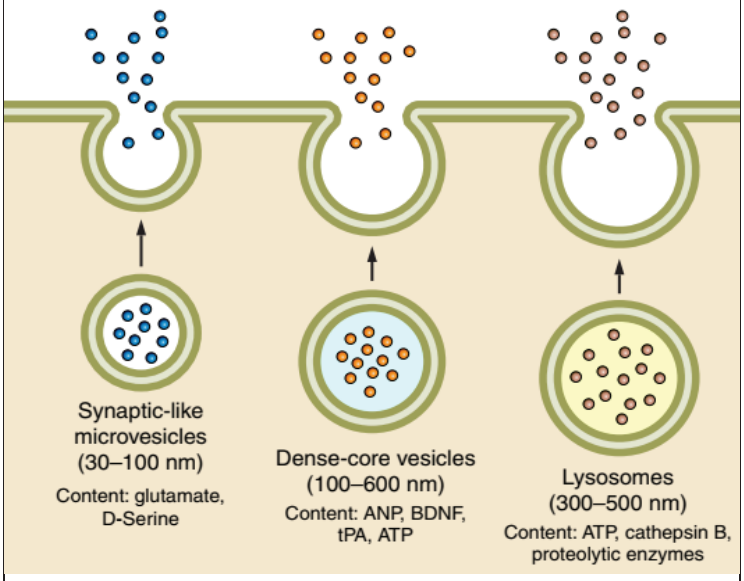

	SLMV	DCV	Lysosomes
Diameter	30-100 nm	100-600 nm	300-500 nm
Biogenesis	Recycling from plasma membrane	BFA-sensitive, Golgi derived vesicles, REST	VNUT LAMP1
Fusion	VAMP2 VAMP3	VAMP2 VAMP3	TI-VAMP/VAMP7
Content	Glutamate D-serine	ANP, BDNF, tPA, ATP	ATP, Cathepsin B Proteolytic enzymes

Abbreviation: ANP: atrial natriuretic peptide, ATP: adenosine 5'-triphosphate, BDNF: brain-derived neurotrophic factor, BFA: brefeldin A, DCV: dense-core vesicles, LAMP1: lysosomal-associated membrane protein 1, REST: RE-1-silencing transcription factor. SLMV: synaptic-like microvesicles, TI-VAMP: tetanus neurotoxin-insensitive vesicle associated membrane protein, tPA: tissue plasminogen activator, VAMP2: vesicle-associated membrane protein 2, VAMP3: vesicle-associated membrane protein 3, VAMP7: vesicle-associated membrane protein 3, VNUT: vesicular nucleotide transporter

Figure 20: Multiple types of vesicular release in Astroglia.
In astrocytes, three different vesicular compartments, with different markers and origin, have been identified to release gliotransmitters: the smallest synaptic like micro vesicles (SLMV); the dense core vesicles (DCV) and the secretory lysosomes. The vesicular nucleotide transporter, transporting ATP from the cytoplasm to the luminal side of the vesicular compartment, has been identified on all three vesicle types in astrocytes. The vesicular fusion of SLMV and DCV with astrocytic plasma membrane utilize similar mechanisms as neuro-transmitter filled vesicles in neuronal synapses. Secretory lysosomes are believed to be responsible for most of the exocytosis-derived extracellular ATP from astrocytes. However, lysosomes do not always release ATP through complete exocytosis but have been shown to partially collapse with the plasma membrane hence opening up a temporary fusion pore that let ATP diffuse into the extracellular environment, and then collapse back into a lysosomal-like vesicular compartment; this mechanism has been named kiss-and-run exocytosis. It has been observed that in places where synaptotagmin IV is present rather than synaptotagmin I, fusion events are more inclined toward kiss-and-run release rather than full fusion (Wang et al., 2001). Vesicles are re-acidified approximately twenty times faster after kiss-and-run compared to full collapsed vesicles, which has a significant impact on the kinetics of ATP (and other molecules that utilize the proton-gradients to enter vesicles) being re-loaded into the luminal side of secretory vesicles (Haydon and Carmignoto, 2006). [Figure modified from: Verkhratsky and Nedergaard, 2018].

Q

the total number of vesicles present in an astrocyte is rather low. It represents about 2% of the VAMP2-positive vesicles present in an astrocyte and therefore does probably not account for a large fraction of the extracellularly released ATP. Instead, secretory lysosomes appear to represent the main vesicular source of ATP released by exocytosis (Verkhratsky et al., 2016).

Lysosomes are crucial intracellular organelles of astrocytes (and most other cells) and are mostly responsible for the degradation of intracellular molecules due to the high concentration of intra-lysosomal proteolytic enzymes, and the recycling of macromolecules such as proteins (Kroemer and Jaattela, 2005). Several groups have reported a role of lysosomes in the secretion of gliotransmitters by astrocytes, in particular in the calcium-dependent release of ATP (Fig. 20 and Table 7) (Jaiswal et al., 2002; Li et al., 2008; Zhang et al., 2007). Secretory lysosomes can be stained with FM-dyes or with the fluorescent ATP analogue MANT-ATP (2'/3=-O- (N'-methylanthraniloyl)adenosine-5=-O-triphosphate) in living astrocytes and their estimated diameter is of 300-500nm (Vardjan et al., 2012; Zhang et al., 2007). As for other vesicles, intra-lysosomal ATP is accumulated via the vesicular nucleotide transporter (Oya et al., 2013). In addition to ATP, the astrocytic secretory lysosomes express lysosome specific markers such as cathepsin D, lysosomal specific marker 1 (LAMP1), and ras-related protein Rab7 (Zhang et al., 2007). Exocytosis of secretory lysosomes is calcium-dependent and is characterized by its slow fusion kinetics (see Table 8). The exocytosis and membrane fusion of secretory lysosomes is triggered by the vesicle-associated protein VAMP 7 and will proceed even in the presence of tetanus toxins (Jaiswal et al., 2002; Li et al., 2008).

1.6.6 Non-vesicular release of gliotransmitters

Several signaling molecules, including gliotransmitters, can be released directly to the extracellular environment through a broad range of membrane-bound proteins in astrocytes. The non-vesicular release pathways include hemichannels, membrane transporters, ionotropic receptor-channels such as purinergic P2X7R (Fig. 15 and Table 7). Among the non-vesicular proteins involved in the gliotransmitter release, the hemichannels, namely the connexins/connexons and pannexins/pannexons have lately received a great amount of attention, partly due to their ability to release ATP to the extracellular environment (Dahl and Locovei, 2006; Hofer and Dermietzel, 1998). The diffusion of ATP across the cell membrane from the cytoplasm to the extracellular environment, through a channel, is driven mostly by the difference in ATP concentration between inside and outside of the

astrocytes. The intracellular concentration of ATP is approximately 5 mM which is about 107 times higher than in the extracellular space, where, under normal physiological conditions, the concentration of ATP is in the low nanomolar range, meaning that there is a substantial chemical driving force favoring the efflux of ATP (Verkhratsky and Nedergaard, 2018). Regarding non-vesicular secretion of gliotransmitters from astrocytes, connexins were probably the first to be identified and seemingly the most well-studied proteins in this context (Hofer and Dermietzel, 1998). Connexons are transmembrane hemichannels formed from the assembly of six connexin (Cx) proteins around a central pore that has a diameter of ~1.2 nm, with some variations between subtypes (Harris, 2007). More than 20 different connexins have been identified and shown to be distributed in different tissues. Each connexin is named after its predicted molecular weight, for example, connexin 30 has a molecular weight of 30k Dalton (see Table 14).

1.6.7 Non-vesicular release of gliotransmitters - Connexon/Connexin hemichannels

Connexon hemichannels are widely associated with the release of extracellular signaling molecules through its central pore, and ATP has been described as one of the most important permeant molecules for this hemichannel (Harris, 2007). Connexons are heavily expressed at perivascular endfeet of astrocytes indicating that ATP release through connexons might be involved in regulating the blood flow in different parts of the central nervous system through astroglia-vasculature signaling (Verkhratsky and Nedergaard, 2018). The first evidence indicating that connexins are involved in ATP release was obtained by utilizing stably transfected Cx43 and Cx32 in non-jap junction expressing glioma cells. The cells transfected with connexins release ten times more ATP compared to control groups when stimulating the purinergic receptors, they express with UTP. In the central nervous system, Cx43 and Cx30 are highly expressed in astrocytes but not in neurons (see Table 14). Release of ATP through astrocytic Cx43 has been suggested to be fundamental in astroglial communication (Chever et al., 2014; Roux et al., 2015). The gating mechanisms of connexin hemichannels is strongly modulated by the membrane potential as well as by the intracellular free calcium concentration. Lowering calcium in glioblastoma cells expressing Cx43 is associated with dye-uptake (<1kD) as well as ATP release (Bargiello et al., 2012; Lopez et al., 2016; Verselis and Srinivas, 2008).

Table 14. Expression of main connexin and pannexin hemichannel subtypes in neurons and glia

Cell type	Connexin	Pannexin
Neurons	Cx30.2, Cx31.1, Cx32, Cx36, Cx40, Cx45, Cx50, Cx57	Panx1, Panx2
Astrocytes	Cx26, Cx30, Cx43, Cx40, Cx45	Panx1, Panx2[a]
Microglia	Cx32, Cx36, Cx43[b]	Panx1
Oligodendrocytes	Cx29, Cx42, Cx27	Panx1, Panx2

Abbreviation: Cx: Connexin, Panx1/2: Pannexin1/2
a: activated astrocyte in the hippocampus during ischemia
b: activated microglia but not expressed in resting state.
[Table modified from: Decrock et al., 2015]

1.6.8 Non-vesicular release of gliotransmitters - Pannexons/Pannexin hemichannels

In addition to the well-studied connexins, a second structurally related channel type termed pannexins/pannexons has recently been identified. Pannexins are evolutionarily unrelated to the connexins but are rather homologs of the invertebrate gap junction protein Innexin. Today, three different pannexin channels have been identified, PAN-1, PAN-2, and PAN-3 and none of them can dimerize and become a gap junction, but they stay rather as individual membrane-bound pannexin channels (Dahl and Locovei, 2006; Panchina et al., 2000). Among the different pannexin channel isomers, the pannexin-1 channel has been studied most extensively. Pannexin-1 channels are expressed in excitable and non-excitable cells and are present in many tissues including in the central nervous system (Medina-Ceja et al., 2019). Table 14 summarizes the distribution of pannexon subtypes in CNS cells.

The pannexin-1 channel can be activated by changes in $[Ca^{2+}]_i$, increases in extracellular potassium concentration, activation of TNF-α receptors, phosphorylation by Src-kinase after NMDA receptor activation, activation of different purinergic signaling pathways by agonists such as ATP or activation of adrenergic α_1 receptors. For a more extensive and detailed description of the activation pathways and regulatory mechanisms of pannexin-1, interested readers are referred to the following detailed reviews (Billaud et al., 2011; Dahl, 2015; Thompson et al., 2008; Weilinger et al., 2016).

It has been demonstrated by several independent groups that pannexin-1 channels are permeable to ATP. The mechanism of release of ATP through pannexin-1 channels was shown to be either calcium-dependent or calcium-independent, depending on the pathway through which the channel is activated (Dahl, 2015; Lazarowski, 2012). Activation through the purinergic receptor $P2X_7$ pathway is calcium-independent, whereas activation of pannexin-1 channels following the stimulation of G-protein coupled P2Y receptors involves calcium-dependent mechanisms (Locovei et al., 2007; Locovei et al., 2006; Zhang et al., 2012b). Interestingly, at higher concentrations (higher than required for the activation of purinergic receptors), ATP acts as a pannexin-1 channel antagonist by inhibiting the opening of the channel. This suggests the coexistence of a positive feed-forward amplification mechanism (at low ATP concentrations) together with autoregulatory inhibition (at high ATP concentrations) most probably to ensure proper regulation of extracellular concentration of ATP and its metabolites.

Nevertheless, pannexin-1 channels are not always permeable to ATP in their open configuration. Indeed, pannexin-1 can exist in three different conformational: a closed state, ATP-permeable state and a non-ATP-permeable (Eskandari et al., 2002). The non-selective, ATP permeable, state has a large conductance, around 500 pS, and is permeable to negative as well as positively charged molecules (approx. 1 kDA), while the non-ATP-permeable configuration is the anion-selective a have a configuration with lower conductance (~ 15 – 75 pS). The permeability to ATP through pannexin-1 is intricately linked to the external [K^+] of the cell. The ATP-permeable configuration seems to be promoted during high extracellular [K^+] while lower K^+ levels appear to favour the non-ATP-permeable configuration (Nomura et al., 2017; Romanov et al., 2012; Wang et al., 2014).

1.6.9 Multiple non-vesicular release pathways with discrete kinetics operate in parallel

In addition to the hemichannels (connexons and pannexons) several other channels present in astrocytes have been shown to display ATP permeability. These include volume regulated ion channels (VRACs), P2X7 receptors, maxi ion channels (MACs) and calcium homeostasis modulator 1 channels (CALHM-1) (Fig. 15 and references in Table 7) (Taruno, 2018). It, therefore, appears that astrocytes utilize multiple pathways in parallel to release gliotransmitters. Interestingly, different channels can differ quite extensively in their conditions of recruitment. Some require G-protein associated signaling while others do not, and some channels require elevation of intracellular calcium while some channels are calcium-independent. This was proven in an elegant series of experiment where the authors utilized human embryonic kidney 293 (HEK293) cells transfected (HEK293T) with glutamate AMPA-receptor (GluR1-L497Y) mRNA as detector-/sniffer-cells to detect glutamate release from astrocytes (Lee et al., 2007). They showed that activation of protease-activated receptors 1 (PAR1-receptors) by the PAR peptide agonist TFLLR, induced two different components of glutamate release, differing by their kinetics, see Fig. 16-18. The first release phase was characterized by activation of inhibitory G-proteins and a fast glutamate release, appearing on a millisecond timescale after stimulation (Woo et al., 2012). In addition to recording glutamate-induced currents in HEK293T cells, the authors simultaneously imaged the variations in intracellular free calcium concentration in the glutamate-releasing astrocyte. The fast glutamate release response upon TFLLR agonist stimulation was calcium-independent, and the channel involved in this fast and early phase of glutamate release was identified as the potassium channel KCNK2 also called TREK-1. The second, more delayed phase of glutamate release was characterized by a much slower

activation rate, appearing with a delay of 5-20 seconds after stimulation (Woo et al., 2012). The release through the slow mechanism required the activation of Gq associated proteins, by PAR-1 receptors. The slow Gq protein-activated channel was identified as the calcium-dependent chloride channel bestrophin-1 (BEST-1). Blocking an increase in intracellular free calcium concentration significantly reduced the release of glutamate through the BEST-1 channels, suggesting that PAR-1 induced glutamate release through BEST-1 channels was calcium-dependent (Woo et al., 2012).

These observations that in astrocytes, gliotransmitter release can involve several distinct pathways that can be recruited either through the activation of a single type of G-protein coupled receptor as demonstrated by Woo (2012) and colleagues or most probably also through simultaneous activation of different types of receptors. The results presented above confirm that astrocytes can take advantage of a variety of different non-vesicular release pathways that have distinct kinetics mechanism of regulation as well as variable calcium-dependence. These pathways coexist with calcium-dependent vesicular release mechanisms and both mechanisms of release are probably involved in the fine regulation of extracellular ATP levels *in vivo*.

However, the secretion of many gliotransmitter in astrocytes is based both on vesicular and non-exocytotic pathways, some gliotransmitters appear to involve exclusively non-vesicular pathways. It appears that GABA is an example of such a gliotransmitter that solely depends on channels/transporters to be released into the extracellular compartment (Verkhratsky and Nedergaard, 2018). Cultured astrocytes from both rodents and humans can release GABA (Gallo et al., 1991; Gallo et al., 1986; Lee et al., 2011). However, there is currently no evidence for the expression of vesicular GABA transporters in astrocytes, making it unlikely that GABA is stored in exocytotic vesicles. Moreover, GABA release has been described to be calcium-independent in situ (Woo et al., 2012). Altogether, this strongly suggests that GABA is exclusively released through non-vesicular mechanisms (Héja et al., 2009; Kirischuk et al., 2016; Le Meur et al., 2012). Several non-vesicular mechanisms have been identified for the release of astrocytic GABA, which include diffusion through the plasma membrane via VRACs or the bestrophin-1 channels (Table 7) (Kozlov et al., 2006; Lee et al., 2010; Yoon and Lee, 2014). However, the most well-described mode of astrocytic release of GABA is through operation in the reverse mode of the plasma membrane GABA transporter, that normally is involved in clearing neuronally released GABA from the synaptic cleft (Angulo et al., 2008; Gallo et al., 1991; Héja et al., 2009; Kirischuk et al., 2016).

Concerning ATP, in addition to the vesicular release, today five groups of ATP release channels have been described (VRACSs, MACs, P2X7R, CALHM-1 and hemichannels) (Fig. 15). Additionally, ATP binding-cassette (ABC) transporters such as multidrug resistance protein 1 (p-glycoprotein) and cystic fibrosis transmembrane conductance regulator have been suggested to support ATP release (Abraham et al., 1993; Reisin et al., 1994; Schwiebert, 1999). Although the pore diameter of certain ABC transporter can expand and would allow ATP diffusion, it is controversial whether or not the ABC transporters are involved in ATP release (Krasilnikov et al., 2011; Linsdell and Hanrahan, 1998). Several groups have provided evidence that directly contradicts involvement of ABC transporters in purinergic signaling, and they are therefore currently not commonly accepted as means through which ATP is released from astrocytes (Grygorczyk et al., 1996; Roman et al., 2001).

1.6.10 Spinal ATP release, astroglia and chronic pain

Although the roles of astrocytes and purinergic signaling in physiological and pathological conditions have been studied, the precise role of glial cells in nociceptive processing remains still to be clarified further. Selective inhibition of spinal astrocyte metabolism by intrathecal (i.t.) injections of fluorocitrate produced a noticeable and reversible reduction of thermal and mechanical hyperalgesia in rats after peripheral injury (Meller et al., 1994) - but not under basal physiological condition - (Lefèvre et al., 2016). Moreover, functional alterations in spinal cord dorsal horn astrocytes have been observed to be fundamental in the development and maintenance of neuropathic pain in animal models, and inhibition of spinal astrocytic function generally produces an anti-nociceptive effect during neuropathy in animals (Gao and Ji, 2010b; Guo et al., 2007; Ji et al., 2006; Okada-Ogawa et al., 2009; Xie et al., 2007). In addition, it is well known that the anti-cancer drug paclitaxel induces pain in patients as early as 1–3 days after the beginning of drug administration (Loprinzi et al., 2011; Reeves et al., 2012) and that this chronic neuropathy can last for years (Rahn et al., 2014). In animal models of paclitaxel-induced neuropathy, it has been reported that astrocytes in the dorsal horn, but not spinal microglial cells, are activated. In such animal models, the neuropathic pain symptoms are strongly decreased when inhibiting the metabolism of astrocytes supporting the idea that astrocytes are the key cells involved in the pathogenesis of certain neuropathies (Zhang et al., 2012a)., For more information concerning the involvement of astrocytes in pain, readers are referred to the excellent review by Ji and colleagues (2019) (Ji et al., 2019).

While acute pain can be managed with opioids and opioid-derivatives, there are currently no drugs suitable for intense, persistent chronic pain symptoms. Long term use of opioids is associated with the development of opioid-tolerance and is, therefore, a serious issue for clinical treatment. Moreover, the possibility of addiction and the accompanying withdrawal symptoms when opioid treatment is interrupted makes the clinical use of opioids for long term pain management inadequate (Liu and Anand, 2001). In rats, opioid-induced withdrawal symptoms are associated with the release of ATP through pannexin-1 channels in the spinal cord from glial cells (Burma et al., 2017), most probably after activation of the purinergic P2X7 receptor. The importance of ATP release in the spinal cord can be appreciated with the pannexin-1 channel blockers mefloquine and probenecid, which are used clinically to block ATP release and thereby diminish the severity of withdrawal symptoms (Burma et al., 2017). This opens the possibility to target pharmacologically the ATP-releasing pannexin hemichannels to minimize the severity of withdrawal symptoms.

Elevation of extracellular ATP in the spinal cord is known to trigger symptoms that mimic neuropathic pain conditions. It was recently established that vesicular, release of ATP is also involved in neuropathic pain in mice (Masuda et al., 2016). Indeed, SLC17A9 $^{-/-}$ mice, with a deletion of both VNUT genes, do not demonstrate an elevation in spinal extracellular ATP concentration following nerve injury and the hypersensitivity, that is normally associated with nerve injury and chronic pain is diminished. This highlights the importance of purinergic signaling in the spinal cord in the establishment of neuropathic pain and it has recently been suggested that VNUT might be an interesting target to reduce neuropathic pain (Masuda et al., 2016; Sakamoto et al., 2014).

It is widely recognized that ATP and purinergic signaling represent a fundamental physiological system that is involved in regulating many neuronal and non-neuronal functions, including exocrine and endocrine secretion, immune responses, inflammation, development and the maintenance of neuropathic inflammatory pain among others (Burnstock, 2006a; Burnstock, 2006b; Burnstock and Knight, 2004; Fields and Burnstock, 2006). Recently, most literature on the role of ATP and pain has focused on chronic pain conditions, However, there is evidence that supports the idea that ATP is also involved in nociceptive processing during acute pain. For further details concerning the role of ATP and purinergic signaling in acute pain please see the extensive reviews by Tsuda, 2010 and Toulme, 2009 (Toulme et al., 2009; Tsuda et al., 2010).

1.7 Aim of the Thesis

As described earlier, noradrenaline, which is released from *Locus coeruleus* axons into the DH, is a strong modulator of nociceptive processing in the spinal cord. Spinal astrocytes express α_1-, α_2- and beta-adrenergic receptors, which might be activated by spinally released noradrenaline. Furthermore, the astrocytic networks, which are present in all layers of the dorsal horn might play an important role in the processing of incoming sensory information by modulating neuronal synaptic communication and transmitting intra- and inter-segmental information through the generation of propagating calcium waves and the release of gliotransmitters such as ATP.

Direct experimental evidence showing that noradrenaline can modulate purinergic signaling in the dorsal horn of the spinal cord is limited. However in 2015, through an elegant series of electrophysiological experiments, Seibt and Schlichter showed that in laminae III-IV of the dorsal horn of the spinal cord, noradrenaline increased the frequency of inhibitory GABAergic (and glycinergic) post-synaptic currents (IPSCs)). Moreover, the same study showed that inhibiting the metabolism of spinal cord glial cells with fluorocitrate or blocking purinergic transmission with the antagonist PPADS significantly reduced the action of noradrenaline on IPSCs frequency. The authors, therefore, concluded that in the dorsal horn of the spinal cord, glial cells, as well as ATP signaling, were key elements for the modulation of inhibitory synaptic transmission in lamina III-IV by noradrenaline (Seibt and Schlichter, 2015). In this context, it might be hypothesized that ATP released from glial cells following the action of noradrenaline might act on inhibitory interneurons to facilitate inhibitory synaptic transmission.

Therefore, the aims of this thesis were:

(1) to characterize the effects of noradrenaline and adrenergic receptor agonists on $[Ca^{2+}]_i$ in DH glial cells,

(2) to develop a method to detect ATP release from spinal astrocytes,

(3) to utilize this technique in order to characterize the effect of noradrenaline on ATP release from DH spinal astroglia.

2 Methods and Results

The results from my thesis work that are presented in this chapter will be divided into two parts. The first part is a reprint of our first published article “Eersapah V, Hugel S and Schlichter R. High-resolution detection of ATP release from single cultured mouse dorsal horn spinal cord glial cells and its modulation by noradrenaline. Purinergic Signal. 2019”. The second part of the results is the unpublished work that followed after the publication and is presented in the form of an article draft.

One major aim of this thesis was to study the release ATP of dorsal horn glial cells. However, from when we started our project there were few or no available method allowing to study ATP release with high sensitivity and high temporal precision. A substantial part of our research during the first study was therefore devoted to developing a novel technique to detect ATP from single dorsal horn glial cells. This technique was subsequently used to study the modulatory action of noradrenaline on ATP release from dorsal horn glia. Because a significant part of our results concerns the technical development that we further utilized as a method to advance our study, the results cannot hence be clearly separated from the methodological part. The methodological aspect is described in detail in the first part of the results (Eersapah et al., 2019).

Therefore we decided not to include a separate specific section on the methods and the cell system used. The methodological approach we used in the second part of the results was virtually identical to that of the first project and will therefore not be repeated here. However, we used several additional substances for the second project. There are presented in the table below.’

Table 15. List of additional chemicals used in the second project

Substance	Supplier	Stock conc.	Solubilized in	Storage
Idazoxan	Sigma-Aldrich[1]	2 mM	H_2O	- 20 ° C
α-methyl -noradrenaline	Sigma-Aldrich	10 mM	DMSO	- 20 ° C
Yohimbine	Tocris[2]	2 mM	H_2O	- 20 ° C
2-(2-Benzofuranyl)-2-imidazoline hydrochloride (2-BFI)	Sigma-Aldrich	5 mM	DMSO[3]	- 20 ° C
Clorgyline	Sigma-Aldrich	2 mM	Ethanol	- 20 ° C
Cimetidine	Sigma-Aldrich	5 mM	H_2O	- 20 ° C

1. Sigma-Aldrich, St. Louis, MO, USA
2. Tocris Bioscience, Bristol, United Kingdom
3. DMSO: Dimethyl sulfoxide

Results Project – 1

Context and main objective project 1

Although few in numbers, the noradrenergic neurons in the brain stem, send projections to virtually all major parts of the central nervous system including the dorsal horn of the spinal cord where noradrenaline has a well-documented role as a powerful modulator of the nociceptive system. Currently, most studies have attributed the analgesic effect of noradrenaline to neuronal α2-adrenoceptors (α2-AR) activation at the spinal level (Aston-Jones and Waterhouse, 2016; Millan, 2002). This effect of spinal α2-AR has also been demonstrated to have significant clinical relevance since intrathecal administration of specific α2-AR agonists (such as clonidine or dexmedetomidine) effectively produce analgesia in humans(Paris and Tonner, 2005). Importantly and often neglected aspect, is that adrenergic receptors have been identified not only in neurons but also in glial cells. This observation raises the possibility that a glial component could be involved in the mechanism through which noradrenaline produces spinal analgesia (Salm and McCarthy, 1990). Furthermore, most noradrenaline in the dorsal horn is not released at classical neuronal synapses, but rather seem to act through volume transmission. Under these conditions, noradrenaline could also reach and act through glial cells. However, although much effort has been devoted to clarifying the neuronal circuits and consequences of noradrenaline and adrenergic receptor activation, many elements underlying the action of noradrenaline within the dorsal horn of the spinal cord remain unidentified.

In 2015, Seibt and Schlichter provided compelling electrophysiological evidence that noradrenaline strongly facilitates inhibitory synaptic transmission in the dorsal horn through a mechanism that was critically dependent on both glial cells and ATP signaling (Seibt and Schlichter, 2015). These observations suggest that in addition to a direct action on neurons, noradrenaline could also act on glial cells to modulate the glial release of ATP. Therefore, in order characterize the mechanisms underlying the initial observations of Seibt and Schlichter, we aimed to investigate if dorsal horn glial cells, in mice, express functional receptors that can be activated by noradrenaline and, if so, how their activity could be related to the modulation of ATP release from glial cells.

Purinergic Signalling
https://doi.org/10.1007/s11302-019-09673-2

ORIGINAL ARTICLE

High-resolution detection of ATP release from single cultured mouse dorsal horn spinal cord glial cells and its modulation by noradrenaline

Varen Eersapah[1] · Sylain Hugel[1] · Rémy Schlichter[1]

Received: 17 May 2019 / Accepted: 12 July 2019

Abstract

Human embryonic kidney 293 (HEK293) cells stably transfected with the rat P2X2 receptor subunit were preincubated with 200 nM progesterone (HEK293-P2X2-PROG), a potent positive allosteric modulator of homomeric P2X2 receptors, and used to detect low nanomolar concentrations of extracellular ATP. Fura-2-loaded HEK293-P2X2-PROG cells were acutely plated on top of cultured DH glial cells to quantify ATP release from single DH glial cells. Application of the α1 adrenoceptor agonist phenylephrine (PHE, 20 μM) or of a low K^+ (0.2 mM) solution evoked reversible increases in the intracellular calcium concentration ($[Ca^{2+}]_i$) in the biosensor cells. A reversible increase in $[Ca^{2+}]_i$ was also detected in half of the biosensor cells following the interruption of general extracellular perfusion. All increases in $[Ca^{2+}]_i$ were blocked in the presence of the P2X2 antagonist PPADS or after preloading the glial cells with the calcium chelator BAPTA, indicating that they were due to calcium-dependent ATP release from the glial cells. ATP release induced by PHE was blocked by -L-phenylalanine 2-naphtylamide (GPN) that permeabilizes secretory lysosomes and bafilomycin A1 (Baf A1), an inhibitor of the H^+-pump of acidic secretory vesicles. By contrast, ATP release induced by application of a low-K^+ solution was abolished by Baf A1 but not by GPN. Finally, spontaneous ATP release observed after interrupting general perfusion was insensitive to both GPN and Baf A1 pretreatment. Our results indicate that ATP is released in a calcium-dependent manner from two distinct vesicular pools and one non-vesicular pool coexisting in DH glial cells and that noradrenaline and PHE selectively target the secretory lysosome pool.

Keywords Astrocyte · Exocytosis · Secretory lysosome · Vesicular release · Non-vesicular release

Introduction

The dorsal horn of the spinal cord (DH) is an important structure for the integration and the transmission of peripheral nociceptive information [1–3]. It is also a strategic site where potentially painful messages can be modulated, in particular by descending controls originating from supraspinal centers [3–5]. Noradrenergic projections from the brainstem have been shown to modulate nociceptive information at the spinal level [5, 6]. These descending noradrenergic projections to the DH originate mainly from the *Locus Coeruleus* (LC) [7] and are recruited during sustained activity of Aδ primary nociceptors [8] or during peripheral inflammation [9, 10].

Noradrenaline (NA) can inhibit glutamate release from primary afferents [11–15], decrease the excitability of DH neurons/interneurons [15, 16], and facilitate inhibitory (GABAergic and glycinergic) transmission in the DH [17–19]. From a behavioral point of view, NA and α adrenoceptor agonists induce antinociceptive effects when administered intrathecally [5, 20].

Adrenoceptors are expressed by DH interneurons [14–17] as well as by DH glial cells, at least in cultures of whole spinal cords [21]. In the DH, NA fibers form synaptic contacts with fine dendrites of intrinsic DH neurons but not with primary afferent terminals [22–24]. However, a large proportion of the contacts of noradrenergic fibers do not have the features of classical synapses suggesting the involvement of volume transmission [25]. Such "non-classical" contacts seem also common

Electronic supplementary material The online version of this article (https://doi.org/10.1007/s11302-019-09673-2) contains supplementary material, which is available to authorized users.

✉ Rémy Schlichter
schlichter@inci-cnrs.unistra.fr

[1] Centre National de la Recherche Scientifique (UPR3212), Institut des Neurosciences Cellulaires et Intégratives, Université de Strasbourg, 67000 Strasbourg, France

Published online: 23 August 2019

for serotonergic and dopaminergic fibers in the DH [26, 27]. Most importantly, more than 60% of contacts formed by noradrenergic and serotoninergic fibers in the DH appear to be of the "non-synaptic" type and to be established with astrocytic profiles [26]. These morphological results suggest that DH glial cells might represent important targets of the descending noradrenergic projections and therefore might participate in the modulation of nociceptive messages by NA at the spinal level.

Recently, we have shown that NA selectively increased inhibitory synaptic transmission in the DH [19]. This phenomenon involved α_1 and α_2 adrenoceptors and functional communication between deep and superficial laminae of the DH [19]. Moreover, blocking the metabolism of DH glial cells with fluorocitrate suppressed the modulatory effect of NA on inhibitory synaptic transmission [19], indicating a fundamental role of DH glia-to-neuron communication during noradrenergic modulation of inhibitory synaptic transmission. In addition, our data indicated that ATP seemed to play a major role as a signaling molecule in this interaction [19].

Therefore, the aim of the present work was to determine whether NA was able to trigger/modulate ATP release from DH glial cells and to characterize the mechanisms involved in this phenomenon. To this end, we developed and improved a sniffer cell/biosensor system that allowed us to detect low nanomolar concentrations of extracellular ATP and to quantify ATP release at the single cell level with excellent spatial and temporal resolutions.

Methods

Animal procedures

Mice were bred and housed in the animal facility Chronobiotron, UMS3415, accredited according to EU Directive 2010/63 and French regulations 2013-118. All procedures were conducted in conformity with the rules of the European Communities Council Directive 2010/63/EU, and the French regulations 2013-118. Pups were kept with their mothers until euthanasia by decapitation which is considered as an ethical method for very young animals.

Primary cultures of DH glial cell

Cultures of primary DH spinal cord glial cells were prepared from neonatal 3- to 6-day-old postnatal C57BL/6 mice pups of either sex. Animals were decapitated and a laminectomy was performed in order to expose the dorsal part of the lumbar spinal cord. After having removed the meninges with thin forceps, the dorsal half of the spinal cord (i.e., the region of the dorsal horn) was harvested and placed in cold (4 °C) Dulbecco's modified Eagle's medium/F-12 containing 15 mM HEPES (Gibco, France).

The collected spinal tissue was then dissociated mechanically using fire-polished Pasteur glass pipettes of decreasing tip diameters until obtaining a turbid solution containing the dissociated cells and tissue debris. This solution was centrifuged at 500 RPM for 5 min. The supernatant containing large debris was removed and discarded, and the pellet containing the glial cells was re-suspended in 2 mL of culture medium composed of Dulbecco's modified Eagle's medium supplemented with 10% (*v*/*v*) heat-inactivated horse serum (Gibco, France) and 0.5% (*v*/*v*) streptomycin/penicillin (at 5000 μg/mL and 5000 U/mL respectively, Gibco, France).

The cell suspension was seeded in the center of sterile 35-mm standard plastic culture dishes (Corning, USA) in which a central hole (18 mm) had been drilled and to the bottom of which a glass coverslip had been glued, thus delimiting a central well in the culture dish. The internal part of the glass bottom of the dishes was coated with poly-D-lysine (0.02 mg/mL, Sigma, France) in order to favor the attachment of the cells. After seeding, the cultures were placed and maintained in a 37 °C water-saturated incubator in an atmosphere containing air and 5% CO_2. Experiments were performed on confluent cells 2–3 weeks after seeding.

Maintenance of HEK293 cells

In order to detect ATP release from cultured DH glial cells, we used a human embryonic kidney 293 (HEK293) cell line that was stably transfected with the rat P2X2 receptor subunit [28]. This cell line, which we will refer to as HEK293-P2X2 later in the text, was kindly provided by Dr. François Rassendren (Institut de Génomique Fonctionnelle, Montpellier France). These cells express homomeric P2X2 receptors [28] and were previously used by us to characterize P2X2 receptor-mediated currents and their modulation by progesterone [29]. HEK293-P2X2 cells were cultured in sterile 75-mm^2 flasks (Thermo Scientific, Denmark) in a culture medium consisting of Dubelcco's modified Eagle's medium with 25 mM HEPES (Gibco) to which were added fetal calf serum (10% *v*/*v*, Gibco), penicillin-streptomycin (50 IU/mL each, Gibco), and glutamax (1% *v*/*v*, Gibco). The transfected sequence contained the rat P2X2 subunit sequence as well as a neomycin resistance cassette [28]. This allowed for the selection of P2X2-expressing HEK293 cells by culturing them in the presence of geneticin (0.5 mg/mL, G418, Gibco). The cultures were kept at 37 °C in a water-saturated incubator in an atmosphere composed of air and 5% CO_2. Before calcium imaging experiments, HEK293P2X2 cells were mechanically detached from the bottom of the culture flask by flushing the cells with a stream of culture medium by means of a 10-mL sterile plastic pipette. The medium containing the detached cells was then transferred to a 15-mL sterile plastic tube (Greiner Bio-One, Germany), and the volume was adjusted to 10 mL with standard culture medium. This solution was centrifuged at

500 RPM for 5 min, and the pellet was re-suspended in culture medium or extracellular medium used for calcium imaging experiments (see below). In order to prepare cultures of HEK293-P2X2 cells alone, cells were re-suspended in 2-mL standard culture medium, seeded on poly-D-lysine coated glass-bottom culture dishes and maintained as described for DH glial cultures in the preceding section. These cultures were used to determine the intrinsic properties of HEK293-P2X2 cells in calcium imaging experiments. Alternatively, HEK293-P2X2 cells were used as biosensor cells to detect ATP release from cultured DH glial cells. To this end, the dissociated HEK293-P2X2 cells were re-suspended in 2 mL of the serum-free HEPES buffer-based extracellular solution used for calcium experiments, loaded with fura-2 and plated on top of cultured DH glial cells just before the beginning of the experiments (see below).

Calcium imaging

Loading of cells with fura-2 Cultured DH glial cells or HEK293-P2X2 cells were washed several times with the extracellular HEPES-based extracellular solution used in all the calcium imaging experiments. This extracellular solution was composed of (in mM): NaCl 135, KCl 5, $CaCl_2$ 2.5, $MgCl_2$ 1, glucose 10, and HEPES 5 (pH = 7.4). Loading of cells was achieved by incubating them for 1 h at room temperature (22–25 °C) in extracellular medium containing 4 μM fura-2 acetoxymethyl ester (fura-2 AM) (Molecular Probes, USA), 0.001% (*w*/*v*) pluronic acid (Molecular Probes, USA) in order to facilitate fura-2 AM uptake by the cells. After loading, the cells were washed with extracellular medium and used for calcium experiments on the experimental setup.

In experiments in which HEK293-P2X2 cells were used as biosensors for ATP release from DH glial cells, the loading with fura-2 was performed on suspensions of HEK293-P2X2 cell (see above). This protocol was performed at room temperature (22–25 °C) following a protocol similar to that described above for glial cultures, except that the "loading-medium" also contained 200 nM progesterone (PROG, Sigma-Aldrich, USA) in order to potentiate P2X2 receptor function [29]. After 1-h incubation, this suspension of HEK293-P2X2 cells was diluted with 9 mL of extracellular solution and centrifuged at 500 RPM for 5 min. The pellet was rinsed two times with 10 mL of extracellular solution and re-suspended in 2 mL of extracellular solution. This suspension of fura-2- and progesterone-loaded HEK293-P2X2 cells was then seeded on top of cultured DH glial cells (200 μL per dish).

Measurements of changes in intracellular free calcium concentration ($[Ca^{2+}]_i$) To monitor changes in $[Ca^{2+}]_i$, culture dishes were transferred to the stage of an inverted fluorescence microscope (Axiovert 35; Zeiss, Gottingen, Germany) and the cells were visualized with a × 40 oil-immersion objective (Fluor 40; NA, 1.30; Nikon, Tokyo, Japan). The cultures were continuously superfused with extracellular medium, the temperature of which was maintained at 34 °C. Cells were allowed to habituate to this temperature for at least 15 min before starting the experiments. In experiments using HEK293-P2X2 cells as ATP biosensors, the fura-2- and progesterone-loaded cells (HEK293-P2X2-PROG cells) were seeded on top of the glial cells once the culture dishes of glial cells had been placed on the microscope stage. This procedure was performed at room temperature and in the absence of extracellular superfusion. Fifteen minutes after seeding, HEK293-P2X2-PROG cells had attached sufficiently to the glial cell layer and superfusion with heated extracellular solution was started. It should be noted that in biosensor experiments, only HEK293-P2X2-PROG cells were loaded with fura-2. Thus, the measured changes in $[Ca^{2+}]_i$ were solely due to changes in calcium levels in HEK293-P2X2-PROG cells since glial cells did not contain fura-2.

Calcium signals were acquired with a quantitative real-time imaging system comprising a cooled CCD camera (CoolSNAP HQ; Roper Scientific, Tucson, AZ, USA) and an image analysis software package (Imaging workbench 4.0; Axon Instruments, Molecular Devices). Cells were alternately excited at wavelengths of 350 and 380 nm with a lambda-10 filter wheel (Sutter instruments, USA), and emitted light was collected above 520 nm. Pairs of images were acquired every 1.1 s. Throughout the manuscript, intracellular calcium levels and their variations are expressed as the ratio of fluorescence signals (ratio F_{350}/F_{380}) measured at 520 nm after alternate excitation at 350 and 380 nm. This ratio was calculated after background signal subtraction. All experiments were performed at 34 °C.

Calcium imaging analysis For analysis, regions of interest (ROIs) corresponding to individual cells were selected manually offline using the Imaging workbench 4.0 software (Axon Instruments, Molecular Devices). ROIs were chosen based on cell responsiveness to a positive control in order to avoid any selection bias by the experimenter. For cultured glial cells, this positive control consisted in the existence of a large transient increase in $[Ca^{2+}]_i$ following the local application of 30 μM ATP at the end of the recording session. For HEK293-P2X2-PROG cells, only those that responded with an increase in $[Ca^{2+}]_i$ to a low (200 nM) concentration of exogenously applied ATP were considered in the analysis. This response corresponded to the change in $[Ca^{2+}]_i$ triggered by the selective activation of P2X2 receptors and attested cell ability to sense low concentrations of extracellular ATP (for details see "Results" section and Fig. 2). In a given field, all cells displaying an increase in $[Ca^{2+}]_i$ following the application of ATP were selected for analysis regardless of the fact that they responded or not to other substances applied during the experiment.

The acquired florescence signals were analyzed in more detail with the Clampfit 10.7.0 software (Molecular Devices) which allowed us to quantify baseline F_{350}/F_{380} ratio values as well as their changes during application of pharmacological substances. Measurements of area under the curve (AUC) of the calcium signals in fura-2-loaded HEK293-P2X2-PROG cells in contact with glial cells were used to quantify ATP release from glia under control and different experimental conditions (e.g., after treatment with vesicular release inhibitors). To this end, the experimental fluorescence values were divided by the mean F_{350}/F_{380} ratio value measured before application of the tested substance. This value was determined over a period of 500 s preceding substance application, and this procedure therefore normalized the basal fluorescence ratio value to 1 and the area under the curve (AUC) value corresponding to this control period to 500 (ratio of 1 during 500 s). Changes in ATP release were quantified by the changes in the AUC value in HEK293-P2X2-PROG cells that were induced by local application of noradrenaline, different adrenoceptor agonists, or a low K^+ containing extracellular solution (see below). These applications lasted 150 s and the AUC was measured over a 500-s period, which included the 150-s lasting application of the substance and a subsequent 350-s period outlasting the application time in order to include delayed/prolonged effects on ATP release from glial cells. The AUC determined during the 500-s period before application was compared to that measured during the 500-s following the onset of application of the substance to be tested. The increase in AUC triggered by the substance reflected the increase in ATP release from glia, since it was blocked by a P2X receptor antagonist (see "Results" section and Fig. 3) and was never observed in HEK293-P2X2-PROG cells cultured alone, i.e., in the absence of glia (online resource Fig. 7).

Pharmacological substances

Pharmacological substances to be tested were prepared as 1000 times concentrated stock solutions and diluted to their final concentration in extracellular solution just before the beginning of the experiments.

D,L-Noradrenaline hydrochloride, phenylephrine hydrochloride, clonidine hydrochloride, isoproterenol hydrochloride, adenosine triphosphate disodium salt (ATP), propranolol hydrochloride, prazosin hydrochloride, yohimbine hydrochloride (all Sigma-Aldrich, USA), and pyridoxalphosphate-6-azophenyl-2′,4′-disulfonic acid (PPADS) (Tocris, UK) were prepared in distilled water and stored at − 20 °C.

Fura-2-AM (Molecular Probes, USA), 1,2-Bis(2-aminophenoxy)ethane-*N*,*N*,*N*′,*N*′-tetraacetic acid tetrakis (BAPTA-AM) (Sigma-Aldrich, USA), bafilomycin A1 (Abcam, Cambridge, UK), and glycyl-L-phenylalanine 2-naphthylamide (GPN) (Abcam, Cambridge, UK) were prepared in dimethyl sulfoxide (DMSO) and stored at 4 °C. Progesterone (PROG, Sigma-Aldrich, USA) was prepared in ethanol 70% (*v*/*v*) and stored at 4 °C.

Application of substances

During all calcium imaging experiments, the cells were continuously superfused with extracellular solution preheated at 34 °C. The total bath volume was 2 mL and perfusion rate was 3 mL/min. Substances to be tested were applied locally by means of a gravity-driven multichannel perfusion device consisting of independent 5-mL syringes connected via separated polyethylene tubings to a common final outlet, i.e., a 0.9-mm metal needle placed just above the cells. The substance to be applied was selected by opening a tap placed between the syringe and the polyethylene tube connected to this syringe. Outside application periods, standard extracellular solution was continuously flowing through the application system to the cells via one of the application channels that remained open. During application of a substance, the tap of the control extracellular solution channel was closed simultaneously with the opening of the tap of the substance to be tested. The reverse procedure was followed at the end of the application period of the substance.

In all experiments, we checked that switching between two channels containing extracellular solution did not produce mechanical artifacts that could trigger an increase in $[Ca^{2+}]_i$. We also verified that application of vehicle/solvents such as ethanol, H_2O, or DMSO in which stock solutions of substances were prepared did not induce changes $[Ca^{2+}]_i$. In some experiments, increases in $[Ca^{2+}]_i$ were triggered by applying a low K^+ solution [30, 31]. To this end, the concentration of KCl in the extracellular solution was reduced from 5 to 0.2 mM, and the NaCl concentration was increased from 135.0 to 139.8 mM. Application of this low K^+ solution never increased $[Ca^{2+}]_i$ in HEK293-P2X2-PROG cells cultured alone (online resource Fig. 7).

Incubation of cells with substances

In some of the experiments, DH glial cells were pre-incubated with pharmacological substances in order to block increases in $[Ca^{2+}]_i$ (BAPTA-AM), release of secretory lysosomes (GPN) or release of acidic vesicles (bafilomycin A1). All incubations were performed at room temperature, and the substances were added at their final concentration to the extracellular HEPES-based medium used for calcium imaging experiments. The concentrations and times of incubation were as follows: BAPTA-AM (10 μM, 1 h), GPN (100 μM; 20 min), and bafilomycin A1 (0.2 μM; 90 min). Concentration and incubation times for the different substances were chosen according to those used in similar studies and published in the scientific literature: BAPTA-AM [32], GPN [33, 34], and bafilomycin A1 [35].

Fitting of dose-response curves

Dose-response curves for ATP were described with the following equation: $y = 100/(1 + (EC_{50}/[ATP])^{\wedge}A_H)$ where y is the proportion of responding cells and A_H a Hill coefficient.

Statistical analysis

Statistical data analyses were performed using the statistical software Kyplot 5.0. (KyensLab, Tokyo, Japan). Proportions in contingency tables were compared with Fisher's exact test (http://quantpsy.org/fisher/fisher.htm). Comparison between means was performed with paired or unpaired (as appropriate) Student's t test. The significance level for statistical tests was set as $\alpha = 0.05$. Symbols to indicate P values that are used in the figures are as follows: $^{****}P < 0.00001 < ^{***}P < 0.0001 < ^{**}P < 0.001 < ^{*}P < 0.05 <$ n.s (not significant).

Most results are expressed as proportion of responsive cells given as X/n where X is the number of responsive cells and n the total number of cells tested.

The other numerical results are given as mean ± s.e.m. (standard error to the mean).

Results

DH glial cell cultures

Our aim was to use a mixed DH glial cell culture rather than isolated "purified" glial cell populations in order to maintain the coexistence and the interaction between the major DH glial cell types in culture. Different considerations indicate that our cultures contained no neurons and mainly astrocytes. The absence of neurons was suggested by calcium imaging experiments showing that the application of a depolarizing extracellular solution containing a high (50 mM) K^+ concentration did not induce an increase in $[Ca^{2+}]_i$ that is typical for neurons, including for DH neurons in culture [30, 36] (online resource Fig. 8). The absence of neurons was most probably due to the purely mechanical dissociation protocol that we used. Indeed, we have a long-standing experience in the preparation of primary postnatal DH mixed neuron-glia cultures [37, 38] and we have clearly established that, in order to obtain viable neurons, it is necessary to use an enzymatic dissociation followed by a very mild mechanical dissociation. When mechanical dissociation is used alone or is too intense, neurons do not survive.

In addition, it has been clearly established that, among glial cells, α_1 adrenoceptors are expressed by astrocytes but not by microglia even in cell culture [39]. In our cultures, 90% of the cells responded to the α_1 adrenoceptor-specific agonist phenylephrine (PHE, see below) suggesting that astrocytes were the main glial cell type present in these cultures. Moreover, during calcium imaging experiments, we observed that the cells displaying an increase in $[Ca^{2+}]_i$ upon stimulation with PHE had a flattened star-shaped morphology that is characteristic of astrocytes in culture.

Taken together, these arguments indicate that the majority of cells present in our cultures appeared to be astrocytes.

Effect of NA and adrenoceptor agonists on intracellular-free calcium concentration ($[Ca^{2+}]_i$) in DH glial cells

Local application of NA (20 μM, 50 s) induced an increase in $[Ca^{2+}]_i$ in 86.0% of the cells tested (172/200). Three types of responses were observed (Fig. 1a). In the majority of cases, cells responded with a type 1 response that consisted of an initial fast transient peak followed by lower amplitude plateau phase that slowly declined but persisted during the whole duration of NA application. Type 1 responses were observed in 85.5% (147/172) of the NA-responsive DH glial cells. A second type of response (type 2) consisted of an initial peak followed by oscillations in $[Ca^{2+}]_i$ that occurred during the plateau phase. Such oscillatory responses were recorded in 11.0% (19/172) of the cells. Finally, a small proportion of cells, i.e., 3.5% (6/172), displayed a type 3 response that consisted of a single initial peak with no detectable plateau phase or oscillations in $[Ca^{2+}]_i$.

We next tested the classical α1, β, and α2 adrenoceptor agonists phenylephrine (PHE, 20 μM), isoproterenol (ISO, 10 μM), and clonidine (CLO, 20 μM), respectively. As illustrated in Fig. 1b, PHE, ISO, and CLO induced increases in $[Ca^{2+}]_i$ in 95.0% (132/139), 23.7% (47/198), and 6.1% (7/114) of the cells, respectively. The proportion of responses to PHE was significantly reduced to 5.1% (4/79) in the presence of the α1 adrenoceptor antagonist prazosin (2 μM) (Fisher's exact test, $P = 9.4 \times 10^{-45}$). Similarly, the proportion of responses to ISO was significantly reduced to 7.0% (4/57) by the β adrenoceptor antagonist propranolol (20 μM) (Fisher's exact test, $P = 0.03$). By contrast, the proportion of responses to CLO was very low (6.1% see above) and not significantly modified by the α2 adrenoceptor antagonist yohimbine (1 μM) (1.7%, 1/58, Fisher's exact test; $P = 0.265$). In agreement with these observations, we found that a cocktail of prazosin, propranolol, and yohimbine virtually abolished the responses to NA (5.1%, 4/79, Fisher's exact test; $P = 4.0 \times 10^{-38}$). Figure 1c summarizes the proportions of types 1, 2, and 3 responses observed following the application of NA, PHE, ISO, and CLO. Interestingly, in the majority of cases (90.2%, 101/112), the responses triggered by PHE could be reproduced at least 2 times in the same cells (online resource Fig. 9).

Taken together, our results suggest that NA increased $[Ca^{2+}]_i$ in about 90% cultured DH glial cells and that this effect was largely mimicked both qualitatively and quantitatively by the α1-agonist PHE. In addition, about 25% of the

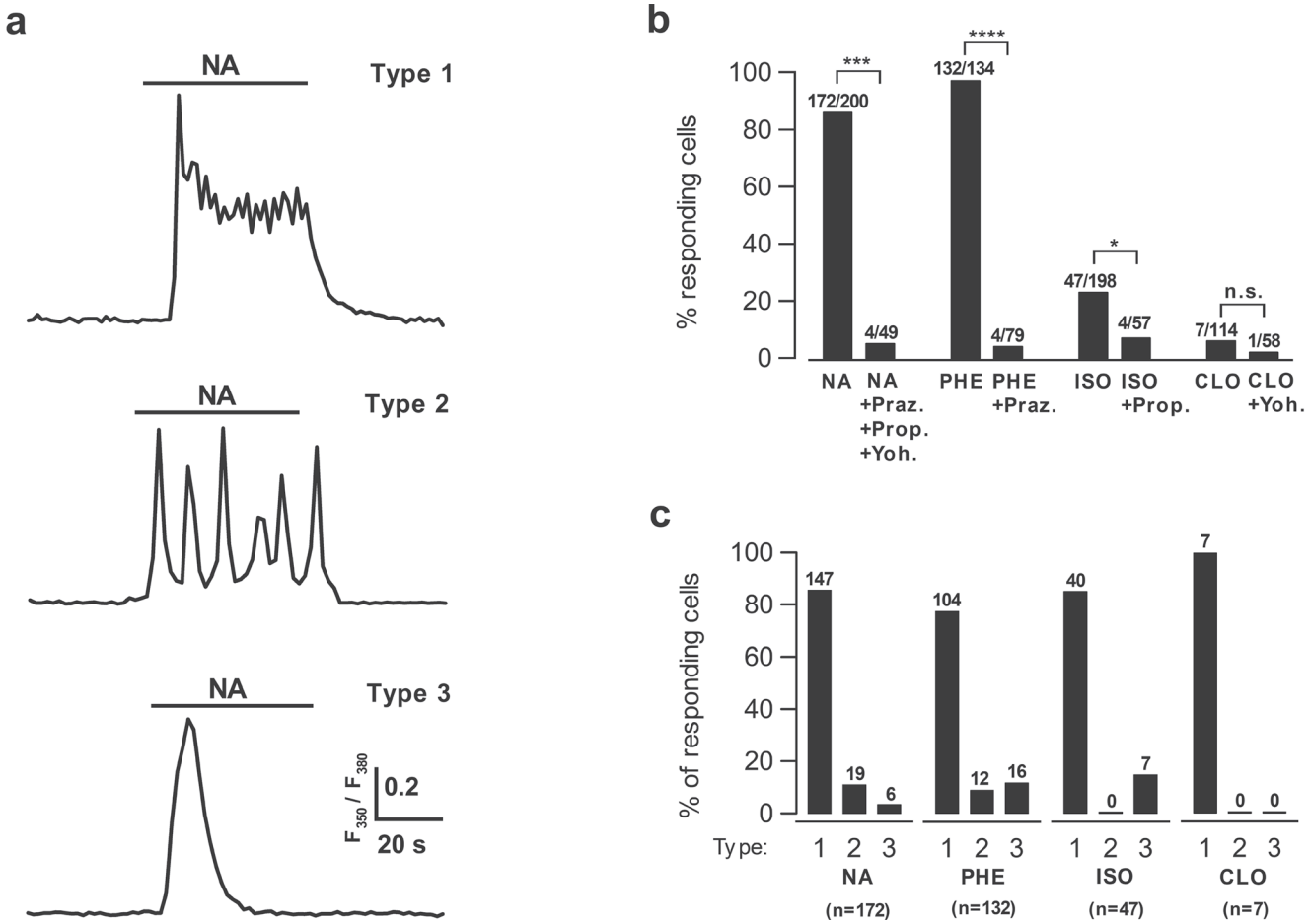

Fig. 1 Effect of noradrenaline (NA) and different adrenoceptor agonists on $[Ca^{2+}]_i$ in cultured fura-2-loaded DH glial cells. **a** Application of NA (20 μM, 50 s) elicited three types of $[Ca^{2+}]_i$ responses that consisted of a peak and a plateau (type 1), oscillations in $[Ca^{2+}]_i$ (type 2), or a single initial peak (type 3). **b** Effect of different classical adrenoceptor agonists on $[Ca^{2+}]_i$ in DH glial cells. Phenylephrine (PHE 20 μM, 50 s), an α1 adrenoceptor agonist, reproduced the effect of NA, whereas isoproterenol (ISO, 10 μM, 50 s), a β adrenoceptor agonist, or clonidine (CLO 20 μM, 50 s), an α2 adrenoceptor agonist, increased $[Ca^{2+}]_i$ in very small fractions of cells. The effects of the adrenoceptor agonists were significantly reduced by classical antagonists of these receptors, i.e., prazosin (Praz, 2 μM), an α1 adrenoceptor antagonist, propranolol (Prop, 20 μM), a β adrenoceptor antagonist but not yohimbine (Yoh, 1 μM), an α2 adrenoceptor antagonist. The effect of NA was potently reduced by a combination of all three antagonists. Fisher's exact test $^{****}P < 0.0001$, $^{***}P < 0.001$, $^{*}P < 0.05$, n.s. not significant. In this and following figures, the ratios of numbers above the columns of the histograms indicate the proportion of responding cells. **c** Occurrence of type 1, 2, and 3 responses among DH glial cells that responded to NA (20 μM), PHE (20 μM), CLO (20 μM), or ISO (10 μM). The total number of cells sampled is given by *n* and indicated below the histograms for each agonist tested. In this and following figures, the single numbers above the columns of the histograms indicate the number of responding cells within the total sample

cells displayed a response to ISO but virtually none to CLO. We therefore decided to investigate in more detail the effects of PHE and NA on the release of ATP from DH glial cells.

Detection of extracellular ATP by an improved biosensor system

In order to detect the release of ATP from DH glial cells and its modulation by NA and PHE, we used a biosensor/sniffer cell approach. We chose this option because, once released in the extracellular space, ATP is rapidly metabolized by ectonucleotidases [40–42] making it difficult to detect accurately this short-lived molecule. We decided to use HEK293 cells stably transfected with rat P2X2 receptors (HEK293-P2X2) [28] as a detection system for extracellular ATP, since these receptors are highly permeable to Ca^{2+} ions [43] and Ca^{2+} influx through these receptors can be detected by calcium indicators such as fura-2. The general idea of our approach was to plate fura-2-loaded HEK293-P2X2 cells on top of cultured DH glial cells. Under these conditions, changes in $[Ca^{2+}]_i$ measured in HEK293-P2X2 cells will reflect and allow to monitor the changes in ATP release from glial cells following the application of NA and PHE (see below) with good spatial and temporal resolutions.

When ATP was applied to HEK293-P2X2 cells cultured alone and loaded with fura-2, we observed an increase in $[Ca^{2+}]_i$. The dose-response relationship illustrating the proportion cells displaying an increase in $[Ca^{2+}]_i$ for increasing

concentrations of ATP applied is illustrated in Fig. 2a. The apparent EC_{50} of ATP was 0.75 ± 0.02 μM. Under these conditions, it was difficult to detect low nanomolar concentrations of ATP. Indeed, application of 200 nM ATP triggered small calcium responses in only 5.3% (4/76) of the cells (Fig. 2b), corresponding approximately to the EC_5 of our dose-response curve. However, we have previously shown that rat P2X2 receptors can be strongly and selectively potentiated by the steroid/neurosteroid progesterone (PROG) [29]. Figure 2b shows that acute application of PROG (5 μM) to HEK293-P2X2 cells for 100 s did not evoke any significant increase in $[Ca^{2+}]_i$. However, when ATP (200 nM), which initially triggered small and rare responses before PROG application, was applied to HEK293-P2X2 cells after they had been exposed to PROG (5 μM), it evoked large increases in $[Ca^{2+}]_i$ in the large majority of the cells (75.9%, 41/54, Fig. 2b). PROG, PROG-

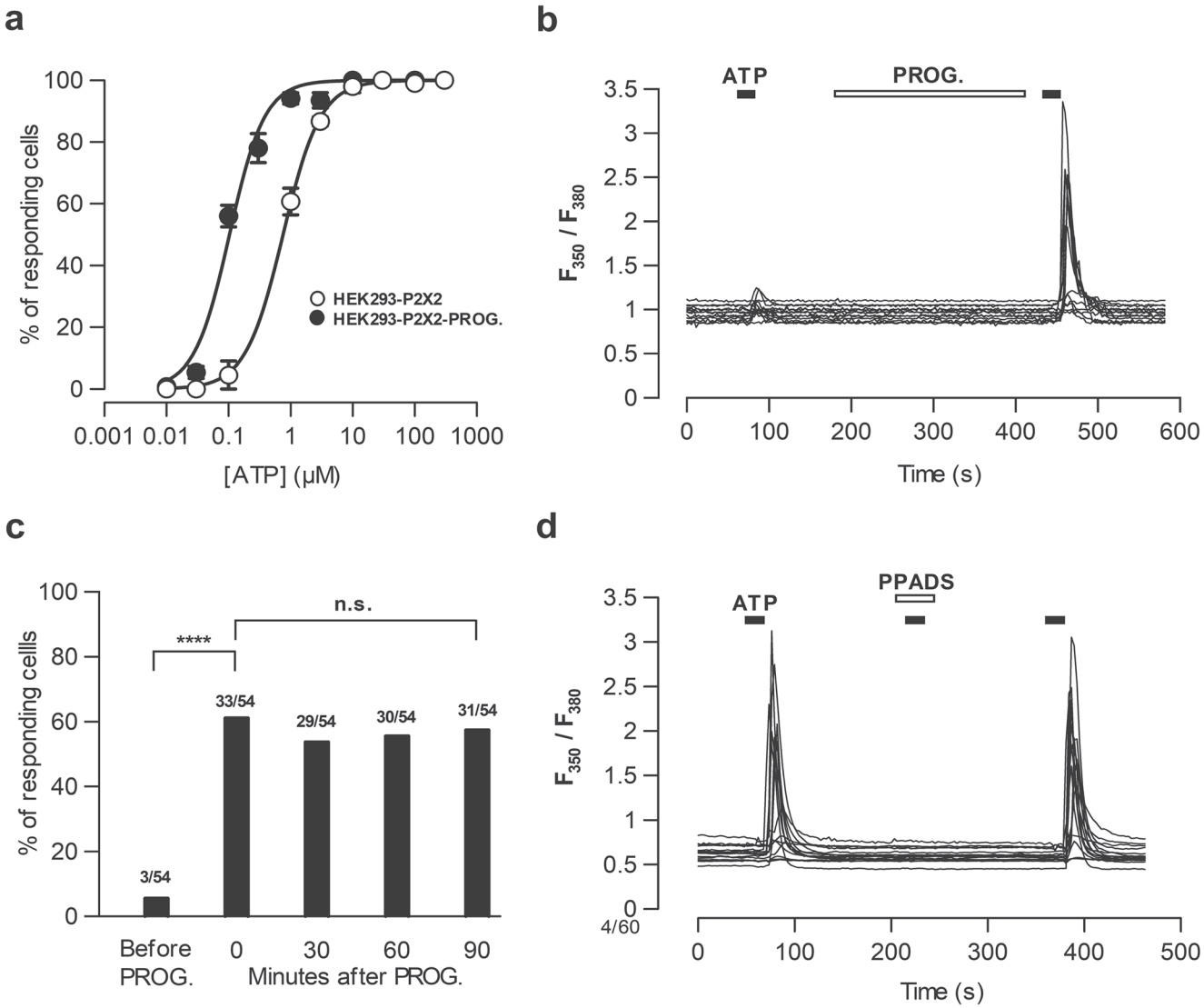

Fig. 2 Characterization of the ATP biosensor detector system. **a** Proportion of HEK293 cells stably transfected with the rat P2X2 subunit (HEK293-P2X2 cells) responding to various concentrations of locally applied ATP. The dose-response relationship of ATP on HEK293-P2X2 cells (open circles) indicated an apparent EC_{50} of 0.75 ± 0.02 μM. When cells were preincubated for 1 h with 200 nM PROG (HEK293-P2X2-PROG, filled circles), the dose-response curve was shifted to the left (EC_{50} of 0.10 ± 0.01 μM) reflecting an increased detection capacity at low ATP concentrations. Each point represents mean ± s.e.m. ($32 \le n \le 142$ cells and $3 \le n \le 5$ experiments per data point). **b** A low concentration of ATP (200 nM) triggered small amplitude increases in $[Ca^{2+}]_i$ in a small fraction of HEK293-P2X2 cells. Application of PROG (5 μM) alone did not induce a change in $[Ca^{2+}]_i$. However, after PROG application, a larger fraction of HEK293-P2X2 displayed $[Ca^{2+}]_i$ responses following ATP (200 nM) application, indicating an increase in detection capacity of ATP by these cells. **c** The fraction of cells responding to 200 nM ATP was significantly increased after incubation with PROG (200 nM, 1h) and persisted for at least 90 min after PROG wash-out without significant attenuation. Fisher's exact test, $^{****}P < 0.00001$, n.s. not significant. n.s. applies to each of the individual time points (30, 60, 90) compared to time point 0. **d** In cells preincubated with a low concentration of PROG (200 nM) for 1 h (HEK293-P2X2-PROG), a low concentration of ATP (200 nM) induced large increases in $[Ca^{2+}]_i$ that were completely and reversibly blocked by the P2X2 receptor antagonist PPADS (50 μM)

derived metabolites, and other steroids are lipophilic molecules that solubilize easily in the hydrophobic part of the plasma membrane where they remain for considerable periods of time [44, 45]. In agreement with this, we noticed that the potentiating effect of PROG (5 μM) persisted after the end of the application of PROG (Fig. 2b). Similar observations were made when HEK293-P2X2 cells were incubated for 1 h with a much lower concentration of PROG (200 nM), and this phenomenon was quantified in a sample of 54 cells (Fig. 2c). After preincubation with 200 nM PROG for 1 h, the potentiating effect of PROG lasted for at least 90 min without significant attenuation (Fig. 2c). The effect of PROG was due to the positive modulation of P2X2 receptors because ATP receptors mediating the increase in $[Ca^{2+}]_i$ were blocked by the P2X2 receptor antagonist PPADS (50 μM) (Fig. 2d). After PROG exposure, none of the cells tested (0/41) displayed an increase $[Ca^{2+}]_i$ to ATP (200 nM) in the presence of PPADS (50 μM) (Fisher's exact test, $P = 1.6 \times 10^{-17}$). Moreover, ATP (200 nM) rarely induced an increase in $[Ca^{2+}]_i$ in non-transfected HEK293 cells (5.3%; 2/38) and these responses were not inhibited by PPADS (50 μM). The complete dose-response relationship for ATP after PROG (200 nM, 1 h) is illustrated in Fig. 2a. After PROG pretreatment, the EC_{50} value decreased to 0.10 ± 0.01 μM yielding a 7.5-fold increase in the sensitivity of ATP detection in our system.

Taken together, these results suggest that PROG-potentiated P2X2 receptors stably expressed by HEK293 cells represent an excellent tool to detect low nanomolar concentrations of extracellular ATP.

Quantification of ATP release from cultured DH glial cells

In order to detect and quantify ATP release from cultured glial cells, HEK293-P2X2 cells were loaded with fura-2-AM and incubated with 200 nM PROG for 1 h at room temperature and then plated on top of confluent DH glial cell cultures (see "Methods" section). Since only HEK293-P2X2 cells were loaded with fura-2, changes in $[Ca^{2+}]_i$ reflected either spontaneously occurring calcium fluctuations in these cells and/or activation of P2X2 receptors by ATP released from DH glial cells in close contact with the HEK293-P2X2 cells.

In an initial set of experiments, we quantified the spontaneously occurring changes in $[Ca^{2+}]_i$ in HEK293-P2X2 cells pre-incubated with PROG but cultured alone (i.e., in the absence of DH glial cells). Under these conditions, the $[Ca^{2+}]_i$ levels were usually very stable and rarely displayed spontaneously occurring peaks in $[Ca^{2+}]_i$ (6.8%; 10/146). When observed, the frequency of peaks was very low ($2.8 \times 10^{-3} \pm 4.4 \times 10^{-4}$ Hz, $n = 10$). Moreover, these cells rarely displayed increases in $[Ca^{2+}]_i$ following the application of NA (20 μM) nor PHE (20 μM). Indeed, we observed an increase in F_{350}/F_{380} ratio in only 2% (2/99) of the cells, and this change consisted of a single peak (type 3 response in Fig. 1a). Calcium peaks occurring spontaneously in HEK293-P2X2-PROG cells plated on top of DH glial cells were also relatively rare and represented 11.9% of the cases (19/160). This proportion of cells was not significantly different from that of HEK293-P2X2-PROG displaying calcium peak in the absence of DH glial cells (Fischer's exact test; $P = 0.17$). Moreover, the mean frequency of peaks was not different from that in the absence of glia ($3.0 \times 10^{-3} \pm 2.1 \times 10^{-4}$ Hz, $n = 42$; Fisher's exact test; $P = 0.75$).

In contrast, when PROG-loaded HEK293-P2X2 cells (HEK293-P2X2-PROG) were seeded on top of DH glial cell cultures, application of NA (20 μM) or PHE (20 μM) induced the appearance of peak-like increases of $[Ca^{2+}]_i$ in the HEK293-P2X2-PROG cells (Fig. 3a1, b1). In 23 cases, HEK293-P2X2-PROG cells displayed spontaneous calcium peaks before the application of NA (20 μM). The mean frequency of peaks was of $3.0 \times 10^{-3} \pm 2.8 \times 10^{-4}$ Hz ($n = 23$). After application of NA (20 μM), the frequency of peaks significantly increased to $4.3 \times 10^{-3} \pm 3.3 \times 10^{-4}$ Hz ($n = 23$, Fisher's exact test; $P = 0.007$). Similarly, in 19 cases, HEK293-P2X2-PROG cells displayed spontaneous calcium

Fig. 3 Detection of ATP release from DH glial cells by HEK293-P2X2-PROG cells and its modulation by NA and PHE. HEK293-P2X2 cells preincubated with PROG (200 nM, 1 h) were plated on top of DH glial cells and served as detectors of ATP released from the glia. Only HEK293-P2X2-PROG cells were loaded with fura-2. **a1** Application of NA (20 μM, 150 s) induced and increase in $[Ca^{2+}]_i$ in a biosensor HEK293-P2X2-PROG cell. The response consisted of peak-like increases in the fura-2 fluorescence ratio (F_{350}/F_{380}) observed not only during NA application but also after the end of the application. **a2** Histogram showing the occurrence of fluorescence ratio peaks before, during, and after application of NA (20 μM, 150 s). The histogram was obtained by pooling the observations from 89 different biosensor cells. Note the very small number of peaks before NA application and the increase in the number of peaks during and following NA application. **b1**, **b2** Application of PHE (20 μM, 150 s) mimicked the effect of NA. Histogram obtained by pooling the observations from 68 biosensor cells. **c** When DH glial cells were preloaded with the calcium chelator BAPTA-AM (10 μM, 1 h) before adding the HEK293-P2X2-PROG cells on top of them, application of PHE (20 μM) failed to induce any change in F_{350}/F_{380} fluorescence ratio, indicating that ATP was no longer released from DH glial cells under these conditions. **d** In the steady presence of PPADS (50 μM) added to the extracellular medium, PHE did not induce changes in $[Ca^{2+}]_i$, demonstrating that the calcium signals induced by PHE were mediated by P2X2 receptors present on the detector HEK293-P2X2-PROG cells. **e** Quantification of ATP release from DH glial cells by calculating the area under the curve (AUC) of the calcium signal measured in the detector HEK293-P2X2-PROG cells. The AUC was determined over a period of 500 s before (baseline, BL) and after the application of PHE for individual cells under different experimental conditions: standard conditions (PHE), when DH glial cells were preloaded with BAPTA (PHE (BAPTA)) and in the steady presence of PPADS in the extracellular medium (PHE + PPADS). Statistical comparisons were made between PHE and corresponding BL for each experimental condition using a paired Student's *t* test. ****$P < 0.0001$; n.s. not significant). Values of AUC are expressed in arbitrary units (a.u.). *n* values are between 68 and 87

peaks before the application of PHE (20 μM). The mean frequency of peaks was of $3.0 \times 10^{-3} \pm 3.2 \times 10^{-4}$ Hz ($n = 19$). After application of PHE (20 μM), the frequency of peaks significantly increased to $4.4 \times 10^{-3} \pm 5.6 \times 10^{-4}$ Hz ($n = 19$, Fisher's exact test; $P = 4.0 \times 10^{-3}$).

In order to facilitate the representation of the effects of NA and PHE on calcium peaks, data from all responsive cells were pooled. These data are presented in Fig. 3a2, b2 under the form of histograms of the number of calcium peaks as a function of time before, during, and after the application of NA and PHE. Application of NA (20 μM) or PHE (20 μM) induced an increase in the number of $[Ca^{2+}]_i$ peaks that outlasted the duration of NA or PHE application.

Interestingly, an increase in the number/frequency of calcium peaks by NA or PHE could be induced only by the first application of these agonists. A second application, even if performed 1000 s after the first application did not induce the appearance or the increase in frequency of $[Ca^{2+}]_i$ peaks, whereas effects on calcium responses in DH glial cells alone could be reproduced at least two times (see above). The

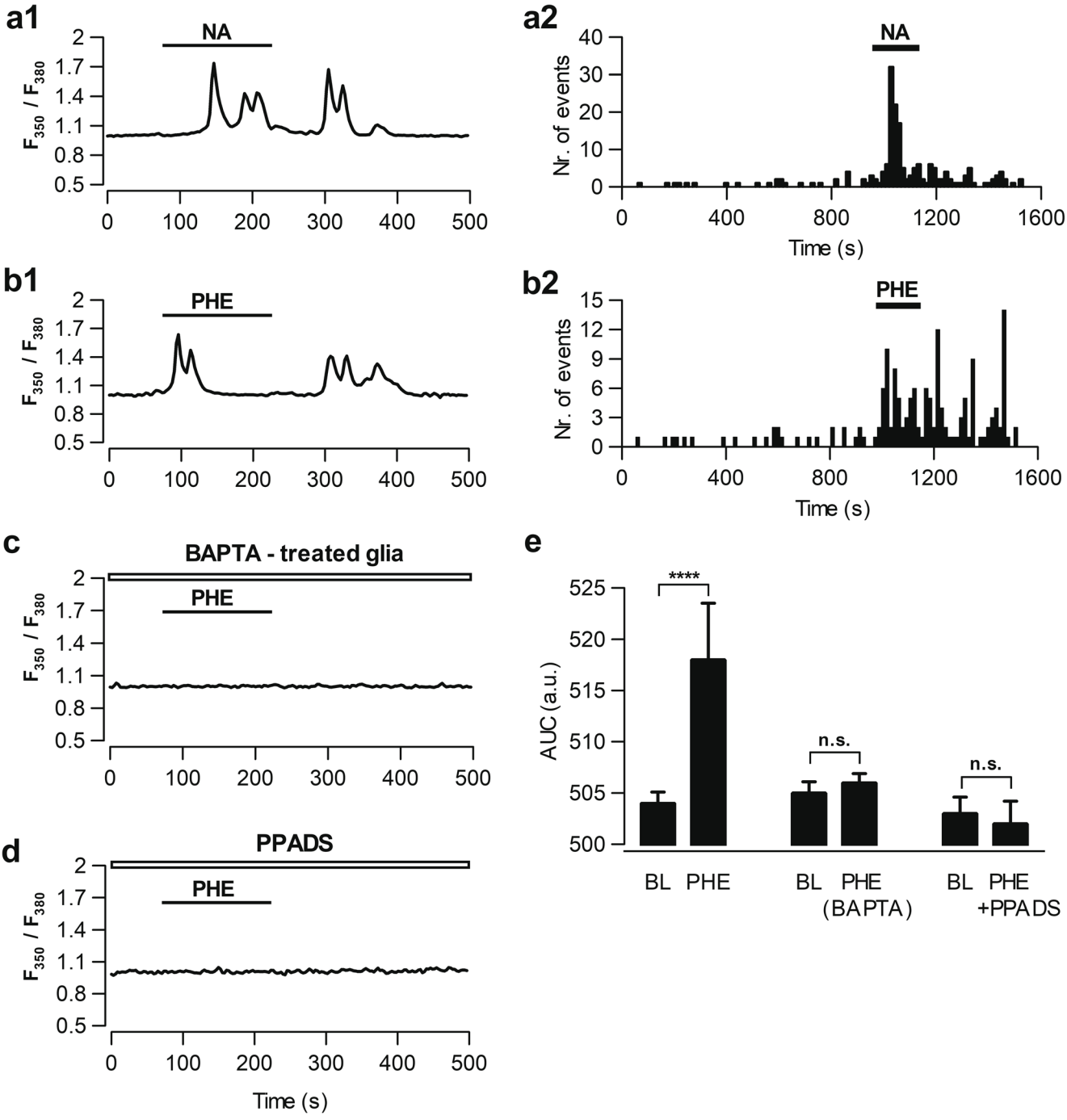

calcium signals induced by PHE were never observed when DH glial cells were pre-loaded with BAPTA-AM (0/87, Fig. 3c) or when PPADS (50 μM) was added to the extracellular medium (0/71, Fig. 3d).

In order to quantify more precisely the changes in $[Ca^{2+}]_i$ that occurred in HEK293-P2X2-PROG cells, we determined the area under the curve (AUC) of the fura-2 signal and normalized each signal by dividing it by the value of the baseline, thus allowing to compare the results between different cells (see "Methods" section for more details). This was done for equivalent periods of time (i.e., 500 s) before and after application of PHE. As shown in Fig. 3e, PHE significantly increased the AUC from 504.8 ± 1.1 a.u. (arbitrary units) to 518.2 ± 5.0 a.u. ($n = 68$, paired Student's t test; $P = 6.2 \times 10^{-4}$). The effect of PHE was abolished by PPADS (50 μM) or after loading the DH glial cells with the calcium chelator BAPTA-AM (Fig. 3e). In the presence of PPADS (50 μM), the AUC was of 503.8 ± 1.6 a.u. before and of 502.0 ± 2.3 a.u. after application of PHE (20 μM) ($n = 70$). These values did not differ significantly (paired Student's t test; $P = 0.37$). When DH glial cells were preincubated with BAPTA-AM, the AUC was of 505.0 ± 1.1 a.u. before and of 506.0 ± 0.9 a.u. after application of PHE (20 μM) ($n = 87$). These values did not differ significantly (paired Student's t test; $P = 0.27$).

These results show that the increase in $[Ca^{2+}]_i$ involved the activation of PPADS-sensitive P2X2 receptors expressed by HEK293-P2X2 cells. Moreover, BAPTA specifically loaded into DH glial cells blocked the changes in $[Ca^{2+}]_i$ observed in HEK293-P2X2 cells indicating that these changes were due to a calcium-dependent release of ATP from the cultured DH glial cells.

Effect of reducing extracellular K^+ concentration on the release of ATP

Since NA and PHE triggered calcium-dependent release of ATP from cultured DH glial cells (see preceding section), we wondered whether other stimuli that increase $[Ca^{2+}]_i$ were able to induce ATP release from these cells.

It has been reported that application of an extracellular solution containing a low concentration of K^+ ions (low K^+) can induce the rise in $[Ca^{2+}]_i$ in astrocytes by activating Ba^{2+}-sensitive Kir4.1 inwardly rectyfing K^+ channels [30, 31]. We therefore first tested the effect of applying a low K^+ solution (in which the concentration of K^+ was reduced from 5 to 0.2 mM) to cultured DH glial cells loaded with fura-2. Application of this low K^+ solution rapidly induced a rise in $[Ca^{2+}]_i$ that lasted for the whole duration of the application (Fig. 4a). Increases in $[Ca^{2+}]_i$ were observed in a large majority cultured DH glial cells tested (87.1%, 54/62). Moreover, this increase in $[Ca^{2+}]_i$ could be reproduced several times in the same cells when applied at an interval of 1000 s (Fig. 4a). This low K^+-induced response was totally blocked (0/31) when 2 mM Ba^{2+} was added to the extracellular solution. Interestingly, when tested under the same experimental conditions, the low K^+ solution never induced a rise in $[Ca^{2+}]_i$ in PROG-treated HEK293-P2X2 cells cultured alone (0/150).

When we applied a low K^+ medium to fura-2-loaded DH glial cells, we observed an increase in $[Ca^{2+}]_i$ in 87.1% (54/62) of them (Fig. 4b). This proportion was unaffected in the presence of PPADS (50 μM) in the extracellular medium (88.6%, 39/4, $P = 1.0$) but significantly reduced after preloading of the glial cells with BAPTA-AM (3.2%, 1/31, $P = 6.0 \times 10^{-16}$).

Application of the low K^+ solution to co-cultures of DH glial cells and PROG-treated fura-2-loaded HEK293-P2X2 resulted in an increase in $[Ca^{2+}]_i$ in the HEK293-P2X2 cells (Fig. 4c). Such an effect was observed in 64.1% (84/131) of the recorded cells. None of the of HEK293-P2X2-PROG on top DH glial cells displayed an increase in $[Ca^{2+}]_i$ in the presence of PPADS (50 μM) in the extracellular medium (0.0%, 0/42, Fisher's exact test, $P = 1.5 \times 10^{-15}$) and the proportion of HEK293-P2X2-PROG with a calcium response was significantly reduced when the DH glial cells were preloaded with BAPTA-AM (0.0%, 0/37, Fisher's exact test; $P = 8.6 \times 10^{-14}$) (data not illustrated).

We further quantified this response by determining the relative AUC for each response (Fig. 4d). In the absence of any treatment, the AUC of the calcium response induced by low K^+ was of 523.0 ± 4.0 a.u. ($n = 131$). The AUC was of 503.7 ± 0.6 a.u. (= 42) in the presence of PPADS and of 503.2 ± 1.1 a.u. (= 37) after preloading the DH glial cells with BAPTA-AM (Fig. 4d). These values were significantly different from the AUC of the low K^+ calcium response measured in the absence of any treatment: PPADS, unpaired Student's t test; $P = 4.9 \times 10^{-4}$; and BAPTA-AM, unpaired Student's t test; $P = 1.9 \times 10^{-4}$).

Taken together, these results suggested that application of a low K^+ solution activated Ba^{2+}-sensitive (most probably Kir4.1) channels that triggered an increase in $[Ca^{2+}]_i$ which in turn led to a calcium-dependent release of ATP that was sensed by the transfected P2X2 receptors.

Distinct vesicular pools of ATP are mobilized by NA and low K^+ stimulation of cultured DH glial cells

In order to check whether calcium-dependent ATP release involved intracellular vesicles, we tested the effects of bafilomycin A1 (Baf A1) and glycyl-L-phenylalanine 2-naphtylamide (GPN). Bafilomycin A1 blocks the activity of the proton pump present on acidic vesicles that generates the pH gradient across the vesicle membrane that is necessary for the loading of the vesicles with the transmitter. Baf A1 acts on all types of acidic vesicles including light clear vesicles and secretory lysosomes [35, 46]. GPN is a substrate of cathepsin C, a lysosomal peptidase present in lysosomes [47]. GPN is

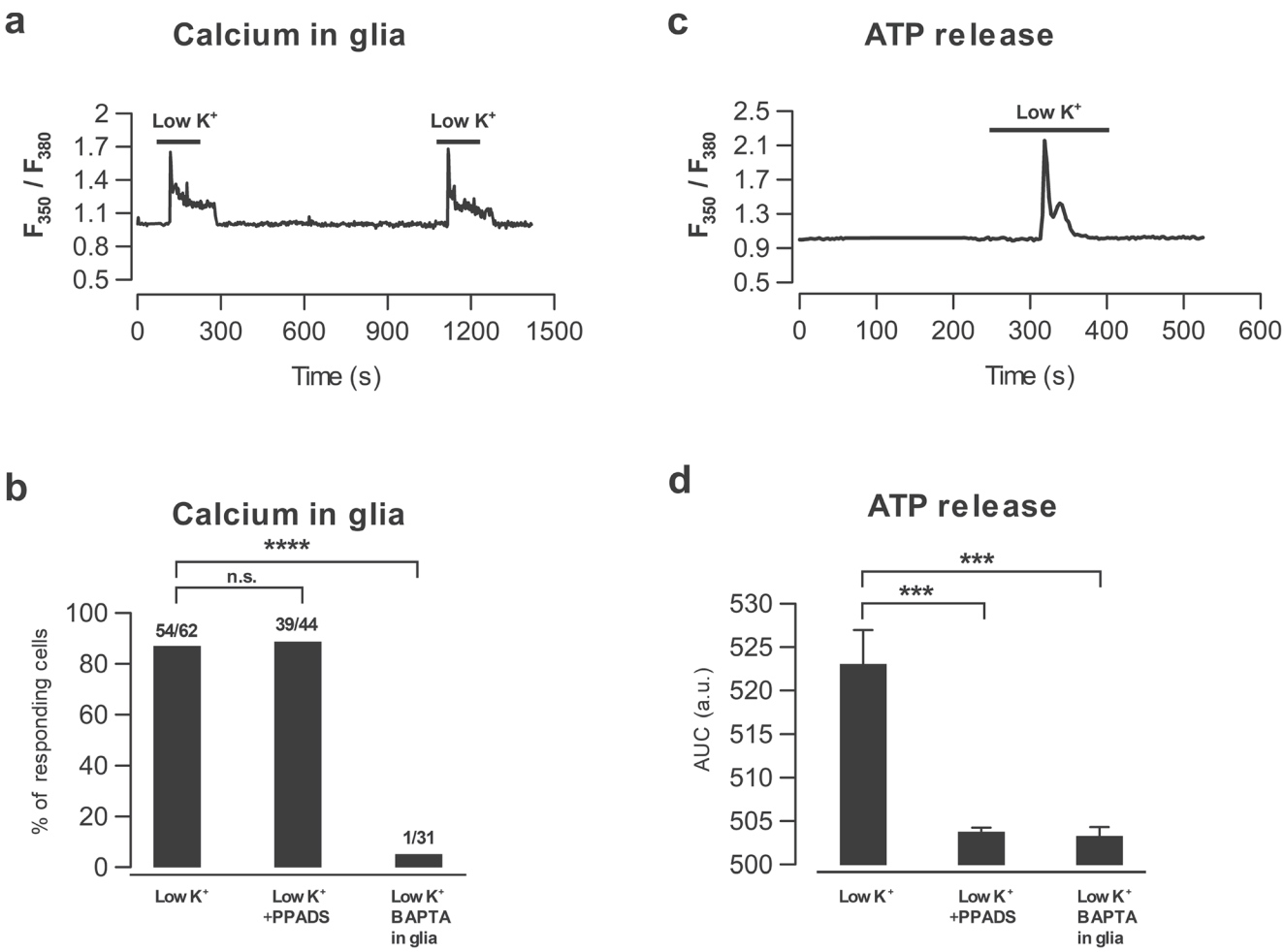

Fig. 4 Application of a low K^+ solution induced calcium-dependent ATP release from DH glial cells. **a** In fura-2-loaded DH glial cells, local application of an extracellular solution in which the concentration of K^+ was lowered to 0.2 mM (low K^+ solution) triggered an increase in $[Ca^{2+}]_i$ that lasted as long as the solution was applied and then rapidly returned to pre-application baseline levels. This effect of the low K^+ solution on $[Ca^{2+}]_i$ could be repeated at least two times in the same cell. **b** The proportion of DH glial cells displaying an increase in $[Ca^{2+}]_i$ following the application of the low K^+ solution was not affected in the presence of PPADS (50 μM) in the extracellular medium (88.6%, 39/44, Fisher's exact test, $P > 0.05$ n.s.) but strongly reduced when the glial cells were preloaded with the calcium chelator BAPTA (Fisher's exact test, ****$P < 0.0001$). **c** When fura-2-loaded HEK293-P2X2-PROG cells were plated on top of DH glial cells, application of a low K^+ solution triggered an increase in $[Ca^{2+}]_i$ indicative of ATP release from DH glial cells. **d** The mean AUC of the calcium signals measured in detector HEK293-P2X2-PROG cells following the application of the low K^+ solution was also significantly reduced when P2X2 receptors were blocked in the steady state presence of PPADS (50 μM) (unpaired Student's *t* test, ***$P < 0.001$) or when DH glial cells were preloaded with BAPTA-AM (unpaired Student's *t* test, ***$P < 0.001$). Number of cells was between 37 and 131

taken up by secretory lysosomes, and following hydrolysis by cathepsin C, it generates fragments that accumulate inside the secretory lysosomes and rapidly induces an intra-lysosomal hypertonic condition that leads to the permeabilization of these secretory lysosomes to low molecular weight substances [33, 34]. Incubation with GPN therefore induces a selective functional perturbation of secretory lysosomes [33, 34, 48]. We first verified that pretreatment with GPN and/or Baf A1 did not directly affect the change in $[Ca^{2+}]_i$ triggered by PHE or low K^+ solution in DH glial cells cultured alone.

Figure 5a summarizes the effects of GPN (Fig. 5a2) and Baf A1 (Fig. 5a3) on changes in $[Ca^{2+}]_i$ measured in fura-2-loaded, PROG-treated HEK293-P2X2 cells plated on top of cultured DH glial cells. When glial cells were pretreated with GPN, the proportion of responses to PHE was strongly decreased (6.3%, 5/80, Fisher's exact test; $P = 2.8 \times 10^{-18}$) and that responding to low K^+ was slightly reduced (41.3%, 33/80, Fisher's exact test; $P = 2.0 \times 10^{-3}$). After preincubation of the glial cells with Baf A1, there was a significant reduction of the proportion of the responses to PHE (11.8%, 8/68, Fisher's exact test; $P = 3.7 \times 10^{-13}$) as well as to low K^+ (5.9%, 3/51, Fisher's exact test; $P = 7.7 \times 10^{-12}$).

When glial cells were pretreated with GPN, the baseline value (BL) of the AUC was of 503.4 ± 1.1 a.u. ($n = 80$) and that after PHE (20 μM), application was of 503.8 ± 1.7 a.u. ($n = 80$). These values were not significantly different (paired

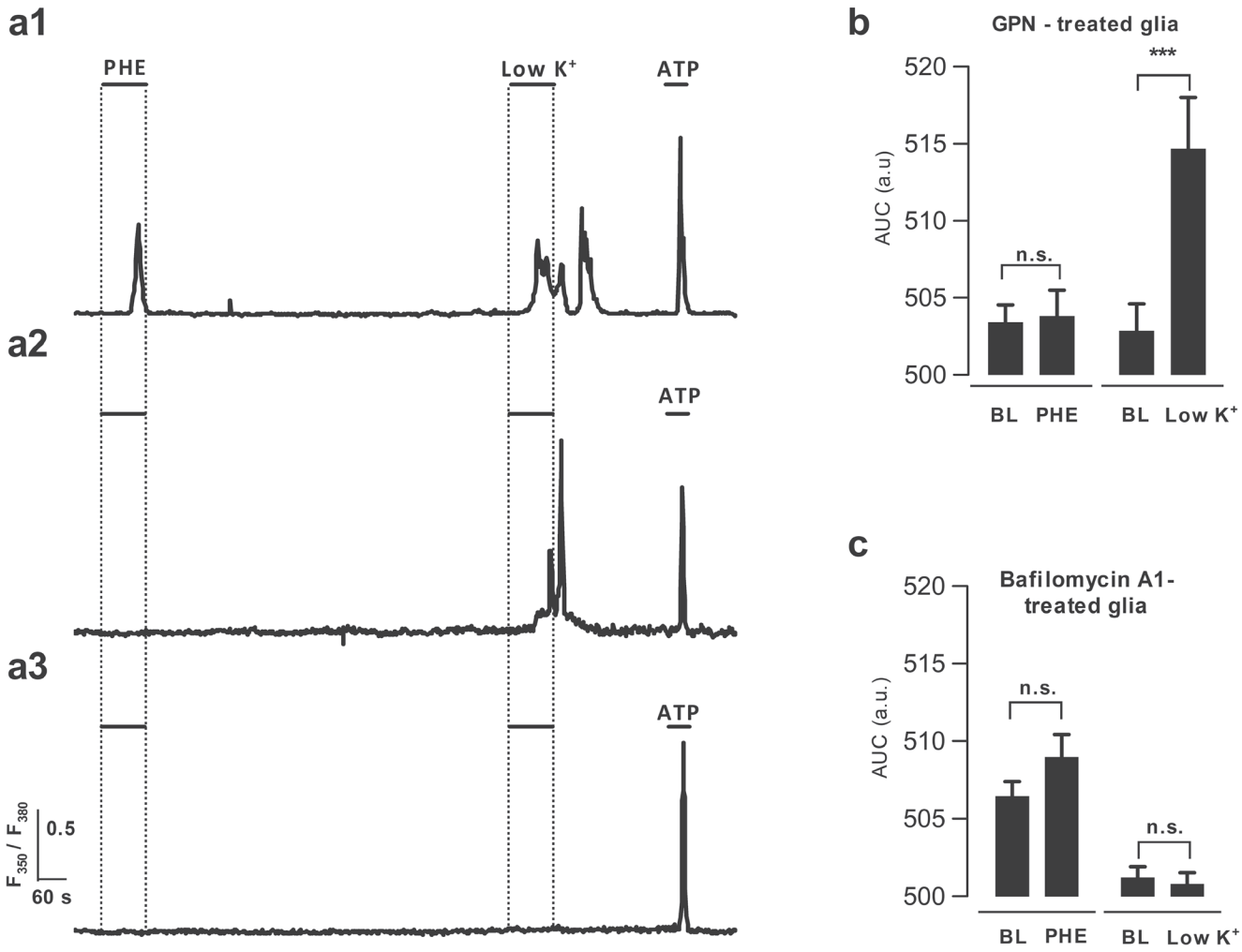

Fig. 5 Characterization of vesicular ATP release from DH glial cells and its modulation by PHE and low K^+. **a** Comparison of calcium responses in detector HEK293-P2X2-PROG cells plated on top of DH cultured glial cells under different experimental conditions: no treatment of glial cells (**a1**), pretreatment of DH glial cell cultures with GPN (100 μM, 20 min, **a2**), or with Baf A1 (0.2 μM, 90 min, **a3**). In each situation, we tested the application of PHE (20 μM), of a low K^+ solution, and of ATP (200 nM). Note that GPN or Baf A1 pretreatment abolished ATP release induced by PHE, but that only Baf A1 but not GPN prevented the release of ATP following low K^+ stimulation. In all cases, application of ATP (200 nM) increased $[Ca^{2+}]_i$ in the detector HEK293-P2X2-PROG cells indicating that they were able to detect low concentrations of ATP. **b**, **c** Quantification of the effects of pretreatment with GPN (**b**) or Baf A1 (**c**) by determination of the area under the curve (AUC) of the recorded calcium signals. The bars indicate mean values and error bars represent s.e.m. Paired Student's *t* test, $***P < 0.001$, n.s. not significant. Number of cells per bar was $n = 80$ for **b** and between 51 and 68 in **c**. BL baseline. Values of AUC are expressed in arbitrary units (a.u.)

Student's *t* test; $P = 0.84$). In the experiments with low K^+ applied to GPN-treated glial cells, the AUC measured in HEK203-P2X2-PROG cells on top of the glia under resting conditions was of 502.7 ± 1.7 a.u. ($n = 80$). This value significantly increased to 514.2 ± 3.1 a.u. ($n = 80$, Paired Student's *t* test; $P = 3.1 \times 10^{-6}$) after application of low K^+.

When glial cells were pretreated with Baf A1, the baseline value (BL) of the AUC was of 504.0 ± 1.0 a.u. ($n = 68$) and that after PHE (20 μM), application was of 505.0 ± 1.3 a.u. ($n = 68$). These values were not significantly different (paired Student's *t* test; $P = 0.16$). In the experiments with low K^+ applied to Baf A1-treated glial cells, the AUC measured in HEK203-P2X2-PROG cells on top of the glia under resting conditions was of 501.9 ± 1.1 a.u. ($n = 51$) and of 501.2 ± 1.2 a.u. ($n = 51$, Paired Student's *t* test; $P = 3.1 \times 10^{-6}$) after application of low K^+. These values were not significantly different (paired Student's *t* test, $P = 0.39$).

To summarize, pretreatment of cultured glial cells with GPN suppressed the increase in $[Ca^{2+}]_i$ induced by PHE (20 μM) application but not that induced by the low K^+ solution, whereas pretreatment with Baf A1 suppressed both responses to PHE and low K^+. These results indicated that ATP can be released from a secretory lysosomal (GPN-sensitive) pool as well as from and a non-lysosomal (Baf A1-senstitive) pool. Our data also show that PHE targets selectively the secretory lysosomal pool.

Spontaneous release of ATP from cultured DH glial cells

As mentioned above, HEK293-P2X2-PROG cells plated on DH glial cells rarely displayed spontaneously occurring peaks/changes in $[Ca^{2+}]_i$, i.e., in the absence of an application of NA or PHE, indicating that spontaneous vesicular release was a rare phenomenon under our basal experimental conditions. One reason for apparently not detecting spontaneous release might be that ATP released from DH glia under basal conditions did not reach a local concentration sufficient to significantly activate P2X2 receptors in the detector cells. We therefore decided to favor accumulation of ATP released from DH glial cells by temporarily interrupting (stopping) the constant superfusion of the cells with extracellular solution. Such stop/flow experiments have been used previously to demonstrate ATP release from cultured astrocytes following mechanical or electrical stimulation of the glial cells [49]. Figure 6a, b shows that stopping the general and local superfusion induced a significant increase in the F_{350}/F_{380} fluorescence ratio in 55.4% (46/83) of the detector HEK293-P2X2-PROG cells. When extracellular superfusion was switched on again, the fluorescence ratio returned to control levels, i.e., to a value close to that recorded before stopping the flow of extracellular solution, thereby indicating that the increase in $[Ca^{2+}]_i$ in the detector cells was reversible. This increase in $[Ca^{2+}]_i$ was due to the activation of P2X2 receptors by ATP because the fraction of cells displaying an increase in fluorescence ratio was significantly reduced (7.6%; 4/60, Fisher's exact test $P = 3.7 \times 10^{-10}$) in the steady state presence of PPADS (50 μM) in the extracellular solution (Fig. 6a, b). There was also a significant reduction of the fraction of cells

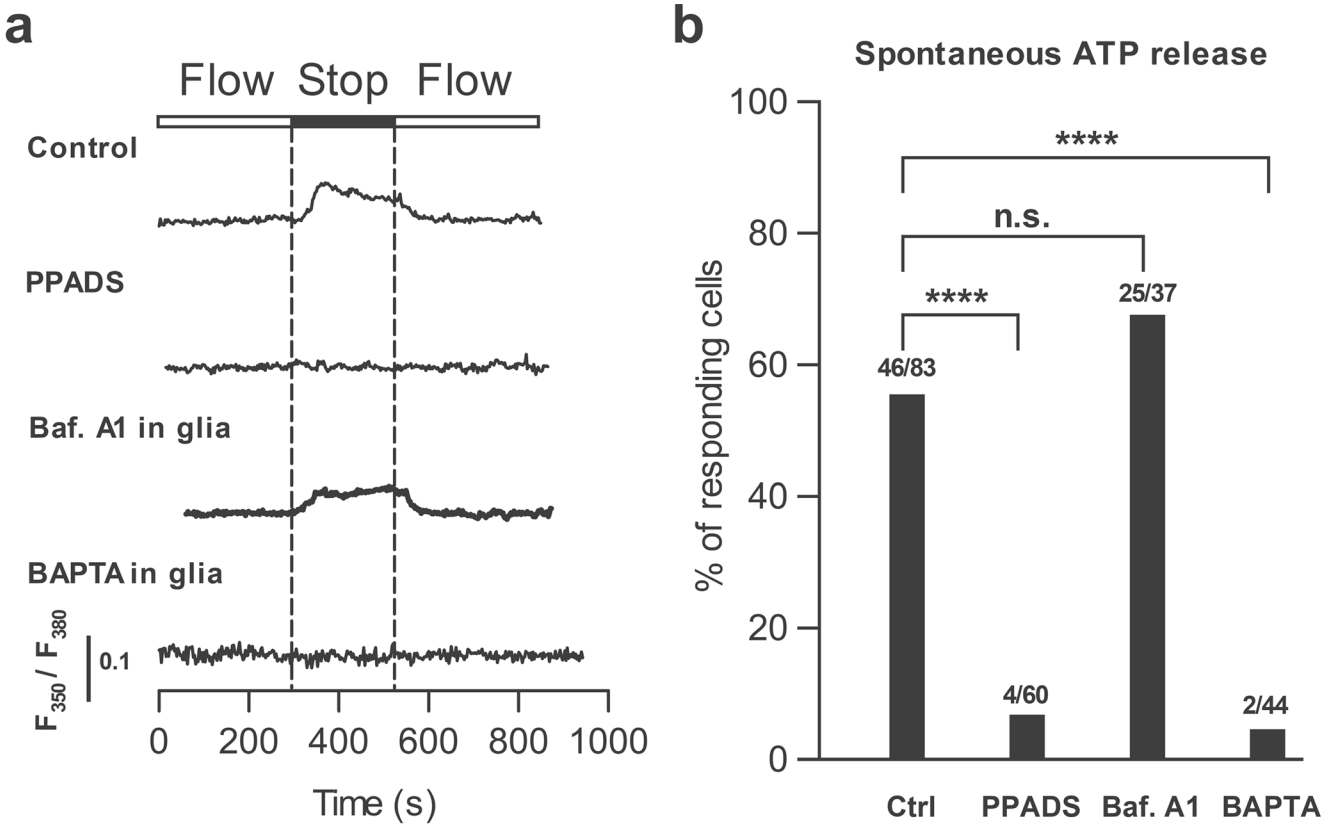

Fig. 6 Identification of a spontaneous calcium-dependent but non-vesicular release of ATP from cultured DH glial cells. In order to detect low levels of spontaneously occurring ATP release from DH glial cells, the continuous superfusion with extracellular medium (flow condition) was interrupted (stop condition) allowing a time-dependent local accumulation of extracellular ATP. **a** Stopping the general and local superfusion triggered a rapid and sustained increase in $[Ca^{2+}]_i$ measured in the HEK293-P2X2-PROG detector cells plated on top of cultured DH glial cells (top trace: control). Note that the $[Ca^{2+}]_i$ value rapidly returned to baseline values once the superfusion was turned on again (flow condition). The change in $[Ca^{2+}]_i$ triggered by stopping general superfusion was not observed when the extracellular medium contained PPADS (50 μM) to block P2X2 receptors (PPADS condition) or when DH glial cells were preloaded with the calcium chelator BAPTA-AM (BAPTA in glia condition), but persisted when glial cells were pretreated with Baf A1 to suppress the release of acidic secretory vesicles (Baf. A1 in glia condition). **b** Quantification of the experiments illustrated in **a**. The percentage of cells responding with an increase in $[Ca^{2+}]_i$ when the general superfusion was stopped is displayed as a function the different experimental conditions. The numbers above the columns indicate the proportions (Fisher's exact test, ****$P < 0.0001$, n.s. not significant)

displaying an increase in F_{350}/F_{380} ratio when glial cells were preloaded with the calcium chelator BAPTA-AM (4.5%, 2/44, Fisher's exact test $P = 2.3 \times 10^{-9}$; Fig. 6). In contrast, pretreating the DH glial cells with Baf A1 in order to block vesicular release of ATP (see above) did not significantly change the fraction of detector cells displaying an increase in $[Ca^{2+}]_i$ following the interruption of extracellular superfusion (Fig. 6a) (67.7%; 25/37, Fisher's exact test $P = 0.23$; Fig. 6).

Taken together, our results suggest the existence of a spontaneous ATP release from DH glial cells. This release is calcium-dependent but does not involve acidic vesicles.

Discussion

Our results demonstrate that NA induced/stimulated the release of ATP from cultured DH glial cells. This effect relied on the activation of α_1 adrenoceptors and the calcium-dependent fusion of secretory lysosomes with the plasma membrane. The detection of the release of low nanomolar concentrations of ATP at the single cell level was possible owing to the development of an improved sniffer cell system consisting of HEK293 cells expressing rat P2X2 receptors that are strongly and selectively potentiated by the steroid progesterone (PROG). This system provided very good sensitivity to ATP and excellent spatial and time resolutions. It also allowed us to demonstrate at the single cell level the coexistence of distinct vesicular and non-vesicular calcium-dependent release mechanisms of ATP [50, 51].

Improved sniffer cell detection system for the detection of ATP release from DH glial cells

ATP is an important extracellular signaling molecule that can be released from various cell types including neurons and glial cells [49, 52–55]. ATP is also recognized as a major gliotransmitter that underlies calcium wave propagation in glial networks and modulation of electrical activity in neuronal networks [49, 54–58] including in the DH of the spinal cord [37, 38, 59]. A major limit for the precise detection and quantification of ATP release is its rapid degradation by extracellular ectonucleotidases [40–42] which strongly reduce the lifetime of ATP in the extracellular space once it has been released. This is a serious challenge when trying to quantify low concentrations of extracellular ATP, in particular at the single cell level. Several approaches have been developed to try to resolve this issue. One of these consists of using calcium-permeable ionotropic ATP receptors (P2X receptors) as detection/detector elements. HEK293 cells transfected with P2X2 or mutant P2X3 receptors have been used successfully for detecting ATP release from glial cells [58, 60]. We found, when using a calcium imaging approach, that simply expressing P2X2 receptors in HEK293 cells did not improve the ATP detecting capacity of these cells that naturally express metabotropic P2Y receptors [61, 62]. Indeed, our results show that non-transfected and HEK293 cells transfected with rat P2X2 receptors displayed a similar EC_{50} for ATP that was in the micromolar range (0.75 μM) and therefore too high for reliably detecting low nanomolar concentrations of ATP (see "Results" section and Fig. 2a). However, we have previously shown that homomeric P2X2 receptors are strongly and selectively potentiated by the steroid/neurosteroid PROG [29]. In line with this finding, preincubation of the HEK293-P2X2 cells with PROG increased by sevenfold the sensitivity of the cells to ATP, shifting the EC_{50} for ATP to 0.1 μM. Moreover, the high oil-water partition coefficient of steroids/neurosteroids such as PROG and PROG derivatives which is > 50,000 [45] provides an ideal situation in which these substances can rapidly gain access to the lipophilic compartment of the plasma membrane where they remain trapped for long periods of time. The residence/dwell time of these lipophilic substances within the membrane will be mainly determined by a combination of slow wash out (diffusion into the extracellular medium) and metabolism of the substances within the cell [44]. Once in the hydrophobic part of the membrane bilayer, these steroids can diffuse laterally and interact with integral membrane proteins to modulate their activity, as it has been shown for the positive allosteric modulation and direct activation of $GABA_A$ receptors [45, 63–65]. A similar effect is probably involved in the potentiation of P2X2 receptors by PROG [29]. Whatever the mechanism involved, we noticed that when the HEK293-P2X2 receptors were in contact with PROG, i.e., 5 μM for 100 s or 200 nM for 1 h, we observed a robust potentiation of P2X2 receptor activity that lasted for at least 3 h after removing PROG from the extracellular solution. We took advantage of this situation and incubated the HEK293-P2X2 cells alone with 200 nM PROG before plating them on top of the cultured DH glial cells, thus avoiding to expose the glial cells directly to PROG. This system allowed us to reliably detect ATP release not only from the DH glial cells (see below) but also from neurons such as primary sensory neurons (online resource Fig. 10). More generally, we think that this detection system could be useful for the study of ATP release from virtually every cell type.

Vesicular ATP release from cultured DH glial cells and its modulation by NA

The improved sniffer cell system described above allowed us to clearly detect NA-evoked ATP release from DH glial cells. Application of NA or the specific α_1 adrenoceptor agonist PHE-induced peak-like $[Ca^{2+}]_i$ transients in the detector HEK293-P2X2-PROG cells. These transients were absent when the DH glial cells were loaded with the calcium chelator BAPTA-AM or when the extracellular medium contained

PPADS, an antagonist of P2X2 receptors. These results indicated that activation of α_1 adrenoceptors in DH glial cells induced calcium-dependent release of ATP that was detected by the HEK293-P2X2-PROG cells. This calcium-dependent release apparently resembled that described for vesicular release of ATP, glutamate, aspartate, or D-serine from astrocytes in the CNS [66, 67]. In line with these studies, ATP release induced by PHE from our cultured DH glial cells was completely blocked when the DH glial cells were pretreated with Baf A1, an inhibitor of the proton pump present on the membrane of acidic secretory vesicles, preventing the loading of the vesicles by the transmitter [35, 46]. Most interestingly, calcium-dependent ATP release induced by α_1 adrenoceptor stimulation was also blocked when DH glial cells were treated with GPN, a small peptide-like molecule that is selectively taken up by secretory lysosomes and leads to their selective functional perturbation [34, 47, 48]. The complete suppression of PHE-induced ATP release by GPN suggested that α_1 adrenoceptor stimulation selectively recruited a pool of secretory lysosomes and induced their exocytosis. This is consistent with previous studies in which it was shown that ATP release from hippocampal and cortical astrocytes seems to involve mainly secretory lysosomes [33, 34, 68, 69].

However, we observed that a release of ATP independent of α_1 adrenoceptor stimulation was still possible after selectively affecting secretory lysosomes with GPN. Indeed, it has been shown that in astrocytes, application of a low K^+ containing solution induced an increase in $[Ca^{2+}]_i$ by activating inwardly rectifying Kir4.1 K^+ channels [30, 31]. In our DH glia cultures, application of a low K^+ solution increased $[Ca^{2+}]_i$ in the vast majority (87%) of cells and this led to the release of ATP that could be detected by the HEK293-P2X2-PROG sniffer cells (see Fig. 5). Like for the PHE effect, low K^+-induced ATP release was blocked by BAPTA loading of the glial cells or by pretreating the cells with Baf A1. Yet, pretreatment of the DH glia with GPN did not block the effect of low K^+ on ATP release, whereas ATP release induced by PHE was completely suppressed under these conditions. This clearly pointed to the existence of a second pool of vesicles mediating calcium-dependent ATP release that was distinct from secretory lysosomes and that could be recruited by application of a low K^+ solution but neither by NA nor PHE. This pool could correspond to the small clear vesicle pool or the large dense-core vesicle pool that are present in astrocytes [69].

Spontaneous release of ATP from DH glial cells

Transiently/temporarily interrupting the continuous superfusion of the cells with extracellular solution allowed us to reveal an increase in $[Ca^{2+}]_i$ in approximately half of the sniffer HEK293-P2X2-PROG cells seeded on top of the DH glial cells. This increase in $[Ca^{2+}]_i$ was inhibited by PPADS or preloading the glial cells with BAPTA indicating that this increase in $[Ca^{2+}]_i$ reflected the release of ATP from at least a subset of glial cells. The fact that only half of the detector cells displayed such an increase in $[Ca^{2+}]_i$ might also reflect that only a fraction of the sniffer cells was appropriately positioned (i.e., close to the release sites of ATP) to detect ATP release. The fraction of responsive cells might therefore be a lower estimate of the fraction of glial cells that are able to release ATP spontaneously. Most importantly, spontaneous ATP release was still present after blocking vesicular ATP release from acidic vesicles by Baf A1 pretreatment but was suppressed when glial cells were preloaded with BAPTA. The study of the exact cellular mechanisms underlying spontaneous ATP release was beyond the main scope of our study and was not further investigated. However, in line with literature concerning ATP release from glial cells, the non-vesicular spontaneous release of ATP observed in our model might possibly involve release of ATP through ATP-permeable membrane channels, or membrane transporters [50, 51, 55].

Physiological considerations

ATP release from DH glia Our results confirm that secretory lysosomes are important for ATP release from DH glial cells. Moreover, this lysosomal pool of ATP is apparently the selective target of NA-mediated regulation of ATP release from these cells. The stimulation of ATP release by NA involved α1 adrenoceptors that are coupled to phospholipase C activation [55]. Lysosome-mediated ATP release has been shown to underlie propagation of calcium waves in glial networks and glia-to-neuron communication [69]. Interestingly, another vesicular but non-lysosomal pool of ATP could be released when $[Ca^{2+}]_i$ was increased by application of a low K^+ solution [30, 31]. In heterologous expression systems transfected with Kir4.1 channels, a decrease in extracellular K^+ concentration ($[K^+]_o$) to a final concentration of 2 mM was sufficient to trigger important increases in $[Ca^{2+}]_i$ in about 40% of the recorded cells [31]. Decreases in $[K^+]_o$ following neuronal activity (K^+ undershoot) have been observed in the cortex [70], the hippocampus [71], and the spinal cord [72]. It remains to be established if the observed decreases in $[K^+]_o$ observed are sufficient to trigger rises in $[Ca^{2+}]_i$ under physiological conditions. Important reductions in $[K^+]_o$ might be achieved in very localized regions where the volume of extracellular space is particularly small. Finally, the spontaneous calcium-dependent and non-vesicular release of ATP is of particular interest. This release might serve homeostatic purposes by locally allowing the production of adenosine [73] but might also represent an important element for basal and activity-dependent signaling within the glial network and between the glial and neuronal networks.

ATP and NA systems in the DH Stimulation of glial ATP release by NA contained in the descending axons of *Locus*

Coeruleus neurons might participate in the control of nociception [5, 19, 74]. ATP is an important extracellular signaling molecule [52, 75] that plays a role in sensory transmission [76], in particular in nociceptive transmission [77]. In the spinal cord, ATP can be released from neurons and glial cells [38, 59] and receptors for ATP are expressed by both cell types [52, 53, 78]. Different P2X receptor subunits are expressed in the DH [79], and their expression appears to increase during the postnatal period, in particular in the deep DH of the spinal cord [80]. Glial cells play a role in setting basal threshold for mechanical nociception [81], and ATP release participates in the development of neuropathic pain [82, 83]. Moreover, P2X receptors have been shown to participate in the processing of nociceptive signals in the DH and glial cells seem to be involved in this phenomenon [84].

The noradrenergic innervation of the DH involves axons of neurons having their cell bodies in the *Locus Coeruleus* [7, 85]. In the rat, noradrenergic axons are observed in the DH at birth and display a high affinity uptake mechanism for NA that reaches its adult-like characteristics during the third postnatal week [86]. The development of functional adrenoceptors follows a similar time course although the presence of noradrenergic fibers is apparently not necessary for the pattern of expression of the receptors [86].

In conclusion, our results show for the first time the coexistence of three distinguishable pools of ATP and mechanisms of ATP release from postnatal DH glial cells. In the DH of the spinal cord, this ATP release and its modulation by NA or other neurotransmitters might play a pivotal role in the modulation of nociceptive signaling.

Acknowledgments We would like to thank Mrs. Catherine Moreau and Mrs. Chantal Fitterer for excellent technical assistance. This work was supported by the Centre National de la Recherche Scientifique, Université de Strasbourg, and the French National Research Agency (ANR) contract ANR-17-EURE-0022.

V.E. was the recipient of an Initiative d'Excellence (IdEx) fellowship in the framework of the Investissement d'Avenir program of the Université de Strasbourg.

Compliance with ethical standards

Conflict of interest The authors declare that they have no conflict of interest.

Ethical approval All applicable international, national, and institutional guidelines for care and use of animals were followed.

References

1. Basbaum AI, Bautista DM, Scherrer G, Julius D (2009) Cellular and molecular mechanisms of pain. Cell 139(2):267–284. https://doi.org/10.1016/j.cell.2009.09.028
2. Cordero-Erausquin M, Inquimbert P, Schlichter R, Hugel S (2016) Neuronal networks and nociceptive processing in the dorsal horn of the spinal cord. Neuroscience 338:230–247. https://doi.org/10.1016/j.neuroscience.2016.08.048
3. Millan MJ (1999) The induction of pain: an integrative review. Prog Neurobiol 57(1):1–164
4. Fields H (2004) State-dependent opioid control of pain. Nat Rev Neurosci 5(7):565–575. https://doi.org/10.1038/nrn1431
5. Pertovaara A (2006) Noradrenergic pain modulation. Prog Neurobiol 80(2):53–83. https://doi.org/10.1016/j.pneurobio.2006.08.001
6. Budai D, Harasawa I, Fields HL (1998) Midbrain periaqueductal gray (PAG) inhibits nociceptive inputs to sacral dorsal horn nociceptive neurons through alpha2-adrenergic receptors. J Neurophysiol 80(5):2244–2254
7. Lyons WE, Fritschy JM, Grzanna R (1989) The noradrenergic neurotoxin DSP-4 eliminates the coeruleospinal projection but spares projections of the A5 and A7 groups to the ventral horn of the rat spinal cord. J Neurosci 9(5):1481–1489
8. Hitoto T, Tsuruoka M, Hiruma Y, Matsui Y (1998) A delta afferent fiber stimulation activates descending noradrenergic system from the locus coeruleus. Neurochem Res 23(12):1461–1465
9. Tsuruoka M, Hitoto T, Hiruma Y, Matsui Y (1999) Neurochemical evidence for inflammation-induced activation of the coeruleospinal modulation system in the rat. Brain Res 821(1):236–240
10. Tsuruoka M, Tamaki J, Maeda M, Hayashi B, Inoue T (2012) Biological implications of coeruleospinal inhibition of nociceptive processing in the spinal cord. Front Integr Neurosci 6:87. https://doi.org/10.3389/fnint.2012.00087
11. Feng YP, Yang K, Li YQ (2002) Norepinephrine depresses the capsaicin-evoked miniature excitatory postsynaptic currents in substantia gelatinosa of the rat spinal cord. Neurosci Lett 322(2):99–102
12. Funai Y, Pickering AE, Uta D, Nishikawa K, Mori T, Asada A, Imoto K, Furue H (2014) Systemic dexmedetomidine augments inhibitory synaptic transmission in the superficial dorsal horn through activation of descending noradrenergic control: an in vivo patch-clamp analysis of analgesic mechanisms. Pain 155(3):617–628. https://doi.org/10.1016/j.pain.2013.12.018
13. Hickey L, Li Y, Fyson SJ, Watson TC, Perrins R, Hewinson J, Teschemacher AG, Furue H, Lumb BM, Pickering AE (2014) Optoactivation of locus ceruleus neurons evokes bidirectional changes in thermal nociception in rats. J Neurosci 34(12):4148–4160. https://doi.org/10.1523/JNEUROSCI.4835-13.2014
14. Kawasaki Y, Kumamoto E, Furue H, Yoshimura M (2003) Alpha 2 adrenoceptor-mediated presynaptic inhibition of primary afferent glutamatergic transmission in rat substantia gelatinosa neurons. Anesthesiology 98(3):682–689 **doi:00000542-200303000-00016 [pii]**
15. Sonohata M, Furue H, Katafuchi T, Yasaka T, Doi A, Kumamoto E, Yoshimura M (2004) Actions of noradrenaline on substantia gelatinosa neurones in the rat spinal cord revealed by in vivo patch recording. J Physiol 555 (Pt 2):515–526. doi:https://doi.org/10.1113/jphysiol.2003.054932
16. North RA, Yoshimura M (1984) The actions of noradrenaline on neurones of the rat substantia gelatinosa in vitro. J Physiol 349:43–55
17. Baba H, Goldstein PA, Okamoto M, Kohno T, Ataka T, Yoshimura M, Shimoji K (2000) Norepinephrine facilitates inhibitory transmission in substantia gelatinosa of adult rat spinal cord (part 2): effects on somatodendritic sites of GABAergic neurons. Anesthesiology 92 (2):485–492
18. Baba H, Shimoji K, Yoshimura M (2000) Norepinephrine facilitates inhibitory transmission in substantia gelatinosa of adult rat spinal cord (part 1): effects on axon terminals of GABAergic and glycinergic neurons. Anesthesiology 92(2):473–484
19. Seibt F, Schlichter R (2015) Noradrenaline-mediated facilitation of inhibitory synaptic transmission in the dorsal horn of the rat spinal cord involves interlaminar communications. Eur J Neurosci 42(9):2654–2665. https://doi.org/10.1111/ejn.13077

20. Yaksh TL (1985) Pharmacology of spinal adrenergic systems which modulate spinal nociceptive processing. Pharmacol Biochem Behav 22(5):845–858
21. Hosli E, Hosli L (1982) Evidence for the existence of alpha- and beta-adrenoceptors on neurones and glial cells of cultured rat central nervous system–an autoradiographic study. Neuroscience 7(11): 2873–2881
22. Hagihira S, Senba E, Yoshida S, Tohyama M, Yoshiya I (1990) Fine structure of noradrenergic terminals and their synapses in the rat spinal dorsal horn: an immunohistochemical study. Brain Res 526(1):73–80. https://doi.org/10.1016/0006-8993(90)90251-6
23. Holstege JC, Bongers CM (1991) Ultrastructural aspects of the coeruleo-spinal projection. Prog Brain Res 88:143–156
24. Satoh K, Kashiba A, Kimura H, Maeda T (1982) Noradrenergic axon terminals in the substantia gelatinosa of the rat spinal cord: an electron-microscopic study using glyoxylic acid-potassium permanganate fixation. Cell Tissue Res 222(2):359–378
25. Rajaofetra N, Ridet JL, Poulat P, Marlier L, Sandillon F, Geffard M, Privat A (1992) Immunocytochemical mapping of noradrenergic projections to the rat spinal cord with an antiserum against noradrenaline. J Neurocytol 21(7):481–494
26. Ridet JL, Rajaofetra N, Teilhac JR, Geffard M, Privat A (1993) Evidence for nonsynaptic serotonergic and noradrenergic innervation of the rat dorsal horn and possible involvement of neuron-glia interactions. Neuroscience 52(1):143–157
27. Ridet JL, Sandillon F, Rajaofetra N, Geffard M, Privat A (1992) Spinal dopaminergic system of the rat: light and electron microscopic study using an antiserum against dopamine, with particular emphasis on synaptic incidence. Brain Res 598(1–2):233–241. https://doi.org/10.1016/0006-8993(92)90188-f
28. Stoop R, Thomas S, Rassendren F, Kawashima E, Buell G, Surprenant A, North RA (1999) Contribution of individual subunits to the multimeric P2X(2) receptor: estimates based on methanethiosulfonate block at T336C. Mol Pharmacol 56(5):973–981
29. De Roo M, Boue-Grabot E, Schlichter R (2010) Selective potentiation of homomeric P2X2 ionotropic ATP receptors by a fast non-genomic action of progesterone. Neuropharmacology 58(3):569–577. https://doi.org/10.1016/j.neuropharm.2009.12.002
30. Dallwig R, Vitten H, Deitmer JW (2000) A novel barium-sensitive calcium influx into rat astrocytes at low external potassium. Cell Calcium 28(4):247–259. https://doi.org/10.1054/ceca.2000.0153
31. Hartel K, Singaravelu K, Kaiser M, Neusch C, Hulsmann S, Deitmer JW (2007) Calcium influx mediated by the inwardly rectifying K+ channel Kir4.1 (KCNJ10) at low external K+ concentration. Cell Calcium 42(3):271–280. https://doi.org/10.1016/j.ceca.2006.12.004
32. Innocenti B, Parpura V, Haydon PG (2000) Imaging extracellular waves of glutamate during calcium signaling in cultured astrocytes. J Neurosci 20(5):1800–1808
33. Li D, Ropert N, Koulakoff A, Giaume C, Oheim M (2008) Lysosomes are the major vesicular compartment undergoing Ca2+-regulated exocytosis from cortical astrocytes. J Neurosci 28(30):7648–7658. https://doi.org/10.1523/JNEUROSCI.0744-08.2008
34. Zhang Z, Chen G, Zhou W, Song A, Xu T, Luo Q, Wang W, Gu XS, Duan S (2007) Regulated ATP release from astrocytes through lysosome exocytosis. Nat Cell Biol 9(8):945–953. https://doi.org/10.1038/ncb1620
35. Yoshimori T, Yamamoto A, Moriyama Y, Futai M, Tashiro Y (1991) Bafilomycin A1, a specific inhibitor of vacuolar-type H(+)-ATPase, inhibits acidification and protein degradation in lysosomes of cultured cells. J Biol Chem 266(26):17707–17712
36. Petitjean H, Hugel S, Barthas F, Bohren Y, Barrot M, Yalcin I, Schlichter R (2014) Activation of transient receptor potential vanilloid 2-expressing primary afferents stimulates synaptic transmission in the deep dorsal horn of the rat spinal cord and elicits mechanical hyperalgesia. Eur J Neurosci 40(8):3189–3201. https://doi.org/10.1111/ejn.12688
37. Hugel S, Schlichter R (2000) Presynaptic P2X receptors facilitate inhibitory GABAergic transmission between cultured rat spinal cord dorsal horn neurons. J Neurosci 20(6):2121–2130
38. Jo YH, Schlichter R (1999) Synaptic corelease of ATP and GABA in cultured spinal neurons. Nat Neurosci 2(3):241–245
39. Hertz L, Lovatt D, Goldman SA, Nedergaard M (2010) Adrenoceptors in brain: cellular gene expression and effects on astrocytic metabolism and [Ca(2+)]i. Neurochem Int 57(4):411–420. https://doi.org/10.1016/j.neuint.2010.03.019
40. Dunwiddie TV, Diao L, Proctor WR (1997) Adenine nucleotides undergo rapid, quantitative conversion to adenosine in the extracellular space in rat hippocampus. J Neurosci 17(20):7673–7682
41. Zimmermann H (1999) Two novel families of ectonucleotidases: molecular structures, catalytic properties and a search for function. Trends Pharmacol Sci 20(6):231–236
42. Zimmermann H (2000) Extracellular metabolism of ATP and other nucleotides. Naunyn Schmiedeberg's Arch Pharmacol 362(4–5): 299–309
43. Egan TM, Khakh BS (2004) Contribution of calcium ions to P2X channel responses. J Neurosci 24(13):3413–3420
44. Akk G, Covey DF, Evers AS, Steinbach JH, Zorumski CF, Mennerick S (2007) Mechanisms of neurosteroid interactions with GABA(A) receptors. Pharmacol Ther 116(1):35–57. https://doi.org/10.1016/j.pharmthera.2007.03.004
45. Akk G, Shu HJ, Wang C, Steinbach JH, Zorumski CF, Covey DF, Mennerick S (2005) Neurosteroid access to the GABAA receptor. J Neurosci 25(50):11605–11613. https://doi.org/10.1523/JNEUROSCI.4173-05.2005
46. Bowman EJ, Siebers A, Altendorf K (1988) Bafilomycins: a class of inhibitors of membrane ATPases from microorganisms, animal cells, and plant cells. Proc Natl Acad Sci U S A 85(21):7972–7976
47. Jadot M, Colmant C, Wattiaux-De Coninck S, Wattiaux R (1984) Intralysosomal hydrolysis of glycyl-L-phenylalanine 2-naphthylamide. Biochem J 219(3):965–970
48. Haller T, Dietl P, Deetjen P, Volkl H (1996) The lysosomal compartment as intracellular calcium store in MDCK cells: a possible involvement in InsP3-mediated Ca2+ release. Cell Calcium 19(2): 157–165
49. Hassinger TD, Guthrie PB, Atkinson PB, Bennett MV, Kater SB (1996) An extracellular signaling component in propagation of astrocytic calcium waves. Proc Natl Acad Sci U S A 93(23):13268–13273
50. Blum AE, Joseph SM, Przybylski RJ, Dubyak GR (2008) Rho-family GTPases modulate Ca(2+) -dependent ATP release from astrocytes. Am J Physiol Cell Physiol 295(1):C231–C241. https://doi.org/10.1152/ajpcell.00175.2008
51. Dubyak GR (2012) Function without form: an ongoing search for maxi-anion channel proteins. Focus on "maxi-anion channel and pannexin 1 hemichannel constitute separate pathways for swelling-induced ATP release in murine L929 fibrosarcoma cells". Am J Physiol Cell Physiol 303(9):C913–C915. https://doi.org/10.1152/ajpcell.00285.2012
52. Burnstock G (2006) Historical review: ATP as a neurotransmitter. Trends Pharmacol Sci 27(3):166–176. https://doi.org/10.1016/j.tips.2006.01.005
53. Fields RD, Burnstock G (2006) Purinergic signalling in neuron-glia interactions. Nat Rev Neurosci 7(6):423–436. https://doi.org/10.1038/nrn1928
54. Guthrie PB, Knappenberger J, Segal M, Bennett MV, Charles AC, Kater SB (1999) ATP released from astrocytes mediates glial calcium waves. J Neurosci 19(2):520–528

55. Verkhratsky A, Nedergaard M (2018) Physiology of Astroglia. Physiol Rev 98(1):239–389. https://doi.org/10.1152/physrev.00042.2016
56. Boue-Grabot E, Pankratov Y (2017) Modulation of central synapses by astrocyte-released ATP and postsynaptic P2X receptors. Neural Plast 2017:9454275. https://doi.org/10.1155/2017/9454275
57. Haydon PG (2001) GLIA: listening and talking to the synapse. Nat Rev Neurosci 2(3):185–193
58. Lalo U, Palygin O, Rasooli-Nejad S, Andrew J, Haydon PG, Pankratov Y (2014) Exocytosis of ATP from astrocytes modulates phasic and tonic inhibition in the neocortex. PLoS Biol 12(1):e1001747. https://doi.org/10.1371/journal.pbio.1001747
59. Scemes E, Suadicani SO, Spray DC (2000) Intercellular communication in spinal cord astrocytes: fine tuning between gap junctions and P2 nucleotide receptors in calcium wave propagation. J Neurosci 20(4):1435–1445
60. Pangrsic T, Potokar M, Stenovec M, Kreft M, Fabbretti E, Nistri A, Pryazhnikov E, Khiroug L, Giniatullin R, Zorec R (2007) Exocytotic release of ATP from cultured astrocytes. J Biol Chem 282(39):28749–28758. https://doi.org/10.1074/jbc.M700290200
61. Atwood BK, Lopez J, Wager-Miller J, Mackie K, Straiker A (2011) Expression of G protein-coupled receptors and related proteins in HEK293, AtT20, BV2, and N18 cell lines as revealed by microarray analysis. BMC Genomics 12:14. https://doi.org/10.1186/1471-2164-12-14
62. Fischer W, Franke H, Groger-Arndt H, Illes P (2005) Evidence for the existence of P2Y1,2,4 receptor subtypes in HEK-293 cells: reactivation of P2Y1 receptors after repetitive agonist application. Naunyn Schmiedeberg's Arch Pharmacol 371(6):466–472. https://doi.org/10.1007/s00210-005-1070-6
63. Hosie AM, Wilkins ME, da Silva HM, Smart TG (2006) Endogenous neurosteroids regulate GABAA receptors through two discrete transmembrane sites. Nature 444(7118):486–489. https://doi.org/10.1038/nature05324
64. Inquimbert P, Rodeau JL, Schlichter R (2008) Regional differences in the decay kinetics of GABA(A) receptor-mediated miniature IPSCs in the dorsal horn of the rat spinal cord are determined by mitochondrial transport of cholesterol. J Neurosci 28(13):3427–3437. https://doi.org/10.1523/JNEUROSCI.5076-07.2008
65. Shu HJ, Eisenman LN, Jinadasa D, Covey DF, Zorumski CF, Mennerick S (2004) Slow actions of neuroactive steroids at GABAA receptors. J Neurosci 24(30):6667–6675. https://doi.org/10.1523/JNEUROSCI.1399-04.2004
66. Gundersen V, Storm-Mathisen J, Bergersen LH (2015) Neuroglial transmission. Physiol Rev 95(3):695–726. https://doi.org/10.1152/physrev.00024.2014
67. Harada K, Kamiya T, Tsuboi T (2015) Gliotransmitter release from astrocytes: functional, developmental, and pathological implications in the brain. Front Neurosci 9:499. https://doi.org/10.3389/fnins.2015.00499
68. Jaiswal JK, Fix M, Takano T, Nedergaard M, Simon SM (2007) Resolving vesicle fusion from lysis to monitor calcium-triggered lysosomal exocytosis in astrocytes. Proc Natl Acad Sci U S A 104(35):14151–14156. https://doi.org/10.1073/pnas.0704935104
69. Verderio C, Cagnoli C, Bergami M, Francolini M, Schenk U, Colombo A, Riganti L, Frassoni C, Zuccaro E, Danglot L, Wilhelm C, Galli T, Canossa M, Matteoli M (2012) TI-VAMP/VAMP7 is the SNARE of secretory lysosomes contributing to ATP secretion from astrocytes. Biol Cell 104(4):213–228. https://doi.org/10.1111/boc.201100070
70. Heinemann U, Lux HD (1975) Undershoots following stimulus-induced rises of extracellular potassium concentration in cerebral cortex of cat. Brain Res 93(1):63–76
71. D'Ambrosio R, Gordon DS, Winn HR (2002) Differential role of KIR channel and Na(+)/K(+)-pump in the regulation of extracellular K(+) in rat hippocampus. J Neurophysiol 87(1):87–102. https://doi.org/10.1152/jn.00240.2001
72. Jendelova P, Sykova E (1991) Role of glia in K+ and pH homeostasis in the neonatal rat spinal cord. Glia 4(1):56–63. https://doi.org/10.1002/glia.440040107
73. Pascual O, Casper KB, Kubera C, Zhang J, Revilla-Sanchez R, Sul JY, Takano H, Moss SJ, McCarthy K, Haydon PG (2005) Astrocytic purinergic signaling coordinates synaptic networks. Science 310(5745):113–116. https://doi.org/10.1126/science.1116916
74. Millan MJ (2002) Descending control of pain. Prog Neurobiol 66(6):355–474
75. Burnstock G (2007) Physiology and pathophysiology of purinergic neurotransmission. Physiol Rev 87(2):659–797. https://doi.org/10.1152/physrev.00043.2006
76. Nakatsuka T, Gu JG (2006) P2X purinoceptors and sensory transmission. Pflugers Arch 452(5):598–607. https://doi.org/10.1007/s00424-006-0057-6
77. Tsuda M, Tozaki-Saitoh H, Inoue K (2010) Pain and purinergic signaling. Brain Res Rev 63(1–2):222–232. https://doi.org/10.1016/j.brainresrev.2009.11.003
78. North RA (2002) Molecular physiology of P2X receptors. Physiol Rev 82(4):1013–1067
79. Collo G, North RA, Kawashima E, Merlo-Pich E, Neidhart S, Surprenant A, Buell G (1996) Cloning of P2X5 and P2X6 receptors and the distribution and properties of an extended family of ATP-gated ion channels. J Neurosci 16(8):2495–2507
80. Shiokawa H, Nakatsuka T, Furue H, Tsuda M, Katafuchi T, Inoue K, Yoshimura M (2006) Direct excitation of deep dorsal horn neurones in the rat spinal cord by the activation of postsynaptic P2X receptors. J Physiol 573 (Pt 3):753–763. doi:https://doi.org/10.1113/jphysiol.2006.108613
81. Foley JC, McIver SR, Haydon PG (2011) Gliotransmission modulates baseline mechanical nociception. Mol Pain 7:93. https://doi.org/10.1186/1744-8069-7-93
82. Ji RR, Berta T, Nedergaard M (2013) Glia and pain: is chronic pain a gliopathy? Pain 154(Suppl 1):S10–S28. https://doi.org/10.1016/j.pain.2013.06.022
83. Masuda T, Ozono Y, Mikuriya S, Kohro Y, Tozaki-Saitoh H, Iwatsuki K, Uneyama H, Ichikawa R, Salter MW, Tsuda M, Inoue K (2016) Dorsal horn neurons release extracellular ATP in a VNUT-dependent manner that underlies neuropathic pain. Nat Commun 7:12529. https://doi.org/10.1038/ncomms12529
84. Aoyama R, Okada Y, Yokota S, Yasui Y, Fukuda K, Shinozaki Y, Yoshida H, Nakamura M, Chiba K, Yasui Y, Kato F, Toyama Y (2011) Spatiotemporal and anatomical analyses of P2X receptor-mediated neuronal and glial processing of sensory signals in the rat dorsal horn. Pain 152(9):2085–2097. https://doi.org/10.1016/j.pain.2011.05.014
85. Fritschy JM, Lyons WE, Mullen CA, Kosofsky BE, Molliver ME, Grzanna R (1987) Distribution of locus coeruleus axons in the rat spinal cord: a combined anterograde transport and immunohistochemical study. Brain Res 437(1):176–180. https://doi.org/10.1016/0006-8993(87)91541-1
86. Singer HS, Coyle JT, Vernon N, Kallman CH, Price DL (1980) The development of catecholaminergic innervation in chick spinal cord. Brain Res 191(2):417–428

Eersapah et al (2019)

Purinergic Signalling

Online Resource

Supplementary Material

Figures 7 to 10

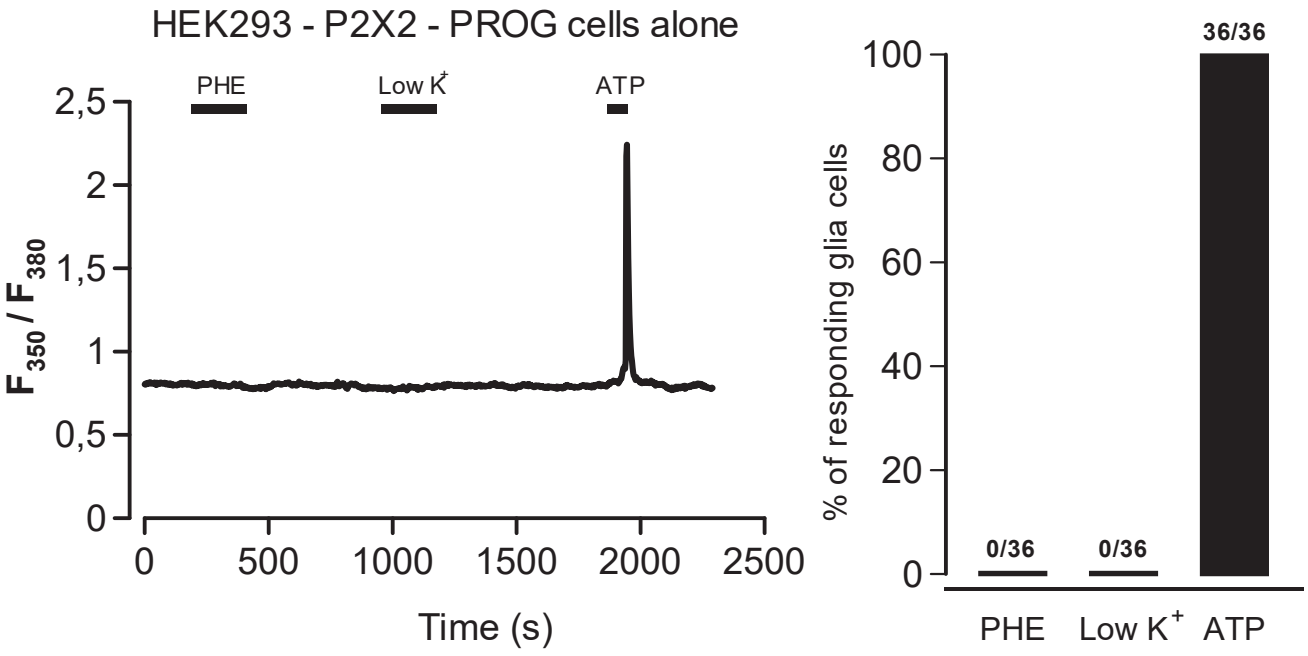

Fig. 7 Absence of effect of PHE and a low K+ solution on $[Ca^{2+}]_i$ in HEK-P2X2-PROG cells cultured alone. Left panel shows that local applications of phenylephrine (PHE, 20 μM) or of an extracellular solution containing a low (0.2 mM) concentration of K^+ (Low K^+) did not trigger an elevation of $[Ca^{2+}]_i$ in HEK-P2X2-PROG cells alone (i.e. in the absence of DH glial cells) indicating that they did not express α1 adrenoceptors and Kir4.1 K^+ channels. However, the cells responded by an increase in $[Ca^{2+}]_i$ to an application of ATP (30 μM). The quantification of these effects on a sample of 36 cells tested is shown in the right panel. The numbers on top of the histogram columns represent the proportion of responsive cells.

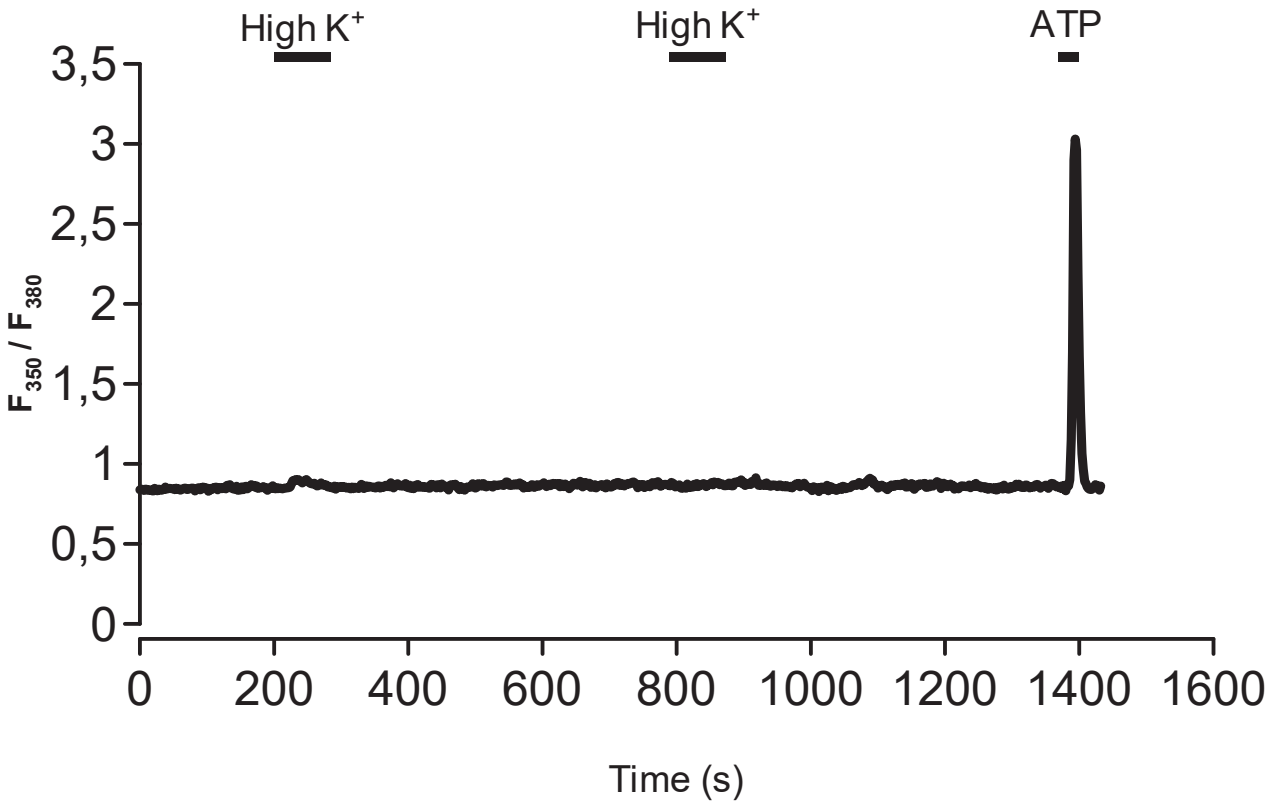

Fig. 8 Application of a depolarizing High K^+ solution to DH glial cells in culture did not increase $[Ca^{2+}]_i$. An extracellular solution in which the K^+ concentration was increased to 50 mM (High K^+) was applied to fura-2 loaded cells primary DH cultures. This depolarizing solution did not increase $[Ca^{2+}]_i$ indicating the absence of voltage-dependent calcium channels in the cells. This result indicates the absence of neurons in our cultures. Application of ATP (30 μM) elicited an increase in $[Ca^{2+}]_i$ indicating that the cells were able generate a calcium signal following the activation of endogenously expressed metabotropic P2Y purinoceptors.

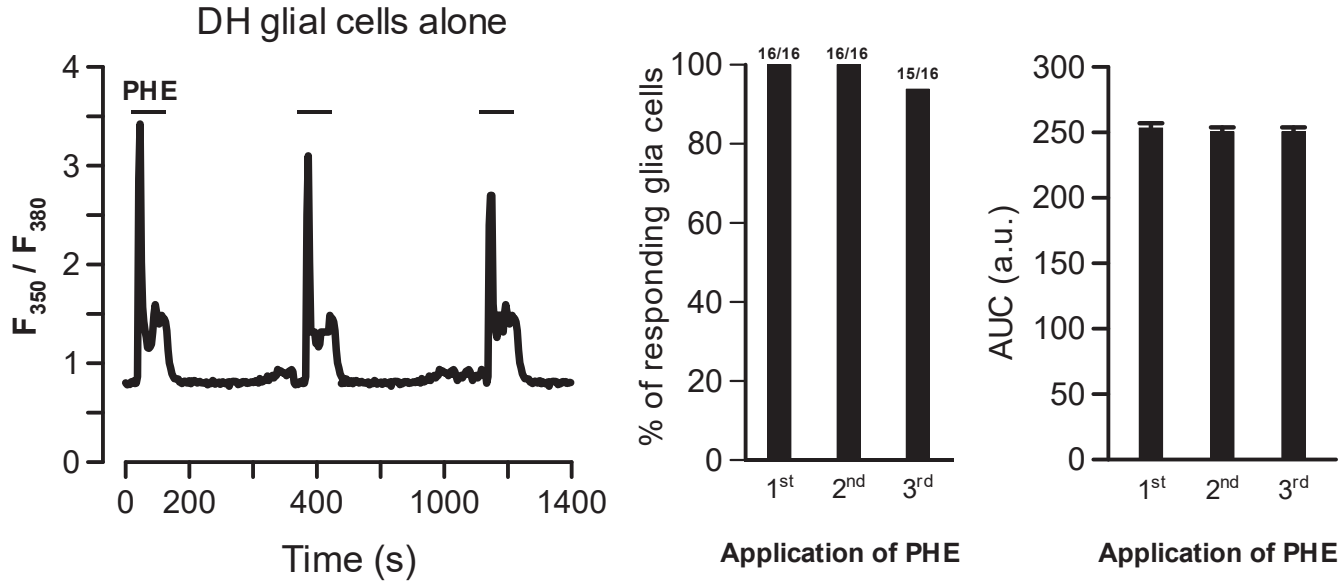

Fig. 9 Calcium responses to PHE can be repeated several times without significant attenuation in cultured DH glial cells. As illustrated in the left panel, application of the α1 adrenoceptor agonist PHE (20 μM, 50s) triggered an increase in $[Ca^{2+}]_i$ that could be reproduced 3 times without significant attenuation both in the proportion of responding cells (middle panel) and the area under the curve (AUC) (right panel) of the recorded signals. *a.u. arbitrary units.*

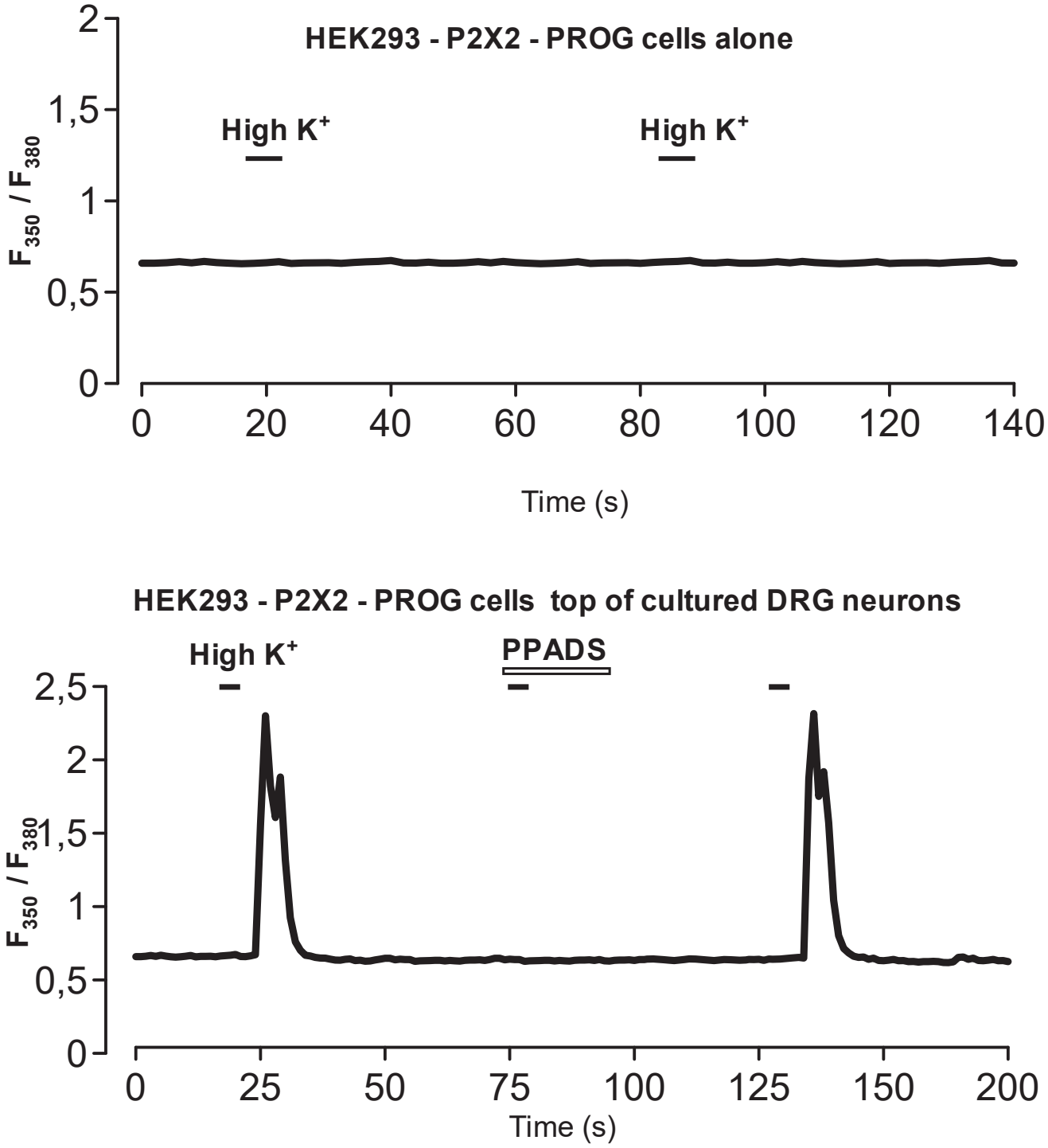

Fig. 10 HEK293-P2X2-PROG cells are efficient biosensors to measure ATP release from cultured mouse dorsal root ganglion neurons. Top panel shows that application of a depolarizing high K^+ (50 mM) solution to HEK293-P2X2-PROG cells cultured alone did not increase $[Ca^{2+}]_i$ in these cells indicating the absence of voltage-dependent Ca^{2+} channels. However, when fura-2 loaded HEK293-P2X2-PROG cells were plated on top of cultured mouse DRG cells (lower panel), application of a high K^+ solution triggered a large increase in $[Ca^{2+}]_i$ in the HEK cell that was reversibly blocked by the P2X2 receptor antagonist PPADS (50 μM). This result suggests that the observed increase in $[Ca^{2+}]_i$ reflected the calcium-dependent release of ATP from DRG neurons following the opening of voltage-dependent Ca^{2+} channels in the neuron in contact with the recorded biosensor cell.

Results Project - 2

Context and main objective project 2

Our previous results have shown that NA increased $[Ca^{2+}]_i$ in cultured DH glial cells via the activation of α_1 adrenoceptors (α_1-ARs) and led to the calcium-dependent and vesicular release of ATP from a pool of secretory lysosomes (see part 1 of results, (Eersapah et al., 2019)). This phenomenon might therefore contribute to the spinal analgesia mediated by NA released from descending noradrenergic axons from *Locus Coeruleus* neurons projecting to the DH of the spinal cord (Lyons et al., 1989; Pertovaara, 2006; Yaksh et al., 1995). Yet, *in vivo* studies have shown that it is mainly the activation of α_2 adrenoceptors (α_2-ARs) that underlies the analgesic effects of NA at the spinal level (Budai et al., 1998; Yaksh et al., 1995). Moreover, our laboratory has recently shown that NA can facilitate inhibitory (GABAergic) synaptic transmission via the activation of glial α_1- and α_2-adrenoceptors (α_1-AR and α_2-AR) that most probably trigger the release of ATP from glia (Seibt and Schlichter, 2015). Surprisingly, the only activation of α_1-AR by phenylephrine (PHE) seemed to increase $[Ca^{2+}]_i$ whereas the application of the α_2-AR agonist clonidine (CLO) did not significantly elevate $[Ca^{2+}]_i$ in cultured DH glial cells. This was rather surprising since, in glial cells, Gq, as well as Gi/o, coupled metabotropic receptors such as $GABA_B$ receptors increase $[Ca^{2+}]_i$ in glial cells (Kang et al., 1998; McCarthy and Salm, 1991; Nilsson et al., 1992). Indeed, CLO has been shown to induce a transient increase in $[Ca^{2+}]_i$ in a fraction of cultured cortical and hippocampal astrocytes (Hertz et al., 2010; Salm and McCarthy, 1990) and this proportion was further increased after pretreatment of the cultures with cAMP promoting agents (Enkvist et al., 1996). Our objective was therefore to check in more detail for the presence of functional α_2-ARs on cultured DH glial cells and to evaluate the consequences of their activation on ATP release from these cells. To this end we carefully (re)examined the effects of α_2-AR agonists on $[Ca^{2+}]_i$ and also examined the possibility that these agonists might perhaps inhibit the increase in $[Ca^{2+}]_i$ evoked by the α_1-AR agonist PHE.

2.1.1 Effect of CLO on $[Ca^{2+}]_i$ in DH glial cells

As reported in the preceding results section, application of CLO (10 µM) induced a transient increase in $[Ca^{2+}]_i$ in a very low (6.1%, 7/114) proportion of DH glial cells (see Part 1 of the results section, (Eersapah et al., 2019)). Moreover, this proportion of responding cells was not significantly changed in the presence of the α_2-AR antagonist yohimbine (1 µM) (1.7%, 1/58, Fisher's exact test; P = 0.265), raising the possibility that this increase in $[Ca^{2+}]_i$ might not be due to the activation of α_2-ARs.

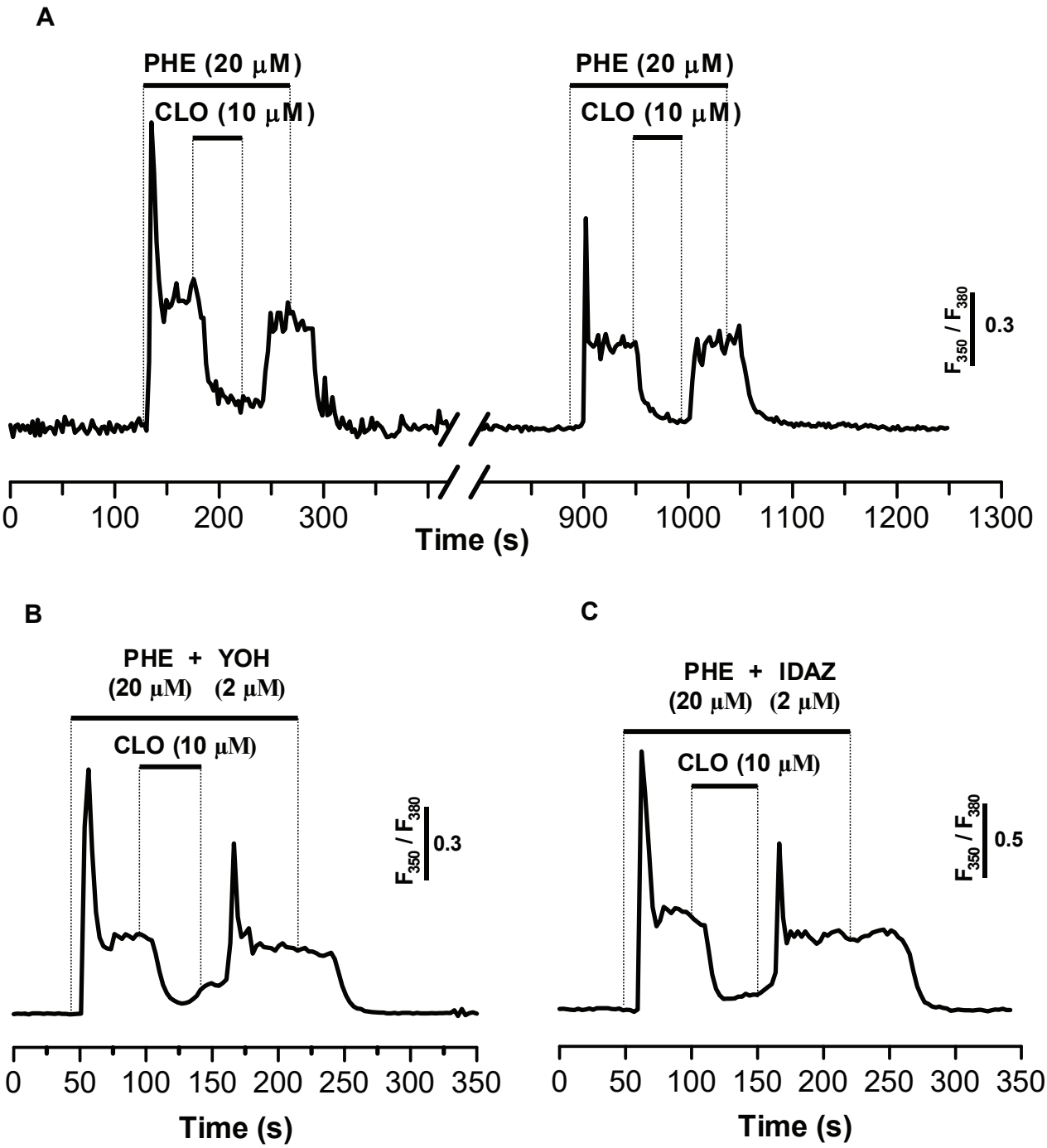

Figure 21. Clonidine inhibited phenylephrine-induced calcium plateau independent of α_2-AR. Example traces of calcium imaging signals from fura-2 loaded DH glial cells. A Application of α_1-adrenergic agonist phenylephrine (PHE, 20μM) induces an increase in intracellular calcium. Co-application of α_2-agonist clonidine (CLO, 10 μM) significantly reduces the $[Ca^{2+}]$i increase induced by PHE. The calcium responses can be reproduced when separated by a 10-minute interval. B The inhibitory effect of CLO on the $[Ca^{2+}]_i$ induced by PHE is not prevented by co-application of α_2-adrenergic specific antagonist yohimbine (YOH, 2μM). C Similarly, the inhibitory effect of CLO on $[Ca^{2+}]_i$ is not reduced in the presence of the α2- antagonist idazoxan (IDAZ, 2μM).

We next wondered whether activation of α_2-ARs might decrease rather than increase $[Ca^{2+}]_i$. Application of CLO (10 µM) did never decrease basal levels of $[Ca^{2+}]_i$ (N = 0/114 cells tested). However, we found that CLO potently and reversibly inhibited the plateau phase of calcium responses induced by PHE, an agonist of α_1-ARs (Fig . 21A). CLO (10 µM) rapidly and reversibly reduced the amplitude of the calcium plateau of PHE responses in 98% (122/125) of the cells tested. The plateau was on average reduced to 16.3 ± 3.9 % (n=89) of the control value, i.e. the plateau amplitude measured just before the application of CLO (10 µM). The effect of CLO (10 µM) was not blocked by the α_2-AR antagonists yohimbine (YOH 2 µM) (Fig.21B) or idazoxan (IDAZ 2 µM) (Fig 21C)

In a set of 6 cells, it was possible to directly compare the effect of the two α_2-AR antagonists on the CLO (10 µM) response in the same cells. In the presence of YOH (2 µM), CLO (10 µM) still inhibited the amplitude of the calcium plateau induced by PHE (20 µM) to 13.8 ± 5.0 % (n=6). This value was not statistically different from that observed in the absence of YOH in the same cells (23.5 ± 7.0 % (n=6); paired Student's t-test; P = 0.223). Similarly, in the presence of IDAZ (2 µM), CLO reduced the PHE-induced plateau to 29.4 ± 12.2 % (n=6), a value that was not different from that observed with CLO alone (23.5 ± 7.0 % (n=6); paired Student's t-test; P = 0.512). These results suggested that the effect of CLO (10 µM) was not due to the activation of α_2-ARs (see below).

It must be emphasized that the slow increase in $[Ca^{2+}]_i$ induced by the local application of a low K+ (0.2 mM) – containing extracellular solution was not affected by the application of 10 µM CLO (Fig 22), indicating that the inhibitory effect of CLO was not a general non-specific effect of intracellular calcium signaling in cultured DH glial cells.

2.1.2 Effects of α-methyl-Noradrenaline (α-me-NA) and low concentrations of CLO on $[Ca^{2+}]_i$

We next tested the effect of α-methyl-Noradrenaline (α-me-NA) that was shown to be a selective agonist at α_2-ARs when used at low (submicromolar) concentrations (Decker and Schwartz, 1985; Piguet and Schlichter, 1998). Application of α-me-NA (0.5 µM) induced an increase in $[Ca^{2+}]_i$ in 21/29 (72.4%) of the DH glial cells from which we recorded (Fig 23). In a given cell, the response to α-me-NA (0.5 µM) could be reproduced at least two times when separated by a delay of 10 minutes (Fig 23). Two consecutive responses to α-me-NA (0.5 µM) could be elicited in 24 out of 30 cells (80%) in which it was tested. The area under the curve (AUC) of

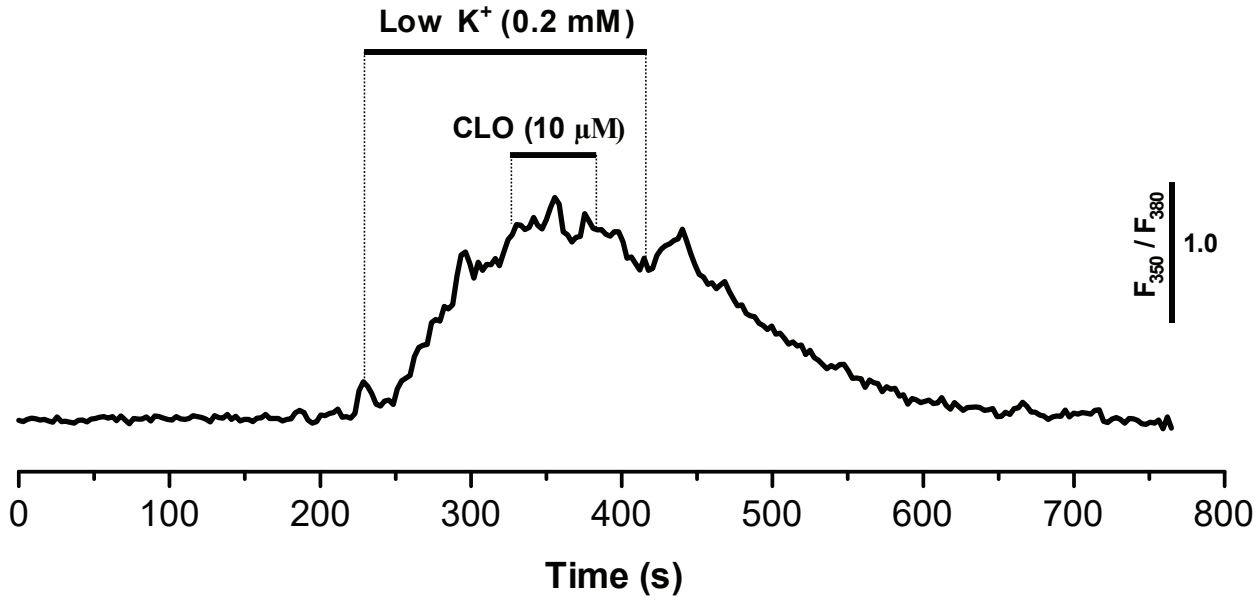

Figure 22. Effect of clonidine on elevated $[Ca^{2+}]_i$ induced by low K^+ solution. Average trace of $[Ca^{2+}]_i$ signals in fura-2-loaded DH glial cells (N= 5). A local application of an extracellular solution in which the concentration of potassium ions was lowered to 0.2 mM (Low K^+ solution) triggered an increase in $[Ca^{2+}]_i$ that lasted as long as the solution was applied and then returned to pre-application baseline levels. Co-application of the α_2-agonist clonidine (CLO, 10 μM) did not induce any change on the elevated $[Ca^{2+}]_i$ levels induced by the Low K^+ solution.

the first response was of 58.8 ± 3.7 a.u. (arbitrary units) (n=24) and that of the second response of 53.0 ± 2.2 a.u. (n=24). These AUCs were not significantly different (paired Student's t-test; P = 0.06). In the presence of YOH (2 µM), α-me-NA (0.5 µM) did not induce any increase in [Ca2+]i (0%; 0/27 cells) (Fig 24A). This result indicated that the response to α-me-NA was due to the activation of α2-ARs. Interestingly, the increase in [Ca2+]i induced by α-me-NA (0.5 µM) was reproduced by a low concentration of CLO (0.3 µM) (Fig 24B). This effect of CLO at low concentration was clearly different from that observed at high concentration (10 µM) (see preceding results and Fig 21)

2.1.3 Dose-response effect of CLO

We then decided to investigate in more detail the effect of various concentrations of CLO on the PHE-induced response. As illustrated in Fig 25, low concentrations of CLO (0.1 µM or 0.3 µM) either had no effect or triggered an increase in $[Ca^{2+}]_i$ whereas high concentrations of CLO (3 µM or 10 µM) induced a decrease of the calcium plateau (Fig 25). Intermediate concentrations (1 µM) displayed either type of response and occasionally triggered biphasic responses consisting in an initial increase in $[Ca^{2+}]_i$ followed by late inhibition of the calcium plateau (Fig 25). The dose-response relationships for the facilitating effect of CLO, i.e. the increase in $[Ca^{2+}]_i$ on top of the PHE plateau, and the inhibitory effect on the plateau phase are illustrated in Fig 26A as the fraction of cells displaying an increase in $[Ca^{2+}]_i$ or an inhibition of the plateau as a function of the CLO concentration applied. The facilitatory response was observed only at low CLO concentrations and had a bell-shaped appearance. The threshold for the facilitatory response was obviously below 0.1 µM, i.e. the lowest concentration of CLO that we tested. Indeed, at 0.1 µM around 30% of the cells already displayed an increase in $[Ca^{2+}]_i$. The maximal fraction of cells displaying an increase in $[Ca^{2+}]_i$ was observed at CLO concentrations of 0.3 to 1 µM, with around 70% of the cells displaying such an increase in $[Ca^{2+}]_i$. At concentrations higher than 1 µM of CLO, increases in $[Ca^{2+}]_i$ were very rarely observed, i.e. in less than 10% of the cells. The inhibitory component of calcium the plateau of the PHE response had a threshold around 0.1 µM and reached a maximum at 3 µM, a concentration at which 98% of the cells displayed an inhibition of the calcium plateau of the PHE response. At a concentration of 1 µM, CLO inhibited the PHE calcium plateau in about 57% of the cells, indicating that the IC_{50} of this effect was close to 1 µM CLO. When the amplitude of the inhibition of the plateau was quantified in individual cells by measuring the amplitude of calcium plateau signal for each CLO

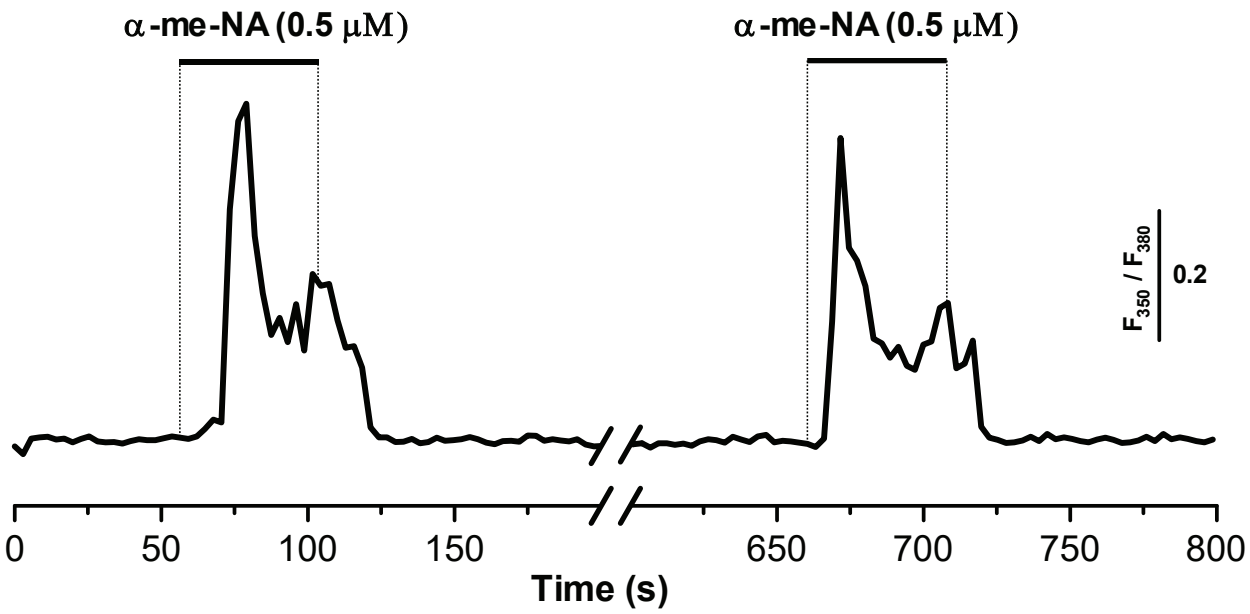

Figure 23. Effect of α_2-AR agonist α-methyl-noradrenaline on $[Ca^{2+}]_i$ DH glia. Example traces of calcium imaging signals from fura-2 loaded DH glial cells. Application of α_2-agonist α-methyl-noradrenaline (α-me-NA 0.5 μM) induced an increase in $[Ca^{2+}]_i$. The calcium response induced by α-me-NA could be replicated at least two times when separated by an interval of 500 seconds.

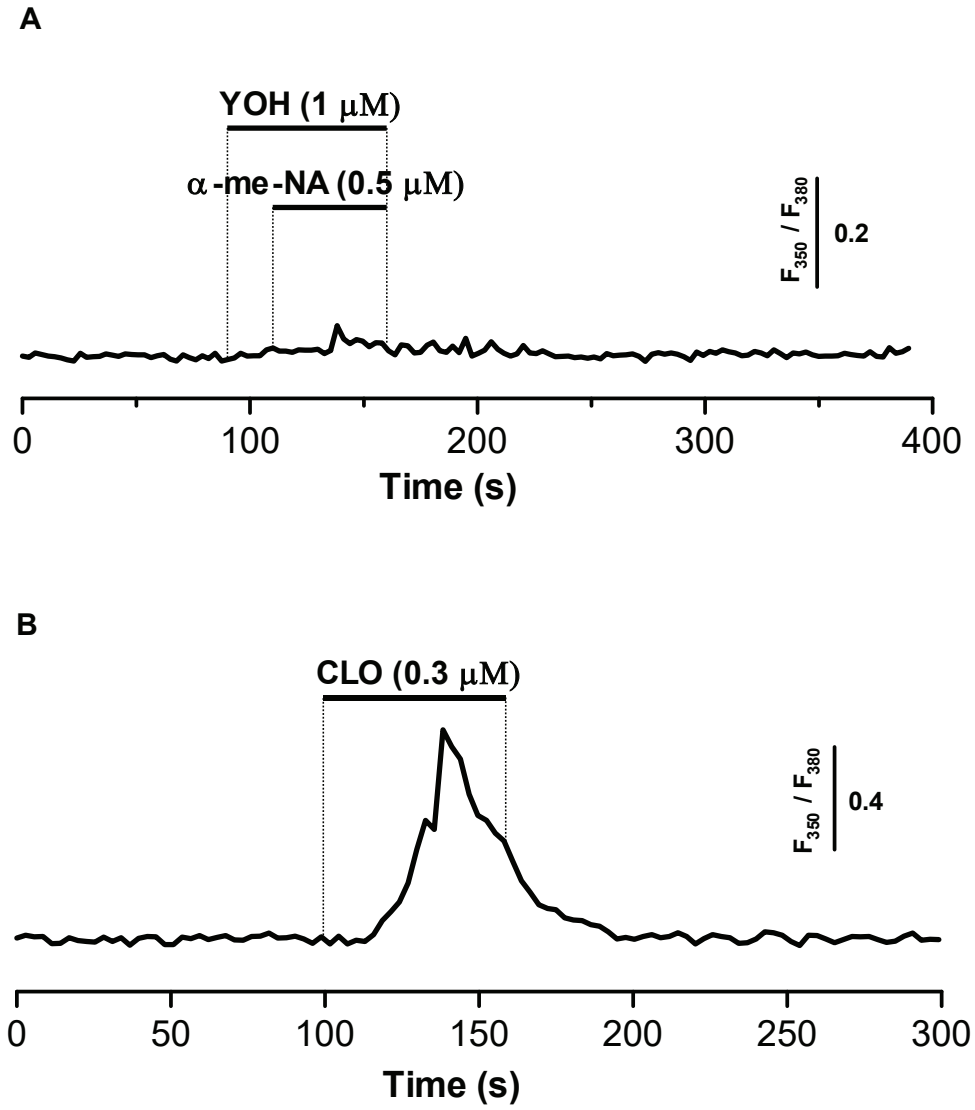

Figure 24. ɑ-methyl-noradrenaline-induced $[Ca^{2+}]_i$ increase is inhibited by yohimbine. Example traces of calcium imaging signals from fura-2 loaded DH glial cells. A Co-application of α_2- antagonist yohimbine (1μM) inhibits the $[Ca^{2+}]_i$ increase normally induced by α_2-agonist α-methyl-noradrenaline (α-me-NA, 0.5 μM). B Low concentration (0.3 μM) of the α_2-agonist clonidine (CLO) induces an increase in $[Ca^{2+}]_i$ levels.

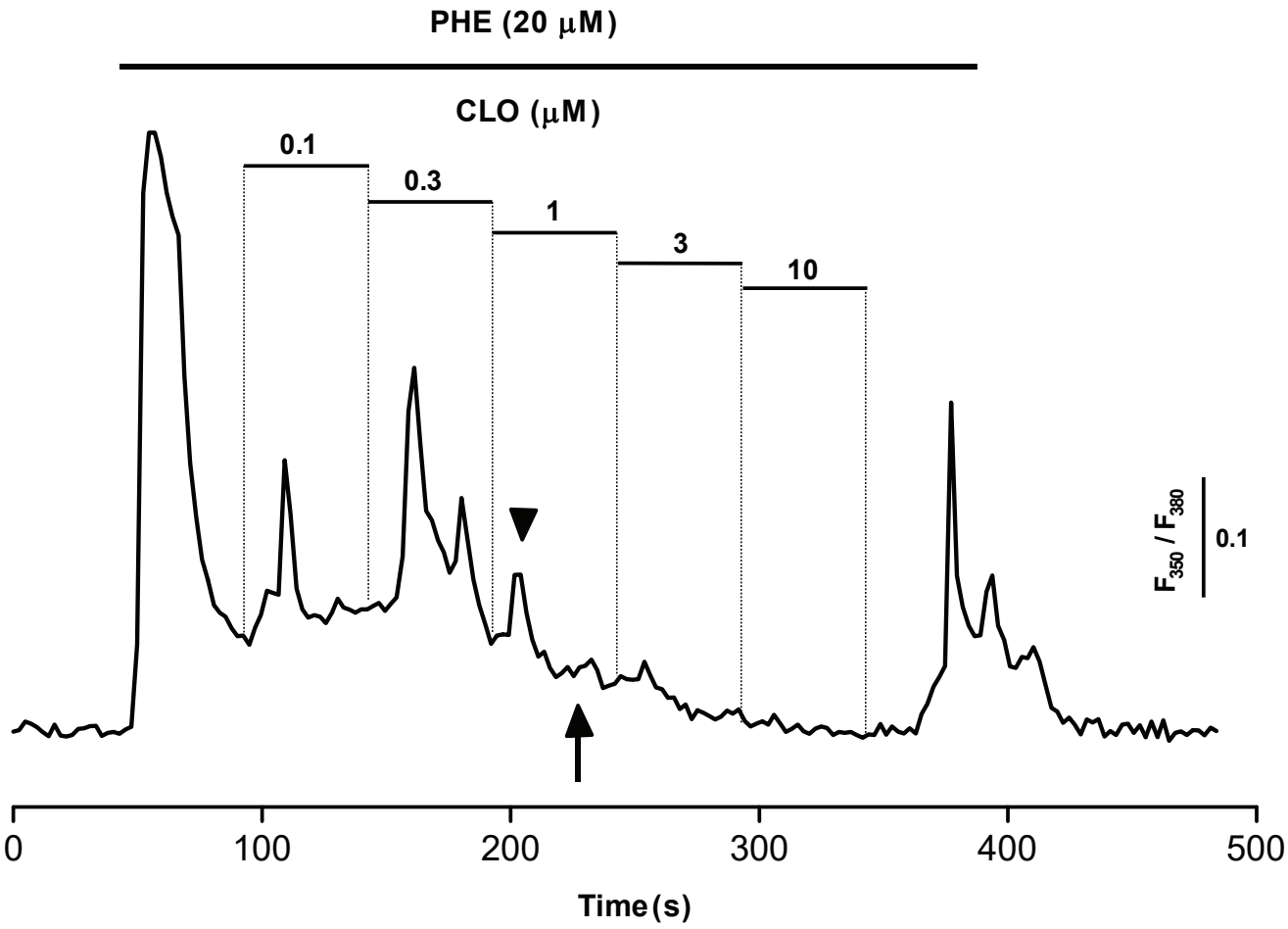

Figure 25. α_2-agonist clonidine (CLO) induced different $[Ca^{2+}]_i$ responses depending on the dose. Example trace of calcium imaging signals from fura-2 loaded DH glial cells. Co-application of different concentrations (0.1-10μM) of CLO on top of the α_1-agonist phenylephrine (PHE, 20 μM) -induced $[Ca^{2+}]_i$ plateau response. At low concentrations (0.1-0.3 μM) CLO induced an increase in $[Ca^{2+}]_i$ on top of the PHE plateau response, while at higher concentration (3-10 μM) CLO inhibited the PHE plateau. At 1 μM of CLO induced two different $[Ca^{2+}]_i$ response patterns, first, an increase in $[Ca^{2+}]_i$ (arrowhead) followed by an inhibition of the PHE-induced calcium plateau (arrow).

concentration during a cumulative application of increasing CLO concentrations, it seemed that the relationship was exponential, i.e. linear when expressed as a function of the logarithm of the CLO concentration (Fig 26B). Such a phenomenon is compatible with a dose-dependent blockade by CLO of the channel(s) underlying the calcium influx during the plateau of the PHE response (i.e. store-operated calcium entry (SOCE) channels or non-store operated calcium entry (non-SOCE) channels). The CLO concentration that induced a 50% inhibition of the plateau was around 1 µM. The main types of PHE responses observed in our cultured glial cells were type 1 responses (see preceding Results Part 1, (Eersapah et al., 2019)) consisting of an initial peak in $[Ca^{2+}]_i$ followed by a sustained plateau lasting for the remaining duration of PHE application. The quantification of the effect of CLO on PHE responses was mainly carried out on this type of responses (see above). We nevertheless had the opportunity to evaluate the effect of CLO on some cells displaying type 2 responses to PHE, i.e. displaying calcium oscillations during the PHE plateau phase, or on type 3 responses consisting of a single early/initial transient calcium peak with no plateau phase following the is peak. As illustrated in Fig 27A; for type 2 PHE responses, CLO at concentrations between 0.1 and 1 µM, did not seem to affect the calcium oscillations. However, at higher concentrations (3 and 10 µM) CLO blocked the calcium oscillations and decreased the amplitude of the calcium plateau. Concerning type 3 responses, CLO induced an increase in $[Ca^{2+}]_i$ at low concentrations (0.1 and 0.3 µM) but such increases in $[Ca^{2+}]_i$ were not observed at CLO concentrations ≥ 1 µM (Fig 27B). This observation was consistent with the appearance of a inhibitory/blocking effect of CLO on the calcium response at higher CLO concentrations that probably masked the increase in $[Ca^{2+}]_i$ observed in isolation at lower CLO concentration (at which the blocking effect was not or less active).

2.1.4 Effect of imidazoline molecules on calcium signals in DH glial cells

The finding that CLO could both increase $[Ca^{2+}]_i$ at low concentrations and block these signals as well as inhibit the plateau response of the PHE response at high concentrations was puzzling and we, therefore, undertook some experiments designed at elucidating this apparent paradox. CLO is an imidazoline molecule that can bind to α2-ARs as well as to imidazoline binding sites/receptors. Three types of imidazoline binding sites/receptors have been identified so far and were termed I1, I2 and I3 (Head and Mayorov, 2006). I1 and I2 are expressed in the CNS (Ernsberger et al., 1995) (Flamez et al., 1997) (Vauquelin et al., 1999). We, therefore, tested the effect of selective agonist of I1 and I2 sites/receptors on the calcium plateau of the PHE response.

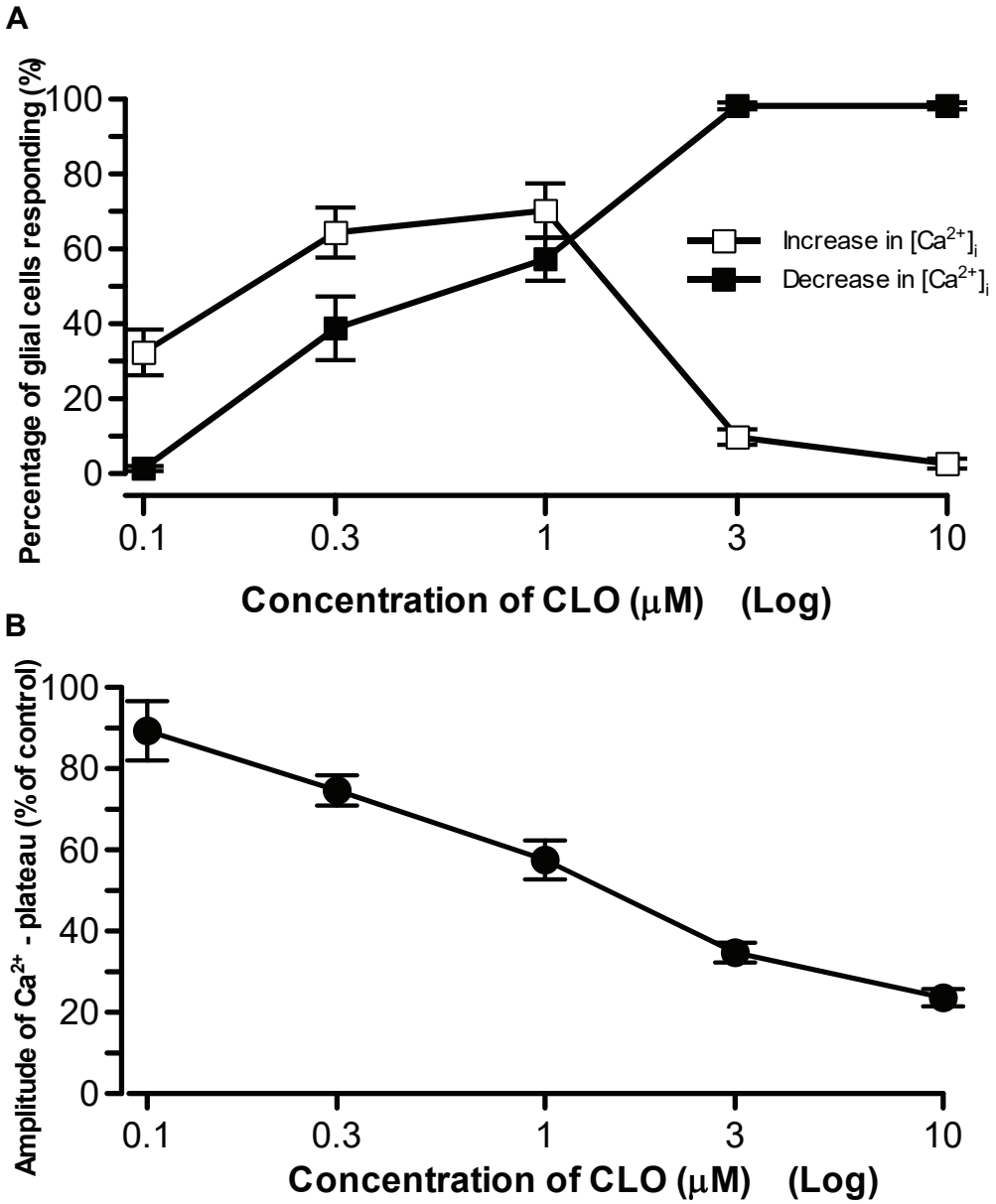

Figure 26. Dose-response curves of clonidine (CLO) responses measured on top of the PHE-induced calcium plateau. A Fraction of cells displaying a change in $[Ca^{2+}]_i$ as a function of different concentration of CLO (0.1-10 μM). For each of the five tested concentration of CLO the cells have been separated into those which showed an increase, represented by white squares, or a decrease, represented by black squares, in $[Ca^{2+}]_i$ (n = 7 experiments, 5-20 cells/experiment) At the highest concentration tested (10 μM) practically all cells showed a decrease in $[Ca^{2+}]_i$ however at the lowest concentration tested (0.1 μM) around 30% of the cells displayed an increase in $[Ca^{2+}]_i$ meaning that the threshold for this type of CLO response was below 0.1 μM of CLO. The IC_{50} for the inhibitory component appeared to be just below 1μM of CLO (at which 57.3 % of the cells showed a decrease in $[Ca^{2+}]_i$. B For each CLO concentration (n = 20 cells, n = 3 experiments) the amplitude of the inhibitory component was quantified in individual cells by measuring the amplitude of calcium plateau signal during the application of CLO concentration, a 50% reduction of the amplitude of the plateau was achieved around 1 μM of CLO.

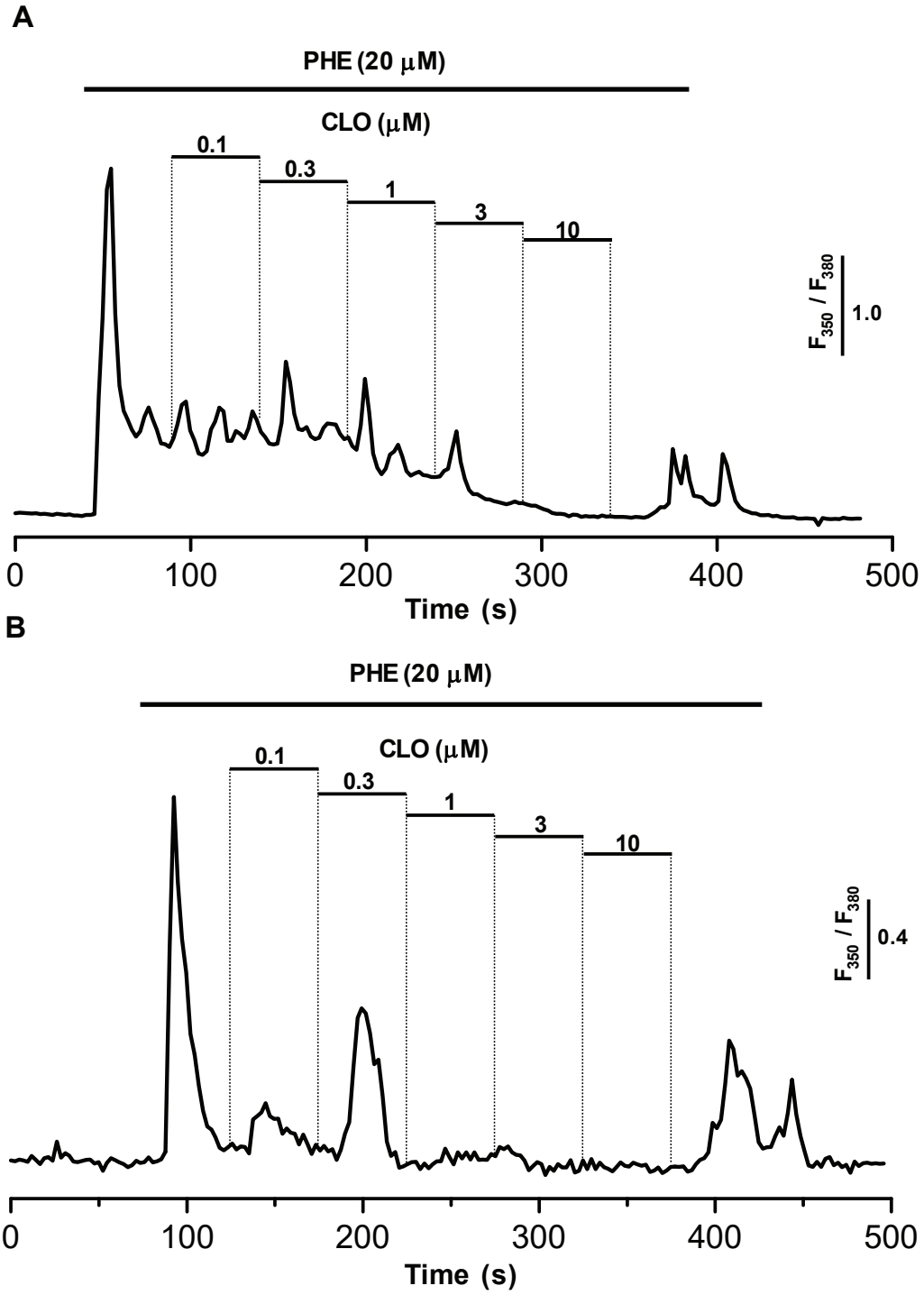

Figure 27. Dose-response relationship of clonidine (CLO) on top of type 2 and type 3 PHE responses. Example trace of calcium imaging signals from fura-2 loaded DH glial cells during the cumulative application of increasing CLO concentrations (0.1-10μM). A Application of CLO during type 2 PHE (20μM) induced $[Ca^{2+}]_i$ responses. CLO at concentrations between 0.1 and 1 μM, did not seem to affect the calcium oscillations significantly while at concentrations above 3μM, CLO inhibited the frequency of the oscillations and decreased the amplitude of the PHE $[Ca^{2+}]_i$ plateau. B Application of CLO during type 3 PHE $[Ca^{2+}]_i$ responses revealed that CLO induced an increase in $[Ca^{2+}]_i$ at low concentrations (0.1 and 0.3 μM) but such increases were not observed at higher CLO concentrations (≥ 1 μM) which is consistent with the previous finding, showing dominating inhibitory/blocking effect of CLO on the $[Ca^{2+}]_i$ response during higher CLO concentrations.

I1 sites/receptors

Cimetidine, an antagonist of H2 type histamine receptors, is considered as a selective I1 agonist (Tsoli et al., 1995). Cimetidine (10 µM) failed to inhibit or to increase the plateau of the PHE (10 µM) response (n=18) (Fig 28A).

I2 sites/receptors

Application of the I2 selective agonist 2-(2-Benzofuranyl)-2-imidazoline hydrochloride (2-BFI, 10 µM) (Sanchez-Blazquez et al., 2000) (Choi et al., 2018), that also acts as an NMDA receptor antagonist (Han et al., 2013b), rapidly reduced the plateau of the PHE (20 µM) response in 47/48 (98%) of the DH glial cells from which we recorded. In these cells, 2-BFI (10 µM) rapidly and reversibly reduced the PHE calcium plateau amplitude to 24.2 ± 4.8 % (n=28) of its initial value (Fig 28B).

2.1.5 Effect of Idazoxan on the 2-BFI response

We next tested the effect of idazoxan (IDAZ) on the 2-BFI-induced inhibition of the calcium plateau of the PHE (20 µM) response (Fig 29). Idazoxan is an antagonist of both α_2-ARs and I2 sites/receptors (Flamez et al., 1997; Hudson et al., 1997). In the presence of IDAZ (2 µM), 2-BFI was still able to inhibit the amplitude of the plateau of the PHE response. However, the amplitude of the PHE plateau was reduced to only 67.9 ± 6.8 % (n=4) in the presence of IDAZ (2 µM) compared to 24.2 ± 4.8 % (n=28) in the absence of IDAZ. These values were significantly different (unpaired Student's t-test; P = 0.002). Since 2-BFI in not an agonist at α_2-ARs (Hudson et al., 1997), the inhibitory effect of IDAZ indicated that 2-BFI reduced the amplitude of the PHE plateau, at leat in part, by acting at I2 sites/receptors.

2.1.6 Effect of clorgyline

It has been suggested that I2 sites/receptors are located on mono-amino-oxidase A (MAO-A) (Anderson et al., 2006) and that these sites are blocked by clorgyline (CLORG) (Raddatz et al., 1999; Sanchez-Blazquez et al., 2000). We, therefore, tested the effect of CLORG on the responses induced by 2-BFI and CLO (Fig 30). In the presence of CLORG (2 µM), 2-BFI reduced the amplitude of the PHE plateau to 72.7 ± 7.0 % (n=13). This effect was significantly smaller than that of 2-BFI applied alone, i.e. in the absence of CLORG (24.2 ± 4.8 %; n=28; unpaired Student's t-test; P < 0.0001) We also tested the effect of CLORG on the inhibition of the PHE plateau by CLO (10 µM). In the presence of CLORG (2 µM), CLO (10 µM) reduced the PHE plateau to 8.6 ±

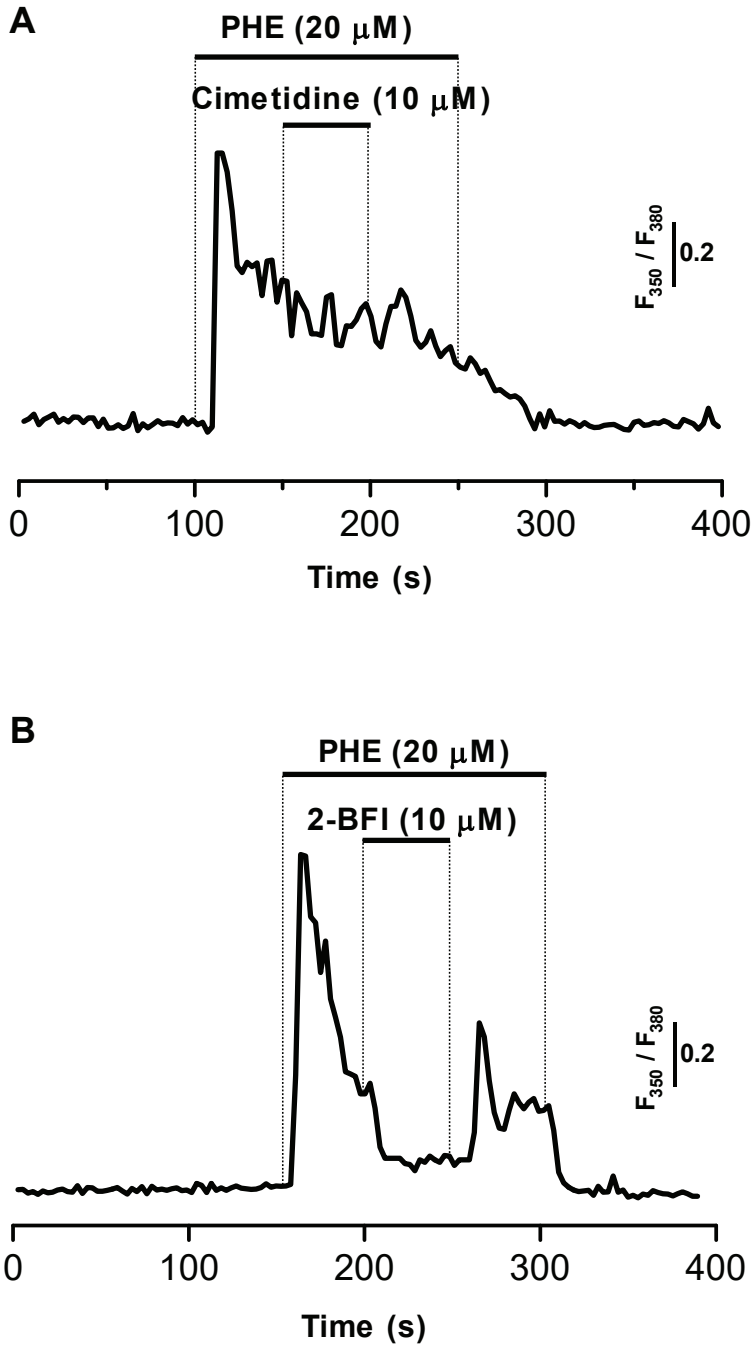

Figure 28. Effect of Imidazoline receptor type 2 and type 1 agonists on PHE-induced $[Ca^{2+}]_i$ plateau. Example trace of calcium imaging signals from fura-2 loaded DH glial cells. A Cimetidine (10 μM), a selective imidazoline receptor type 1 agonist failed to either increase or inhibit the $[Ca^{2+}]_i$ plateau induced by the α_1-receptor agonist phenylephrine (PHE, 20 μM). B 2-(2-Benzofuranyl)-2-imidazoline hydrochloride (2-BFI, 10 μM), a selective imidazoline receptor type 2 agonist, strongly reduced the plateau of the PHE (20 μM) response.

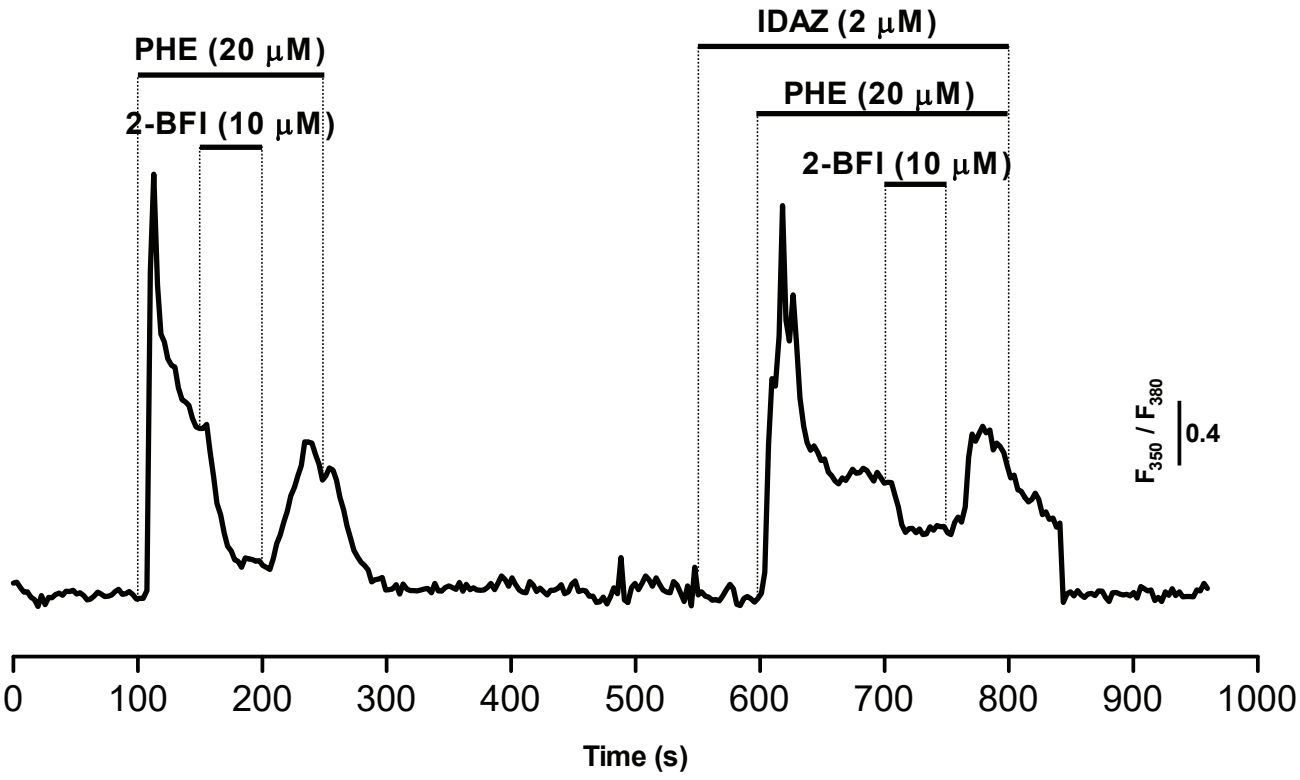

Figure 29. α_2-AR- and I2 receptor- antagonist reduced the inhibitory effect of 2-BFI on PHE-induced $[Ca^{2+}]_i$ plateau. Example trace of calcium imaging signals from fura-2 loaded DH glial cells. Application of the imidazoline receptor type 2 (I2) agonist 2-BFI (10 μM), induced an inhibition of the calcium plateau of the PHE (20 μM) response (as shown also in figure R8). In a second application, 2-BFI was applied in the presence of idazoxan (IDAZ, 2μM), an antagonist of both α_2-ARs and I2 sites/receptors, which indeed reduced the effect/inhibition of 2-BFI on the calcium plateau of the PHE (20 μM) response.

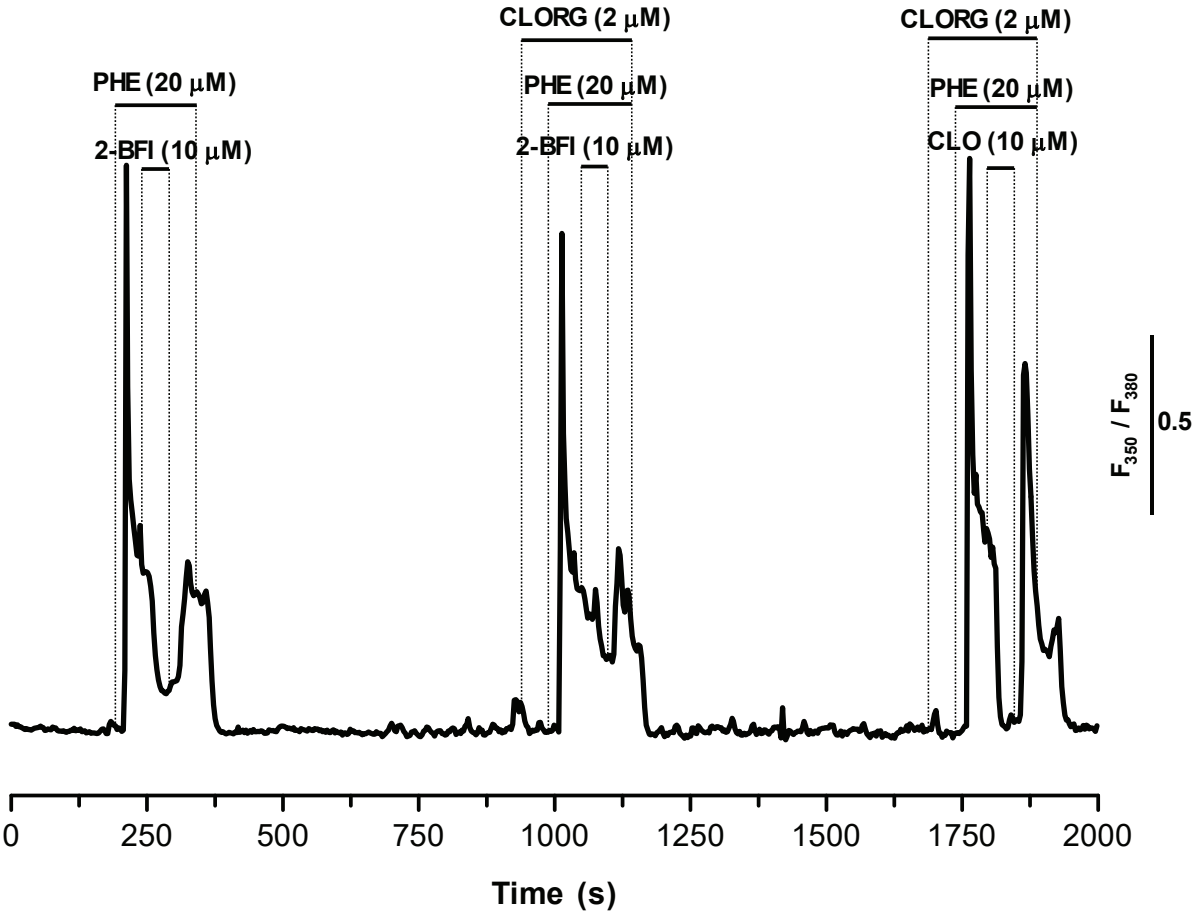

Figure 30. 2-BFI and CLO inhibit PHE-induced $[Ca^{2+}]_i$ plateau by partially non-overlapping mechanism. Average trace of calcium imaging signals from fura-2 loaded DH glial cells (N= 4 cells). Application of the I2 agonist 2-BFI (10 μM) induced an inhibition of the calcium plateau of the PHE (20 μM) response (see figure R8 and R9 for details). When in the same cells, 2-BFI was applied in the presence of clorgyline (CLORG, 2 μM) an antagonist of I2 receptors the inhibitory effect of 2-BFI on the calcium plateau of the PHE (20 μM) response was decreased. However, the inhibitory effect of CLO on the calcium plateau of the PHE was not affected by the presence of CLORG.

1.5 % (n=13) whereas, in the absence of CLORG, CLO reduced the plateau to 16.3 ± 4.0 % (n=29). These values were not significantly different (unpaired Student's t-test; P = 0.15). These results indicated that the 2-BFI-induced inhibition of the PHE plateau was in part due to the activation of I2 receptors. However, neither the I2 antagonist IDAZ nor the MAO-A inhibitor CLORG did completely suppress the effect of 2-BFI on the PHE plateau (see discussion section 2.2 below)

2.1.7 Effects of α-me-NA, 2-BFI and CLO on ATP release from cultured DH glial cells

In the preceding section, we have shown that α-me-NA increased basal [Ca2+]i and CLO and 2-BFI inhibited PHE-evoked changes $[Ca^{2+}]_i$. We, therefore, evaluated the effects of these molecules on basal or PHE-evoked ATP release from cultured DH glial cells. To this end, we used our sniffer system approach (see Results Part 1 section, Eersapah et al (2019)) in which HEK293-P2X2-PROG cells were plated on top of the cultured DH glial cells.

Effect on basal ATP release

Application of α-me-NA (0.5 μM) to HEK293-P2X2-PROG cells cultured alone never induced any change in $[Ca^{2+}]_i$. However, application of α-me-NA (0.5 μM) induced an increase in $[Ca^{2+}]_i$ in 16/29 (55.2%) of HEK293-P2X2-PROG cells plated on top of DH glial cells (Fig 31) indicating that α-me-NA (0.5 μM) stimulated the release of ATP from DH glial cells. The A.U.C of the calcium signal in the HEK293-P2X2-PROG cells was of 101.75 ± 0.14 a.u (n=28) before application of α-me-NA (0.5 μM) and of 108.91 ± 1.40 a.u (n=28) after α-me-NA application. These values were significantly different (paired Student's t-test, P = 1.5 10^{-5}). Application of 2–BFI (10 μM) alone did not increase $[Ca^{2+}]_i$ in HEK293-P2X2-PROG cells plated on top of DH glial cells. The A.U.C of the calcium signal was of 100.8 ± 0.21 a.u (n=26) before 2-BFI application and of 100.6 ± 0.21 a.u (n=26) during the 100 seconds lasting 2-BFI (10 μM) application (paired Student's t-test, P = 0.49). Similarly, application of CLO (10 μM) alone did not increase $[Ca^{2+}]_i$ in HEK293-P2X2-PROG cells plated on top of DH glial cells. The A.U.C of the calcium signal was of 101.6 ± 0.11 a.u (n=45) before CLO application and of 101.6 ± 0.30 a.u (n=45) during the 100 seconds lasting CLO (10 μM) application (paired Student's t-test, P = 0.94).

In summary, α-me-NA stimulated the release of ATP whereas 2-BFI and CLO did neither evoke ATP release nor modulate basal release of ATP.

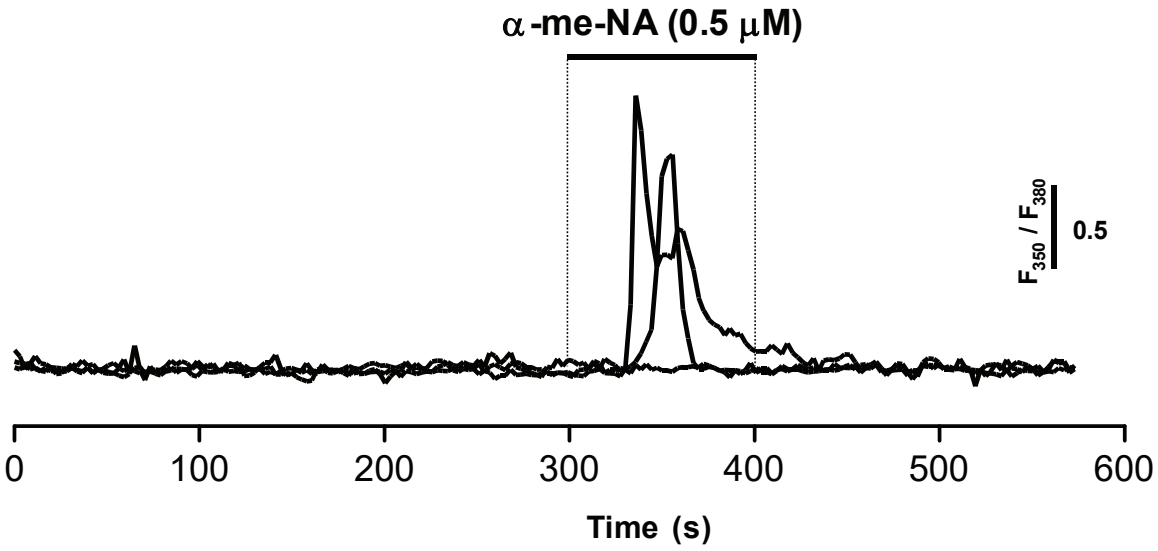

Figure 31. Characterization of ATP release from DH glial cells and its modulation by α-methyl-noradrenaline (α-me-NA, 0.5 μM). Fura-2 loaded HEK293-P2X2-PROG cells were plated on top of DH glial cells, application of a α-me-NA triggered an increase in $[Ca^{2+}]_i$ the detector HEK293 cells, indicating ATP release from DH glial cells (see Eersapah et al., 2019). The illustration shows the superimposed $[Ca^{2+}]_i$ signals from 3 different HEK293-P2X2-PROG cells (on top of DH glial cells) before, during and after the application of 0.5 μM α-me-NA.

Effect on PHE-evoked ATP release

In these experiments we first applied 2-BFI or CLO alone for 50 seconds, then we coapplied 2-BFI and PHE or CLO and PHE for 100 seconds and finally we washed out 2-BFI or CLO in order apply PHE alone for another 50 seconds (Fig 32). The calcium signals in the detector HEK293-P2X2-PROG cells were quantified by the A.U.C in the absence of any application (baseline for 100 s), during the co-application of 2-BFI or CLO with PHE (for 100 s) and during PHE alone (for 100 s) after wash-out of 2-BFI or CLO. The period analyzed for PHE alone included the 50 seconds of application of PHE and the 50 seconds period that immediately followed the termination of PHE application (100 s in total). These A.U.C were then compared statistically.

As illustrated in Fig 32A, when PHE (20 µM) was coapplied with 2-BFI (10 µM), it failed to increase $[Ca^{2+}]_i$ in the detector HEK293-P2X2-PROG cells. The A.U.C under baseline conditions, i.e. in the absence of any application, was of 102.0 ± 0.38 a.u (n=16) and 102.09 ± 0.49 a.u (n=16) during the coapplication of 2-BFI and PHE. These values were not significantly different (paired Student's t-test, P = 0.75). When 2-BFI was washed out and PHE was applied alone, an increase in [Ca2+]i was observed and the A.U.C of this signal was of 112.77 ± 1.76 a.u (n=16) which was significantly larger than that observed during the co-application of PHE with 2-BFI (paired Student's t-test, P = 3.76 10-6). These results indicated that 2-BFI (10 µM) reversibly blocked the ATP release induced by PHE (20 µM). Similar results were obtained with CLO (10 µM) (Fig 32B). Co-application of CLO (10 µM) and PHE (20 µM) failed to increase [Ca2+]i in the detector HEK293-P2X2-PROG cells. The A.U.C under baseline conditions, i.e. in the absence of any application, was of 101.22 ± 0.24 a.u (n=29) and of 101.58 ± 0.02 a.u (n=29) during the co-application of CLO and PHE. These values were not significantly different (paired Student's t-test, P = 0.14). When CLO was washed out and PHE was applied alone, an increase in [Ca2+]i was observed. The A.U.C of this signal was of 120.60 ± 2.98 a.u (n=29) which was significantly larger than that observed during the co-application of PHE with CLO (paired Student's t-test, P = 6.67 10-7). These results indicated that CLO (10 µM) also reversibly blocked the ATP release induced by PHE (20 µM). It must be emphasized that the increases in [Ca2+]i in the detector HEK293-P2X2-PROG cells evoked by PHE after washout of 2-BFI or CLO were comparable to those obtained in experiments in which only PHE was applied (A.U.C 115.06 ± 2.24 a.u (n=34) (unpaired Student's t-test: PHE vs PHE after washout of 2-BFI, P = 0.51 and PHE vs PHE after washout of CLO, P = 0.14). Therefore, it appeared that α-me-NA

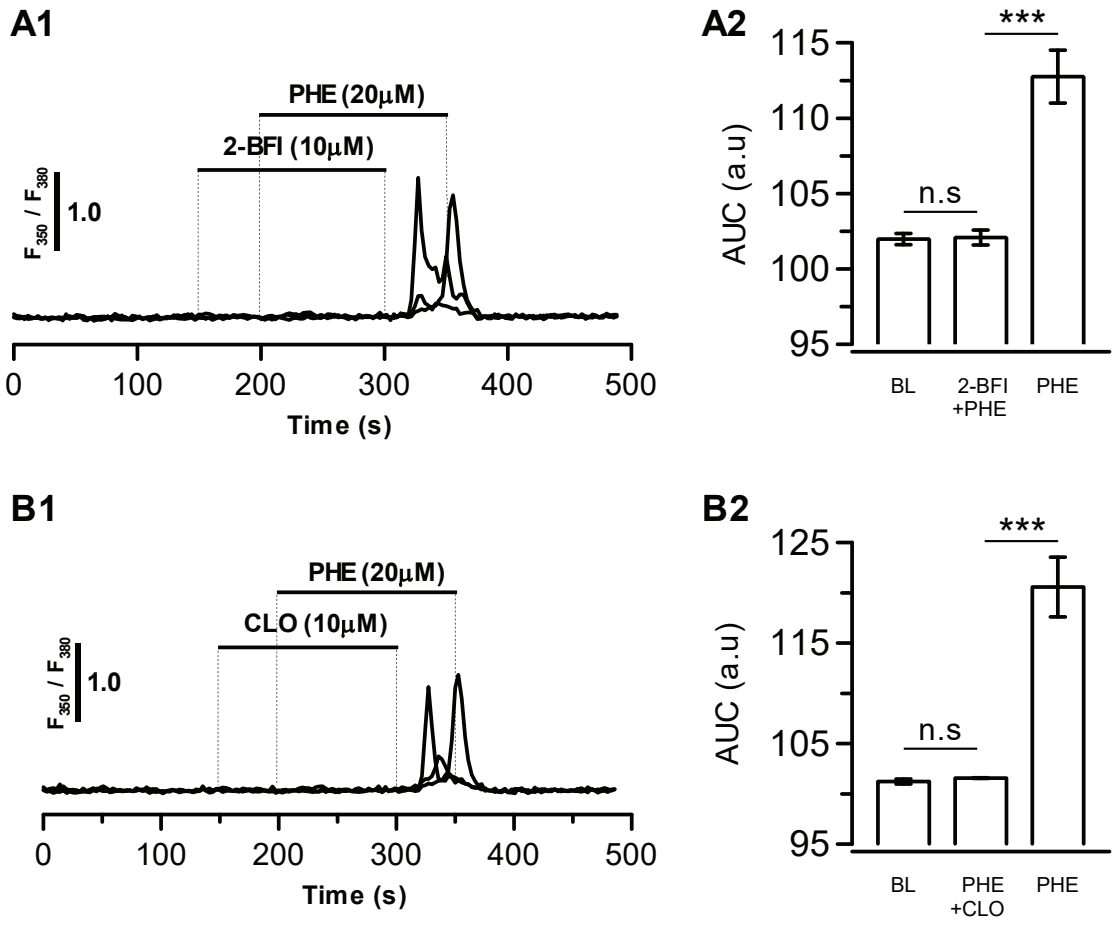

Figure 32. Interaction between AR-agonists and imidazolines on ATP release from DH glial cells. Fura-2 loaded HEK293-P2X2-PROG cells were plated on top of DH glial cells and used as detector cells for ATP release (see Eersapah et al., 2019). **A1** Superimposed $[Ca^{2+}]_i$ signal from 3 HEK293-P2X2-PROG cells (on top of DH glial cells) before, during and after the application of 2-BFI and PHE. Co-application of 2-BFI (10μM) and PHE (20μM) showed that 2-BFI inhibited ATP release normally induced by PHE (see Eersapah et al., 2019). However, shortly after stopping the 2-BFI perfusion, PHE induced a significant increase in the $[Ca^{2+}]_i$ signals from the ATP detector cells. **A2** Mean area under the curve (AUC) measured in the HEK293-P2X2-PROG cells under the different experiment conditions. **B1**/ **B2** illustrate similar experiments as **A1**/**A2** but with co-application of CLO and PHE. CLO also inhibited the PHE induced ATP release when co-applied with PHE. After wash-out of CLO, PHE rapidly induced the release of ATP as indicated by the presence calcium peaks (pair Students test, ***P< 0.001, N=7 -19).

increased the release of ATP from cultured DH glial cells whereas 2-BFI and CLO inhibited the PHE-evoked release of ATP from these glial cells.

2.1.8 Effects of 2-BFI and CLO on PHE-evoked calcium signals in cultured DH glial cells

In order to clarify the blocking effect of 2-BFI and CLO on ATP release, we next investigated their effect of the PHE–induced increases in $[Ca^{2+}]_i$ in cultured DH glial cells. The protocol of co-application of 2-BFI or CLO and PHE and sequential wash out of 2-BFI or CLO was the same as that used in the ATP release experiments described above. Fig 33 illustrates that when 2-BFI (10 μM) or CLO (10 μM) were co-applied with PHE (20 μM), there was no increase in $[Ca^{2+}]_i$ in cultured DH glial cells. However, upon wash out of 2BFI or CLO, a large increase in $[Ca^{2+}]_i$ was observed in the same cells. These observations indicated that 2-BFI or CLO reversibly blocked the increase in $[Ca^{2+}]_i$ induced by PHE.

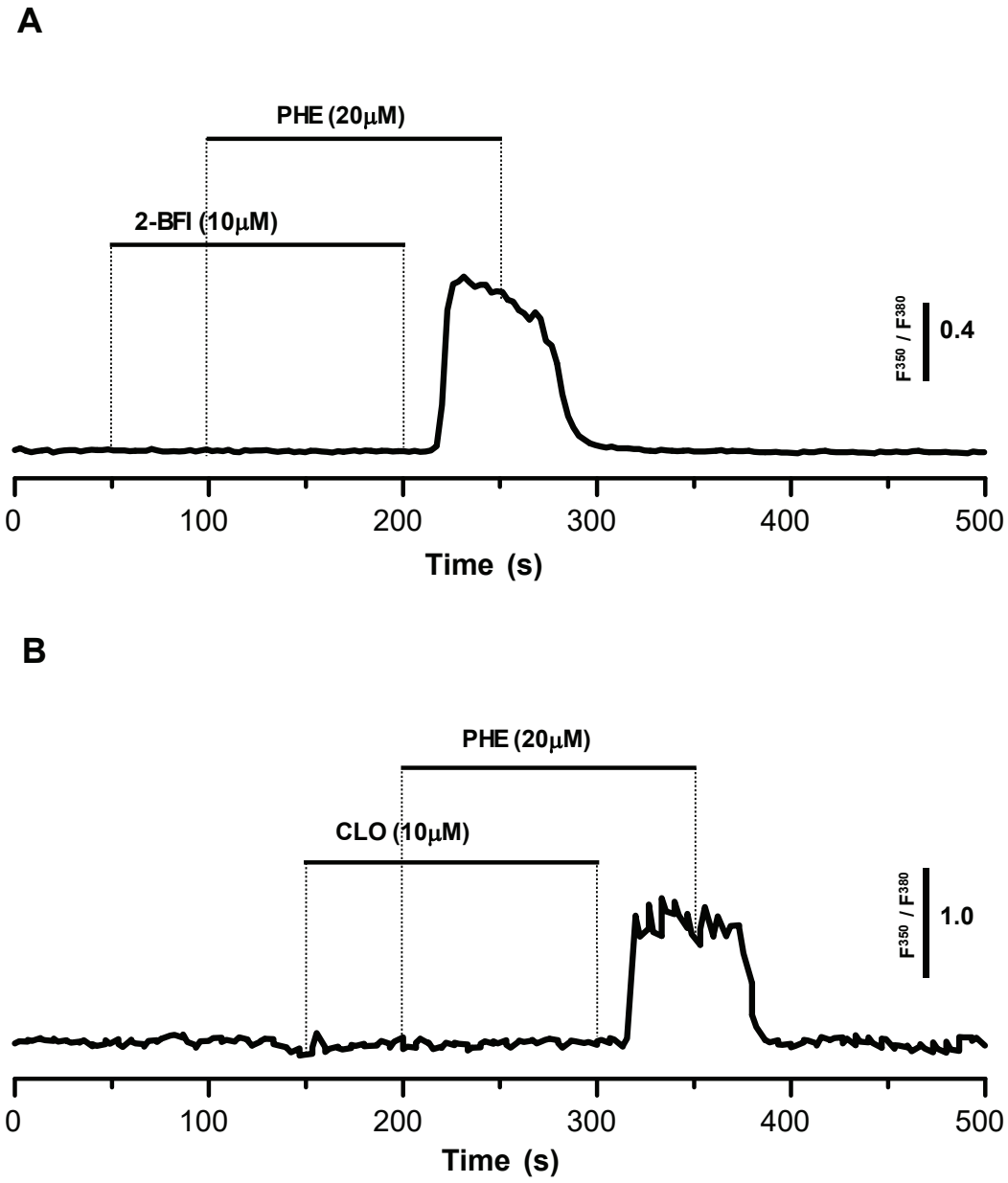

Figure 33. Interaction between AR-agonists and imidazolines on $[Ca^{2+}]_i$ in DH glial cells. Example trace of $[Ca^{2+}]_i$ signals from fura-2 loaded DH glial cells. A 2-BFI (10μM) inhibited the PHE (20μM) -induced $[Ca^{2+}]_i$ increase during co-application in DH glial cells. Shortly after stopping the 2-BFI application, the inhibition was removed and PHE induced an increase in [Ca2+]i. B Similarly to 2-BFI, co-application of CLO inhibited the PHE-induced $[Ca^{2+}]_i$ elevation during the period it was present, but rapidly allowed $[Ca^{2+}]_i$ elevation from PHE after washout.

2.2 Discussion - project 2

Our results show that a majority (approximately 70%) of cultured DH glial cells express functional α_2-ARs, the activation of which increased $[Ca^{2+}]_i$ and facilitated the release of ATP. These receptors were selectively activated by low concentrations of α-me-NA and CLO. At higher concentrations, CLO inhibited the calcium plateau phase of the response evoked by the α_1-AR agonist PHE and this inhibition appeared to involve a blockade of the calcium influx channels that underlie the calcium plateau of the PHE response. In addition, virtually all cultured DH glial cells (98%) expressed functional I2 imidazoline receptors, the activation of which also reversibly reduced the amplitude of the calcium plateau of the PHE response. Moreover, when CLO or 2-BFI were pre-applied and subsequently co-applied with PHE, both the initial peak and plateau of the α_1-AR response were blocked. These blocking effects were rapidly reversed upon washout of CLO or 2-BFI. In line with these observations, at high concentration (10 μM) both CLO and the I2 agonist 2-BFI reversibly blocked the PHE-evoked release of ATP.

2.2.1 DH glial express functional α_2-ARs that increase $[Ca^{2+}]i$

α-me-NA and CLO at low concentration increased $[Ca^{2+}]_i$ in cultured DH glial cells. This effect was reproducible upon repeated application and reversibly blocked by the selective α_2-AR antagonist YOH. Interestingly, low concentrations of α-me-NA and CLO also elevated $[Ca^{2+}]_i$ when applied during the calcium plateau observed following the activation of α_1-ARs by PHE, indicating that both responses were at least additive. It will be interesting, in future studies to test the additivity or eventual synergy of the calcium responses induced by the two receptor types, in particular by using sub-maximally effective concentrations of agonists for the two receptors. Since 95% of the DH glial cells in our cultures express functional α_1-ARs (see part 1 of results and Eersapah et al (2019)) and 70% had functional α_2-ARs, it appears that about 70% cultured DH glial cells co-express both types of α-ARs. A direct proof of such colocalization was evident from our experiments since all cells displaying responses to α-me-NA also responded to PHE with an increase in $[Ca^{2+}]_i$. These receptors, which both trigger an increase in $[Ca^{2+}]_i$ in cultured DH glial cells, might be co-stimulated upon NA release in the DH under physiological conditions and act in concert to finely tune ATP release (see general discussion section for more details).

2.2.2 High concentrations of CLO inhibit α_1-AR-induced elevations in $[Ca^{2+}]_i$

At concentrations ≥ 0.3 μM, CLO also inhibited rather than increased $[Ca^{2+}]_i$. Interestingly both an increase or a decrease of the PHE-induced calcium plateau could be observed at concentrations between 0.3 and 1 μM. Usually, we observed either an increase or a decrease in a given cell, but occasionally an increase could be followed by a decrease, see Fig 24-25. The inhibitory effect was dose-dependent and appeared to be maximal between 3 and 10 μM at which an almost complete inhibition of the PHE-induced calcium plateau was observed. Interestingly, in cells with type 3 responses to PHE, i.e., in which only a peak increase without a subsequent plateau phase was present, low concentrations of CLO (0.1 and 0.3 μM) increased $[Ca^{2+}]_i$, whereas no change in $[Ca^{2+}]_i$ was observed in the same cells at higher CLO concentrations. These observations reinforced the idea that the facilitating response was blocked at high CLO concentrations. Further experiments will be needed to clarify the mechanisms involved in these phenomena and will require to find pharmacological tools to separate the facilitatory and inhibitory effects of CLO on the PHE-evoked calcium response. It is well established that, in glial cells, the plateau phase of the calcium response induced by PHE and other G protein-coupled metabotropic receptors is due to calcium influx. Such an influx can be triggered following the initial release of calcium from intracellular calcium stores by a phenomenon termed store-operated calcium entry (SOCE) (Ong et al., 2019; Prakriya and Lewis, 2015). Alternatively, calcium influx can be independent of an initial depletion of intracellular calcium stores and activated by arachidonic acid. This phenomenon is termed non-store operated calcium entry (non-SOCE) (Shuttleworth, 2012). Future experiments aimed at isolating pharmacologically SOCE and non-SOCE components of calcium influx should allow determining if CLO inhibits SOCE, non-SOCE or both.

2.2.3 Presence of functional imidazoline I2 sites/receptors on cultured DH glial cells

Among imidazoline-related molecules, some, like CLO, bind to specific sites/receptors distinct from α_2-ARs and induce the modulation of physiological functions (Ernsberger et al., 1995; Head and Mayorov, 2006). Three types of imidazoline sites/receptors (I1, I2 and I3) have been described (Head and Mayorov, 2006). I3 receptors are apparently only expressed in pancreatic β cells in which they regulate insulin secretion. I1 and I2 receptors are expressed in the nervous system. I1 receptors are best known and play a central role in the regulation of cardiovascular function. They apparently underlie the non α_2-AR-mediated hypotensive effect of CLO by acting

within brainstem structures to regulate blood pressure (Ernsberger et al., 1997; Nikolic and Agbaba, 2012). I2 receptors have been less characterized and it has been proposed that I2 sites are situated mostly on monoamine oxidases (MAO) located in mitochondria (Regunathan and Reis, 1996). More recently a binding site for I2 ligands has also been characterized on brain-type creatine kinase (CK-B) (Kimura et al., 2009).

In our system, the I2 agonist 2-BFI (10 μM) clearly inhibited the plateau of the PHE calcium plateau in a reversible manner and in virtually all cells tested. This effect of 2-BFI was significantly reduced in the presence of the I2 antagonist idazoxan but not by the α_2-AR antagonist yohimbine. However, IDAZ only partly blocked the effect of 2-BFI, suggesting that the IDAZ-resistant effect of 2-BFI on the PHE-induced calcium plateau involved a mechanism that was independent of I2 receptors (see next section of discussion). CLO is also an agonist at imidazoline receptors. CLO binds with high affinity to I1 receptors (K_i=1 nM) and with rather low affinity to I2 receptors (K_i between 8 and 14 μM) (Ernsberger et al., 1997; Ernsberger et al., 1990; Head and Mayorov, 2006). Using our calcium imaging approach, we found no evidence for the presence of functional I1 receptors on cultured DH glial cells, since cimetidine (10 μM), an agonist of I1 receptors (Tsoli et al., 1995) had no effect on $[Ca^{2+}]_i$ or on the calcium plateau of PHE responses. This finding was consistent with earlier studies indicating that astrocytes express I2 but not I1 sites/receptors (Ernsberger et al., 1995; Regunathan et al., 1993). It is therefore unlikely that the effect of CLO in our experiments was mediated by its interaction with I1 receptors.

Our results also showed that the effect of the I2 agonist 2-BFI was significantly reduced but not totally blocked by CLORG, an inhibitor of MAO (Sanchez-Blazquez et al., 2000). These results are consistent with the involvement of I2 sites located on MAO in the inhibition of the calcium plateau by 2-BFI. The intracellular transduction pathways that follow binding of I2 ligands to I2 sites/receptors located on MAO or CK-B are presently unknown. One possibility could be that these I2 ligands modulate the enzymatic activities of MAOs or CK-B.

The I2 binding site at CK-B is distinct from the active site of the enzyme and binds 2-BFI with nanomolar affinity (Kimura et al., 2009). It was shown that even at high concentration (20 μM), 2-BFI did not affect the enzymatic activity of CK-B (Kimura et al., 2009). It is therefore unlikely that the inhibition of the calcium plateau of the PHE-induced plateau was due to a reduction (or an increase) in the activity of CK-B by 2-BFI.

There are currently no data available concerning the binding characteristics of CLO and IDAZ to CK-B as well as on their eventual consequences on CK-B activity.

It is generally accepted that the typical I2 binding site/receptor are mainly located on MAOs at the outer membrane of mitochondria (Regunathan and Reis, 1996) (Bousquet et al., 2020). Binding studies with I2 ligands on I2 sites and the high-affinity site of MAO are generally in good agreement: i.e. for I2 sites CLO, IDAZ and 2-BFI possess K_is of 8-14 µM, 11 nM and 10 nM, respectively (Ferrari et al., 2011; Molderings et al., 1998); and for the high-affinity site of MAO the Ki are of 750 nM, 2.2 nM and 4-6 nM, respectively (Ferrari et al., 2011; Ozaita et al., 1997). For the low-affinity site of MAO the I2 ligands have Kis > 25 µM (range 25-46 µM) (Ferrari et al., 2011; Ozaita et al., 1997). I2 ligands were shown to inhibit the activity of both subtypes of MAO termed MAO-A and MAO-B (Ferrari et al., 2011; Ozaita et al., 1997). The IC_{50} of CLO, IDAZ and 2-BFI are between 11 µM and 700 µM for MAO-A and between 23 µM and 6000 µM for MAO-B (Ferrari et al., 2011; Ozaita et al., 1997).

The I2 ligands that we tested were applied extracellularly at micromolar concentrations (CLO 10 µM, IDAZ 2 µM, 2-BFI 10 µM). To bind to I2 sites these molecules have to cross the plasma membrane in order to reach I2 sites that are located intracellularly. This can occur via direct diffusion across the membrane for very hydrophobic molecules like CLO and/or via organic cation or anion transporters (OCT and OAT respectively) (Ullrich et al., 1993). CLO can very rapidly enter the cell by diffusing across the cell membrane that can reduce the extracellular concentration CLO by about 70% as it was shown for contra-luminal CLO influx into rat kidney cells in vivo (Ullrich et al., 1993). In the same preparation, it was also shown that CLO can enter the cells via OAT and OCT but the K_i for these transports are 2.8 mM and 1 mM, respectively. IDAZ can also be transported to the cell interior by OCT with a K_i of 0.4 mM. There are unfortunately no data available concerning the mechanisms by which 2-BFI is transported across plasma membranes. For example, if one speculates that inside the cells the I2 ligands tested could reach a concentration that was 100 times lower than its concentration outside the cell, this would result in expected intracellular concentrations of 100 nM for CLO and 2-BFI and 20 nM for IDAZ. At these concentrations, one should observe significant binding of 2-BFI and IDAZ to I2 sites/rec (close to EC90/IC90) but only a modest binding, if any, of CLO (<EC1). At these intracellular concentrations neither CLO nor 2-BFI is likely to significantly affect MAO activity (see preceding paragraph of this discussion section). Even if CLO would be present at a 10 times higher intracellular concentration, i.e. 1 µM, this would

only correspond to the EC_{10} of this ligand for I2 sites/receptors. This might explain why IDAZ had no significant effect on the inhibition of the PHE-induced calcium plateau induced by CLO.

We next asked whether the CLO- and 2-BFI-induced reductions of the amplitude of the PHE-triggered calcium plateau could be due to the inhibition of MAO activity by CLO and 2-BFI. We therefore tested the effect of the MAO inhibitor CLORG (at a concentration of 2 μM). Acute application or pre-incubation of the glial cell cultures with CLORG never directly interfered with the PHE-triggered calcium response but reduced the effect of 2-BFI on the calcium plateau. If, as speculated before, the intracellular CLORG concentration would reach 20 nM this would lead only to a reduction of 50% of MAO-A activity and would not affect MAO-B activity. At 200 nM one would expect a 90% inhibition of MAO-A activity (IC90) and still no effect on MAO-B (Ferrari et al., 2011; Ozaita et al., 1997). It should also be emphasized that, when used at the same concentration (10 μM), CLO was more potent that 2-BFI in reducing the PHE-induced calcium plateau although its IC_{50} for the inhibition of MAO activity is almost two orders of magnitude higher than that of 2-BFI (CLO: 700 μM; 2-BFI 11 μM) (Ozaita et al., 1997).

Since (1) CLORG, an inhibitor of MAO, applied alone did not inhibit the PHE-calcium response and (2) that at the concentrations used, neither CLO nor 2-BFI would significantly affect MAO-A or MAO-B activities, it was unlikely that the observed effects of CLO and 2-BFI were mediated by an inhibition of MAO activity. One possible explanation for the "antagonistic" effect of CLORG on the I2 receptor/site-mediated component of 2-BFI, could be that the binding of CLORG to MAO might mask the I2 binding site and therefore block the access of I2 agonists to their binding sites on MAO. Indeed, it has been shown that imidazoline ligands bind to a site that is distinct from the active site of the enzyme where CLORG binds (Raddatz et al., 1995). Taken together, our results indicate that I2 sites receptors are located on MAO but that the action of the imidazolines tested was certainly not related to their inhibition of MAO enzymatic activity.

2.2.4 Inhibition of SOCE and non-SOCE calcium entry and intracellular calcium release by high concentrations of CLO and 2-BFI

Our results clearly showed that IDAZ and CLORG decreased but did not fully block the inhibitory effect of 2-BFI (10 μM) on the calcium plateau of the PHE response see Fig.29-30. Moreover, CLORG failed to inhibit the effect of CLO on the plateau of the PHE-response. This suggested that these molecules had an additional

effect that was not mediated by I2 sites/receptors. This effect could involve a yet to unravel receptor-mediated effect or could reflect the direct blockade by these two imidazoline-related molecules of (a) calcium influx pathway(s) that is (are) active during the PHE plateau phase.

2.2.4.1 Direct blockade of Ca^{2+}-influx channels

Molecules having an imidazoline ring might directly interact with the channels underlying SOCE and/or non-SOCE, since SKF96365 which possesses an imidazole ring was shown to inhibit selectively non-SOCE at low (100 nM) concentrations (Moneer et al., 2005) and SOCE at higher (micromolar) concentrations (Jairaman and Prakriya, 2013).

Imidazolines such as CLO, IDAZ and 2-BFI have been shown to inhibit cation-permeable ionotropic neurotransmitter receptors. Indeed, CLO and IDAZ inhibit nicotinic acetylcholine receptors (nAChR) (Molderings et al., 1995b) and 5-HT_3 serotonin receptors (5-HT_3R) (Molderings et al., 1995a) with an IC_{50} > 10 µM. The blocking effects of CLO and IDAZ on nAChRs and 5-HT_3Rs at high micromolar concentrations was shown to be independent of I1 and I2 receptors (Molderings et al., 1995b) and it has been suggested that CLO could bind to the cation binding site within the nAChR channel pore in a way similar to phencyclidine (Musgrave et al., 1996). The effect of 2-BFI on nAChRs and 5-HT_3R has not been tested, but 2-BFI was reported to inhibit NMDA glutamate receptors (NMDAR) (Han et al., 2013a; Jiang et al., 2010). Both 2-BFI and IDAZ dose dependently inhibited calcium entry induced by activation of NMDARs in cortical neurons. The threshold of these effects was around 10 µM for both 2-BFI or IDAZ, 2-BFI being however more potent than IDAZ (Jiang et al., 2010). Whole-cell patch-clamp recordings from cortical neurons showed that 2-BFI inhibited membrane currents triggered by NMDAR-activation in a voltage-independent and non-competitive manner. The IC_{50} of the 2-BFI effect on NMDAR currents was of 125 µM and 2-BFI had no effect on AMPA receptor-mediated currents (Han et al., 2013a). Calcium imaging experiments in the same preparation showed that 2-BFI produced a progressive and rapidly reversible inhibition of Ca^{2+} influx through NMDARs. This effect was reproduced by memantine, a blocker of NMDARs, and the onset and offset kinetics of the blocking effect s of 2-BFI and memantine matched perfectly (Han et al., 2013a). It therefore appears that imidazolines that act as Imidazoline site/receptor ligands such as CLO, IDAZ and 2-BFI can also inhibit Ca^{2+} influx through cationic ion channels

independently of their effects on I1 and I2 sites/receptors. Such blocking effects might also occur for other cationic channels such as those that underlie SOCE and non SOCE.

Indeed, during SOCE and non-SOCE the association of the endoplasmic reticulum protein STIM1 and the membrane channel proteins Orai1 and/or Orai3 form calcium-selective calcium entry pathways (Shaw et al., 2013) (Parekh, 2010; Shuttleworth, 2009; Shuttleworth, 2012; Soboloff et al., 2012; Thompson and Shuttleworth, 2013). These calcium-permeable channels underlie the calcium plateau phase following the activation of metabotropic G-protein coupled receptors, and their blockade could explain the fast and reversible inhibition of the PHE-induced calcium plateau by CLO and 2-BFI. SOCE can be potently inhibited by the trivalent cation La3+ (Aussel et al., 1996; Hoth and Penner, 1993; Jairaman and Prakriya, 2013; Mason et al., 1991). The IC50 of this fast and reversible blocking effect of La^{3+} is of 20 nM (Aussel et al., 1996). La^{3+} also blocks cationic ionotropic neurotransmitter receptors such as nAChRs (Rangel-Gonzalez et al., 2002), 5-HT3Rs (Emerit et al., 1993) and NMDARs (Reichling and MacDermott, 1991). Interestingly, the receptors blocked by La^{3+} are the same as those known to be blocked by CLO and 2-BFI. It is therefore tempting to speculate that SOCE channels, that are blocked by La^{3+} might also be blocked by CLO and 2-BFI. An argument in favor of this hypothesis comes from experiments using SKF96365, an imidazole molecule that blocks SOCE at low micromolar concentrations (Jairaman and Prakriya, 2013; Merritt et al., 1990) and also inhibits the PHE-induced calcium plateau in our preparation (data not shown).

In summary, the most likely mechanism involved in the inhibition of the PHE-induced calcium plateau by CLO and 2-BFI is a direct and rapidly reversible block of SOCE (and perhaps non-SOCE) channels. In future experiments, it will be interesting to test the effects of CLO and 2-BFI on pharmacologically separated/isolated SOCE and non-SOCE calcium entry pathways.

2.2.4.2 Receptor-mediated inhibition of SOCE and non SOCE

In addition, to the reduction of the PHE-induced calcium plateau, we also noticed that when CLO or 2-BFI were pre-applied alone and then coapplied with PHE (see Fig. 21, 28, 33), the increase in $[Ca^{2+}]_i$ normally triggered by PHE was completely blocked during the co-application but was very rapidly and fully restored upon washout of CLO or 2-BFI. This phenomenon was also observed in our experiments on ATP release in which no PHE-induced ATP release was observed during pre-and co-application of CLO or 2-BFI and PHE, but a significant

and often large release of ATP occurred very soon after stopping the co-application and rinsing CLO or 2-BFI (see Fig. 32). The observation that the initial peak of the PHE-induced calcium response in glial cells was blocked by these imidazolines could be explained in several ways: (1) CLO and 2-BFI could either block the production of IP_3 and or directly block IP_3 receptors (IP_3R) by acting intracellularly, or alternatively (2) by decreasing the coupling of α1-ARs to IP_3 production. There is currently no evidence for either of these possibilities in the literature. However, a recent study carried out on hippocampal astrocytes revealed an interesting relationship between SOCE and refilling of calcium stores in the endoplasmic reticulum (Sakuragi et al., 2017). In this study, SOCE was inhibited by preventing the interaction between STIM and Orai with DPB162-AE (Goto et al., 2010; Hendron et al., 2014). DPB162-AE not only blocked the spontaneously-occurring calcium transients in astrocytes but also prevented the refilling of calcium stores of the endoplasmic reticulum (Sakuragi et al., 2017) as it was observed for other non-excitable cells (Bittremieux et al., 2017). When DPB162-AE was pre-applied for 4 min, the increase in $[Ca^{2+}]_i$ normally induced by stimulation of metabotropic glutamate receptors with DHPG was totally abolished including the initial calcium rise triggered by the release of Ca^{2+} from intracellular stores (Sakuragi et al., 2017). This observation is very similar to what we observed in our experiments. It might be that pre-application of CLO or 2-BFI blocks SOCE channels, a phenomenon that will lead to impaired refilling of intracellular calcium stores. As a consequence, there will be a reduction/suppression of the PHE-induced calcium response in DH glial cells and a decrease/suppression of calcium-dependent ATP release from these cells.

2.3 Conclusion

Our results clearly indicate that about 70% of cultured DH glial cells co-express α_1 and α_2-ARs that increase $[Ca^{2+}]_i$ and that virtually all DH glial cells also express I2 imidazoline sites/receptors. From a functional point of view, our results showed that activation of α_2-ARs stimulated whereas activation of I2 receptors inhibited the release of ATP from DH glial cells. At high concentrations of imidazoline-related molecules such as CLO and 2-BFI, a direct blockade of calcium influx channels leading to decrease in the refilling of intracellular calcium stores seemed to occur and these phenomena led to a blockade of ATP release from DH glial cells.

3 General Discussion

The major aim of our work was to determine whether glial cells from the DH of the mouse spinal cord express functional receptors for noradrenaline and what would be the consequences of their activation on the release of the gliotransmitter ATP. To this end, we developed a mixed culture of DH glial cells from postnatal mice containing mainly astrocytes (>95%). Our results show that virtually all of these astrocytes possess functional α_1-adrenoceptors and about 70% express α_2-adrenoceptors (α_1 and α_2-ARs). Activation of these receptors increased intracellular free calcium concentration ($[Ca^{2+}]_i$) and induced the release of ATP from DH glial cells via the exocytosis of secretory lysosomes. A more detailed analysis of the effects of the classical α_2-AR agonist clonidine revealed complex effects of this imidazoline molecule that included the activation of α_2-ARs and a direct block of store-operated and non-store operated calcium entry channels (SOCE and non-SOCE channels). Activation of I2 imidazoline sites/receptors present on monoaminoxidases (MAOs) led to an IDAZ-sensitive inhibition of SOCE and/or non-SOCE as well as a direct blockade of these calcium influx channels. This direct blockade resembled that indued by CLO at micromolar concentrations. These blocking effects seemed to be linked to the imidazolinic structure of the ligands. For example, it was also observed with the imidazolinic α_2-AR agonist dexmedetomidine (10 µM, results not shown). Alternatively, this decrease in SOCE and non-SOCE might be due to a receptor-mediated effect, but the identity of the eventual receptor(s) involved and of the underlying inhibitory mechanism(s) of SOCE- and/or non-SOCE-mediated calcium influx remain(s) to be elucidated. Most importantly, activation of I2 sites/receptors and direct inhibition of SOCE and non-SOCE led to the suppression of α_1-AR triggered ATP release from DH glial cells and this phenomenon might have important consequences in the pharmacological management of chronic pain.

Most aspects concerning the development of our biosensor system allowing high-resolution detection of ATP release from single glial cells, the characterization of α_1- and α_2-ARs and their consequences on $[Ca^{2+}]_i$ and on ATP release, the presence of I2 sites/receptors and the direct blocking effect of CLO on SOCE and non-SOCE, have been already discussed in detail at the end of the first and second parts of the Results section of this thesis and will therefore not be re-discussed in depth in the following general discussion. In the next

sections, we would like to comment in more detail on the physiological importance of our results and their possible clinical applications.

Illustration of Result part 1

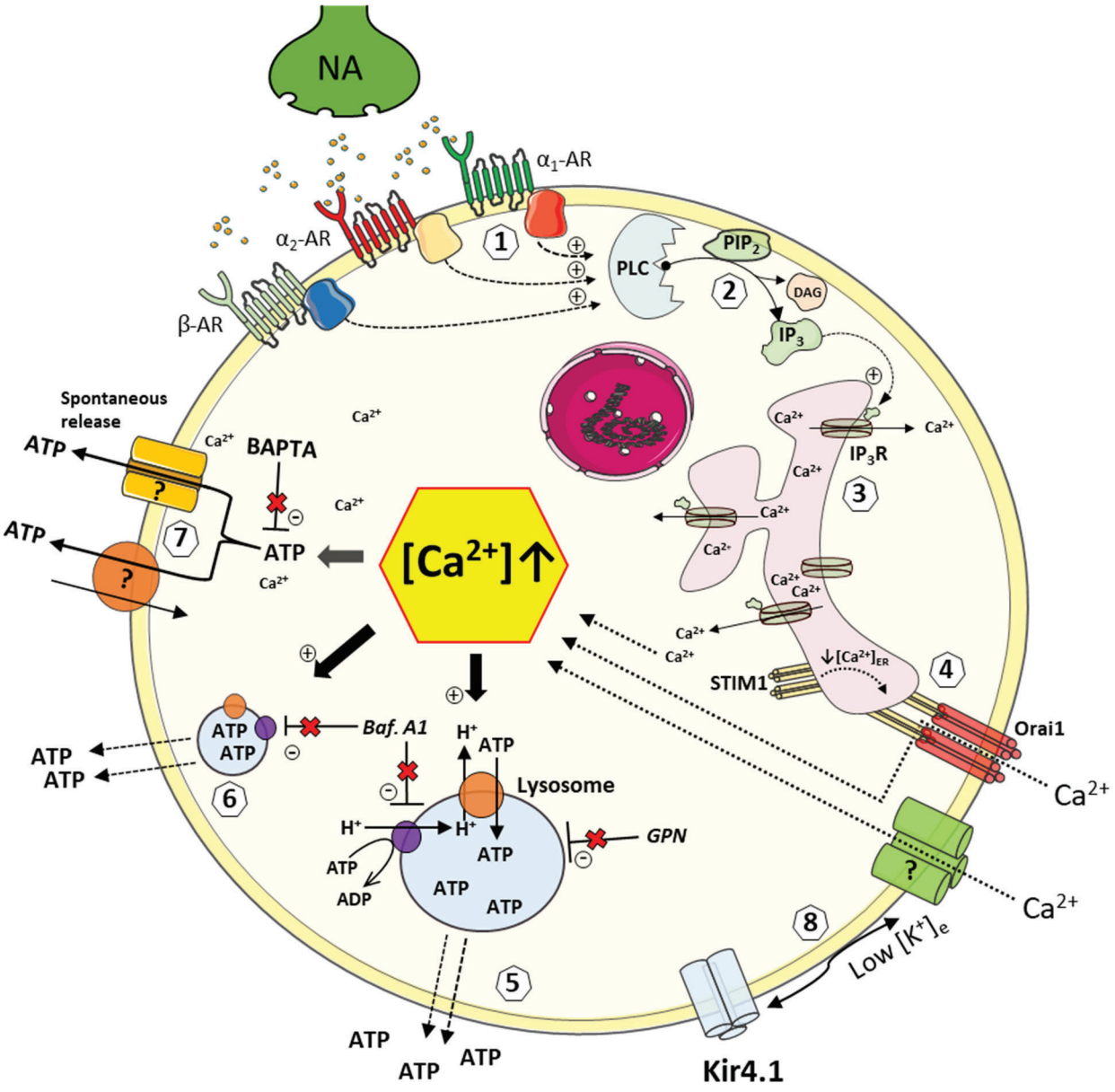

Figure 34. Legend on next page

Figure 34. Summary of results from project one – effect of noradrenaline on intracellular calcium and ATP release in DH glia. **1)** Astrocytes expresse G-protein coupled adrenoceptors (α_1, α_2 and β) that, when stimulated by noradrenaline (NA, 20μM), lead to the activation of phospholipase C (PLC). **2)** Activated PLC cleaves the membrane-bound phosphatidylinositol 4,5-bisphosphate (PIP2) to diacylglycerol (DAG) and inositol 1,4,5-trisphosphate (IP_3) which can diffuse into the cytoplasm. **3)** Free IP_3 can bind to the IP_3 receptors (IP_3R) located on the membrane of the endoplasmic reticulum (ER). Binding of IP_3 to the IP_3R, which act as calcium channels, leads to the release of Ca^{2+} from the lumen of the ER to the cytoplasm. **4)** Low ER concentrations of calcium trigger the migration and aggregation/accumulation of the $[Ca^{2+}]_{ER}$ - sensor stromal interaction molecule 1 (STIM1) near the plasma membrane. STIM1 proteins near the plasma membrane can interact with the calcium release-activated calcium channel protein 1 called Orai1. The Ca^{2+} permeable STIM-Orai complexes allow calcium influx from the external environment into the cytoplasm and thereby further prolong the elevation of free intracellular calcium concentration in the cytoplasm. 5) Prolonged elevated $[Ca^{2+}]_i$ induced by NA or α_1-agonist phenylephrine (PHE, 20μM) results in vesicular ATP release that can be blocked by the lysosomal disrupting molecule GPN (glycyl-L-phenylalanine 2-naphthylamide) indicating that lysosomes are the primary ATP sources of NA-induced ATP release. **6)** However, a second non-lysosomal vesicular ATP-pool, composed of smaller vesicles resistant to GPN-treatment, was released from astroglia when increasing $[Ca^{2+}]_i$ by lowering the external $[K^+]_e$ (0.2 mM). **8)** Exposing astroglia to reduced $[K^+]_e$ causes a conformational shift in the inward-rectifying potassium channel Kir.4.1 which allows influx of external Ca^{2+} and thereby the release of the second vesicular ATP-pool. Both the lysosomal and the small vesicular sources of ATP release are blocked by Bafilomycin A (Baf. A1) which prevents the acidification of vesicles (and therefore also the loading of ATP into the vesicles) by blocking the H^+-ATPase. 7) Astroglia also release ATP spontaneously through a non-vesicular mechanism (not blocked by Baf. A1). However, the spontaneous non-vesicular ATP release mechanism is dependent on$[Ca^{2+}]_i$, as it is blocked by the calcium chelator BAPTA-AM. It is important to note that BAPTA-AM blocks all pathways of ATP release, indicating that they are all calcium-dependent.

3.1 Noradrenaline and the DH of the spinal cord

3.1.1 Functional adrenoceptors on DH glial cells and their role in the control of ATP release in the spinal nociceptive system.

The study of astroglial cells in the nervous system over the past 40 to 50 years has clearly shown that they express a large diversity of ionotropic and metabotropic receptors to classical neurotransmitters, neuropeptides or other extracellular messengers (Verkhratsky and Nedergaard, 2018). An interesting feature of metabotropic receptors in glial cells, and in particular in astrocytes, is that both Gq-coupled and Gi/o coupled receptors increase $[Ca^{2+}]_i$ whereas in neurons only Gq coupled receptors have such an effect (Durkee et al., 2019). Indeed, in neurons, Gi/o coupled pathways generally activate an inwardly rectifying K^+ conductance (post-synaptic effect) or inhibit voltage-dependent Ca^{2+} channels (presynaptic effect) (Huang and Thathiah, 2015). Moreover, it appears as a general rule that changes in $[Ca^{2+}]_i$ in glial cells are fundamental for the integration of extra and intracellular signals and intercellular communication (Verkhratsky and Nedergaard, 2018). Therefore, most substances that act on glia trigger changes (increases or decreases) in $[Ca^{2+}]_i$ that can be studied by calcium imaging approaches using synthetic or genetically-encoded calcium-sensitive probes. Using the ratiometric calcium dye fura-2, were could demonstrate that 95% of cultured postnatal mouse DH glial cells expressed functional α_1-ARs that increased $[Ca^{2+}]_i$. This finding was consistent with studies on cortical (Hertz et al., 2010; Pankratov and Lalo, 2015; Salm and McCarthy, 1990) and hippocampal (Duffy and MacVicar, 1995; Shelton and McCarthy, 2000) astrocytes in which noradrenaline also increases $[Ca^{2+}]_i$ by activating α_1-ARs. However, to our knowledge, our results are the first showing such a phenomenon in DH glial cells. The presence of α_2-ARs on glial cells has been more controversial because apparently only a limited fraction of CNS astrocytes responded with small increases in $[Ca^{2+}]_i$ following the application of classically used α_2-AR agonist clonidine (CLO) (Enkvist et al., 1996; Salm and McCarthy, 1990). This was also the case in our DH glial cultures, where only a small fraction of cells responded to a high concentration of CLO (10 μM). High concentrations of CLO were also used in most of the studies on cortical or hippocampal astrocytes. When testing the effect of α-me-NA (0.3 μM), an agonist that is considered selective of α_2-ARs when used at low concentration (Decker and Schwartz, 1985; Piguet and Schlichter, 1998), we observed that 70% of the cultured DH glial cells responded with an increase in $[Ca^{2+}]_i$. Moreover, the effect of α-me-NA was blocked by the α_2-AR antagonist yohimbine

and reproduced by a low concentration of CLO (0.3 μM). These results indicated the presence of functional α_2-AR on DH glial cells and that the activation of these receptors induced an increase in $[Ca^{2+}]_i$. In contrast, we observed that high concentrations of CLO (≥1μM) decreased the plateau of PHE-induced calcium responses. Therefore, the use of high CLO concentration in our and other studies on glial cells have led to a large underestimation of the presence of functional α_2-AR on these cells. This underestimation was due to the inhibition of the increase in $[Ca^{2+}]_i$ triggered by α_1- and α_2-AR activation by high concentrations of CLO (see Part 2 of the *Results* section). The exact targets and mechanisms underlying this inhibition remain to be clarified, but most probably involves a direct blockade of SOCE and/or non-SOCE channels by imidazoline-related-molecules.

The presence of adrenoceptors on spinal glial cells in culture has been suggested in 1982 using an autoradiography approach (Hösli and Hösli, 1982). Our results demonstrate that at least 70% of the glial cells present in our cultures co-express functional α_1- and α_2-ARs. These glial cells are probably astrocytes since because astrocytes appear to express functional α_1-ARs (Hertz et al., 2010). Activation of α_1-AR as well as α_2-ARs increased $[Ca^{2+}]_i$. Since a α_2 response could be evoked on top of the calcium plateau of a α_1 response, it appeared that the two types of responses were additive. Future studies will tell whether there is additivity or synergy of these responses and whether the calcium pool(s) involved in the two responses are the same or different.

Most importantly, we show that activation of α_1-ARs triggered the release of ATP via the calcium-dependent exocytosis of secretory lysosomes. The involvement of lysosomes in the release of ATP has been documented in astrocytes (Zhang et al., 2007). We confirm this point and show for the first time that this pool of secretory lysosomes is selectively targeted by noradrenaline via α_1-AR stimulation in DH glial cells. Although we have not tested it directly, we believe that the ATP release evoked by the selective α_2-AR stimulation might also involve secretory lysosomes. Indeed, after pretreatment of the glial cells with GPN that selectively inactivates lysosomes, ATP release triggered by PHE as well as by the natural agonist noradrenaline were completely blocked. Noradrenaline activates both α_1 and α_2-ARs and if α_2-AR would have targeted a vesicular pool different from lysosomes, it should have been intact after GPN treatment and therefore detectable in our experimental system.

Concerning ATP release, our results also show for the first time the coexistence of 3 distinct types of ATP release from DH glial cells. All three types of ATP release were dependent on an increase in $[Ca^{2+}]_i$. Two of these ATP pools are vesicular and involve acidic vesicles since these vesicular ATP releases were blocked by bafilomycin A1 pretreatment. The lysosomal pool targeted by noradrenaline was also blocked/inactivated after GPN pretreatment whereas that triggered by the application of a low K^+ solution was not affected by GPN and therefore represented a distinct acidic vesicular pool. Application of a low K^+ solution was shown to increase $[Ca^{2+}]_i$ in astrocytes from various CNS regions (Dallwig et al., 2000) by a mechanism involving inwardly rectifying Kir4.1 K^+ channels (Härtel et al., 2007). How the modulation of Kir4.1 K^+ channels leads to an elevation in $[Ca^{2+}]_i$ is not clear but it is reproducible upon repeated stimulation and consistently observed in virtually all astrocytes in slices or cultures from different CNS regions as well as in our DH glia culture system (see Results Part 1, Eersapah et al (2019)). It is, however, possible to suggest that the mechanisms of increase in $[Ca^{2+}]_i$ evoked by α_1-AR (application of PHE) and by low-K^+ are different since 2-BFI (10 µM, I2 site/receptor agonist) and CLO (10 µM) inhibited the calcium plateau of the PHE response but had no effect of the change in $[Ca^{2+}]_i$ evoked by the low-K^+ solution.

In addition, our results are the first to show that application of a low-K^+ solution not only increased $[Ca^{2+}]_i$ in DH glial cells but also triggered calcium-dependent vesicular ATP release from these cells (see Results Part 1 section, (Eersapah et al., 2019)).

Interestingly DH glial cells also displayed a basal/tonic calcium-dependent release of ATP that was resistant to inhibition by bafilomycin A1 and therefore did not involve acidic secretory vesicles. This non-vesicular ATP release will need further investigation in order to characterize the underlying mechanisms.

3.1.2 Glia to neuron interaction in the DH of the spinal cord

In the DH of the spinal cord, noradrenergic fibers originate mainly from the Locus Coeruleus (Lyons et al., 1989). These axons form synaptic like contacts with a subset of DH interneurons but not with primary afferent fibers (Rajaofetra et al., 1992) (Hagihira et al., 1990) (Holstege and Bongers, 1991; Satoh et al., 1982) although noradrenaline inhibits the release of glutamate from primary nociceptors (Travagli and Williams, 1996). This suggests that noradrenaline released from coeruleo-spinal axons might act via volume transmission at least in the case of primary afferent terminals (Rajaofetra et al., 1992). A similar mode of transmission has been

suggested for noradrenergic transmission in other structures of the CNS (Borroto-Escuela et al., 2015). In the DH of the spinal cord, noradrenergic axons also form frequent contacts with glial cells (Ridet et al., 1993), an observation suggesting a role of DH glia (mostly astrocytes) as effectors of noradrenaline.

Thus, our results suggest that noradrenaline released from noradrenergic fibers is likely to activate α_1-ARs as well as α_2-ARs present on glial cells. Moreover, the increase in $[Ca^{2+}]_i$ triggered by the activation of α_1- and α_2-ARs in DH glia seemed at least additive and therefore the co-activation of these receptors is likely to reinforce and warrant ATP secretion from glial cells following the local release of noradrenaline from descending noradrenergic fibers.

3.1.3 Direct postsynaptic effects of noradrenaline

Noradrenaline hyperpolarizes a large majority (70-80%) of lamina II DH neurons by activation of α_2-ARs (Grudt et al., 1995; North and Yoshimura, 1984). Noradrenaline less frequently depolarizes lamina II interneurons (3%-33%) by activating α1-Ars (Grudt et al., 1995; North and Yoshimura, 1984). In some cases the two types of effects can coexist yielding a biphasic response. Using transgenic mice that express EGFP under the GAD67 promoter in order to identify GABAergic neurons, it was shown that α_2-ARs are mainly expressed by non-GABAergic (probably excitatory glutamatergic) interneurons and α_1-ARs by inhibitory GABAergic neurons (Gassner et al., 2009). However, in lamina III of the DH of the spinal cord, the situation was very different from that in lamina II. Indeed, in lamina III, EGFP positive neurons were never depolarized by noradrenaline and 25% of them were hyperpolarized (Gassner et al., 2009). These findings indicate important differences in the effect of noradrenaline in different laminae of the DH.

3.1.3.1 Effects of noradrenaline on synaptic transmission

In lamina II, the activation of α_1-ARs had no effect of the frequency of spontaneously-occurring glutamatergic excitatory post-synaptic currents (sEPSCs) and increased the frequency of spontaneous but not miniature inhibitory postsynaptic currents (IPSCs) in lamina II (Baba et al., 2000). This finding indicated that α_1-ARs were located on the cell bodies of inhibitory (GABAergic and glycinergic) neurons (Baba et al., 2000). This finding was confirmed in mice expressing EGFP under the GAD67 promoter (Gassner et al., 2009). The absence of effect on miniature IPSCs (mIPSCs), i.e. recorded in the presence tetrodotoxin (TTX), in order to prevent

action potential generation and propagation, indicated that these receptors were absent from presynaptic terminals of inhibitory neurons. Activation of α_2-ARs did not affect the frequency of sIPSCs or sEPSCs in lamina II neurons (Baba et al., 2000) but inhibited the electrically evoked synaptic release of glutamate after Aδ and C primary afferent stimulation (Kawasaki et al., 2003; Pan et al., 2002). These results indicated the presence of inhibitory α_2-ARs on primary afferent nociceptors that inhibit the synaptic release of glutamate.

Interestingly, in lamina II, activation of α_2-ARs did not affect the frequency of sEPSCs and sIPSCs. This is in contrast with the situation in deeper laminae of the DH. Indeed, our laboratory has shown that in laminae III-IV, application of noradrenaline (20 μM) increased the frequency of sIPSCs (GABAergic or glycinergic) in 90% of the neurons (Seibt and Schlichter, 2015) but had no effect on sEPSCs or miniature IPSCs (mIPSCs). This effect was reproduced by the α_1-AR agonist PHE in all cell tested but also, rather surprisingly, by the α_2-AR agonist CLO. Indeed CLO increased the frequency of sIPSCs in 36% of the neurons from which we recorded.

Since CLO hyperpolarizes DH neurons and has no stimulatory effect on glutamatergic transmission, it is difficult to explain a CLO-mediated a facilitation of inhibitory synaptic transmission by a purely neuronal. It is therefore important to consider a contribution of glial cells to the effect of CLO and, in a more general context, of noradrenaline in the DH of the spinal cord (see below)

3.1.4 Glia to neuron interaction in the DH and effect of noradrenaline

We have shown that selective blockade of glial metabolism by fluorocitrate, significantly reduced the proportion of neurons in which PHE increased the frequency of sIPSCs (from 100% to 32%) in laminae III-IV of the DH and completely abolished the effect of CLO on sIPSC frequency (Seibt and Schlichter, 2015). This observation indicated that a large fraction of the α1-AR-mediated effect and the totality of the α_2-AR-mediated effect in laminae III-IV implicated an action at glial cells. In the light of the results presented in this thesis, this phenomenon might point to a fundamental role for the activation of glial α_1- and α_2-ARs in the control of inhibitory synaptic transmission in the DH. In line with this hypothesis, pharmacological blockade of P2X receptors strongly decreased the facilitatory effect of PHE and abolished the effect of CLO on sIPSC frequency, thereby mimicking the effect of metabolic inhibition of glial cells (Seibt and Schlichter, 2015). This suggested that a substantial fraction of the α_1-AR-mediated effect and the totality of the α_2-AR-mediated effect were due

to the release of ATP from DH glial cells that in turn activated P2X (and eventually P2Y) receptors of DH inhibitory (GABAergic or glycinergic) neurons. Postsynaptic as well as presynaptic P2X receptors are present on DH neurons (Hugel et al., 2009; Jo and Schlichter, 1999; Shiokawa et al., 2006). Activation of postsynaptic receptors triggers inward currents (Hugel et al., 2009; Jo and Schlichter, 1999) and therefore membrane depolarization, a phenomenon that might resemble activation of α_1-ARs. If the neurons expressing these post-synaptic P2X receptors were GABAergic or glycinergic, such depolarizations could facilitate the generation of action potentials in these neurons and lead to the synaptic release of GABA or glycine. This has not been directly verified by characterizing the neurochemistry of the recorded neurons but is very likely since activation of P2X receptors in the DH never increased the frequency of glutamatergic sEPSCs (Hugel et al., 2009; Rhee et al., 2000). Concerning DH interneurons, presynaptic P2X receptors are specifically expressed by inhibitory GABAergic, and to a lesser extent glycinergic, neurons and might contribute to the increase in the frequency of sIPSCs (Hugel and Schlichter, 2000; Rhee et al., 2000). Activation of α_2-ARs on neurons is purely inhibitory (hyperpolarization, inhibition of neurotransmitter release). The increase in sIPSC frequency might therefore be explained by the α_2-AR mediated release of ATP from DH glial cells which in turn could activate post- and presynaptic P2X receptors on inhibitory (GABAergic and glycinergic) interneurons and lead to an increase in sIPSC frequency.

Our work was focused on the mechanism of ATP release and its modulation by noradrenaline. However, many other extracellular messengers among which small gliotransmitters (glutamate, D-serine), neuropeptides (Atrial Natriuretic factor, Neuropeptide Y) and pro-inflammatory cytokines (Tumor necrosis Factor α, Interleukin 1β, Interleukin 6) can be released from glial cells (Verkhratsky and Nedergaard, 2018). The two former are released by calcium-dependent exocytosis (Verkhratsky and Nedergaard, 2018). The mechanism of secretion of cytokines is less well known and might occur via diverse mechanisms including regulated exocytosis, constitutive exocytosis or through recycling endosomes(Lacy and Stow, 2011; Stanley and Lacy, 2010). There is evidence that signal peptide-containing cytokines can be secreted in a calcium-dependent and SNARE-dependent manner (Han et al., 2009). ATP is contained in all acidic secretory vesicles. Therefore, it might be co-released with other transmitters, in particular with glutamate and D-serine. In line with this possibility, previous results from our laboratory on inhibitory synaptic transmission in laminae III-V of the DH in rat spinal

cord slices have shown that AMPA and NMDA- receptors are partly involved, along with purinoceptors, in the modulatory action of NA (Seibt and Schlichter, 2015). Thus it appears ha NA could also trigger the release of glutamate and perhaps D-serine (a co-agonist on NMDA receptors) from DH glial cells. The glial origin of glutamate and/or D-serine was attested by the fact that the effects of NA were blocked by preincubation of the spinal cord slices with the gliotoxin fluorocitrate (Seibt and Schlichter, 2015). In a more general context, gliotransmitter release or co-release (glutamate, GABA) might play an important role in modulating the excitability and the synchronization of the electrical activity in neuronal networks (Angulo et al., 2004; Kozlov et al., 2006).

In conclusion, it appears that, in the DH of the spinal cord, activation of glial α_1- and α_2-ARs represents an important aspect of noradrenaline-mediated control of synaptic transmission by descending noradrenergic controls.

3.1.5 Possible implication of DH glial cells in the spinal analgesic effects of noradrenaline

There is abundant literature showing the analgesic effect of noradrenaline at the spinal level. Intrathecal administration of noradrenaline or of α_1- or α_2-ARs agonists are anti-nociceptive (Yaksh et al., 1995) (Asano et al., 2000; Buerkle and Yaksh, 1998; Howe et al., 1983; Monroe et al., 1995; Reddy et al., 1980) whereas β-AR agonists or antagonists are without effect on nociceptive thresholds (Reddy et al., 1980). *In vivo* electrophysiological recordings have provided evidence that α_2-ARs might be of predominant importance. Indeed activation of α_2-ARs but not of α_1-ARs by local application of α_2-AR ligands (Fleetwood-Walker et al., 1985) or activation of descending controls (Budai et al., 1998) inhibit the activity of DH neurons receiving synaptic inputs from noxious heat-sensitive nociceptors.

Most of the studies examining the role of α_2-ARs in nociception have used CLO as a selective agonist of these receptors. However, CLO can also bind to imidazoline receptors/sites (see below). Such binding sites are present in the DH of the spinal cord of the rat and represent approximately 20% of the CLO binding sites (Monroe et al., 1995). However, under basal conditions, i.e. in the absence of chronic inflammation or neuropathy, these imidazoline receptors/binding sites do not participate in the analgesic effect of CLO, which is entirely mediated by activation of α_2-ARs (Monroe et al., 1995). Moreover, under basal physiological conditions, blocking the metabolism of DH glial cells by intrathecal infusion of fluoroacetate did not change the nociceptive thresholds

(Lefèvre et al., 2016). In vivo calcium imaging in astrocytes of the superficial laminae of the DH in mice revealed that nociceptive mechanical stimulation (pinching) did not induce any change in $[Ca^{2+}]_i$ in these astrocytes. However, a "stronger" nociceptive stimulation obtained by intraplatar injection of formalin produces a transient increase in $[Ca^{2+}]_i$ that lasted for about 5 minutes (Yoshihara et al., 2018).

Following nociceptive stimulation, increased action potential discharges in Aδ and C peripheral nociceptors activate the Locus Coeruleus and recruit descending noradrenergic controls (Tyce and Yaksh, 1981; Yaksh and Tyce, 1981). Similar recruitment was observed following peripheral inflammation (Maeda et al., 2009; Tsuruoka et al., 2003). A recent study has shown that a subset of DH glial cells responded by an increase in $[Ca^{2+}]_i$ following a peripheral stimulation of primary afferent nociceptors with capsaicin and that the effect on these DH astrocytes was due to the activation of *Locus Coeruleus* neurons that released NA in the DH and increased $[Ca^{2+}]_i$ in the astrocytes via the activation of α_{1A}-ARs (Kohro et al., 2020). Previous work from our laboratory on rat spinal cord slices has indicated that inhibition of noradrenaline uptake by nortryptiline increased the frequency of sIPSCs in laminae III-IV and that this increase could be blocked by pretreatment of the slices with fluorocitrate (Seibt and Schlichter, 2015). It, therefore, appears that a small release of noradrenaline occurs in the DH under basal physiological conditions and that the amount of noradrenaline present in the extracellular compartment can become sufficient to significantly stimulate glial adrenoceptors when noradrenaline uptake is blocked or when descending spinally projecting noradrenergic axons from *Locus* Coeruleus neurons are activated (e.g. after strong nociceptive stimulation or under inflammatory conditions).

3.2 Spinal I2 imidazoline receptors/sites and analgesia

Our results show that 98% of cultured mouse DH glial cells express functional I2 imidazoline receptors/sites that could be activated by 2-BFI and led to a rapid inhibition of the PHE-induced calcium plateau. This effect was reversibly antagonized by IDAZ. We have used 2-BFI at a single concentration (10 μM) at which this imidazoline molecule also inhibited SOCE and/or non-SOCE in an IDAZ-insensitive manner. This phenomenon was most probably due to a direct blockade of the SOCE and/or non-SOCE channels as it was also observed with the imidazoline molecule CLO at micromolar concentrations. In future experiments, it will be important to characterize the dose-response effects of 2-BFI on the PHE-induced calcium plateau.

Imidazoline receptors/sites can be activated (or antagonized) by synthetic imidazolinic molecules but several endogenously occurring molecules have been suggested to be natural agonists of imidazoline receptors/sites. Among these substances are agmatine (Regunathan and Reis, 1996) and imidazole-4-acetic acid-ribotide (IAA-RP, (Prell et al., 2004)). IAAP-RP can bind to both I1 and I2 receptors/sites but appears to preferentially act at I2 receptor/sites (Regunathan and Reis, 1996). In the CNS, IAAP is obtained mainly after transamination of histidine and subsequently, IAAP is conjugated with phosphoribosyl-pyrophosphate to form IAAP-RP and can be released in a calcium-dependent manner (Prell et al., 2004). IAA-RP is present in neurons but not in glial cells (Friedrich et al., 2007) and binds preferentially to I1 and I3 receptors/sites (Prell et al., 2004). We will therefore not further discuss the effects of IAA-RP in the nervous system and rather focus our attention on agmatine.

Agmatine is produced by decarboxylation of the amino-acid L-arginine (Laube and Bernstein, 2017) and meets many criteria of a neurotransmitter. Agmatine has diverse physiological effects including antinociceptive, anti-depressive, anxiolytic, neuroprotective, anticonvulsant, cardiovascular, gastric and renal effects (Molderings and Haenisch, 2012). It has attracted much interest in the context of clinical neuroscience because of its potential therapeutic effects, in particular in the field of neuropathic pain (Laube and Bernstein, 2017).

Agmatine is synthesized in neurons as well as in astrocytes (Regunathan et al., 1995; Regunathan and Reis, 1996). In humans, agmatine can be detected in cerebrospinal fluid as well as in plasma (Regunathan et al., 2009). In the rat spinal cord, agmatine is released in a calcium-dependent manner (Goracke-Postle et al., 2006) as well as from capsaicin-sensitive primary afferent nociceptor terminals in the DH of the spinal cord (Goracke-

Postle et al., 2007). It is therefore possible to speculate that after the persistent and sustained activity of primary afferent nociceptors and/or DH spinal cord interneurons, agmatine might reach local concentrations sufficient to activate I2 receptors present in DH glial cells. An additional possibility is a local synthesis from L-arginine that is transported into the glial cells. Interestingly arginine decarboxylase (the enzyme responsible for agmatine synthesis from L-arginine) is located in the outer mitochondrial membrane, i.e. in the proximity of MAOs that carry the I2 receptors/sites (Regunathan and Reis, 1996).

Indeed, I2 receptors represent an interesting target in pain management (Bektas et al., 2015). I2 agonists such as 2-BFI and CR4056 (2-phenyl-6-(1H-imidazol-1il) quinazoline), have no or very small effects on basal nociceptive thresholds, respectively. However, they display potent analgesic effects in inflammatory and neuropathic pain models (Ferrari et al., 2011; Li et al., 2014) (Siemian et al., 2018), (Thorn et al., 2016). CR4056 went in phase II clinical trials for pain management. It is well tolerated and significantly reduced osteoarthritic pain in humans (Rovati et al., 2020). Moreover, I2 agonists potentiate the analgesic effects of morphine without inducing tolerance or addiction (Laube and Bernstein, 2017; Regunathan, 2006; Roerig, 2003; Siemian et al., 2016). In addition, intracellular calcium signaling is essential for the antinociceptive effect of 2-BFI in rats (Siemian et al., 2017). However, it is not known if I2 receptors/sites present in glial cells contribute to the analgesic effects of CR4056 or other I2 agonists.

Considering the data available in the scientific literature, it appears that the activation of I2 receptors/sites triggers antinociceptive effects in inflammatory and neuropathic pain conditions. The exact mechanism of this action is currently not known. However, our results provide novel information concerning the effect of I2 receptor/site activation at the spinal level under basal physiological conditions. Indeed we show for the first time (1) that I2 receptors/sites are expressed by DH spinal cord glial cells and (2) that activation of these receptors inhibits SOCE and/or non-SOCE thereby reducing calcium influx in glial cells and calcium-dependent-gliotransmitter release from these glial cells. We speculate that such inhibition of gliotransmitter release might also occur in inflammatory and neuropathic conditions. Therefore activation of I2 receptors/sites by exogenously administered imidazoline agonists or by the endogenous agonist agmatine might represent powerful means to induce analgesia. Moreover, since, at micromolar concentrations, exogenous imidazolines also directly block the calcium influx channels underlying SOCE and/or non-SOCE (see part 2 of the Results

section) this phenomenon might add to the effect of I2 receptor activation by increasing/reinforcing the inhibitory effect of these molecules on calcium influx and thus to the inhibition of gliotransmitter release.

3.2.1 DH glial cells and pain

The first evidence for the role of glial cells in the development of pathological pain was obtained in 1991 by Garrisson and coworkers in the rat (Garrison et al., 1991). These authors noticed that a peripheral nerve constriction injury-induced a strong upregulation of the expression of Glial Fibrillary Acidic Protein (GFAP) in the DH of the spinal cord ipsilateral to the constriction. Moreover, the degree of expression of GFAP, a marker of glial cells and in particular of "activated" astrocytes, was correlated with the magnitude of the measured thermal heat hyperalgesia in the ipsilateral hind paw. After this initial description, many laboratories and studies have examined the role of glial cells in acute and chronic pain. We will only briefly describe below the main results obtained in these numerous studies. Interested readers can refer to the reviews on this topic that appeared during the past 30 years, e.g. (Ji et al., 2016; Nakagawa and Kaneko, 2010; Scholz and Woolf, 2007; Watkins and Maier, 2003).

3.2.2 Acute nociception/pain

In vivo calcium imaging experiments have shown that light (brushing) or strong (pinching) mechanical stimulation or application of acetone to mimic a thermal non-noxious cold stimulus did not increase $[Ca^{2+}]_i$ in DH astrocytes of anaesthetized mice. However subcutaneous injection of formalin in a hind paw triggered an increase in DH astrocytes ipsilateral to the stimulation (Yoshihara et al., 2018). In freely moving mice, innocuous and noxious peripheral stimulation increased $[Ca^{2+}]_i$ in groups of neurons in the DH of the spinal cord. However, in astrocytes low and moderate mechanical stimulations had no effect on $[Ca^{2+}]_i$. Only very high-intensity mechanical stimulation induced an increase in $[Ca^{2+}]_i$ in astrocytes (Sekiguchi et al., 2016). In addition, both the neuronal and astrocytic responses were inhibited by anesthesia.

Thus, it appears that under acute nociceptive mechanical stimulation, DH neurons respond with an increase in $[Ca^{2+}]_i$ whereas astrocytes display such an increase only following very intense mechanical stimulation or after a mild peripheral inflammatory stimulus (formalin injection).

3.2.3 Inflammatory and neuropathic pain

Following chronic inflammation or neuropathy, glial cells in the DH of the spinal cord change/adapt their functional properties to the homeostatic perturbation of their environment. This situation is currently designated under the term of "glial activation" that refers to the "*ability of these glial cells to perform functions beyond those present in the basal state*" (Watkins and Maier, 2003). Such activation is observed for both microglial cells and astrocytes (Inoue and Tsuda, 2009; Nakagawa and Kaneko, 2010; Watkins and Maier, 2003) and underlies the plastic changes that occur in the integration of nociceptive message in DH neuronal networks in chronic pain situations.

Morphological aspects. Activation of microglia is characterized by an increase in the number of microglia, an increased expression of *ionized calcium-binding adaptor molecule 1* (Iba1) in these cells and a change in their morphology, from elongated to rounded (Inoue and Tsuda, 2009; Inoue and Tsuda, 2018; Watkins and Maier, 2003). The activation of astrocytes is associated with an increase in the expression of GFAP (Inoue and Tsuda, 2009; Watkins and Maier, 2003) (Nakagawa and Kaneko, 2010).

Central sensitization. Central sensitization refers to the increase in efficacy of transmission of nociceptive messages from the primary afferent nociceptors to the central nociceptive neurons in the spinal cord or the brain stem (Woolf and Salter, 2000). Such activity-dependent modifications in nociceptive transmission and processing have been documented in the DH in the case of inflammatory and neuropathic pain (Ikeda et al., 2012). Central sensitization was associated with and increase in Ox42 (a monoclonal antibody that recognizes Cd11b) staining in microglia and of GFAP staining in astrocytes indicating an activation of both cell types under inflammatory and neuropathic conditions. Interestingly, the increase in transmission between primary afferent nociceptors and DH neurons was strongly dependent on ATP release in the DH. Pharmacological analysis of the action of endogenously released ATP on excitation of DH neurons indicated a fundamental role of P2X4 purinergic receptors and microglia in neuropathic pain, and of P2X1,2,3 receptors and astrocytes in inflammatory pain (Ikeda et al., 2012). A role for microglial P2X4 receptors in the development of neuropathic pain has been well established using knock-down (Tsuda et al., 2003) and knock-out (Ulmann et al., 2008) approaches. P2X4 receptors have also been implicated in the development of chronic (but not mild) inflammatory pain (Ulmann et al., 2010) (Lalisse et al., 2018) and central sensitization in the DH of the spinal cord (Aby et al., 2018). Most importantly, central sensitization precedes eventual longer lasting (chronic)

modifications in the processing of nociceptive information as observed during chronic inflammatory and neuropathic pain states.

3.2.4 Chronic inflammatory and neuropathic pain.

Development of chronic pain is also accompanied by an increased synthesis and release of intercellular signaling molecules, such as chemokines, cytokines and ATP, that allow the coordinated communication between microglia and astrocytes but also between glia and neurons. Activation of microglia is initiated by the activity-dependent release of chemokines such as fraktalkine (CX3CL1) and CCL2 (also known as Monocyte Chemoattractant Protein 1 (MCP-1)) from highly active primary afferents (Nakagawa and Kaneko, 2010; White et al., 2007) (Gao and Ji, 2010a). The extracellular messengers involved in the activation of astrocytes are less well characterized but include neurotransmitters and neuropeptides (glutamate, substance P, calcitonin gene-related peptide (CGRP)), ATP, prostaglandins). Activation of microglia leads to the increased production and release of pro-inflammatory cytokines such as Tumor Necrosis factor α (TNF-α), interleukin 1β (IL-1β) and interleukin 6 (IL-6) from microglia and astrocytes, that can in turn act on neighboring microglia and astrocytes (amplification mechanism) as well as on neurons to modulate synaptic transmission (increase in excitatory glutamatergic transmission and decrease in inhibitory GABAergic transmission in the DH of the spinal cord) (Ji et al., 2013; Kawasaki et al., 2008; Nakagawa and Kaneko, 2010). Interestingly, microglia also produce and release interleukin 18 (IL-18) that acts specifically on astrocytes and might therefore be involved in microglia to astrocyte communication (Miyoshi et al., 2008; Nakagawa and Kaneko, 2010). Intrathecal administration of pro-inflammatory cytokines induces mechanical hyperalgesia and allodynia, indicating the important role of cytokines as initiators of the plastic changes that occur in DH neuronal networks and underlie the development of hyperalgesia and allodynic states (Reeve et al., 2000).

ATP is an extracellular messenger that plays a major role in the activation of glial cells, and the communication between glia as well as between glia and neurons (Di Virgilio et al., 2009; Fields and Burnstock, 2006) (Ji et al., 2013; Wang et al., 2009). A single intrathecal injection of ATP in the rat was shown to activate microglia and astrocytes in the DH of the spinal cord and to produce long lasting (> 1 week) mechanical allodynia that resembled that observed in chronic pain models (Nakagawa et al., 2007). Interestingly, it was recently shown

that vesicular release of ATP from DH neurons was a key element for the development of neuropathic pain (Masuda et al., 2016) (Inoue and Tsuda, 2018).

The induction of neuropathic pain is due to an early activation of microglia that is followed by a more delayed activation of astrocytes (Inoue and Tsuda, 2009; Watkins and Maier, 2003; Zhang and De Koninck, 2006) (Inoue and Tsuda, 2018). This initial recruitment of microglia is rather involved in the induction phase and the more delayed activation of astrocytes in the maintenance phase of the plastic changes associated with neuropathic pain. Therefore it appears that interfering with chemokine, cytokine and ATP release fom glial cells and neurons or with their signaling pathways in target cells represent interesting therapeutic options for the management of chronic inflammatory and neuropathic pain (see below).

3.2.5 SOCE and non-SOCE as targets for analgesia in chronic pain

As outlined above cytokines released from microglia play a key role in the development of hyperalgesic and allodynic states associated with inflammatory and neuropathic pain. Moreover a single intrathecal administration of ATP induced an activation of microglia and astrocytes in the DH of the spinal cord and triggered long lasting mechanical allodynia (Nakagawa et al., 2007). Cytokine release from glial cells can occur by different routes including a vesicular calcium- and SNARE-dependent manner and a calcium-dependent but non-vesicular manner (Stanley and Lacy, 2010) (Andrei et al., 2004; Gardella et al., 2001; Han et al., 2009; Lacy and Stow, 2011) (Murray and Stow, 2014; Shieh et al., 2014; Suttles et al., 1990).

Our thesis work has shown that ATP can be released from DH glial cells in a calcium-dependent fashion via secretory lysosomes and another acidic vesicular pool distinct from lysosomes. Moreover, we have observed a calcium-dependent non-vesicular release of ATP from these glial cells. So far, we did not have the opportunity to examine how these mechanisms of ATP secretion would be affected under pathological conditions, e.g. for example under inflammatory conditions that can be mimicked in culture by incubation of the cells with lipopolysaccharide (LPS) or a cocktail of pro-inflammatory cytokines (TNF-α, IL-1β, IL-6). However, since all acidic secretory vesicles including lysosomes contain high concentrations of ATP, we speculate that quantifying the kinetics and amplitude of ATP release might probably be a good indicator of vesicular release in general and of other gliotransmitters (e.g. glutamate of D-serine) or neuropeptides in particular. It follows that measuring and quantifying increases or decreases of ATP release might reflect the size and amplitude of the

modulation of the calcium-dependent release of other extracellular messengers (glutamate, D-serine, neuropeptides, cytokines) via acidic vesicles. However, this point will have to be clarified in future experiments. Our results with imidazoline molecules indicated that activation of I2 receptors (by 2-BFI) inhibited the amplitude of the calcium plateau induced by PHE. This plateau is due to calcium influx via SOCE channels and/or non-SOCE channels. These channels are made of associations of Orai subunits (4 Orai 1 subunits for SOCE and 3 Orai 1 + 2 Orai 2 subunits for non-SOCE channels) that are gated by an aggregate of STIM 1 roteins (Prakriya and Lewis, 2015; Shuttleworth, 2012).

Calcium influx via SOCE and/or non-SOCE channels is important for the calcium-dependent release of transmitters/signaling molecules from non-excitable cells including glial cells (Putney, 2018; Toth et al., 2019). It this case inhibiting SOCE and/or non-SOCE channels should affect the calcium-dependent release of messenger molecules from glia and other non excitable cells (e.g. immune cells).

3.2.6 Inhibition of SOCE and non-SOCE to decrease cytokine release

As discussed above cytokine production and release from DH glial cells plays an important role in the central sensitization of nociceptive networks in the DH of the spinal cord as well as in the development of hyperalgesia and allodynia associated with chronic pain states. Since cytokine can be released via a vesicular and calcium-dependent pathway (Lacy and Stow, 2011; Stanley and Lacy, 2010), it might be expected that this release would also depend on calcium-influx via SOCE and non-SOCE channels. It has been shown that pharmacological inhibition of SOCE and/or non-SOCE channels inhibits the release of proinflammatory cytokines from non-excitable cells (Heo et al., 2015; Wang et al., 2016) (Beringer et al., 2019) including from murine astrocytes (Gao et al., 2016) and microglia (Heo et al., 2015). Inhibition of calcium influx and cytokine release was also observed after knock-down of STIM1 or Orai 1 in the same preparations of murine astrocytes and microglia (Heo et al., 2015; Wang et al., 2016).

3.2.7 SOCE/non SOCE and excitability of nociceptive neurons.

Recent studies have shown that SOCE channels are also functionally expressed in a majority of primary afferent nociceptors (Wei et al., 2017) and DH spinal cord neurons (Xia et al., 2014). In both types of neurons, emptying intracellular calcium stores with thapsigargin led to the activation of SOCE monitored as an inward current under voltage-clamp conditions or a membrane depolarization under current-clamp conditions. This led to an

increase in excitability of the neurons that was reduced/blocked by antagonists of SOCE/non SOCE channels or by knocking-down STIM or Orai (Wei et al., 2017; Xia et al., 2014). In DH neurons application of substance P activated Gq-coupled Neurokinin type 1 (NK1) receptors that increased $[Ca^{2+}]_i$. This response to substance P was strongly reduced after pharmacological blockade of SOCE/non-SOCE or knock-down of STIM and Orai (Xia et al., 2014).

These results indicate that SOCE/non-SOCE channels play an important role in the excitability of DH neurons and primary afferent nociceptors and modulate $[Ca^{2+}]_i$ responses triggered by metabotropic neurotransmitter/ neuropeptide receptors.

3.2.8 SOCE, non-SOCE and nociception/pain.

Pharmacological inhibition of SOCE/non-SOCE channels with YM-58483 also known as BTP2, reduced dose-dependently thermal and mechanical hyperalgesia in chronic inflammatory and neuropathic murine pain models (Gao et al., 2013; Gao et al., 2015). Most interestingly, YM-58483 was effective when given orally (*per os*) and prevented the development of inflammatory and neuropathic (pre-treatment protocol) as well as established inflammatory and neuropathic pain hypersensitivity (post-treatment protocol). Acute/basal nociceptive thresholds were increased by YM-58483 but only at the highest dose tested (30 $mg.kg^{-1}$) (Gao et al., 2013). It has not been investigated whether these effects of YM-58483 on chronic pain involved a contribution of glial cells. However, concerning acute pain thresholds, glial cells are probably not implicated because chronic infusion of fluoroacetate over 2 weeks did not affect basal nociceptive thresholds in rats (Lefèvre et al., 2016). Therefore, it is most likely that the effects of YM-58483 on acute/basal pain threshold, that were observed only at the highest dose tested, were due to an inhibition of SOCE channels in DH nociceptive and/or primary afferent nociceptors that led to a reduction in excitability of these neurons (Wei et al., 2017; Xia et al., 2014).

3.3 Speculations on possible therapeutic strategies for inducing analgesia in chronic pain situations

From the elements presented in the previous sections of this discussion, it appears that there are two attractive targets for pain management, i.e. I2 imidazoline receptors/sites and SOCE and/or non-SOCE channels (or the cellular mechanisms leading to SOCE and/or non-SOCE). Both targets are found in neurons as well as in glial cells. In particular they are involved in neuronal and glial plasticities associated with inflammatory and neuropathic pain.

3.3.1 Agonists of I2 receptors/sites and other imidazoline molecules.

We have not studied the effect of I2 receptor/site activation on $[Ca^{2+}]_i$ or membrane excitability in primary nociceptors or DH spinal cord neurons, but our results clearly showed that imidazolinic molecules (such as 2-BFI) that act as agonists on I2 receptors/sites inhibit SOCE and non-SOCE and ATP release in cultured DH glial cells (astrocytes). Moreover, at higher concentration imidazolines (i.e. 2-BFI, CLO, Dexmedetomidine) can also directly block the SOCE and/or non-SOCE channels and thereby increase the inhibitory action of I2 agonists on calcium influx. Some of these molecules, like 2-BFI, also inhibit NMDA receptors at high concentrations (>10 μM) and could therefore also reduce NMDA receptor-dependent plasticity in central nociceptive pathways. CR4056 is a synthetic imidazolinic I2 receptors/site agonist that has powerful analgesic effects in animal models of inflammatory and neuropathic pain (Ferrari et al., 2011). It is well tolerated in humans and was shown to significantly reduce arthritic pain (Rovati et al., 2020). However, today, it is not known if CR4056 inhibits SOCE and/or non-SOCE channels in glial cells and/or neurons, and if glial cells participate in its analgesic actions. I2 agonists having properties similar to CR4056 might be promising molecules for pain management in humans. In particular, they are active when given orally and might also be co-administered with other analgesic molecules (see below).

3.3.2 Inhibitors of SOCE and non-SOCE.

Calcium influx through SOCE or non-SOCE channels plays a fundamental role in the release of messenger molecules from glial cells and in particular of ATP (Toth et al., 2019). Moreover inhibition of interaction between STIM and Orai proteins, that prevent calcium influx rapidly inhibit/block calcium transients in glial cells and their modulation by stimulation of metabotropic receptors (Sakuragi et al., 2017). There is also

Illustration of Result part 2

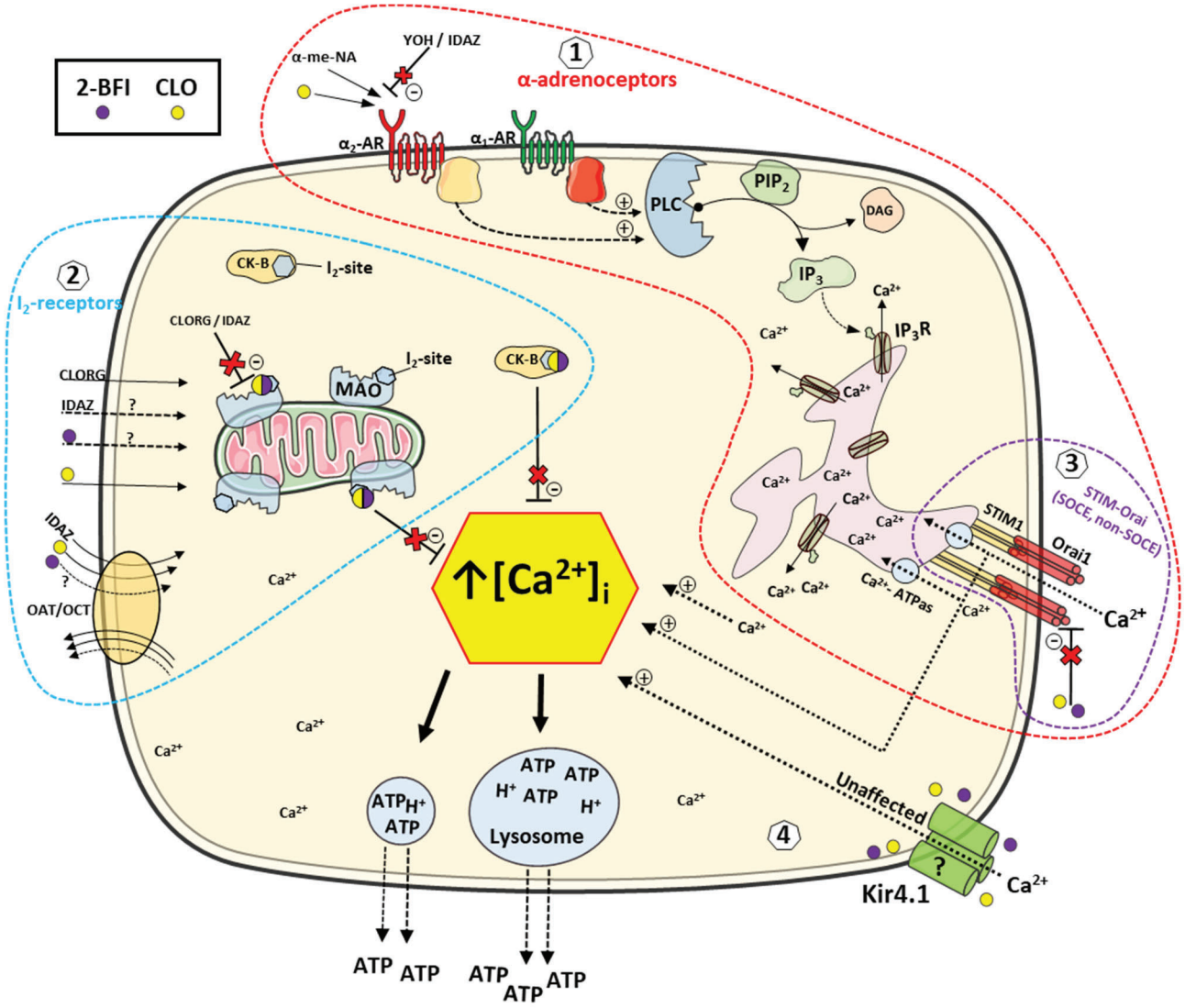

Figure 35. Legend on next page

Figure 35 - Summary of result part two. The effect of α_2-AR and imidazoline receptors (I-receptors) agonists on $[Ca^{2+}]_i$ and ATP release in DH glia. Our previous results showed that NA (20 μM) increased $[Ca^{2+}]_i$ primarily through activation of α_1-AR (mimicked by α_1-AR agonist phenylephrine (PHE)) while, the α_2-adrenoceptor agonist clonidine (CLO, 10 μM) had no significant effect on $[Ca^{2+}]_i$ in glia. (see Fig. 34 and Eersapah et al., 2019). **1) α-adrenoceptor signaling (red dotted line).** α-methyl-noradrenaline (α-me-NA, 0.5 μM) a selective α_2-AR agonist and low concentrations(<μM) of CLO both bind to the α_2-AR and increase $[Ca^{2+}]_i$ in DH glia and consequently induce the release of ATP. Both the increase in $[Ca^{2+}]_i$ and the release of ATP were blocked by the selective α_2-AR antagonist yohimbine (YOH, 2 μM). **2) I2-receptors (blue dotted line).** I2-receptors/sites are located on the monoaminoxidase (MAO) enzyme on the outer membrane of mitochondria as well as on creatine kinase B (CK-B). Binding of imidazoline molecules/agonists such as CLO (10 μM) or 2-(Benzofuranyl)-2-imidazoline (2-BFI, 10 μM) to I2-receptors inhibits the adrenoceptor (PHE) mediated increase in $[Ca^{2+}]_i$ and the subsequent ATP release in DH glial cells. The inhibitory effect mediated by I_2-recepor agonists on $[Ca^{2+}]_i$ can be decreased by the MAO-inhibitor clorgyline (CLORG, 2 μM) and the I2-receptor antagonist Idazoxan (IDAZ). CLO (and possibly 2-BFI) can enter the cells through organic cation/anion transporters (OCT/OAT) or direct diffusion through the plasma membrane. However, the down-stream mechanism through which I-receptors inhibit the $[Ca^{2+}]_i$ in DH glia induced by adrenoceptor (α_1-AR, PHE) agonists remains unclear. **3) Stim-Orai (SOCE) (purple dotted line)**. Adrenoceptor activation leads to the production of inositol trisphosphate (IP_3) which binds to IP_3 receptor (IP_3R) and to subsequent Ca^{2+} release from the endoplasmic reticulum (ER). Low ER concentration will trigger the formation of STIM-Orai complexes at ER-plasma membrane juncctions (see Fig. 34) that will allow Store Operated Calcium Entry (SOCE) from the external environment into the cytoplasm and thereby prolong the elevated cytoplasmic free intracellular calcium concentration. One possible mechanism through which CLO and 2-BFI could inhibit the $[Ca^{2+}]_i$ increase (and the release of ATP) in DH glia induced by adrenoceptor (α_1-AR, PHE) could be by directly blocking SOCE channels. **4).** Interestingly, neither $[Ca^{2+}]_i$ increase nor ATP release induced by local application of external solution containing a low concentration of potassium (0.2 mM) was affected by neither CLO nor by 2-BFI. This suggests that one of the inhibitory mechanisms through which CLO and 2-BFI are acting, is by most likely specifically targeting the SOCE-channels, or a step upstream the SOCE activation.

evidence that inhibiting SOCE and/or non-SOCE will have consequences on the refilling of internal calcium stores (Bittremieux et al., 2017) and therefore on responses depending on the activation of metabotropic (calcium-mobilizing) receptors (Sakuragi et al., 2017). Inhibition of SOCE and/or non-SOCE channels with YM-58483 (also known as BTP2) had potent analgesic effect in murine models of inflammatory and neuropathic pain (Gao et al., 2013) (Gao et al., 2015).

In humans YM-58483 has not been tested. There are some molecules approved by the the U.S. Food and Drug Administration (FDA) for the treatment of various pathologies that were shown also to block SOCE and/or non-SOCE channels. Ten of these molecules were tested for their capacity to block SOCE and non-SOCE (Rahman and Rahman, 2017). Among these molecules, 3 have been reported to reduce pain although the studies mentioning these effects were not always specifically designed to test the analgesic effects of these molecules. Leflunomide is used as a non-steroidal anti-inflammatory agent in rheumatoid arthritis and reduced significantly arthritic pain (Osiri et al., 2009). Lansoprasole is an inhibitor of gastric H^+-pump and reduces also abdominal pain (Graham et al., 2002). Tolvaptan is an antagonist of V2 vasopressin receptors and used in the treatment of Autosomal Dominant Polycystic Kidney Disease (ADPKD) and was shown to slowly but significantly improve renal pain with prolonged treatment duration (Casteleijn et al., 2017). To our knowledge, there is currently no specific and selective blocker of SOCE or non-SOCE channels that has been approved for clinical use and tested in humans, although there is an active research in the field of specific inhibitors of these channels by pharmaceutical companies (Sweeney et al., 2009).

3.3.3 Association of I2 agonists and/or SOCE non-SOCE inhibitors and classical analgesics.

Certainly one of the promising options for the management of pain would be the association of several molecules having analgesic effects. This should allow to reduce the concentration/dose of each molecule and therefore reduce the side effects of these molecules. Additivity/synergy of several molecules have been already described in animal studies (see below).

I2 agonists. I2 agonists, such as CR4056 or 2-BFI, were shown to have analgesic effects in rodents and did not display marked tolerance upon repeated application (Ferrari et al., 2011; Li et al., 2014). Most importantly, CR4056 was shown to have a synergistic effect with morphine in a model in chronic inflammatory pain induced by complete Freund's adjuvant (CFA). During co-administration, it was possible to reduce the concentration of

morphine used thereby decreasing tolerance to morphine and to reducingside effects of morphine such as constipation, sedation, physical dependence and abuse (Sala et al., 2020). It would be interesting to test whether the analgesic effect following co-administration of CR4056 and morphine would be further increased by additional administration of a SOCE and/or non-SOCE channel blocker. If this was the case, it could be envisaged to decrease even further the concentration of morphine used in the analgesic strategy.

α_2-AR agonists. Clonidine has been used for its analgesic properties over the last 50 years. However, its clinical use is limited by serious adverse effects that include hypotension and sedation (Carroll et al., 1993; J.E. Neil, 2011). CLO crosses the Blood Brain Barrier (BBB) (Foster et al., 2002) (André et al., 2009) but can be used only at low intra-veinous doses because of a rapid appearance of adverse effects (Carroll et al., 1993). The hypotensive effect of CLO is due to its high affinity for imidazoline I1 receptors/sites in the brain stem (Ernsberger et al., 1997; Ernsberger et al., 1987). Alternatively, one could think of using dexmedetomidine (DEX), that has a 10 fold higher affinity than CLO for α_2-AR but unfortunately DEX also binds to I1 receptors and in addition produces opposite effects on human platelet aggregation when activating I1 receptors/sites or α_2-ARs (Kawamoto et al., 2015). In humans undergoing surgery, perioperative administration of CLO or DEX was shown to reduce pain intensity and post-operative morphine consumption (Blaudszun et al., 2012). Moreover, in mice, association of CLO and morphine synergize to improve their analgesic effects (Roerig et al., 1992; Stone et al., 2014). This synergy allowed to reduce the undesired side effects (sedation and cardiovascular depression) by allowing a reduction in the therapeutic doses used (Stone et al., 2014).

3.4 Hypotheses

As mentioned above I2 receptor agonist (2-BFI, CR4056), α_2-AR agonists (CLO, DEX), morphine and SOCE/non-SOCE channel inhibitors have analgesic effects. Combination or I2 agonists and morphine (Li et al., 2014; Sala et al., 2020) as well as of α_2-AR agonists and morphine (Roerig et al., 1992) (Stone et al., 2014) are clearly beneficial and reduce the dose of morphine required to produce efficient analgesia, thereby reducing undesirable side effects induced by treatments using a single type of molecule (nausea, hypotension, bradycardia, sedation). However, interaction between SOCE/non-SOCE inhibitors and I2 agonist, α_2-AR agonists or morphine have not been investigated so far and might be promising since SOCE/non-SOCE inhibitors have been shown to reduce calcium influx and gliotransmitter/cytokine release in astrocytes and to decrease excitability of primary afferents nociceptors and DH spinal cord neurons (Wei et al., 2017) (Xia et al., 2014). These phenomena probably underlie the potent analgesic effect of the SOCE/non-SOCE inhibitor YM-58483 (BTP2) in inflammatory and neuropathic pain (Gao et al., 2013; Gao et al., 2015). It would therefore be interesting to evaluate the analgesic effects of a SOCE/non-SOCE inhibitors (e.g. YM-58483) given in combination with an I2 receptor agonist (2-BFI, CR4056), a α_2-AR agonist (CLO, DEX) or morphine. It will be particularly important and interesting to evaluate the analgesic action of a combination of 3 of these molecules (SOCE/non-SOCE inhibitor, I2 agonist, α_2-AR agonist). Indeed, in case of a powerful interaction, this might allow to reduce the dose of the α_2-AR agonist used (to further limit its undesirable side-effects) and perhaps to avoid the use of morphine in the analgesic protocol.

3.5 Future Perspectives

To further expand our study and potentially answer some of the questions raised in the above-mentioned hypotheses we would like to propose someadditional experiments.

Point 1:

First of all, it is important to know whether stimulation of α-ARs (α_1 and α_2) trigger calcium influx by activation SOCE or non-SOCE channels or both and if the blocking effect of I2 receptor agonists or of high (micromolar) doses of CLO on Ca^{2+} influx concerns SOCE, non-SOCE or both. To this end, one coud use pharmacological tools either to selectively inhibit the SOCE and non-SOCE components (see below) or to selectively activate SOCE (thapsigargin, cyclopiazinic acid) or non-SOCE (arachidonic acid). Relatively selective agents that inhibit SOCE include La^{3+} ions at low nanomolar concentrations (e.g 20 nM) or BTP2 (also known as YM5483 (IC50 = 10 nM)). On the other hand, LOE-908 at low micromolar concentrations (e.g. 3 μM) will specifically inhibit non-SOCE (Jairaman and Prakriya, 2013).

Testing the effect of the α_2-AR agonist α-me-NA, the I2-agonist (2-BFI) and micromolar concentrations of CLO on SOCE induced by Thapsigargin or cyclopiazonic acid would give valuable information on the calcium influx mechanism(s) they target. This should be relatively simple to test on cultured DH glial cells, but might be more tricky in ATP release experiments, because Thapsigargin will also induce calcium release from intracellular stores in the detector HEK293-P2X2 cells. This proble might be perhaps overcome by preteating the HEK293-P2X2 cells with thapsigargin before plating them on top of the DH glial cells. Indeed, thapsigargin is known as an irreversible (or very slowly reversible) blocker of the ER Ca^{2+} ATPase.

Point 2:

So far, the effects of α_2-AR agonist α-me-NA and the I2-agonist (2-BFI) have been tested at single concentrations. It will be important to obtain full dose-response curves of the agonists in order to better characterise their effects. In additions, it will be important to determine in more detail the effects of CLO at sub-micromolar, i.e. nanomolar, concentrations. All these dose-response experiments could be performed in the absence of pharmacological blockers or in the presence selective blockers of SOCE and non-SOCE.

Point 3:

It would also be interesting to determine if the calcium signalling in DH glial cells and the modulation of ATP release from these cells is affected under ”pathological” conditions. Therefore it would be interesting to characterise the effects of α_1- and α_2-AR agonists as well as of I2-agonists on $[Ca^{2+}]_i$ after pretreating the cultures with lipopolysaccharide (LPS) that is known to recapitulate and mimick the effect of inflammation on glial cells.

Point 4:

It would also be of interest to determine the relationship between $[Ca^{2+}]_i$ in different astrocytic compartments (cell body versus processes) and its relationship to ATP release. Such experiments would allow to determine whether release of ATP from astroglia requires a global $[Ca^{2+}]_i$ increase or if local calcium influx in the thin processes could be sufficient to induce a regional release ATP of from those local calcium influx zones. Such experiments should be possible by measuring calcium changes in the cell body and the processes of astrocytes after the transfection of the DH glial cells with a genetically encoded calcium probe such as GCaMP6. In this context, it will also be interesting to determine whether there are differential modulatory effects of α_1, α_2 and I2 agonists on calcium signalling and/or ATP release in the processes or the cell bodies

Point 5:

Finally, it would be interesting to use the results from the above-mentioned experiments to evaluate the role and the interplay of SOCE, non-SOCE, I2-agonist and α_2-AR on pain thresholds and nociceptive behavioural tests in rodents.This aspect could be studied in naïve mice as well as in models of inflammatory and neuropathic pain. This approach would allow us to determine whether the interactions of the molecules tested in our *in vitro* model (as discussed in the General Discussion section) will have consequences on nociceptive thresholds and/or on mechanical and thermal hyperalgesia in inflammatory and neuropathic models. To this end the effect of each individual molecule will be tested alone before assessing the effects of combinations of these molecules. Such experiments would allow to determine whether the co-administration of molecules results additive or supra – additive effects providing an improvement of the analgesic effects.

4 References

Abbracchio, M.P., G. Burnstock, A. Verkhratsky, and H. Zimmermann. 2009. Purinergic signalling in the nervous system: an overview. *Trends Neurosci*. 32:19-29.

Abraham, E.H., A.G. Prat, L. Gerweck, T. Seneveratne, R.J. Arceci, R. Kramer, G. Guidotti, and H.F. Cantiello. 1993. The multidrug resistance (mdr1) gene product functions as an ATP channel. *Proceedings of the National Academy of Sciences of the United States of America*. 90:312-316.

Aby, F., S. Whitestone, M. Landry, L. Ulmann, and P. Fossat. 2018. Inflammatory-induced spinal dorsal horn neurons hyperexcitability is mediated by P2X4 receptors. *Pain Reports*. 3:e660.

Al Ghamdi, K.S., E. Polgár, and A.J. Todd. 2009. Soma size distinguishes projection neurons from neurokinin 1 receptor-expressing interneurons in lamina I of the rat lumbar spinal dorsal horn. *Neuroscience*. 164:1794-1804.

Aldskogius, H., and E.N. Kozlova. 1998. Central neuron-glial and glial-glial interactions following axon injury. *Progress in Neurobiology*. 55:1-26.

Alvarez, F.J., R.M. Villalba, R. Zerda, and S.P. Schneider. 2004. Vesicular Glutamate Transporters in the Spinal Cord, with Special Reference to Sensory Primary Afferent Synapses. *Journal of Comparative Neurology*. 472:257-280.

Anderson, N.J., I. Seif, D.J. Nutt, A.L. Hudson, and E.S. Robinson. 2006. Autoradiographical distribution of imidazoline binding sites in monoamine oxidase A deficient mice. *J Neurochem*. 96:1551-1559.

André, P., M. Debray, J.M. Scherrmann, and S. Cisternino. 2009. Clonidine transport at the mouse blood-brain barrier by a new H antiporter that interacts with addictive drugs. *Journal of Cerebral Blood Flow and Metabolism*. 29:1293-1304.

Andrei, C., P. Margiocco, A. Poggi, L.V. Lotti, M.R. Torrisi, and A. Rubartelli. 2004. Phospholipases C and A2 control lysosome-mediated IL-1β secretion: Implications for inflammatory processes. *Proceedings of the National Academy of Sciences of the United States of America*. 101:9745-9750.

Angelova, P.R., V. Kasymov, I. Christie, S. Sheikhbahaei, E. Turovsky, N. Marina, A. Korsak, J. Zwicker, A.G. Teschemacher, G.L. Ackland, G.D. Funk, S. Kasparov, A.Y. Abramov, and A.V. Gourine. 2015. Functional oxygen sensitivity of astrocytes. *Journal of Neuroscience*. 35:10460-10473.

Angulo, M.C., A.S. Kozlov, S. Charpak, and E. Audinat. 2004. Glutamate released from glial cells synchronizes neuronal activity in the hippocampus. *Journal of Neuroscience*. 24:6920-6927.

Angulo, M.C., K. Le Meur, A.S. Kozlov, S. Charpak, and E. Audinat. 2008. GABA, a forgotten gliotransmitter. *Prog Neurobiol*. 86:297-303.

Araque, A., G. Carmignoto, P.G. Haydon, S.H. Oliet, R. Robitaille, and A. Volterra. 2014. Gliotransmitters travel in time and space. *Neuron*. 81:728-739.

Arcuino, G., J.H.C. Lin, T. Takano, C. Liu, L. Jiang, Q. Gao, J. Kang, and M. Nedergaard. 2002. Intercellular calcium signaling mediated by point-source burst release of ATP. *Proceedings of the National Academy of Sciences of the United States of America*. 99:9840-9845.

Asano, T., S. Dohi, S. Ohta, H. Shimonaka, and H. Iida. 2000. Antinociception by epidural and systemic α2-adrenoceptor agonists and their binding affinity in rat spinal cord and brain. *Anesthesia and Analgesia*. 90:400-407.

Aston-Jones, G., and B. Waterhouse. 2016. Locus coeruleus: From global projection system to adaptive regulation of behavior. *Brain Res*. 1645:75-78.

Aussel, C., R. Marhaba, C. Pelassy, and J.P. Breittmayer. 1996. Submicromolar La3+ concentrations block the calcium release-activated channel, and impair CD69 and CD25 expression in CD3- or thapsigargin-activated Jurkat cells. *Biochem J*. 313 (Pt 3:909-913.

Baba, H., K. Shimoji, and M. Yoshimura. 2000. Norepinephrine facilitates inhibitory transmission in substantia gelatinosa of adult rat spinal cord (Part 1): Effects of axon terminals of GABAergic and glycinergic neurons. *Anesthesiology*. 92:473-484.

Baillie, G.S., A. Sood, I. McPhee, I. Gall, S.J. Perry, R.J. Lefkowitz, and M.D. Houslay. 2003. β-arrestin-mediated PDE4 cAMP phosphodiesterase recruitment regulates β-adrenoceptor switching from Gs to Gi. *Proceedings of the National Academy of Sciences of the United States of America*. 100:940-945.

Bar El, Y., S. Kanner, A. Barzilai, and Y. Hanein. 2018. Activity changes in neuron-astrocyte networks in culture under the effect of norepinephrine. *PLoS One*. 13:e0203761.

Barg, S., X. Ma, L. Eliasson, J. Galvanovskis, S.O. Gö Pel, S. Obermüller, J. Platzer, E. Renström, M. Trus, D. Atlas, J. Striessnig, and P. Rorsman. 2001. Fast exocytosis with few Ca^{2+} channels in insulin-secreting mouse pancreatic B cells. *Biophysical Journal*. 81:3308-3323.

Bargiello, T.A., Q. Tang, S. Oh, and T. Kwon. 2012. Voltage-dependent conformational changes in connexin channels. *Biochim Biophys Acta*. 1818:1807-1822.

Basarsky, T.A., D. Feighan, and B.A. MacVicar. 1999. Glutamate release through volume-activated channels during spreading depression. *Journal of Neuroscience*. 19:6439-6445.

Basbaum, A.I., D.M. Bautista, G. Scherrer, and D. Julius. 2009. Cellular and Molecular Mechanisms of Pain. *Cell*. 139:267-284.

Bazargani, N., and D. Attwell. 2016. Astrocyte calcium signaling: the third wave. *Nat Neurosci*. 19:182-189.

Bektas, N., D. Nemutlu, and R. Arslan. 2015. The imidazoline receptors and ligands in pain modulation. *Indian J Pharmacol*. 47:472-478.

Belai, A., and G. Burnstock. 1994. Evidence for coexistence of ATP and nitric oxide in non-adrenergic, non-cholinergic (NANC) inhibitory neurones in the rat ileum, colon and anococcygeus muscle. *Cell and Tissue Research*. 278:197-200.

Bergersen, L.H., C. Morland, L. Ormel, J.E. Rinholm, M. Larsson, J.F.H. Wold, A.T. Røe, A. Stranna, M. Santello, D. Bouvier, O.P. Ottersen, A. Volterra, and V. Gundersen. 2012. Immunogold detection of L-glutamate and D-serine in small synaptic-like microvesicles in adult hippocampal astrocytes. *Cerebral Cortex*. 22:1690-1697.

Beringer, A., Y. Gouriou, F. Lavocat, M. Ovize, and P. Miossec. 2019. Blockade of store-operated calcium entry reduces IL-17/TNF cytokine induced inflammatory response in human myoblasts. *Frontiers in Immunology*. 9:3170.

Bezzi, P., V. Gundersen, J.L. Galbete, G. Seifert, C. Steinhäuser, E. Pilati, and A. Volterra. 2004. Astrocytes contain a vesicular compartment that is competent for regulated exocytosis of glutamate. *Nature Neuroscience*. 7:613-620.

Billaud, M., A.W. Lohman, A.C. Straub, R. Looft-Wilson, S.R. Johnstone, C.A. Araj, A.K. Best, F.B. Chekeni, K.S. Ravichandran, S. Penuela, D.W. Laird, and B.E. Isakson. 2011. Pannexin1 regulates α1-adrenergic receptor-mediated vasoconstriction. *Circulation Research*. 109:80-85.

Bittremieux, M., J.V. Gerasimenko, M. Schuermans, T. Luyten, E. Stapleton, K.J. Alzayady, H. De Smedt, D.I. Yule, K. Mikoshiba, P. Vangheluwe, O.V. Gerasimenko, J.B. Parys, and G. Bultynck. 2017. DPB162-AE, an inhibitor of store-operated Ca^{2+} entry, can deplete the endoplasmic reticulum Ca^{2+} store. *Cell Calcium*. 62:60-70.

Blaudszun, G., C. Lysakowski, N. Elia, and M.R. Tramèr. 2012. Effect of perioperative systemic α2 agonists on postoperative morphine consumption and pain intensity: Systematic review and meta-analysis of randomized controlled trials. *Anesthesiology*. 116:1312-1322.

Bodnar, R.J., R.F. Ackermann, D.D. Kelly, and M. Glusman. 1978. Elevations in nociceptive thresholds following locus coeruleus lesions. *Brain Research Bulletin*. 3:125-130.

Bollmann, J.H., B. Sakmann, and J.G.G. Borst. 2000. Calcium sensitivity of glutamate release in a calyx-type terminal. *Science*. 289:953-957.

Borges, G.S., E. Berrocoso, A. Ortega-Alvaro, J.A. Mico, and F.L. Neto. 2013. Extracellular signal-regulated kinase activation in the chronic constriction injury model of neuropathic pain in anaesthetized rats. *European Journal of Pain (United Kingdom)*. 17:35-45.

Bornhövd, K., M. Quante, V. Glauche, B. Bromm, C. Weiller, and C. Büchel. 2002. Painful stimuli evoke different stimulus-response functions in the amygdala, prefrontal, insula and somatosensory cortex: A single-trial fMRI study. *Brain*. 125:1326-1336.

Borroto-Escuela, D.O., L.F. Agnati, K. Bechter, A. Jansson, A.O. Tarakanov, and K. Fuxe. 2015. The role of transmitter diffusion and flow versus extracellular vesicles in volume transmission in the brain neural-glial networks. *Philos Trans R Soc Lond B Biol Sci*. 370.

Boue-Grabot, E., and Y. Pankratov. 2017. Modulation of Central Synapses by Astrocyte-Released ATP and Postsynaptic P2X Receptors. *Neural Plast*. 2017:9454275.

Bousquet, P., A. Hudson, J.A. Garcia-Sevilla, and J.X. Li. 2020. Imidazoline Receptor System: The Past, the Present, and the Future. *Pharmacol Rev*. 72:50-79.

Brightwell, J.J., and B.K. Taylor. 2009. Noradrenergic neurons in the locus coeruleus contribute to neuropathic pain. *Neuroscience*. 160:174-185.

Budai, D., I. Harasawa, and H.L. Fields. 1998. Midbrain periaqueductal gray (PAG) inhibits nociceptive inputs to sacral dorsal horn nociceptive neurons through alpha2-adrenergic receptors. *J Neurophysiol*. 80:2244-2254.

Buerkle, H., and T.L. Yaksh. 1998. Pharmacological evidence for different alpha2-adrenergic receptor sites mediating analgesia and sedation in the rat. *British Journal of Anaesthesia*. 81:208-215.

Burgoyne, R.D., and A. Morgan. 2003. Secretory granule exocytosis. *Physiol Rev*. 83:581-632.

Burma, N.E., R.P. Bonin, H. Leduc-Pessah, C. Baimel, Z.F. Cairncross, M. Mousseau, J.V. Shankara, P.L. Stemkowski, D. Baimoukhametova, J.S. Bains, M.C. Antle, G.W. Zamponi, C.M. Cahill, S.L. Borgland, Y. De Koninck, and T. Trang. 2017. Blocking microglial pannexin-1 channels alleviates morphine withdrawal in rodents. *Nature Medicine*. 23:355-360.

Burnstock, G. 1993. Introduction: Changing Face of Autonomic and Sensory Nerves in the Circulation. *In* Vascular Innervation and Receptor Mechanisms. 1-22.

Burnstock, G. 2006a. Pathophysiology and therapeutic potential of purinergic signaling. *Pharmacological Reviews*. 58:58-86.

Burnstock, G. 2006b. Purinergic signalling. *British Journal of Pharmacology*. 147:S172-181.

Burnstock, G. 2007. Purine and pyrimidine receptors. *Cellular and Molecular Life Sciences*. 64:1471-1483.

Burnstock, G., and G.E. Knight. 2004. Cellular distribution and functions of P2 receptor subtypes in different systems. *International Review of Cytology*. 240:31-304.

Bushong, E.A., M.E. Martone, and M.H. Ellisman. 2004. Maturation of astrocyte morphology and the establishment of astrocyte domains during postnatal hippocampal development. *International Journal of Developmental Neuroscience*. 22:73-86.

Bushong, E.A., M.E. Martone, Y.Z. Jones, and M.H. Ellisman. 2002. Protoplasmic astrocytes in CA1 stratum radiatum occupy separate anatomical domains. *Journal of Neuroscience*. 22:183-192.

Butt, A.M. 2011. ATP: a ubiquitous gliotransmitter integrating neuron-glial networks. *Semin Cell Dev Biol*. 22:205-213.

Bylund, D.B., D.C. Eikenberg, J.P. Hieble, S.Z. Langer, R.J. Lefkowitz, K.P. Minneman, P.B. Molinoff, R.R. Ruffolo, and U. Trendelenburg. 1994. IV. International union of pharmacology nomenclature of adrenoceptors. *Pharmacological Reviews*.

Carroll, D., A. Jadad, V. King, P. Wiffen, C. Glynn, and H. McQuay. 1993. Single-dose, randomized, double-blind, double-dummy cross-over comparison of extradural and I.V. Clonidine in chronic pain. *British Journal of Anaesthesia*. 71:665-669.

Casteleijn, N.F., J.D. Blais, A.B. Chapman, F.S. Czerwiec, O. Devuyst, E. Higashihara, A.M. Leliveld, J. Ouyang, R.D. Perrone, V.E. Torres, and R.T. Gansevoort. 2017. Tolvaptan and Kidney Pain in Patients With Autosomal Dominant Polycystic Kidney Disease: Secondary Analysis From a Randomized Controlled Trial. *American Journal of Kidney Diseases*. 69:210-219.

Castro-Lopes, J.M., T.R. Tölle, B. Pan, and W. Zieglgänsberger. 1994. Expression of GAD mRNA in spinal cord neurons of normal and monoarthritic rats. *Molecular Brain Research*. 26:169-176.

Charles, A. 1998. Intercellular calcium waves in glia. *GLIA*. 24:39-49.

Charles, A.C., J.E. Merrill, E.R. Dirksen, and M.J. Sandersont. 1991. Intercellular signaling in glial cells: Calcium waves and oscillations in response to mechanical stimulation and glutamate. *Neuron*. 6:983-992.

Chen, J.I., B. Ha, M. Catherine Bushnell, B. Pike, and G.H. Duncan. 2002. Differentiating noxious- and innocuous-related activation of human somatosensory cortices using temporal analysis of fMRI. *Journal of Neurophysiology*. 88:464-474.

Chen, Y., Z. Zhao, W.E. Code, and L. Hertz. 2000. A correlation between dexmedetomidine-induced biphasic increases in free cytosolic calcium concentration and energy metabolism in astrocytes. *Anesthesia and Analgesia*. 91:353-357.

Chever, O., C.Y. Lee, and N. Rouach. 2014. Astroglial connexin43 hemichannels tune basal excitatory synaptic transmission. *Journal of Neuroscience*. 34:11228-11232.

Choe, K.Y., J.E. Olson, and C.W. Bourque. 2012. Taurine release by astrocytes modulates osmosensitive glycine receptor tone and excitability in the adult supraoptic nucleus. *Journal of Neuroscience*. 32:12518-12527.

Choi, D.H., J.H. Yun, and J. Lee. 2018. Protective effect of the imidazoline I2 receptor agonist 2-BFI on oxidative cytotoxicity in astrocytes. *Biochem Biophys Res Commun*. 503:3011-3016.

Choi, H.S., D.H. Roh, S.Y. Yoon, J.Y. Moon, S.R. Choi, S.G. Kwon, S.Y. Kang, H.J. Han, H.W. Kim, A.J. Beitz, S.B. Oh, and J.H. Lee. 2015. Microglial interleukin-1β in the ipsilateral dorsal horn inhibits the development of mirror-image contralateral mechanical allodynia through astrocyte activation in a rat model of inflammatory pain. *Pain*. 156:1046-1059.

Coco, S., F. Calegari, E. Pravettoni, D. Pozzi, E. Taverna, P. Rosa, M. Matteoli, and C. Verderio. 2003. Storage and release of ATP from astrocytes in culture. *Journal of Biological Chemistry*. 278:1354-1362.

Coggeshall, R.E., R.B. Leonard, M.L. Applebaum, and W.D. Willis. 1978. Organization of peripheral nerves and spinal roots of the Atlantic stingray, Dasyatis sabina. *J Neurophysiol*. 41:97-107.

Cohen, S.P., and J. Mao. 2014. Neuropathic pain: mechanisms and their clinical implications. *Bmj*. 348:f7656.

Colloca, L., T. Ludman, D. Bouhassira, R. Baron, A.H. Dickenson, D. Yarnitsky, R. Freeman, A. Truini, N. Attal, N.B. Finnerup, C. Eccleston, E. Kalso, D.L. Bennett, R.H. Dworkin, and S.N. Raja. 2017. Neuropathic pain. *Nature Reviews Disease Primers*. 3:17002.

Cordero-Erausquin, M., P. Inquimbert, R. Schlichter, and S. Hugel. 2016. Neuronal networks and nociceptive processing in the dorsal horn of the spinal cord. *Neuroscience*. 338:230-247.

Cotrina, M.L., J.H.C. Lin, A. Alves-Rodrigues, S. Liu, J. Li, H. Azmi-Ghadimi, J. Kang, C.C.G. Naus, and M. Nedergaard. 1998. Connexins regulate calcium signaling by controlling ATP release. *Proceedings of the National Academy of Sciences of the United States of America*. 95:15735-15740.

Cox, J.J., F. Reimann, A.K. Nicholas, G. Thornton, E. Roberts, K. Springell, G. Karbani, H. Jafri, J. Mannan, Y. Raashid, L. Al-Gazali, H. Hamamy, E.M. Valente, S. Gorman, R. Williams, D.P. McHale, J.N. Wood, F.M. Gribble, and C.G. Woods. 2006. An SCN9A channelopathy causes congenital inability to experience pain. *Nature*. 444:894-898.

Craig, A.D. 1992. Spinal and trigeminal lamina I input to the locus coeruleus anterogradely labeled with Phaseolus vulgaris leucoagglutinin (PHA-L) in the cat and the monkey. *Brain Research*. 584:325-328.

Crippa, D., U. Schenk, M. Francolini, P. Rosa, C. Verderio, M. Zonta, T. Pozzan, M. Matteoli, and G. Carmignoto. 2006. Synaptobrevin2-expressing vesicles in rat astrocytes: Insights into molecular characterization, dynamics and exocytosis. *Journal of Physiology*. 570:567-582.

Daaka, Y., L.M. Luttrell, and R.J. Lefkowitz. 1997. Switching of the coupling of the β2-adrenergic receptor to different g proteins by protein kinase A. *Nature*. 390:88-91.

Dahl, G. 2015. ATP release through pannexon channels. *Philosophical Transactions of the Royal Society B: Biological Sciences*. 370.

Dahl, G., and S. Locovei. 2006. Pannexin: to gap or not to gap, is that a question? *IUBMB Life*. 58:409-419.

Dallwig, R., H. Vitten, and J.W. Deitmer. 2000. A novel barium-sensitive calcium influx into rat astrocytes at low external potassium. *Cell Calcium*. 28:247-259.

Day, H.E.W., S. Campeau, S.J. Watson, and H. Akil. 1997. Distribution of α(1a)-, α(1b)- and α(1d)-adrenergic receptor mRNA in the rat brain and spinal cord. *Journal of Chemical Neuroanatomy*. 13:115-139.

Decker, N., and J. Schwartz. 1985. Postjunctional alpha-1 and alpha-2 adrenoceptors in the coronaries of the perfused guinea-pig heart. *J Pharmacol Exp Ther*. 232:251-257.

Decrock, E., M. De Bock, N. Wang, G. Bultynck, C. Giaume, C.C. Naus, C.R. Green, and L. Leybaert. 2015. Connexin and pannexin signaling pathways, an architectural blueprint for CNS physiology and pathology? *Cell Mol Life Sci*. 72:2823-2851.

DeLeo, J.A. 2006. Basic Science of Pain. *The Journal of Bone and Joint Surgery (American)*. 88 Suppl 2:58-62.

Di Virgilio, F., S. Ceruti, P. Bramanti, and M.P. Abbracchio. 2009. Purinergic signalling in inflammation of the central nervous system. *Trends Neurosci*. 32:79-87.

Ding, F., J. O'Donnell, A.S. Thrane, D. Zeppenfeld, H. Kang, L. Xie, F. Wang, and M. Nedergaard. 2013. α1-Adrenergic receptors mediate coordinated Ca^{2+} signaling of cortical astrocytes in awake, behaving mice. *Cell Calcium*. 54:387-394.

Djouhri, L. 2016. L5 spinal nerve axotomy induces sensitization of cutaneous L4 Aβ-nociceptive dorsal root ganglion neurons in the rat in vivo. *Neuroscience Letters*. 624:72-77.

Djouhri, L., and S.N. Lawson. 2004. Aβ-fiber nociceptive primary afferent neurons: A review of incidence and properties in relation to other afferent A-fiber neurons in mammals. *Brain Research Reviews*. 46:131-145.

Du, T., B. Li, H. Li, M. Li, L. Hertz, and L. Peng. 2010. Signaling pathways of isoproterenol-induced ERK1/2 phosphorylation in primary cultures of astrocytes are concentration-dependent. *Journal of Neurochemistry*. 115:1007-1023.

Duan, B., L. Cheng, S. Bourane, O. Britz, C. Padilla, L. Garcia-Campmany, M. Krashes, W. Knowlton, T. Velasquez, X. Ren, S.E. Ross, B.B. Lowell, Y. Wang, M. Goulding, and Q. Ma. 2014. Identification of spinal circuits transmitting and gating mechanical pain. *Cell*. 159:1417-1432.

Duan, S., C.M. Anderson, E.C. Keung, Y. Chen, Y. Chen, and R.A. Swanson. 2003. P2X7 receptor-mediated release of excitatory amino acids from astrocytes. *Journal of Neuroscience*. 23:1320-1328.

Dubin, A.E., and A. Patapoutian. 2010. Nociceptors: The sensors of the pain pathway. *The Journal of Clinical Investigation*. 120:3760–3772.

Duffy, S., and B.A. MacVicar. 1995. Adrenergic calcium signaling in astrocyte networks within the hippocampal slice. *Journal of Neuroscience*. 15:5535-5550.

Durkee, C.A., A. Covelo, J. Lines, P. Kofuji, J. Aguilar, and A. Araque. 2019. G i/o protein-coupled receptors inhibit neurons but activate astrocytes and stimulate gliotransmission. *GLIA*. 67:1076-1093.

Eersapah, V., S. Hugel, and R. Schlichter. 2019. High-resolution detection of ATP release from single cultured mouse dorsal horn spinal cord glial cells and its modulation by noradrenaline. *Purinergic Signalling*. 15:403-420.

Emerit, M.B., M. Riad, C.M. Fattaccini, and M. Hamon. 1993. Characteristics of [14C]guanidinium accumulation in NG 108-15 cells exposed to serotonin 5-HT3 receptor ligands and substance P. *J Neurochem*. 60:2059-2067.

Enkvist, M.O., H. Hamalainen, C.C. Jansson, J.P. Kukkonen, R. Hautala, M.J. Courtney, and K.E. Akerman. 1996. Coupling of astroglial alpha 2-adrenoreceptors to second messenger pathways. *J Neurochem*. 66:2394-2401.

Erickson, J.D., M.K.H. Schäfer, T.I. Bonner, L.E. Eiden, and E. Weihe. 1996. Distinct pharmacological properties and distribution in neurons and endocrine cells of two isoforms of the human vesicular monoamine transporter. *Proceedings of the National Academy of Sciences of the United States of America*. 93:5166-5171.

Ernsberger, P., J.E. Friedman, and R.J. Koletsky. 1997. The I1-imidazoline receptor: from binding site to therapeutic target in cardiovascular disease. *J Hypertens Suppl*. 15:S9-23.

Ernsberger, P., R. Giuliano, R.N. Willette, and D.J. Reis. 1990. Role of imidazole receptors in the vasodepressor response to clonidine analogs in the rostral ventrolateral medulla. *J Pharmacol Exp Ther*. 253:408-418.

Ernsberger, P., M.E. Graves, L.M. Graff, N. Zakieh, P. Nguyen, L.A. Collins, K.L. Westbrooks, and G.G. Johnson. 1995. I1-imidazoline receptors. Definition, characterization, distribution, and transmembrane signaling. *Ann N Y Acad Sci*. 763:22-42.

Ernsberger, P., M.P. Meeley, J.J. Mann, and D.J. Reis. 1987. Clonidine binds to imidazole binding sites as well as alpha 2-adrenoceptors in the ventrolateral medulla. *Eur J Pharmacol*. 134:1-13.

Eskandari, S., G.A. Zampighi, D.W. Leung, E.M. Wright, and D.D.F. Loo. 2002. Inhibition of gap junction hemichannels by chloride channel blockers. *Journal of Membrane Biology*. 185:93-102.

Fellin, T., T. Pozzan, and G. Carmignoto. 2006. Purinergic receptors mediate two distinct glutamate release pathways in hippocampal astrocytes. *Journal of Biological Chemistry*. 281:4274-4284.

Ferrari, F., S. Fiorentino, L. Mennuni, P. Garofalo, O. Letari, S. Mandelli, A. Giordani, M. Lanza, and G. Caselli. 2011. Analgesic efficacy of CR4056, a novel imidazoline-2 receptor ligand, in rat models of inflammatory and neuropathic pain. *Journal of Pain Research*. 4:111-125.

Feske, S. 2010. CRAC channelopathies. *Pflügers Archiv*. 460:417-435.

Feske, S., Y. Gwack, M. Prakriya, S. Srikanth, S.H. Puppel, B. Tanasa, P.G. Hogan, R.S. Lewis, M. Daly, and A. Rao. 2006. A mutation in Orai1 causes immune deficiency by abrogating CRAC channel function. *Nature*. 441:179-185.

Feustel, P.J., Y. Jin, and H.K. Kimelberg. 2004. Volume-regulated anion channels are the predominant contributors to release of excitatory amino acids in the ischemic cortical penumbra. *Stroke*. 35:1164-1168.

Fields, R.D., and G. Burnstock. 2006. Purinergic signalling in neuron-glia interactions. *Nature Reviews Neuroscience*. 7(6):423-436.

Fierro, L., and A.B. Parekh. 2000. Substantial depletion of the intracellular Ca^{2+} stores is required for macroscopic activation of the Ca^{2+} release-activated Ca^{2+} current in rat basophilic leukaemia cells. *Journal of Physiology*. 522 Pt 2:247-257.

Flamez, A., J.P. De Backer, E. Czerwiec, P. Ladure, and G. Vauquelin. 1997. Pharmacological characterization of I1 and I2 imidazoline receptors in human striatum. *Neurochem Int*. 30:25-29.

Fleetwood-Walker, S.M., R. Mitchell, P.J. Hope, V. Molony, and A. Iggo. 1985. An α2 receptor mediates the selective inhibition by noradrenaline of nociceptive responses of identified dorsal horn neurones. *Brain Research*. 334:243-254.

Florian, C., C.G. Vecsey, M.M. Halassa, P.G. Haydon, and T. Abel. 2011. Astrocyte-derived adenosine and A1 receptor activity contribute to sleep loss-induced deficits in hippocampal synaptic plasticity and memory in mice. *Journal of Neuroscience*. 31:6956-6962.

Foster, K.A., M. Weiss, and M.S. Roberts. 2002. Distribution kinetics of solutes in the isolated in-situ perfused rat head using the multiple indicator dilution technique and a physiological two-barrier model. *Journal of Pharmacy and Pharmacology*. 54:373-382.

Friedrich, V.L., Jr., G.P. Martinelli, G.D. Prell, and G.R. Holstein. 2007. Distribution and cellular localization of imidazoleacetic acid-ribotide, an endogenous ligand at imidazol(in)e and adrenergic receptors, in rat brain. *J Chem Neuroanat*. 33:53-64.

Fukui, M., A. Takishita, N. Zhang, T. Nakagawa, M. Minami, and M. Satoh. 2004. Involvement of Locus Coeruleus Noradrenergic Neurons in Supraspinal Antinociception by α,β-Methylene-ATP in Rats. *Journal of Pharmacological Sciences*. 94:153-160.

Fuxe, K., L.F. Agnati, M. Marcoli, and D.O. Borroto-Escuela. 2015. Volume Transmission in Central Dopamine and Noradrenaline Neurons and Its Astroglial Targets. *Neurochemical Research*. 40:2600-2614.

Gallo, V., M. Patrizio, and G. Levi. 1991. GABA release triggered by the activation of neuron-like non-NMDA receptors in cultured type 2 astrocytes is carrier-mediated. *Glia*. 4:245-255.

Gallo, V., R. Suergiu, and G. Levi. 1986. Kainic acid stimulates GABA release from a subpopulation of cerebellar astrocytes. *European Journal of Pharmacology*. 132:319-322.

Gao, R., X. Gao, J. Xia, Y. Tian, J.E. Barrett, Y. Dai, and H. Hu. 2013. Potent analgesic effects of a store-operated calcium channel inhibitor. *Pain*. 154:2034-2044.

Gao, X., J. Xia, F.M. Munoz, M.T. Manners, R. Pan, O. Meucci, Y. Dai, and H. Hu. 2016. STIMs and Orai1 regulate cytokine production in spinal astrocytes. *Journal of Neuroinflammation*. 13:126.

Gao, X.H., R. Gao, Y.Z. Tian, P. McGonigle, J.E. Barrett, Y. Dai, and H. Hu. 2015. A store-operated calcium channel inhibitor attenuates collagen-induced arthritis. *British Journal of Pharmacology*. 172:2991-3002.

Gao, Y.J., and R.R. Ji. 2010a. Chemokines, neuronal-glial interactions, and central processing of neuropathic pain. *Pharmacol Ther*. 126:56-68.

Gao, Y.J., and R.R. Ji. 2010b. Targeting Astrocyte Signaling for Chronic Pain. *Neurotherapeutics*. 7:482-493.

Gardella, S., C. Andrei, L.V. Lotti, A. Poggi, M. Rosaria Torrisi, M. Raffaella Zocchi, and A. Rubartelli. 2001. CD8+ T lymphocytes induce polarized exocytosis of secretory lysosomes by dendritic cells with release of interleukin-1β and cathepsin D. *Blood*. 98:2152-2159.

Garraway, S.M., and S. Hochman. 2001. Modulatory actions of serotonin, norepinephrine, dopamine, and acetylcholine in spinal cord deep dorsal horn neurons. *Journal of Neurophysiology*. 86:2183-2194.

Garrison, C.J., P.M. Dougherty, K.C. Kajander, and S.M. Carlton. 1991. Staining of glial fibrillary acidic protein (GFAP) in lumbar spinal cord increases following a sciatic nerve constriction injury. *Brain Research*. 565:1-7.

Gasnier, B. 2000. The loading of neurotransmitters into synaptic vesicles. *Biochimie*. 82:327-337.

Gassner, M., R. Ruscheweyh, and J. Sandkühler. 2009. Direct excitation of spinal GABAergic interneurons by noradrenaline. *Pain*. 145:204-210.

Giaume, C., L. Leybaert, C.C. Naus, and J.C. Saez. 2013. Connexin and pannexin hemichannels in brain glial cells: properties, pharmacology, and roles. *Front Pharmacol*. 4:88.

Giesecke, T., R.H. Gracely, M.A.B. Grant, A. Nachemson, F. Petzke, D.A. Williams, and D.J. Clauw. 2004. Evidence of Augmented Central Pain Processing in Idiopathic Chronic Low Back Pain. *Arthritis and Rheumatism*. 50:613-623.

Giesler, G.J., D. Menétrey, G. Guilbaud, and J.M. Besson. 1976. Lumbar cord neurons at the origin of the spinothalamic tract in the rat. *Brain Research*. 118:320-324.

Giesler, G.J., R.P. Yezierski, K.D. Gerhart, and W.D. Willis. 1981. Spinothalamic tract neurons that project to medial and/or lateral thalamic nuclei: Evidence for a physiologically novel population of spinal cord neurons. *Journal of Neurophysiology*. 46:1285-1308.

Giuliani, A.L., A.C. Sarti, and F. Di Virgilio. 2019. Extracellular nucleotides and nucleosides as signalling molecules. *Immunol Lett*. 205:16-24.

Goldberg, Y.P., J. Macfarlane, M.L. Macdonald, J. Thompson, M.P. Dube, M. Mattice, R. Fraser, C. Young, S. Hossain, T. Pape, B. Payne, C. Radomski, G. Donaldson, E. Ives, J. Cox, H.B. Younghusband, R. Green, A. Duff, E. Boltshauser, G.A. Grinspan, J.H. Dimon, B.G. Sibley, G. Andria, E. Toscano, J. Kerdraon, D. Bowsher, S.N. Pimstone, M.E. Samuels, R. Sherrington, and M.R. Hayden. 2007. Loss-of-function mutations in the Nav1.7 gene underlie congenital indifference to pain in multiple human populations. *Clinical Genetics*. 71:311-319.

Gonzalez-Lopez, E., and K.E. Vrana. 2020. Dopamine beta-hydroxylase and its genetic variants in human health and disease. *J Neurochem*. 152:157-181.

Goracke-Postle, C.J., H.O. Nguyen, L.S. Stone, and C.A. Fairbanks. 2006. Release of tritiated agmatine from spinal synaptosomes. *Neuroreport*. 17:13-17.

Goracke-Postle, C.J., A.C. Overland, M.S. Riedl, L.S. Stone, and C.A. Fairbanks. 2007. Potassium- and capsaicin-induced release of agmatine from spinal nerve terminals. *J Neurochem*. 102:1738-1748.

Goto, J.I., A.Z. Suzuki, S. Ozaki, N. Matsumoto, T. Nakamura, E. Ebisui, A. Fleig, R. Penner, and K. Mikoshiba. 2010. Two novel 2-aminoethyl diphenylborinate (2-APB) analogues differentially activate and inhibit store-operated Ca^{2+} entry via STIM proteins. *Cell Calcium*. 47:1-10.

Graham, D.Y., N.M. Agrawal, D.R. Campbell, M.M. Haber, C. Collis, N.L. Lukasik, and B. Huang. 2002. Ulcer prevention in long-term users of nonsteroidal anti-inflammatory drugs: Results of a double-blind, randomized, multicenter, active- and placebo-controlled study of misoprostol vs lansoprazole. *Archives of Internal Medicine*. 162:169-175.

Graham, R.M., D.M. Perez, J. Hwa, and M.T. Piascik. 1996. alpha 1-adrenergic receptor subtypes. Molecular structure, function, and signaling. *Circ Res*. 78:737-749.

Grudt, T.J., and E.R. Perl. 2002. Correlations between neuronal morphology and electro-physiological features in the rodent superficial dorsal horn. *Journal of Physiology*. 540:189-207.

Grudt, T.J., J.T. Williams, and R.A. Travagli. 1995. Inhibition by 5-hydroxytryptamine and noradrenaline in substantia gelatinosa of guinea-pig spinal trigeminal nucleus. *The Journal of Physiology*. 485 (Pt 1):113-120.

Grygorczyk, R., J.A. Tabcharani, and J.W. Hanrahan. 1996. CFTR channels expressed in CHO cells do not have detectable ATP conductance. *Journal of Membrane Biology*. 151:139-148.

Grzanna, R., and M.E. Molliver. 1980. The locus coeruleus in the rat: An immunohistochemical delineation. *Neuroscience*. 5:21-40.

Guo, W., H. Wang, M. Watanabe, K. Shimizu, S. Zou, S.C. LaGraize, F. Wei, R. Dubner, and K. Ren. 2007. Glial-cytokine-neuronal interactions underlying the mechanisms of persistent pain. *Journal of Neuroscience*. 27:6006-6018.

Guo, W., S. Zou, Y. Guan, T. Ikeda, M. Tal, R. Dubner, and K. Ren. 2002. Tyrosine phosphorylation of the NR2B subunit of the NMDA receptor in the spinal cord during the development and maintenance of inflammatory hyperalgesia. *Journal of Neuroscience*. 22:6208-6217.

Guthrie, P.B., J. Knappenberger, M. Segal, M.V.L. Bennett, A.C. Charles, and S.B. Kater. 1999. ATP released from astrocytes mediates glial calcium waves. *Journal of Neuroscience*. 19:520-528.

H Miller, R., and M. C Raff. 1984. Fibrous and protoplasmic astrocytes are biochemically and developmentally distinct. *Journal of Neuroscience*. 4:585-592.

Hagihira, S., E. Senba, S. Yoshida, M. Tohyama, and I. Yoshiya. 1990. Fine structure of noradrenergic terminals and their synapses in the rat spinal dorsal horn: an immunohistochemical study. *Brain Res*. 526:73-80.

Halassa, M.M., T. Fellin, H. Takano, J.H. Dong, and P.G. Haydon. 2007. Synaptic islands defined by the territory of a single astrocyte. *Journal of Neuroscience*. 27:6473-6477.

Halassa, M.M., C. Florian, T. Fellin, J.R. Munoz, S.Y. Lee, T. Abel, P.G. Haydon, and M.G. Frank. 2009. Astrocytic Modulation of Sleep Homeostasis and Cognitive Consequences of Sleep Loss. *Neuron*. 61:213-219.

Hamilton, N.B., and D. Attwell. 2010. Do astrocytes really exocytose neurotransmitters? *Nat Rev Neurosci*. 11:227-238.

Han, C., T. Chen, M. Yang, N. Li, H. Liu, and X. Cao. 2009. Human SCAMP5, a Novel Secretory Carrier Membrane Protein, Facilitates Calcium-Triggered Cytokine Secretion by Interaction with SNARE Machinery. *The Journal of Immunology*. 182:2986-2996.

Han, X., M. Chen, F. Wang, M. Windrem, S. Wang, S. Shanz, Q. Xu, N.A. Oberheim, L. Bekar, S. Betstadt, A.J. Silva, T. Takano, S.A. Goldman, and M. Nedergaard. 2013a. Forebrain engraftment by human glial progenitor cells enhances synaptic plasticity and learning in adult mice. *Cell Stem Cell*. 12:342-353.

Han, Z., J.L. Yang, S.X. Jiang, S.T. Hou, and R.Y. Zheng. 2013b. Fast, non-competitive and reversible inhibition of NMDA-activated currents by 2-BFI confers neuroprotection. *PLoS One*. 8:e64894-e64894.

Harris, A.L. 2007. Connexin channel permeability to cytoplasmic molecules. *Prog Biophys Mol Biol*. 94:120-143.

Hassinger, T.D., P.B. Guthrie, P.B. Atkinson, M.V.L. Bennett, and S.B. Kater. 1996. An extracellular signaling component in propagation of astrocytic calcium waves. *Proceedings of the National Academy of Sciences of the United States of America*. 93:13268-13273.

Hawkins, A., and J. Olszewski. 1957. Glia/nerve cell index for cortex of the whale. *Science*. 126:76-77.

Hayashida, K.I., C.M. Peters, S. Gutierrez, and J.C. Eisenach. 2012. Depletion of endogenous noradrenaline does not prevent spinal cord plasticity following peripheral nerve injury. *Journal of Pain*. 13:49-57.

Haydon, P.G. 2001. Glia: Listening and talking to the synapse. *Nature Reviews Neuroscience*. 2:185-193.

Haydon, P.G., and G. Carmignoto. 2006. Astrocyte control of synaptic transmission and neurovascular coupling. *Physiol Rev*. 86:1009-1031.

Head, G.A., and D.N. Mayorov. 2006. Imidazoline receptors, novel agents and therapeutic potential. *Cardiovasc Hematol Agents Med Chem*. 4:17-32.

Heidelberger, R., C. Heinemann, E. Neher, and G. Matthews. 1994. Calcium dependence of the rate of exocytosis in a synaptic terminal. *Nature*. 371:513-515.

Héja, L., P. Barabás, G. Nyitrai, K.A. Kékesi, B. Lasztóczi, O. Töke, G. Tárkányi, K. Madsen, A. Schousboe, Á. Dobolyi, M. Palkovits, and J. Kardos. 2009. Glutamate uptake triggers transporter-mediated GABA release from astrocytes. *PLoS ONE*. 4:e7153.

Hendron, E., X. Wang, Y. Zhou, X. Cai, J.I. Goto, K. Mikoshiba, Y. Baba, T. Kurosaki, Y. Wang, and D.L. Gill. 2014. Potent functional uncoupling between STIM1 and Orai1 by dimeric 2-aminodiphenyl borinate analogs. *Cell Calcium*. 56:482-492.

Heo, D.K., H.M. Lim, J.H. Nam, M.G. Lee, and J.Y. Kim. 2015. Regulation of phagocytosis and cytokine secretion by store-operated calcium entry in primary isolated murine microglia. *Cellular Signalling*. 27:177-186.

Hepp, R., M. Perraut, S. Chasserot-Golaz, T. Galli, D. Aunis, K. Langley, and N.J. Grant. 1999. Cultured glial cells express the SNAP-25 analogue SNAP-23. *GLIA*. 27:181-187.

Herculano-Houzel, S. 2014. The glia/neuron ratio: how it varies uniformly across brain structures and species and what that means for brain physiology and evolution. *Glia*. 62:1377-1391.

Hertz, L., D. Lovatt, S.A. Goldman, and M. Nedergaard. 2010. Adrenoceptors in brain: Cellular gene expression and effects on astrocytic metabolism and $[Ca^{2+}]i$. *Neurochemistry International*. 57:411-420.

Hickey, L., Y. Li, S.J. Fyson, T.C. Watson, R. Perrins, J. Hewinson, A.G. Teschemacher, H. Furue, B.M. Lumb, and A.E. Pickering. 2014. Optoactivation of locus ceruleus neurons evokes bidirectional changes in thermal nociception in rats. *Journal of Neuroscience*. 34:4148-4160.

Hochman, S. 2007. Spinal cord. *Curr Biol*. 17:R950-955.

Hodge, C.J., A.V. Apkarian, M.P. Owen, and B.S. Hanson. 1983. Changes in the effects of stimulation of locus coeruleus and nucleus raphe magnus following dorsal rhizotomy. *Brain Research*. 288:325-329.

Hofer, A., and R. Dermietzel. 1998. Visualization and functional blocking of gap junction hemichannels (connexons) with antibodies against external loop domains in astrocytes. *GLIA*. 24:141-154.

Holstege, J.C., and C.M. Bongers. 1991. Ultrastructural aspects of the coeruleo-spinal projection. *Prog Brain Res*. 88:143-156.

Hoth, M., and R. Penner. 1992. Depletion of intracellular calcium stores activates a calcium current in mast cells. *Nature*. 355:353-356.

Hoth, M., and R. Penner. 1993. Calcium release-activated calcium current in rat mast cells. *J Physiol*. 465:359-386.

Hou, X., L. Pedi, M.M. Diver, and S.B. Long. 2012. Crystal structure of the calcium release-activated calcium channel orai. *Science*. 338:1308-1313.

Howe, J.R., J.Y. Wang, and T.L. Yaksh. 1983. Selective antagonism of the antinociceptive effect of intrathecally applied alpha adrenergic agonists by intrathecal prazosin and intrathecal yohimbine. *Journal of Pharmacology and Experimental Therapeutics*. 224:552-558.

Hoyle, C.H.V. 1996. Purinergic cotransmission: parasympathetic and enteric nerves. *Seminars in Neuroscience*. 8:207-215.

Hua, X., E.B. Malarkey, V. Sunjara, S.E. Rosenwald, W.H. Li, and V. Parpura. 2004. Ca^{2+}-Dependent Glutamate Release Involves Two Classes of Endoplasmic Reticulum Ca^{2+} Stores in Astrocytes. *Journal of Neuroscience Research*. 76:86-97.

Huang, Y., W.D. Stamer, T.L. Anthony, D.V. Kumar, P.A. St. John, and J.W. Regan. 2002. Expression of α2-adrenergic receptor subtypes in prenatal rat spinal cord. *Developmental Brain Research*. 133:93-104.

Huang, Y., and A. Thathiah. 2015. Regulation of neuronal communication by G protein-coupled receptors. *FEBS Lett*. 589:1607-1619.

Hudson, A.L., C.B. Chapleo, J.W. Lewis, S. Husbands, K. Grivas, N.J. Mallard, and D.J. Nutt. 1997. Identification of ligands selective for central I2-imidazoline binding sites. *Neurochem Int*. 30:47-53.

Hugel, S., Y.H. Jo, and R. Schlichter. 2009. Synaptic Co-Release of ATP and GABA. *In* Co-Existence and Co-Release of Classical Neurotransmitters. 1-21.

Hugel, S., and R. Schlichter. 2000. Presynaptic P2X receptors facilitate inhibitory GABAergic transmission between cultured rat spinal cord dorsal horn neurons. *The Journal of neuroscience : the official journal of the Society for Neuroscience*. 20:2121-2130.

Hughes, D.I., S. Sikander, C.M. Kinnon, K.A. Boyle, M. Watanabe, R.J. Callister, and B.A. Graham. 2012. Morphological, neurochemical and electrophysiological features of parvalbumin-expressing cells: A likely source of axo-axonic inputs in the mouse spinal dorsal horn. *Journal of Physiology*. 590:3927-3951.

Hylden, J.L.K., F. Anton, and R.L. Nahin. 1989. Spinal lamina I projection neurons in the rat: Collateral innervation of parabrachial area and thalamus. *Neuroscience*. 28:27-37.

Härtel, K., K. Singaravelu, M. Kaiser, C. Neusch, S. Hülsmann, and J.W. Deitmer. 2007. Calcium influx mediated by the inwardly rectifying K+ channel Kir4.1 (KCNJ10) at low external K+ concentration. *Cell Calcium*. 42:271-280.

Hösli, E., and L. Hösli. 1982. Evidence for the existence of α- and β-adrenoceptors on neurones and glial cells of cultured rat central nervous system-an autoradiographic study. *Neuroscience*. 7:2873-2881.

Ikeda, H., T. Kiritoshi, and K. Murase. 2012. Contribution of microglia and astrocytes to the central sensitization, inflammatory and neuropathic pain in the juvenile rat. *Molecular Pain*. 8:43.

Inoue, K., and M. Tsuda. 2009. Microglia and neuropathic pain. *Glia*. 57:1469-1479.

Inoue, K., and M. Tsuda. 2018. Microglia in neuropathic pain: cellular and molecular mechanisms and therapeutic potential. *Nat Rev Neurosci*. 19:138-152.

J. D. Loeser, S.D.B.C.R.C., and D.C. Turk. 2000. Borknica's Management of Pain. Lippincott Williams & Wilkins. 17-25 pp.

J.E. Neil, M. 2011. Clonidine: Clinical Pharmacology and Therapeutic Use in Pain Management. *Current Clinical Pharmacology*. 6:280-287.

Jacobson, K.A., and C.E. Muller. 2016. Medicinal chemistry of adenosine, P2Y and P2X receptors. *Neuropharmacology*. 104:31-49.

Jaggi, A.S., and N. Singh. 2011. Role of different brain areas in peripheral nerve injury-induced neuropathic pain. *Brain Research*. 1381:187-201.

Jairaman, A., and M. Prakriya. 2013. Molecular pharmacology of store-operated CRAC channels. *Channels (Austin)*. 7:402-414.

Jaiswal, J.K., N.W. Andrews, and S.M. Simon. 2002. Membrane proximal lysosomes are the major vesicles responsible for calcium-dependent exocytosis in nonsecretory cells. *Journal of Cell Biology*. 159:625-635.

Janss, A.J., and G.F. Gebhart. 1988. Brainstem and spinal pathways mediating descending inhibition from the medullary lateral reticular nucleus in the rat. *Brain Research*. 440:109-122.

Jasmin, L., A. Boudah, and P.T. Ohara. 2003. Long-term effects of decreased noradrenergic central nervous system innervation on pain behavior and opioid antinociception. *Journal of Comparative Neurology*. 460:38-55.

Ji, R.R., T. Berta, and M. Nedergaard. 2013. Glia and pain: is chronic pain a gliopathy? *Pain*. 154 Suppl 1:S10-S28.

Ji, R.R., A. Chamessian, and Y.Q. Zhang. 2016. Pain regulation by non-neuronal cells and inflammation. *Science*. 354:572-577.

Ji, R.R., C.R. Donnelly, and M. Nedergaard. 2019. Astrocytes in chronic pain and itch. *Nat Rev Neurosci*. 20:667-685.

Ji, R.R., Y. Kawasaki, Z.Y. Zhuang, Y.R. Wen, and I. Decosterd. 2006. Possible role of spinal astrocytes in maintaining chronic pain sensitization: Review of current evidence with focus on bFGF/JNK pathway. *Neuron Glia Biology*. 2:259-269.

Jiang, S.X., R.Y. Zheng, J.Q. Zeng, X.L. Li, Z. Han, and S.T. Hou. 2010. Reversible inhibition of intracellular calcium influx through NMDA receptors by imidazoline I(2) receptor antagonists. *Eur J Pharmacol*. 629:12-19.

Jo, Y.H., and L.W. Role. 2002. Coordinate Release of ATP and GABA at in Vitro Synapses of Lateral Hypothalamic Neurons. *Journal of Neuroscience*. 22:4794-4804.

Jo, Y.H., and R. Schlichter. 1999. Synaptic corelease of ATP and GABA in cultured spinal neurons. *Nature Neuroscience*. 2:241-245.

Johnson, R.G., Jr. 1988. Accumulation of biological amines into chromaffin granules: a model for hormone and neurotransmitter transport. *Physiol Rev*. 68:232-307.

Jones, S.L., and G.F. Gebhart. 1986. Characterization of coeruleospinal inhibition of the nociceptive tail-flick reflex in the rat: Mediation by spinal α2-adrenoceptors. *Brain Research*. 364:315-330.

Jones, S.L., and G.F. Gebhart. 1988. Inhibition of spinal nociceptive transmission from the midbrain, pons and medulla in the rat: activation of descending inhibition by morphine, glutamate and electrical stimulation. *Brain Research*. 460:281-296.

Jourdain, P., L.H. Bergersen, K. Bhaukaurally, P. Bezzi, M. Santello, M. Domercq, C. Matute, F. Tonello, V. Gundersen, and A. Volterra. 2007. Glutamate exocytosis from astrocytes controls synaptic strength. *Nature Neuroscience*. 10:331-339.

Julius, D., and A.I. Basbaum. 2001. Molecular mechanisms of nociception. *Nature*. 413:203-210.

Kang, J., L. Jiang, S.A. Goldman, and M. Nedergaard. 1998. Astrocyte-mediated potentiation of inhibitory synaptic transmission. *Nat Neurosci*. 1:683-692.

Kang, J., N. Kang, D. Lovatt, A. Torres, Z. Zhao, J. Lin, and M. Nedergaard. 2008. Connexin 43 hemichannels are permeable to ATP. *Journal of Neuroscience*. 28:4702-4711.

Kasymov, V., O. Larina, C. Castaldo, N. Marina, M. Patrushev, S. Kasparov, and A.V. Gourine. 2013. Differential sensitivity of brainstem versus cortical astrocytes to changes in pH reveals functional regional specialization of astroglia. *Journal of Neuroscience*. 33:435-441.

Kawamoto, S., H. Hirakata, N. Sugita, and K. Fukuda. 2015. Bidirectional effects of dexmedetomidine on human platelet functions in vitro. *European Journal of Pharmacology*. 766:122-128.

Kawasaki, Y., E. Kumamoto, H. Furue, and M. Yoshimura. 2003. α2 adrenoceptor-mediated presynaptic inhibition of primary afferent glutamatergic transmission in rat substantia gelatinosa neurons. *Anesthesiology*. 98:682-689.

Kawasaki, Y., L. Zhang, J.K. Cheng, and R.R. Ji. 2008. Cytokine mechanisms of central sensitization: Distinct and overlapping role of interleukin-1β, interleukin-6, and tumor necrosis factor-α in regulating synaptic and neuronal activity in the superficial spinal cord. *Journal of Neuroscience*. 28:5189-5194.

Khakh, B.S., and K.D. McCarthy. 2015. Astrocyte calcium signaling: From observations to functions and the challenges therein. *Cold Spring Harbor Perspectives in Biology*. 7:a020404.

Khakh, B.S., and M.V. Sofroniew. 2015. Diversity of astrocyte functions and phenotypes in neural circuits. *Nature Neuroscience*. 18:942-952.

Kimelberg, H.K. 2010. Functions of mature mammalian astrocytes: a current view. *Neuroscientist*. 16:79-106.

Kimelberg, H.K., S.K. Goderie, S. Higman, S. Pang, and R.A. Waniewski. 1990. Swelling-induced release of glutamate, aspartate, and taurine from astrocyte cultures. *Journal of Neuroscience*. 10:1583-1591.

Kimura, A., R.J. Tyacke, J.J. Robinson, S.M. Husbands, M.C. Minchin, D.J. Nutt, and A.L. Hudson. 2009. Identification of an imidazoline binding protein: creatine kinase and an imidazoline-2 binding site. *Brain Res*. 1279:21-28.

Kirischuk, S., L. Héja, J. Kardos, and B. Billups. 2016. Astrocyte sodium signaling and the regulation of neurotransmission. *GLIA*. 64:1655-1666.

Kohro, Y., T. Matsuda, K. Yoshihara, K. Kohno, K. Koga, R. Katsuragi, T. Oka, R. Tashima, S. Muneta, T. Yamane, S. Okada, K. Momokino, A. Furusho, K. Hamase, T. Oti, H. Sakamoto, K. Hayashida, R. Kobayashi, T. Horii, I. Hatada, H. Tozaki-Saitoh, K. Mikoshiba, V. Taylor, K. Inoue, and M. Tsuda. 2020. Spinal astrocytes in superficial laminae gate brainstem descending control of mechanosensory hypersensitivity. *Nature Neuroscience*. 23:1376-1387.

Kozlov, A.S., M.C. Angulo, E. Audinat, and S. Charpak. 2006. Target cell-specific modulation of neuronal activity by astrocytes. *Proceedings of the National Academy of Sciences of the United States of America*. 103:10058-10063.

Krasilnikov, O.V., R.Z. Sabirov, and Y. Okada. 2011. ATP hydrolysis-dependent asymmetry of the conformation of CFTR channel pore. *Journal of Physiological Sciences*. 61:267-278.

Kreft, M., D. Križaj, S. Grilc, and R. Zorec. 2003. Properties of exocytotic response in vertebrate photoreceptors. *Journal of Neurophysiology*. 90:218-225.

Kreft, M., M. Stenovec, M. Rupnik, S. Grilc, M. Kržan, M. Potokar, T. Pangršič, P.G. Haydon, and R. Zorec. 2004. Properties of Ca^{2+}-dependent exocytosis in cultured astrocytes. *GLIA*. 46:437-445.

Kroemer, G., and M. Jaattela. 2005. Lysosomes and autophagy in cell death control. *Nat Rev Cancer*. 5:886-897.

Krugel, U., H. Kittner, H. Franke, and P. Illes. 2003. Purinergic modulation of neuronal activity in the mesolimbic dopaminergic system in vivo. *Synapse*. 47:134-142.

Krzan, M., M. Stenovec, M. Kreft, T. Pangršič, S. Grilc, P.G. Haydon, and R. Zorec. 2003. Calcium-dependent exocytosis of atrial natriuretic peptide from astrocytes. *Journal of Neuroscience*. 23:1580-1583.

Kudo, T., T. Kushikata, M. Kudo, T. Kudo, and K. Hirota. 2011. Antinociceptive effects of neurotropin in a rat model of central neuropathic pain: DSP-4 induced noradrenergic lesion. *Neuroscience Letters*. 503:20-22.

Kudo, T.T., T. Kushikata, M. Kudo, T.T. Kudo, and K. Hirota. 2010. A central neuropathic pain model by DSP-4 induced lesion of noradrenergic neurons: Preliminary report. *Neuroscience Letters*. 481:102-104.

Lacruz, R.S., and S. Feske. 2015. Diseases caused by mutations in ORAI1 and STIM1. *Annals of the New York Academy of Sciences*. 1356:45-79.

Lacy, P., and J.L. Stow. 2011. Cytokine release from innate immune cells: association with diverse membrane trafficking pathways. *Blood*. 118:9-18.

Lalisse, S., J. Hua, M. Lenoir, N. Linck, F. Rassendren, and L. Ulmann. 2018. Sensory neuronal P2RX4 receptors controls BDNF signaling in inflammatory pain. *Scientific Reports*. 8:964.

Laube, G., and H.G. Bernstein. 2017. Agmatine: multifunctional arginine metabolite and magic bullet in clinical neuroscience? *Biochem J*. 474:2619-2640.

Lazarowski, E.R. 2012. Vesicular and conductive mechanisms of nucleotide release. *Purinergic Signal*. 8:359-373.

Le Meur, K., J. Mendizabal-Zubiaga, P. Grandes, and E. Audinat. 2012. GABA release by hippocampal astrocytes. *Frontiers in Computational Neuroscience*. 6:59.

Lee, C.J., G. Mannaioni, H. Yuan, D.H. Woo, M.B. Gingrich, and S.F. Traynelis. 2007. Astrocytic control of synaptic NMDA receptors. *Journal of Physiology*. 581:1057-1081.

Lee, M., C. Schwab, and P.L. McGeer. 2011. Astrocytes are GABAergic cells that modulate microglial activity. *GLIA*. 59:152-165.

Lee, S., B.E. Yoon, K. Berglund, S.J. Oh, H. Park, H.S. Shin, G.J. Augustine, and C.J. Lee. 2010. Channel-mediated tonic GABA release from glia. *Science*. 330:790-796.

Lee, S.Y., and P.G. Haydon. 2011. A cytokine-dependent switch for glial-neuron interactions. *Neuron*. 69:835-837.

Lefèvre, Y., A. Amadio, P. Vincent, A. Descheemaeker, S.H.R. Oliet, R. Dallel, and D.L. Voisin. 2016. Effects of glia metabolism inhibition on nociceptive behavioral testing in rats. *Data in Brief*. 7:372-375.

Lewis, R.S. 2020. Store-Operated Calcium Channels: From Function to Structure and Back Again. *Cold Spring Harbor Perspectives in Biology*. 12:a035055-a035055.

Leybaert, L., K. Paemeleire, A. Strahonja, and M.J. Sanderson. 1998. Inositol-trisphosphate-dependent intercellular calcium signaling in and between astrocytes and endothelial cells. *GLIA*. 24:398-407.

Li, D., N. Ropert, A. Koulakoff, C. Giaume, and M. Oheim. 2008. Lysosomes are the major vesicular compartment undergoing Ca 2+-regulated exocytosis from cortical astrocytes. *Journal of Neuroscience*. 28:7648-7658.

Li, J.X., D.A. Thorn, Y. Qiu, B.W. Peng, and Y. Zhang. 2014. Antihyperalgesic effects of imidazoline I2 receptor ligands in rat models of inflammatory and neuropathic pain. *British Journal of Pharmacology*. 171:1580-1590.

Lima, D., and A. Coimbra. 1986. A Golgi study of the neuronal population of the marginal zone (lamina I) of the rat spinal cord. *Journal of Comparative Neurology*. 244:53-71.

Linsdell, P., and J.W. Hanrahan. 1998. Adenosine triphosphate-dependent asymmetry of anion permeation in the cystic fibrosis transmembrane conductance regulator chloride channel. *Journal of General Physiology*. 111:601-614.

Liu, J.G., and K.J. Anand. 2001. Protein kinases modulate the cellular adaptations associated with opioid tolerance and dependence. *Brain Res Brain Res Rev*. 38:1-19.

Liu, R.H., and Z.Q. Zhao. 1992. Selective blockade by yohimbine of descending spinal inhibition from lateral reticular nucleus but not from locus coeruleus in rats. *Neuroscience Letters*. 142:65-68.

Liu, T., L. Sun, Y. Xiong, S. Shang, N. Guo, S. Teng, Y. Wang, B. Liu, C. Wang, L. Wang, L. Zheng, C.X. Zhang, W. Han, and Z. Zhou. 2011. Calcium triggers exocytosis from two types of organelles in a single astrocyte. *Journal of Neuroscience*. 31:10593-10601.

Liu, Y., R.r. Liu, L. Wang, L. Zeng, Z.y. Long, and Y.m. Wu. 2012. The effects of different phenotype astrocytes on neural stem cells differentiation in co-culture. *Neuroscience Letters*. 508:61-66.

Llorca-Torralba, M., G. Borges, F. Neto, J.A. Mico, and E. Berrocoso. 2016. Noradrenergic Locus Coeruleus pathways in pain modulation. *Neuroscience*. 338:93-113.

Locovei, S., E. Scemes, F. Qiu, D.C. Spray, and G. Dahl. 2007. Pannexin1 is part of the pore forming unit of the P2X7 receptor death complex. *FEBS Letters*. 581:483-488.

Locovei, S., J. Wang, and G. Dahl. 2006. Activation of pannexin 1 channels by ATP through P2Y receptors and by cytoplasmic calcium. *FEBS Letters*. 580:239-244.

Lopez, W., J. Ramachandran, A. Alsamarah, Y. Luo, A.L. Harris, and J.E. Contreras. 2016. Mechanism of gating by calcium in connexin hemichannels. *Proceedings of the National Academy of Sciences of the United States of America*. 113:E7986-E7995.

Loprinzi, C.L., B.N. Reeves, S.R. Dakhil, J.A. Sloan, S.L. Wolf, K.N. Burger, A. Kamal, N.A. Le-Lindqwister, G.S. Soori, A.J. Jaslowski, P.J. Novotny, and D.H. Lachance. 2011. Natural history of paclitaxel-associated acute pain syndrome: prospective cohort study NCCTG N08C1. *J Clin Oncol*. 29:1472-1478.

Loughlin, S.E., S.L. Foote, and F.E. Bloom. 1986. Efferent projections of nucleus locus coeruleus: topographic organization of cells of origin demonstrated by three-dimensional reconstruction. *Neuroscience*. 18:291-306.

Lu, G.W., and W.D. Willis. 1999. Branching and/or collateral projections of spinal dorsal horn neurons. *Brain Research Reviews*. 29:50-82.

Lu, Y., and E.R. Perl. 2003. A specific inhibitory pathway between substantia gelatinosa neurons receiving direct C-fiber input. *Journal of Neuroscience*. 23:8752-8758.

Lyons, W.E., J.M. Fritschy, and R. Grzanna. 1989. The noradrenergic neurotoxin DSP-4 eliminates the coeruleospinal projection but spares projections of the A5 and A7 groups to the ventral horn of the rat spinal cord. *J Neurosci*. 9:1481-1489.

Ma, W., and R. Quirion. 2002. Partial sciatic nerve ligation induces increase in the phosphorylation of extracellular signal-regulated kinase (ERK) and c-Jun N-terminal kinase (JNK) in astrocytes in the lumbar spinal dorsal horn and the gracile nucleus. *Pain*. 99:175-184.

Mackie, M., D.I. Hughes, D.J. Maxwell, N.J.K. Tillakaratne, and A.J. Todd. 2003. Distribution and colocalisation of glutamate decarboxylase isoforms in the rat spinal cord. *Neuroscience*. 119:461-472.

MacKinnon, C.D. 2018. Sensorimotor anatomy of gait, balance, and falls. *In* Handbook of Clinical Neurology.

Maeda, M., M. Tsuruoka, B. Hayashi, I. Nagasawa, and T. Inoue. 2009. Descending pathways from activated locus coeruleus/subcoeruleus following unilateral hindpaw inflammation in the rat. *Brain Research Bulletin*. 78:170-174.

Maienschein, V., M. Marxen, W. Volknandt, and H. Zimmermann. 1999. A plethora of presynaptic proteins associated with ATP-storing organelles in cultured astrocytes. *Glia*. 26:233-244.

Malmberg, A.B., C. Chen, S. Tonegawa, and A.I. Basbaum. 1997. Preserved acute pain and reduced neuropathic pain in mice lacking PKCγ. *Science*. 278:279-283.

Marchaland, J., C. Calì, S.M. Voglmaier, H. Li, R. Regazzi, R.H. Edwards, and P. Bezzi. 2008. Fast subplasma membrane Ca^{2+} transients control exo-endocytosis of synaptic-like microvesicles in astrocytes. *Journal of Neuroscience*. 28:9122-9132.

Marieb, E.N., and K. Hoehn. 2010. Human Anatomy & Physiology. Pearson Education, San Francisco.

Martin, S.C., and T.J. Shuttleworth. 1994. Ca^{2+} influx drives agonist-activated $[Ca^{2+}]i$ oscillations in an exocrine cell. *FEBS Letters*. 352:32-36.

Martin, W.J., N.K. Gupta, C.M. Loo, D.S. Rohde, and A.I. Basbaum. 1999. Differential effects of neurotoxic destruction of descending noradrenergic pathways on acute and persistent nociceptive processing. *Pain*. 80:57-65.

Mason, M.J., M.P. Mahaut-Smith, and S. Grinstein. 1991. The role of intracellular Ca^{2+} in the regulation of the plasma membrane Ca^{2+} permeability of unstimulated rat lymphocytes. *J Biol Chem*. 266:10872-10879.

Mason, S.T., and H.C. Fibiger. 1979. Regional topography within noradrenergic locus coeruleus as revealed by retrograde transport of horseradish peroxidase. *Journal of Comparative Neurology*. 187:703-724.

Masuda, T., Y. Ozono, S. Mikuriya, Y. Kohro, H. Tozaki-Saitoh, K. Iwatsuki, H. Uneyama, R. Ichikawa, M.W. Salter, M. Tsuda, and K. Inoue. 2016. Dorsal horn neurons release extracellular ATP in a VNUT-dependent manner that underlies neuropathic pain. *Nature Communications*. 7:12529.

McCarthy, K.D., and A.K. Salm. 1991. Pharmacologically-distinct subsets of astroglia can be identified by their calcium response to neuroligands. *Neuroscience*. 41:325-333.

McGrath, P.A. 1994. Psychological aspects of pain perception. *Archives of Oral Biology*. 39 Suppl:55S-62S.

Medina-Ceja, L., F. Villalpando-Vargas, G.I. Girón de la Cruz, A.M. Lara- Vazquez, L. Flores-Mancilla, J.C. Salazar-Sánchez, and A. Morales-Villagrán. 2019. Effect of Chronic Krill Oil Supplement on Seizures Induced by Pentylenetetrazole in the Hippocampus of Adult Rats with Previous Febrile Seizures. *Journal of Food Science*. 84:1703-1711.

Meller, S.T., C. Dykstra, D. Grzybycki, S. Murphy, and G.F. Gebhart. 1994. The possible role of glia in nociceptive processing and hyperalgesia in the spinal cord of the rat. *Neuropharmacology*. 33:1471-1478.

Merritt, J.E., W.P. Armstrong, C.D. Benham, T.J. Hallam, R. Jacob, A. Jaxa-Chamiec, B.K. Leigh, S.A. McCarthy, K.E. Moores, and T.J. Rink. 1990. SK&F 96365, a novel inhibitor of receptor-mediated calcium entry. *Biochem J*. 271:515-522.

Mignen, O., and T.J. Shuttleworth. 2000. I(ARC), a novel arachidonate-regulated, noncapacitative Ca^{2+} entry channel. *Journal of Biological Chemistry*. 275:9114-9119.

Mika, J., M. Zychowska, K. Popiolek-Barczyk, E. Rojewska, and B. Przewlocka. 2013. Importance of glial activation in neuropathic pain. *Eur J Pharmacol*. 716:106-119.

Millan, M.J. 1999. The induction of pain: an integrative review. *Prog Neurobiol*. 57:1-164.

Millan, M.J. 2002. Descending control of pain. *Prog Neurobiol*. 66:355-474.

Miller, K.E., E.M. Hoffman, M. Sutharshan, and R. Schechter. 2011. Glutamate pharmacology and metabolism in peripheral primary afferents: physiological and pathophysiological mechanisms. *Pharmacol Ther*. 130:283-309.

Miyoshi, K., K. Obata, T. Kondo, H. Okamura, and K. Noguchi. 2008. Interleukin-18-mediated microglia/astrocyte interaction in the spinal cord enhances neuropathic pain processing after nerve injury. *Journal of Neuroscience*. 28:12775-12787.

Mizukami, T. 2004. Immunocytochemical Localization of β2-Adrenergic Receptors in the Rat Spinal Cord and Their Spatial Relationships to Tyrosine Hydroxylase-immunoreactive Terminals. *Kurume Medical Journal*. 51:175-183.

Molderings, G.J., K. Donecker, M. Burian, W.A. Simon, D.W. Schroder, and M. Gothert. 1998. Characterization of I2 imidazoline and sigma binding sites in the rat and human stomach. *J Pharmacol Exp Ther*. 285:170-177.

Molderings, G.J., K. Donecker, and M. Gothert. 1995a. Characterization of non-adrenergic [3H]clonidine binding sites in rat stomach: high affinity of imidazolines, guanidines and sigma ligands. *Naunyn Schmiedebergs Arch Pharmacol*. 351:561-564.

Molderings, G.J., and B. Haenisch. 2012. Agmatine (decarboxylated L-arginine): physiological role and therapeutic potential. *Pharmacol Ther*. 133:351-365.

Molderings, G.J., K. Ruppert, H. Bonisch, and M. Gothert. 1995b. No relationship of I1- and I2-imidazoline binding sites to inhibitory effects of imidazolines on ligand-gated ion channels. An investigation in the adrenal medulla and in neuroblastoma cells. *Ann N Y Acad Sci*. 763:420-432.

Moneer, Z., I. Pino, E.J. Taylor, L.M. Broad, Y. Liu, S.C. Tovey, L. Staali, and C.W. Taylor. 2005. Different phospholipase-C-coupled receptors differentially regulate capacitative and non-capacitative Ca^{2+} entry in A7r5 cells. *Biochem J*. 389:821-829.

Monroe, P.J., D.L. Smith, H.R. Kirk, and D.J. Smith. 1995. Spinal nonadrenergic imidazoline receptors do not mediate the antinociceptive action of intrathecal clonidine in the rat. *Journal of Pharmacology and Experimental Therapeutics*.

Montana, V., Y. Ni, V. Sunjara, X. Hua, and V. Parpura. 2004. Vesicular glutamate transporter-dependent glutamate release from astrocytes. *The Journal of neuroscience : the official journal of the Society for Neuroscience*. 24:2633-2642.

Morandini, A.C., L.E. Savio, and R. Coutinho-Silva. 2014. The role of P2X7 receptor in infectious inflammatory diseases and the influence of ectonucleotidases. *Biomed J*. 37:169-177.

Mori, M., C. Heuss, B.H. Gähwiler, and U. Gerber. 2001. Fast synaptic transmission mediated by P2X receptors in CA3 pyramidal cells of rat hippocampal slice cultures. *Journal of Physiology*. 535:115-123.

Moriyama, Y., M. Hiasa, S. Sakamoto, H. Omote, and M. Nomura. 2017. Vesicular nucleotide transporter (VNUT): appearance of an actress on the stage of purinergic signaling. *Purinergic Signalling*. 13:387-404.

Mothet, J.P., L. Pollegioni, G. Ouanounou, M. Martineau, P. Fossier, and G. Baux. 2005. Glutamate receptor activation triggers a calcium-dependent and SNARE protein-dependent release of the gliotransmitter D-serine. *Proceedings of the National Academy of Sciences of the United States of America*. 102:5606-5611.

Murray, R.Z., and J.L. Stow. 2014. Cytokine Secretion in Macrophages: SNAREs, Rabs, and Membrane Trafficking. *Front Immunol*. 5:538.

Musgrave, I.F., D. Krautwurst, and G. Schultz. 1996. Imidazoline binding sites and signal transduction pathways. *Clin Exp Pharmacol Physiol*. 23:990-994.

Muyderman, H., E. Hansson, and M. Nilsson. 1997. Adrenoceptor-induced changes of intracellular K+ and Ca^{2+} in astrocytes and neurons in rat cortical primary cultures. *Neuroscience Letters*. 238:33-36.

Nakagawa, T., and S. Kaneko. 2010. Spinal astrocytes as therapeutic targets for pathological pain. *J Pharmacol Sci*. 114:347-353.

Nakagawa, T., K. Wakamatsu, N. Zhang, S. Maeda, M. Minami, M. Satoh, and S. Kaneko. 2007. Intrathecal administration of ATP produces long-lasting allodynia in rats: Differential mechanisms in the phase of the induction and maintenance. *Neuroscience*. 147:445-455.

Nakatsuka, T., J.S. Park, E. Kumamoto, T. Tamaki, and M. Yoshimura. 1999. Plastic changes in sensory inputs to rat substantia gelatinosa neurons following peripheral inflammation. *Pain*. 82:39-47.

Nayak, D., T.L. Roth, and D.B. McGavern. 2014. Microglia development and function. *Annu Rev Immunol*. 32:367-402.

Nedergaard, M., B. Ransom, and S.A. Goldman. 2003. New roles for astrocytes: redefining the functional architecture of the brain. *Trends Neurosci*. 26:523-530.

Nicholas, M., J.W.S. Vlaeyen, W. Rief, A. Barke, Q. Aziz, R. Benoliel, M. Cohen, S. Evers, M.A. Giamberardino, A. Goebel, B. Korwisi, S. Perrot, P. Svensson, S.J. Wang, and R.D. Treede. 2019. The IASP classification of chronic pain for ICD-11: Chronic primary pain. *Pain*. 160:28-37.

Nikolic, K., and D. Agbaba. 2012. Imidazoline antihypertensive drugs: selective i(1) -imidazoline receptors activation. *Cardiovasc Ther*. 30:209-216.

Nilsson, M., E. Hansson, and L. Ronnback. 1992. Agonist-evoked Ca^{2+} transients in primary astroglial cultures--modulatory effects of valproic acid. *Glia*. 5:201-209.

Nomura, T., A. Taruno, M. Shiraishi, T. Nakahari, T. Inui, M. Sokabe, D.C. Eaton, and Y. Marunaka. 2017. Current-direction/amplitude-dependent single channel gating kinetics of mouse pannexin 1 channel: A new concept for gating kinetics. *Scientific Reports*. 7:10512.

North, R.A. 2002. Molecular physiology of P2X receptors. *Physiol Rev*. 82:1013-1067.

North, R.A., and M. Yoshimura. 1984. The actions of noradrenaline on neurones of the rat substantia gelatinosa in vitro. *The Journal of Physiology*. 349:43-55.

Oberheim, N.A., T. Takano, X. Han, W. He, J.H.C. Lin, F. Wang, Q. Xu, J.D. Wyatt, W. Pilcher, J.G. Ojemann, B.R. Ransom, S.A. Goldman, and M. Nedergaard. 2009. Uniquely Hominid Features of Adult Human Astrocytes *The Journal of Neuroscience*.

Oberheim, N.A., X. Wang, S. Goldman, and M. Nedergaard. 2006. Astrocytic complexity distinguishes the human brain. *Trends in Neurosciences*. 29:547-553.

Oe, Y., X. Wang, T. Patriarchi, A. Konno, K. Ozawa, K. Yahagi, H. Hirai, L. Tian, T.J. McHugh, and H. Hirase. 2020. Distinct temporal integration of noradrenaline signaling by astrocytic second messengers during vigilance. *Nature Communications*. 11:471.

Okada-Ogawa, A., I. Suzuki, B.J. Sessle, C.Y. Chiang, M.W. Salter, J.O. Dostrovsky, Y. Tsuboi, M. Kondo, J. Kitagawa, A. Kobayashi, N. Noma, Y. Imamura, and K. Iwata. 2009. Astroglia in medullary dorsal horn (trigeminal spinal subnucleus caudalis) are involved in trigeminal neuropathic pain mechanisms. *Journal of Neuroscience*. 29:11161-11171.

Ong, H.L., K.P. Subedi, G.Y. Son, X. Liu, and I.S. Ambudkar. 2019. Tuning store-operated calcium entry to modulate Ca(2+)-dependent physiological processes. *Biochim Biophys Acta Mol Cell Res*. 1866:1037-1045.

Ormel, L., M.J. Stensrud, F.A. Chaudhry, and V. Gundersen. 2012. A distinct set of synaptic-like microvesicles in atroglial cells contain VGLUT3. *GLIA*. 60:1289-1300.

Osiri, M., B. Shea, V. Welch, M.E. Suarez-Almazor, V. Strand, P. Tugwell, and G.A. Wells. 2009. Leflunomide for the treatment of rheumatoid arthritis. *The Cochrane database of systematic reviews*:CD002047.

Ossipov, M.H., T.K. Chatterjee, and G.F. Gebhart. 1985. Locus coeruleus lesions in the rat enhance the antinociceptive potency of centrally administered clonidine but not morphine. *Brain Research*. 341:320-330.

Ossipov, M.H., K. Morimura, and F. Porreca. 2014. Descending pain modulation and chronification of pain. *Curr Opin Support Palliat Care*. 8:143-151.

Oya, M., T. Kitaguchi, Y. Yanagihara, R. Numano, M. Kakeyama, K. Ikematsu, and T. Tsuboi. 2013. Vesicular nucleotide transporter is involved in ATP storage of secretory lysosomes in astrocytes. *Biochemical and Biophysical Research Communications*. 438:145-151.

Ozaita, A., G. Olmos, M.A. Boronat, J.M. Lizcano, M. Unzeta, and J.A. Garcia-Sevilla. 1997. Inhibition of monoamine oxidase A and B activities by imidazol(ine)/guanidine drugs, nature of the interaction and distinction from I2-imidazoline receptors in rat liver. *Br J Pharmacol*. 121:901-912.

Paco, S., M.A. Margelí, V.M. Olkkonen, A. Imai, J. Blasi, R. Fischer-Colbrie, and F. Aguado. 2009. Regulation of exocytotic protein expression and Ca^{2+}-dependent peptide secretion in astrocytes. *Journal of Neurochemistry*. 110:143-156.

Palty, R., A. Raveh, I. Kaminsky, R. Meller, and E. Reuveny. 2012. SARAF inactivates the store operated calcium entry machinery to prevent excess calcium refilling. *Cell*. 149:425-438.

Pan, Y.Z., D.P. Li, and H.L. Pan. 2002. Inhibition of glutamatergic synaptic input to spinal lamina IIo neurons by presynaptic α2-adrenergic receptors. *Journal of Neurophysiology*. 87:1938-1947.

Panchina, Y., I. Kelmanson, M. Matz, K. Lukyanov, N. Usman, and S. Lukyanov. 2000. A ubiquitous family of putative gap junction molecules [2]. *Current Biology*. 10:R473-R474.

Pankratov, Y., and U. Lalo. 2015. Role for astroglial α1-adrenoreceptors in gliotransmission and control of synaptic plasticity in the neocortex. *Frontiers in Cellular Neuroscience*. 9:230.

Papay, R., R. Gaivin, A. Jha, D.F. McCune, J.C. McGrath, M.C. Rodrigo, P.C. Simpson, V.A. Doze, and D.M. Perez. 2006. Localization of the mouse α 1A-adrenergic receptor (AR) in the brain: α 1AAR is expressed in neurons, GABAergic interneurons, and NG2 oligodendrocyte progenitors. *Journal of Comparative Neurology*. 497:209-222.

Papay, R., R. Gaivin, D.F. McCune, B.R. Rorabaugh, W.B. Macklin, J.C. McGrath, and D.M. Perez. 2004. Mouse α1B-adrenergic receptor is expressed in neurons and NG2 oligodendrocytes. *Journal of Comparative Neurology*. 478:1-10.

Parekh, A.B. 2010. Store-operated CRAC channels: function in health and disease. *Nat Rev Drug Discov*. 9:399-410.

Parekh, A.B., A. Fleig, and R. Penner. 1997. The store-operated calcium current I(CRAC): Nonlinear activation by InsP3 and dissociation from calcium release. *Cell*. 89:973-980.

Paris, A., and P.H. Tonner. 2005. Dexmedetomidine in anaesthesia. *Curr Opin Anaesthesiol*. 18:412-418.

Parpura, V., T.A. Basarsky, F. Liu, K. Jeftinija, S. Jeftinija, and P.G. Haydon. 1994. Glutamate-mediated astrocyte-neuron signalling. *Nature*. 369:744-747.

Parpura, V., Y. Fang, T. Basarsky, R. Jahn, and P.G. Haydon. 1995. Expression of synaptobrevin II, cellubrevin and syntaxin but not SNAP-25 in cultured astrocytes. *FEBS Letters*. 377:489-492.

Pascual, O., K.B. Casper, C. Kubera, J. Zhang, R. Revilla-Sanchez, J.Y. Sul, H. Takano, S.J. Moss, K. McCarthy, and P.G. Haydon. 2005. Neurobiology: Astrocytic purinergic signaling coordinates synaptic networks. *Science*. 310:113-116.

Peferoen, L., M. Kipp, P. van der Valk, J.M. van Noort, and S. Amor. 2014. Oligodendrocyte-microglia cross-talk in the central nervous system. *Immunology*. 141:302-313.

Peirs, C., S.P.G. Williams, X. Zhao, C.E. Walsh, J.Y. Gedeon, N.E. Cagle, A.C. Goldring, H. Hioki, Z. Liu, P.S. Marell, and R.P. Seal. 2015. Dorsal Horn Circuits for Persistent Mechanical Pain. *Neuron*. 87:797-812.

Pertovaara, A. 2006. Noradrenergic pain modulation. *Prog Neurobiol*. 80:53-83.

Pertovaara, A. 2013. The noradrenergic pain regulation system: A potential target for pain therapy. *Eur J Pharmacol*. 716:2-7.

Philips, T., and J.D. Rothstein. 2017. Oligodendroglia: Metabolic supporters of neurons. *J Clin Invest*. 127:3271-3280.

Pickel, V.M., M. Segal, and F.E. Bloom. 1974. A radioautographic study of the efferent pathways of the nucleus locus coeruleus. *Journal of Comparative Neurology*. 155:15-42.

Piguet, P., and R. Schlichter. 1998. Lability of the pacemaker activity in the rat rostro-ventrolateral medulla: effects of noradrenaline. *Brain Res*. 796:1-12.

Polgár, E., D.I. Hughes, J.S. Riddell, D.J. Maxwell, Z. Puskár, and A.J. Todd. 2003. Selective loss of spinal GABAergic or glycinergic neurons is not necessary for development of thermal hyperalgesia in the chronic constriction injury model of neuropathic pain. *Pain*. 104:229-239.

Polgár, E., S.A.S. Shehab, C. Watt, and A.J. Todd. 1999. GABAergic neurons that contain neuropeptide Y selectively target cells with the neurokinin I receptor in laminae III and IV of the rat spinal cord. *Journal of Neuroscience*. 19:2637-2646.

Potokar, M., M. Stenovec, M. Gabrijel, L. Li, M. Kreft, S. Grilc, M. Pekny, and R. Zorec. 2010. Intermediate filaments attenuate stimulation-dependent mobility of endosomes/lysosomes in astrocytes. *GLIA*. 58:1208-1219.

Potokar, M., M. Stenovec, M. Kreft, M.E. Kreft, and R. Zorec. 2008. Stimulation inhibits the mobility of recycling peptidergic vesicles in astrocytes. *GLIA*. 56:135-144.

Prakriya, M., and R.S. Lewis. 2015. Store-Operated Calcium Channels. *Physiological Reviews*. 95:1383-1436.

Prato, V., F.J. Taberner, J.R.F. Hockley, G. Callejo, A. Arcourt, B. Tazir, L. Hammer, P. Schad, P.A. Heppenstall, E.S. Smith, and S.G. Lechner. 2017. Functional and Molecular Characterization of Mechanoinsensitive "Silent" Nociceptors. *Cell Reports*. 21:3102-3115.

Prell, G.D., G.P. Martinelli, G.R. Holstein, J. Matulic-Adamic, K.A. Watanabe, S.L. Chan, N.G. Morgan, M.A. Haxhiu, and P. Ernsberger. 2004. Imidazoleacetic acid-ribotide: an endogenous ligand that stimulates imidazol(in)e receptors. *Proc Natl Acad Sci U S A*. 101:13677-13682.

Putney, J.W. 2018. Forms and functions of store-operated calcium entry mediators, STIM and Orai. *Adv Biol Regul*. 68:88-96.

Putney, J.W., N. Steinckwich-Besançon, T. Numaga-Tomita, F.M. Davis, P.N. Desai, D.M. D'Agostin, S. Wu, and G.S. Bird. 2017. The functions of store-operated calcium channels. *Biochimica et Biophysica Acta (BBA) - Molecular Cell Research*. 1864:900-906.

Raddatz, R., A. Parini, and S.M. Lanier. 1995. Imidazoline/guanidinium binding domains on monoamine oxidases. Relationship to subtypes of imidazoline-binding proteins and tissue-specific interaction of imidazoline ligands with monoamine oxidase B. *J Biol Chem*. 270:27961-27968.

Raddatz, R., S.L. Savic, and S.M. Lanier. 1999. Imidazoline binding domains on MAO-B. Localization and accessibility. *Ann N Y Acad Sci*. 881:26-31.

Rahman, S., and T. Rahman. 2017. Unveiling some FDA-Approved drugs as inhibitors of the store-operated Ca^{2+} entry pathway. *Scientific Reports*. 7:12881.

Rahn, E.J., L. Deng, G.A. Thakur, K. Vemuri, A.M. Zvonok, Y.Y. Lai, A. Makriyannis, and A.G. Hohmann. 2014. Prophylactic cannabinoid administration blocks the development of paclitaxel-induced neuropathic nociception during analgesic treatment and following cessation of drug delivery. *Molecular Pain*. 10:27.

Rajaofetra, N., J.L. Ridet, P. Poulat, L. Marlier, F. Sandillon, M. Geffard, and A. Privat. 1992. Immunocytochemical mapping of noradrenergic projections to the rat spinal cord with an antiserum against noradrenaline. *Journal of Neurocytology*. 21:481-494.

Rangel-Gonzalez, F.J., J. Garcia-Colunga, and R. Miledi. 2002. Inhibition of neuronal nicotinic acetylcholine receptors by La(3+). *Eur J Pharmacol*. 441:15-21.

Reddy, S.V.R., J.L. Maderdrut, and T.L. Yaksh. 1980. Spinal cord pharmacology of adrenergic agonist-mediated antinociception. *Journal of Pharmacology and Experimental Therapeutics*. 213:525-533.

Reeve, A.J., S. Patel, A. Fox, K. Walker, and L. Urban. 2000. Intrathecally administered endotoxin or cytokines produce allodynia, hyperalgesia and changes in spinal cord neuronal responses to nociceptive stimuli in the rat. *European Journal of Pain*. 4:247-257.

Reeves, B.N., S.R. Dakhil, J.A. Sloan, S.L. Wolf, K.N. Burger, A. Kamal, N.A. Le-Lindqwister, G.S. Soori, A.J. Jaslowski, J. Kelaghan, P.J. Novotny, D.H. Lachance, and C.L. Loprinzi. 2012. Further data supporting that paclitaxel-associated acute pain syndrome is associated with development of peripheral neuropathy: North Central Cancer Treatment Group trial N08C1. *Cancer*. 118:5171-5178.

Regunathan, S. 2006. Agmatine: Biological role and therapeutic potentials in morphine analgesia and dependence. *AAPS J*. 8:E479-484.

Regunathan, S., D. Dozier, R. Takkalapalli, and W.J. Phillips. 2009. Agmatine levels in the cerebrospinal fluid of normal human volunteers. *J Pain Palliat Care Pharmacother*. 23:35-39.

Regunathan, S., D.L. Feinstein, W. Raasch, and D.J. Reis. 1995. Agmatine (decarboxylated arginine) is synthesized and stored in astrocytes. *Neuroreport*. 6:1897-1900.

Regunathan, S., D.L. Feinstein, and D.J. Reis. 1993. Expression of non-adrenergic imidazoline sites in rat cerebral cortical astrocytes. *J Neurosci Res*. 34:681-688.

Regunathan, S., and D.J. Reis. 1996. Imidazoline receptors and their endogenous ligands. *Annu Rev Pharmacol Toxicol*. 36:511-544.

Reichling, D.B., and A.B. MacDermott. 1991. Lanthanum actions on excitatory amino acid-gated currents and voltage-gated calcium currents in rat dorsal horn neurons. *J Physiol*. 441:199-218.

Reisin, I.L., A.G. Prat, E.H. Abraham, J.F. Amara, R.J. Gregory, D.A. Ausiello, and H.F. Cantiello. 1994. The cystic fibrosis transmembrane conductance regulator is a dual ATP and chloride channel. *Journal of Biological Chemistry*.

Ren, K., and R. Dubner. 2008. Neuron-glia crosstalk gets serious: Role in pain hypersensitivity. *Curr Opin Anaesthesiol*. 21:570-579.

Rhee, J.S., Z.M. Wang, J. Nabekura, K. Inoue, and N. Akaike. 2000. ATP facilitates spontaneous glycinergic IPSC frequency at dissociated rat dorsal horn interneuron synapses. *Journal of Physiology*. 524 Pt 2:471-483.

Ribeiro-da-Silva, A., and Y. De Koninck. 2008. Morphological and Neurochemical Organization of the Spinal Dorsal Horn. *In* The Senses: A Comprehensive Reference. 279-310.

Richardson, P.J., and S.J. Brown. 1987. ATP Release from Affinity-Purified Rat Cholinergic Nerve Terminals. *Journal of Neurochemistry*. 48:622-630.

Ridet, J.L., N. Rajaofetra, J.R. Teilhac, M. Geffard, and A. Privat. 1993. Evidence for nonsynaptic serotonergic and noradrenergic innervation of the rat dorsal horn and possible involvement of neuron-glia interactions. *Neuroscience*. 52:143-157.

Ritz, L.A., and J.D. Greenspan. 1985. Morphological features of lamina V neurons receiving nociceptive input in cat sacrocaudal spinal cord. *Journal of Comparative Neurology*. 238:440-452.

Roerig, S.C. 2003. Spinal and Supraspinal Agmatine Activate Different Receptors to Enhance Spinal Morphine Antinociception. *In* Annals of the New York Academy of Sciences Vol. 1009. 116–126.

Roerig, S.C., S. Lei, K. Kitto, J.K.L. Hylden, and G.L. Wilcox. 1992. Spinal interactions between opioid and noradrenergic agonists in mice: Multiplicativity involves delta and alpha-2 receptors. *Journal of Pharmacology and Experimental Therapeutics*.

Roman, R.M., N. Lomri, G. Braunstein, A.P. Feranchak, L.A. Simeoni, A.K. Davison, E. Mechetner, E.M. Schwiebert, and J.G. Fitz. 2001. Evidence for multidrug resistance-1 P-glycoprotein-dependent regulation of cellular ATP permeability. *Journal of Membrane Biology*. 183:165-173.

Romanov, R.A., M.F. Bystrova, O.A. Rogachevskaya, V.B. Sadovnikov, V.I. Shestopalov, and S.S. Kolesnikov. 2012. The ATP permeability of pannexin 1 channels in a heterologous system and in mammalian taste cells is dispensable. *Journal of Cell Science*. 125:5514-5523.

Roux, L., A. Madar, M.M. Lacroix, C. Yi, K. Benchenane, and C. Giaume. 2015. Astroglial connexin 43 hemichannels modulate olfactory bulb slow oscillations. *Journal of Neuroscience*. 35:15339-15352.

Rovati, L.C., N. Brambilla, T. Blicharski, J. Connell, C. Vitalini, A. Bonazzi, G. Giacovelli, F. Girolami, and M. D'Amato. 2020. Efficacy and safety of the first-in-class imidazoline-2 receptor ligand CR4056 in pain from knee osteoarthritis and disease phenotypes: a randomized, double-blind, placebo-controlled phase 2 trial. *Osteoarthritis and Cartilage*. 28:22-30.

Rupnik, M., M. Kreft, S.K. Sikdar, S. Grilc, R. Romih, G. Zupančič, T.F.J. Martin, and R. Zorec. 2000. Rapid regulated dense-core vesicle exocytosis requires the CAPS protein. *Proceedings of the National Academy of Sciences of the United States of America*. 97:5627-5632.

Sahlender, D.A., I. Savtchouk, and A. Volterra. 2014. What do we know about gliotransmitter release from astrocytes? *Philos Trans R Soc Lond B Biol Sci*. 369:20130592.

Sakaba, T. 2008. Two Ca^{2+}-Dependent Steps Controlling Synaptic Vesicle Fusion and Replenishment at the Cerebellar Basket Cell Terminal. *Neuron*. 57:406-419.

Sakamoto, S., T. Miyaji, M. Hiasa, R. Ichikawa, A. Uematsu, K. Iwatsuki, A. Shibata, H. Uneyama, R. Takayanagi, A. Yamamoto, H. Omote, M. Nomura, and Y. Moriyama. 2014. Impairment of vesicular ATP release affects glucose metabolism and increases insulin sensitivity. *Scientific Reports*. 4:6689.

Sakuragi, S., F. Niwa, Y. Oda, K. Mikoshiba, and H. Bannai. 2017. Astroglial Ca^{2+} signaling is generated by the coordination of IP_3R and store-operated Ca^{2+} channels. *Biochemical and Biophysical Research Communications*. 486:879-885.

Sala, E., F. Ferrari, M. Lanza, C. Milia, C. Sabatini, A. Bonazzi, E. Comi, M. Borsi Franchini, G. Caselli, and L.C. Rovati. 2020. Improved efficacy, tolerance, safety, and abuse liability profile of the combination of CR4056 and morphine over morphine alone in rodent models. *British Journal of Pharmacology*. 177:3291-3308.

Salm, A.K., and K.D. McCarthy. 1990. Norepinephrine-evoked calcium transients in cultured cerebral type 1 astroglia. *Glia*. 3:529-538.

Sanchez-Blazquez, P., M.A. Boronat, G. Olmos, J.A. Garcia-Sevilla, and J. Garzon. 2000. Activation of I(2)-imidazoline receptors enhances supraspinal morphine analgesia in mice: a model to detect agonist and antagonist activities at these receptors. *Br J Pharmacol*. 130:146-152.

Sasa, M., K. Munekiyo, Y. Osumi, and S. Takaori. 1977. Attenuation of morphine analgesia in rats with lesions of the locus coeruleus and dorsal raphe nucleus. *European Journal of Pharmacology*. 42:53-62.

Satoh, K., A. Kashiba, H. Kimura, and T. Maeda. 1982. Noradrenergic axon terminals in the substantia gelatinosa of the rat spinal cord: an electron-microscopic study using glyoxylic acid-potassium permanganate fixation. *Cell Tissue Res*. 222:359-378.

Sawada, M., H. Sawada, and T. Nagatsu. 2008. Effects of aging on neuroprotective and neurotoxic properties of microglia in neurodegenerative diseases. *Neurodegenerative Diseases*. 5:254-256.

Sawynok, J., and A. Reid. 1986. Role of ascending and descending noradrenergic pathways in the antinociceptive effect of baclofen and clonidine. *Brain Research*. 386:341-350.

Schneggenburger, R., and E. Neher. 2000. Intracellular calcium dependence of transmitter release rates at a fast central synapse. *Nature*. 406:889-893.

Schneider, S.P. 1992. Functional properties and axon terminations of interneurons in laminae III-V of the mammalian spinal dorsal horn in vitro. *Journal of Neurophysiology*. 68:1746-1759.

Schneider, S.P. 2005. Mechanosensory afferent input and neuronal firing properties in rodent spinal laminae III-V: Re-examination of relationships with analysis of responses to static and time-varying stimuli. *Brain Research*. 1034:71-89.

Schneider, S.P., and T.M. Walker. 2007. Morphology and electrophysiological properties of hamster spinal dorsal horn neurons that express VGLUT2 and enkephalin. *Journal of Comparative Neurology*. 501:790-809.

Scholz, J., and C.J. Woolf. 2007. The neuropathic pain triad: Neurons, immune cells and glia. *Nat Neurosci*. 10:1361-1368.

Schwarz, L.A., K. Miyamichi, X.J. Gao, K.T. Beier, B. Weissbourd, K.E. Deloach, J. Ren, S. Ibanes, R.C. Malenka, E.J. Kremer, and L. Luo. 2015. Viral-genetic tracing of the input-output organization of a central noradrenaline circuit. *Nature*. 524:88-92.

Schwiebert, E.M. 1999. ABC transporter-facilitated ATP conductive transport. *Am J Physiol*. 276:C1-8.

Seal, R.P., X. Wang, Y. Guan, S.N. Raja, C.J. Woodbury, A.I. Basbaum, and R.H. Edwards. 2009. Injury-induced mechanical hypersensitivity requires C-low threshold mechanoreceptors. *Nature*. 462:651-655.

Seibt, F., and R. Schlichter. 2015. Noradrenaline-mediated facilitation of inhibitory synaptic transmission in the dorsal horn of the rat spinal cord involves interlaminar communications. *European Journal of Neuroscience*. 42:2654-2665.

Sekiguchi, K.J., P. Shekhtmeyster, K. Merten, A. Arena, D. Cook, E. Hoffman, A. Ngo, and A. Nimmerjahn. 2016. Imaging large-scale cellular activity in spinal cord of freely behaving mice. *Nature communications*. 7:11450.

Shaw, P.J., B. Qu, M. Hoth, and S. Feske. 2013. Molecular regulation of CRAC channels and their role in lymphocyte function. *Cell Mol Life Sci*. 70:2637-2656.

Shelton, M.K., and K.D. McCarthy. 2000. Hippocampal astrocytes exhibit Ca^{2+}-elevating muscarinic cholinergic and histaminergic receptors in situ. *Journal of Neurochemistry*. 74:555-563.

Shieh, C.H., A. Heinrich, T. Serchov, D. van Calker, and K. Biber. 2014. P2X7-dependent, but differentially regulated release of IL-6, CCL2, and TNF-α in cultured mouse microglia. *GLIA*. 62:592-607.

Shiokawa, H., T. Nakatsuka, H. Furue, M. Tsuda, T. Katafuchi, K. Inoue, and M. Yoshimura. 2006. Direct excitation of deep dorsal horn neurones in the rat spinal cord by the activation of postsynaptic P2X receptors. *Journal of Physiology*. 573:753-763.

Shuttleworth, T.J. 1996. Arachidonic acid activates the noncapacitative entry of Ca^{2+} during [Ca^{2+}](i) oscillations. *Journal of Biological Chemistry*. 271:21720-21725.

Shuttleworth, T.J. 2009. Arachidonic acid, ARC channels, and Orai proteins. *Cell Calcium*. 45:602-610.

Shuttleworth, T.J. 2012. STIM and Orai proteins and the non-capacitative ARC channels. *Front Biosci (Landmark Ed)*. 17:847-860.

Shuttleworth, T.J., J.L. Thompson, and O. Mignen. 2007. STIM1 and the noncapacitative ARC channels. *Cell Calcium*. 42:183-191.

Siemian, J.N., Z.M. LaMacchia, V. Spreuer, J. Tian, T.A. Ignatowski, P.M. Paez, Y. Zhang, and J.X. Li. 2018. The imidazoline I2 receptor agonist 2-BFI attenuates hypersensitivity and spinal neuroinflammation in a rat model of neuropathic pain. *Biochem Pharmacol*. 153:260-268.

Siemian, J.N., J. Li, Y. Zhang, and J.X. Li. 2016. Interactions between imidazoline I2 receptor ligands and acetaminophen in adult male rats: antinociception and schedule-controlled responding. *Psychopharmacology (Berl)*. 233:873-882.

Siemian, J.N., Z. Xue, B.E. Blough, and J.X. Li. 2017. Comparison of some behavioral effects of d- and l-methamphetamine in adult male rats. *Psychopharmacology (Berl)*. 234:2167-2176.

Silinsky, E.M., and J.I. Hubbard. 1973. Biological sciences: Release of ATP from Rat motor nerve terminals. *Nature*. 243:404-405.

Simard, M., G. Arcuino, T. Takano, Q.S. Liu, and M. Nedergaard. 2003. Signaling at the gliovascular interface. *Journal of Neuroscience*. 23:9254-9262.

Simons, M., and K.A. Nave. 2016. Oligodendrocytes: Myelination and axonal support. *Cold Spring Harb Perspect Biol*. 8:a020479.

Smith, E.S.J., and G.R. Lewin. 2009. Nociceptors: a phylogenetic view. *Journal of Comparative Physiology. A, Neuroethology, Sensory, Neural, and Behavioral Physiology*. 195(12):1089–1106.

Soboloff, J., B.S. Rothberg, M. Madesh, and D.L. Gill. 2012. STIM proteins: dynamic calcium signal transducers. *Nat Rev Mol Cell Biol*. 13:549-565.

Sofroniew, M.V., and H.V. Vinters. 2010. Astrocytes: Biology and pathology. *Acta Neuropathol*. 119:7-35.

Sperlágh, B., Z. Maglóczky, E.S. Vizi, and T.F. Freund. 1998. The triangular septal nucleus as the major source of ATP release in the rat habenula: A combined neurochemical and morphological study. *Neuroscience*. 86:1195-1207.

Stanley, A.C., and P. Lacy. 2010. Pathways for cytokine secretion. *Physiology (Bethesda)*. 25:218-229.

Stehberg, J., R. Moraga-Amaro, C. Salazar, A. Becerra, C. Echeverría, J.A. Orellana, G. Bultynck, R. Ponsaerts, L. Leybaert, F. Simon, J.C. Sáez, and M.A. Retamal. 2012. Release of gliotransmitters through astroglial connexin 43 hemichannels is necessary for fear memory consolidation in the basolateral amygdala. *The FASEB Journal*. 26:3649-3657.

Stenovec, M., M. Kreft, S. Grilc, M. Potokar, M.E. Kreft, T. Pangršič, and R. Zorec. 2007. Ca^{2+}-dependent mobility of vesicles capturing anti-VGLUT1 antibodies. *Experimental Cell Research*. 313:3809-3818.

Stone, L.S., J.P. German, K.F. Kitto, C.A. Fairbanks, and G.L. Wilcox. 2014. Morphine and clonidine combination therapy improves therapeutic window in mice: Synergy in antinociceptive but not in sedative or cardiovascular effects. *PLoS ONE*.

Stone, L.S., L.B. MacMillan, K.F. Kitto, L.E. Limbird, and G.L. Wilcox. 1997. The α(2a) adrenergic receptor subtype mediates spinal analgesia evoked by α2 agonists and is necessary for spinal adrenergic-opioid synergy. *Journal of Neuroscience*. 17:7157-7165.

Stout, C.E., J.L. Costantin, C.C.G. Naus, and A.C. Charles. 2002. Intercellular calcium signaling in astrocytes via ATP release through connexin hemichannels. *Journal of Biological Chemistry*. 277:10482-10488.

Suadicani, S.O., C.F. Brosnan, and E. Scemes. 2006. P2X7 receptors mediate ATP release and amplification of astrocytic intercellular Ca^{2+} signaling. *Journal of Neuroscience*. 26:1378-1385.

Suadicani, S.O., R. Iglesias, J. Wang, G. Dahl, D.C. Spray, and E. Scemes. 2012. ATP signaling is deficient in cultured pannexin1-null mouse astrocytes. *GLIA*. 60:1106-1116.

Sung, B., G. Lim, and J. Mao. 2003. Altered expression and uptake activity of spinal glutamate transporters after nerve injury contribute to the pathogenesis of neuropathic pain in rats. *Journal of Neuroscience*. 23:2899-2910.

Suttles, J., L.M. Carruth, and S.B. Mizel. 1990. Detection of IL-1 alpha and IL-1 beta in the supernatants of paraformaldehyde-treated human monocytes. Evidence against a membrane form of IL-1. *Journal of immunology (Baltimore, Md. : 1950)*. 144:170-174.

Svensson, C.I., and E. Brodin. 2010. Spinal astrocytes in pain processing: Non-neuronal cells as therapeutic targets. *Mol Interv*. 10:25-38.

Swanson, L.W. 1976. The locus coeruleus: A cytoarchitectonic, golgi and immunohistochemical study in the albino rat. *Brain Research*. 110:39-56.

Sweeney, Z.K., A. Minatti, D.C. Button, and S. Patrick. 2009. Small-molecule inhibitors of store-operated calcium entry. *ChemMedChem*. 4:706-718.

Szucs, P., L.L. Luz, R. Pinho, P. Aguiar, Z. Antal, S.Y.X. Tiong, A.J. Todd, and B.V. Safronov. 2013. Axon diversity of lamina I local-circuit neurons in the lumbar spinal cord. *Journal of Comparative Neurology*. 521:2719-2741.

Takano, T., J. Kang, J.K. Jaiswal, S.M. Simon, J.H.C. Lin, Y. Yu, Y. Li, J. Yang, G. Dienel, H.R. Zielke, and M. Nedergaard. 2005. Receptor-mediated glutamate release from volume sensitive channels in astrocytes. *Proceedings of the National Academy of Sciences of the United States of America*. 102:16466-16471.

Taruno, A. 2018. ATP release channels. *Int J Mol Sci*. 19.

Taylor, B.K., R.E. Roderick, and A.I. Basbaum. 2000. Brainstem noradrenergic control of nociception is abnormal in the spontaneously hypertensive rat. *Neuroscience Letters*. 291:139-142.

Thomas, P., J.G. Wong, A.K. Lee, and W. Almers. 1993. A low affinity Ca^{2+} receptor controls the final steps in peptide secretion from pituitary melanotrophs. *Neuron*. 11:93-104.

Thompson, J.L., and T.J. Shuttleworth. 2013. Exploring the unique features of the ARC channel, a store-independent Orai channel. *Channels (Austin)*. 7:364-373.

Thompson, R.J., M.F. Jackson, M.E. Olah, R.L. Rungta, D.J. Hines, M.A. Beazely, J.F. MacDonald, and B.A. MacVicar. 2008. Activation of pannexin-1 hemichannels augments aberrant bursting in the hippocampus. *Science*. 322:1555-1559.

Thoreson, W.B., K. Rabl, E. Townes-Anderson, and R. Heidelberger. 2004. A highly Ca^{2+}-sensitive pool of vesicles contributes to linearity at the rod photoreceptor ribbon synapse. *Neuron*. 42:595-605.

Thorn, D.A., Y. Zhang, and J.X. Li. 2016. Effects of the imidazoline I2 receptor agonist 2-BFI on the development of tolerance to and behavioural/physical dependence on morphine in rats. *Br J Pharmacol*. 173:1363-1372.

Todd, A.J. 2010. Neuronal circuitry for pain processing in the dorsal horn. *Nature Reviews Neuroscience*. 11:823-836.

Todd, A.J., D.I. Hughes, E. Polgár, G.G. Nagy, M. Mackie, O.P. Ottersen, and D.J. Maxwell. 2003. The expression of vesicular glutamate transporters VGLUT1 and VGLUT2 in neurochemically defined axonal populations in the rat spinal cord with emphasis on the dorsal horn. *European Journal of Neuroscience*. 17:13-27.

Todd, A.J., and J. McKenzie. 1989. GABA-immunoreactive neurons in the dorsal horn of the rat spinal cord. *Neuroscience*. 31:799-806.

Todd, A.J., and A.C. Sullivan. 1990. Light microscope study of the coexistence of GABA-like and glycine-like immunoreactivities in the spinal cord of the rat. *Journal of Comparative Neurology*. 296:496-505.

Todd, A.J., C. Watt, R.C. Spike, and W. Sieghart. 1996. Colocalization of GABA, glycine, and their receptors at synapses in the rat spinal cord. *Journal of Neuroscience*. 16:974-982.

Torres, A., F. Wang, Q. Xu, T. Fujita, R. Dobrowolski, K. Willecke, T. Takano, and M. Nedergaard. 2012. Extracellular Ca 2+ acts as a mediator of communication from neurons to glia. *Science Signaling*. 5:ra8.

Torres, G.E., R.R. Gainetdinov, and M.G. Caron. 2003. Plasma membrane monoamine transporters: Structure, regulation and function. *Nature Reviews Neuroscience*. 4:13-25.

Torsney, C., and A.B. MacDermott. 2006. Disinhibition opens the gate to pathological pain signaling in superficial neurokinin 1 receptor-expressing neurons in rat spinal cord. *Journal of Neuroscience*. 26:1833-1843.

Toth, A.B., K. Hori, M.M. Novakovic, N.G. Bernstein, L. Lambot, and M. Prakriya. 2019. CRAC channels regulate astrocyte Ca^{2+} signaling and gliotransmitter release to modulate hippocampal GABAergic transmission. *Science Signaling*. 12.

Toulme, E., M. Tsuda, B.S. Khakh, and K. Inoue. 2009. On the role of ATP-gated P2X receptors in acute, inflammatory and neuropathic pain. *In* Translational Pain Research: From Mouse to Man.

Travagli, R.A., and J.T. Williams. 1996. Endogenous monoamines inhibit glutamate transmission in the spinal trigeminal nucleus of the guinea-pig. *Journal of Physiology*. 491 (Pt 1):177-185.

Trebak, M., and J.W. Putney. 2017. ORAI calcium channels. *Physiology (Bethesda)*. 32:332-342.

Treede, R.D., W. Rief, A. Barke, Q. Aziz, M.I. Bennett, R. Benoliel, M. Cohen, S. Evers, N.B. Finnerup, M.B. First, M.A. Giamberardino, S. Kaasa, B. Korwisi, E. Kosek, P. Lavand'Homme, M. Nicholas, S. Perrot, J. Scholz, S. Schug, B.H. Smith, P. Svensson, J.W.S. Vlaeyen, and S.J. Wang. 2019. Chronic pain as a symptom or a disease: The IASP Classification of Chronic Pain for the International Classification of Diseases (ICD-11). *Pain*. 160:19-27.

Tsoli, E., S.L. Chan, and N.G. Morgan. 1995. The imidazoline I1 receptor agonist, moxonidine, inhibits insulin secretion from isolated rat islets of Langerhans. *Eur J Pharmacol*. 284:199-203.

Tsuda, M., Y. Shigemoto-Mogami, S. Koizumi, A. Mizokoshi, S. Kohsaka, M.W. Salter, and K. Inoue. 2003. P2X4 receptors induced in spinal microglia gate tactile allodynia after nerve injury. *Nature*. 424:778-783.

Tsuda, M., H. Tozaki-Saitoh, and K. Inoue. 2010. Pain and purinergic signaling. *Brain Res Rev*. 63:222-232.

Tsuruoka, M., Y.C.P. Arai, H. Nomura, K. Matsutani, and W.D. Willis. 2003. Unilateral hindpaw inflammation induces bilateral activation of the locus coeruleus and the nucleus subcoeruleus in the rat. *Brain Research Bulletin*. 61:117-123.

Tsuruoka, M., M. Maeda, and T. Inoue. 2004. Persistent hindpaw inflammation produces coeruleospinal antinociception in the non-inflamed forepaw of rats. *Neuroscience Letters*. 367:66-70.

Tsuruoka, M., J. Tamaki, M. Maeda, B. Hayashi, and T. Inoue. 2011. The nucleus locus coeruleus/subcoeruleus contributes to antinociception during freezing behavior following the air-puff startle in rats. *Brain Research*. 1393:52-61.

Tsuruoka, M., and W.D. Willis. 1996a. Bilateral lesions in the area of the nucleus locus coeruleus affect the development of hyperalgesia during carrageenan-induced inflammation. *Brain Research*. 726:233-236.

Tsuruoka, M., and W.D. Willis. 1996b. Descending modulation from the region of the locus coeruleus on nociceptive sensitivity in a rat model of inflammatory hyperalgesia. *Brain Research*. 743:86-92.

Tyce, G.M., and T.L. Yaksh. 1981. Monoamine release from cat spinal cord by somatic stimuli: an intrinsic modulatory system. *The Journal of Physiology*. 314:513-529.

Ullrich, K.J., G. Rumrich, C. David, and G. Fritzsch. 1993. Bisubstrates: substances that interact with renal contraluminal organic anion and organic cation transport systems. I. Amines, piperidines, piperazines, azepines, pyridines, quinolines, imidazoles, thiazoles, guanidines and hydrazines. *Pflugers Arch*. 425:280-299.

Ulmann, L., J.P. Hatcher, J.P. Hughes, S. Chaumont, P.J. Green, F. Conquet, G.N. Buell, A.J. Reeve, I.P. Chessell, and F. Rassendren. 2008. Up-regulation of P2X4 receptors in spinal microglia after peripheral nerve injury mediates BDNF release and neuropathic pain. *Journal of Neuroscience*. 28:11263-11268.

Ulmann, L., H. Hirbec, and F. Rassendren. 2010. P2X4 receptors mediate PGE2 release by tissue-resident macrophages and initiate inflammatory pain. *EMBO Journal*. 29:2290-2300.

Unichenko, P., A. Dvorzhak, and S. Kirischuk. 2013. Transporter-mediated replacement of extracellular glutamate for GABA in the developing murine neocortex. *European Journal of Neuroscience*. 38:3580-3588.

Unichenko, P., O. Myakhar, and S. Kirischuk. 2012. Intracellular Na + concentration influences short-term plasticity of glutamate transporter-mediated currents in neocortical astrocytes. *GLIA*. 60:605-614.

Vanegas, H., and H.G. Schaible. 2004. Descending control of persistent pain: Inhibitory or facilitatory? *Brain Res Brain Res Rev*. 46:295-309.

Vardjan, N., M. Gabrijel, M. Potokar, U. Švajger, M. Kreft, M. Jeras, Y. de Pablo, M. Faiz, M. Pekny, and R. Zorec. 2012. IFN-γ-induced increase in the mobility of MHC class II compartments in astrocytes depends on intermediate filaments. *Journal of Neuroinflammation*. 9:144.

Vardjan, N., M. Kreft, and R. Zorec. 2014. Regulated Exocytosis in Astrocytes is as Slow as the Metabolic Availability of Gliotransmitters: Focus on Glutamate and ATP. *In* Glutamate and ATP at the Interface of Metabolism and Signaling in the Brain. 81-101.

Vauquelin, G., J.P. De Backer, P. Ladure, and A. Flamez. 1999. Identification of I1 and I2 imidazoline receptors in striatum membranes from different species. *Ann N Y Acad Sci*. 881:135-143.

Ventura, R., and K.M. Harris. 1999. Three-dimensional relationships between hippocampal synapses and astrocytes. *Journal of Neuroscience*. 19:6897-6906.

Verderio, C., C. Cagnoli, M. Bergami, M. Francolini, U. Schenk, A. Colombo, L. Riganti, C. Frassoni, E. Zuccaro, L. Danglot, C. Wilhelm, T. Galli, M. Canossa, and M. Matteoli. 2012. TI-VAMP/VAMP7 is the SNARE of secretory lysosomes contributing to ATP secretion from astrocytes. *Biology of the Cell*. 104:213-228.

Verderio, C., S. Coco, O. Rossetto, C. Montecucco, and M. Matteoli. 1999. Internalization and proteolytic action of botulinum toxins in CNS neurons and astrocytes. *Journal of Neurochemistry*. 73:372-379.

Verkhratsky, A., M. Matteoli, V. Parpura, J.P. Mothet, and R. Zorec. 2016. Astrocytes as secretory cells of the central nervous system: idiosyncrasies of vesicular secretion. *The EMBO Journal*. 35:239-257.

Verkhratsky, A., and M. Nedergaard. 2018. Physiology of astroglia. *Physiological Reviews*. 98:239-389.

Verselis, V.K., and M. Srinivas. 2008. Divalent cations regulate connexin hemichannels by modulating intrinsic voltage-dependent gating. *Journal of General Physiology*. 132:315-327.

Vig, M., C. Peinelt, A. Beck, D.L. Koomoa, D. Rabah, M. Koblan-Huberson, S. Kraft, H. Turner, A. Fleig, R. Penner, and J.P. Kinet. 2006. CRACM1 is a plasma membrane protein essential for store-operated Ca 2+ entry. *Science*. 312:1220-1223.

Viisanen, H., and A. Pertovaara. 2007. Influence of peripheral nerve injury on response properties of locus coeruleus neurons and coeruleospinal antinociception in the rat. *Neuroscience*. 146:1785-1794.

Voets, T. 2000. Dissection of three Ca^{2+}-dependent steps leading to secretion in chromaffin cells from mouse adrenal slices. *Neuron*. 28:537-545.

Voisin, D.L., N. Guy, M. Chalus, and R. Dallel. 2005. Nociceptive stimulation activates locus coeruleus neurones projecting to the somatosensory thalamus in the rat. *Journal of Physiology*. 566:929-937.

von Bartheld, C.S., J. Bahney, and S. Herculano-Houzel. 2016. The search for true numbers of neurons and glial cells in the human brain: A review of 150 years of cell counting. *J Comp Neurol*. 524:3865-3895.

Wall, P.D. 1967. The laminar organization of dorsal horn and effects of descending impulses. *The Journal of Physiology*. 188:403-423.

Wan, Q.F., Y. Dong, H. Yang, X. Lou, J. Ding, and T. Xu. 2004. Protein kinase activation increases insulin secretion by sensitizing the secretory machinery to Ca^{2+}. *J Gen Physiol*. 124:653-662.

Wang, C.T., R. Grishanin, C.A. Earles, P.Y. Chang, T.F.J. Martin, E.R. Chapman, and M.B. Jackson. 2001. Synaptotagmin modulation of fusion pore kinetics in regulated exocytosis of dense-core vesicles. *Science*. 294:1111-1115.

Wang, G., J. Zhang, C. Xu, X. Han, Y. Gao, and H. Chen. 2016. Inhibition of SOCs Attenuates Acute Lung Injury Induced by Severe Acute Pancreatitis in Rats and PMVECs Injury Induced by Lipopolysaccharide. *Inflammation*. 39:1049-1058.

Wang, J., C. Ambrosi, F. Qiu, D.G. Jackson, G. Sosinsky, and G. Dahl. 2014. The membrane protein Pannexin1 forms two open-channel conformations depending on the mode of activation. *Science Signaling*. 7:ra69.

Wang, S., G. Lim, Q. Zeng, B. Sung, L. Yang, and J. Mao. 2005. Central glucocorticoid receptors modulate the expression and function of spinal NMDA receptors after peripheral nerve injury. *Journal of Neuroscience*. 25:488-495.

Wang, W.W., W.W. Wang, X. Mei, J. Huang, Y. Wei, Y. Wang, S. Wu, and Y. Li. 2009. Crosstalk between spinal astrocytes and nuerons in nerve injury-injuced neuropathic pain. *PLoS ONE*. 4:e6973.

Watkins, E.A., P.C. Wollan, L.J. Melton, and B.P. Yawn. 2008. A population in pain: Report from the Olmsted County health study. *Pain Medicine*. 9:166-174.

Watkins, L.R., and S.F. Maier. 2003. Glia: A novel drug discovery target for clinical pain. *Nat Rev Drug Discov*. 2:973-985.

Watkins, L.R., E.D. Milligan, and S.F. Maier. 2001. Glial activation: A driving force for pathological pain. *Trends Neurosci*. 24:450-455.

Wei, D., Y. Mei, J. Xia, and H. Hu. 2017. Orai1 and orai3 mediate store-operated calcium entry contributing to neuronal excitability in dorsal root ganglion neurons. *Frontiers in Cellular Neuroscience*. 11:400.

Wei, F., R. Dubner, S. Zou, K. Ren, G. Bai, D. Wei, and W. Guo. 2010. Molecular depletion of descending serotonin unmasks its novel facilitatory role in the development of persistent pain. *Journal of Neuroscience*. 30:8624-8636.

Weihe, E., M.K.H. Schäfer, J.D. Erickson, and L.E. Eiden. 1994. Localization of vesicular monoamine transporter isoforms (VMAT1 and VMAT2) to endocrine cells and neurons in rat. *Journal of Molecular Neuroscience*. 5:149-164.

Weilinger, N.L., A.W. Lohman, B.D. Rakai, E.M.M. Ma, J. Bialecki, V. Maslieieva, T. Rilea, M.V. Bandet, N.T. Ikuta, L. Scott, M.A. Colicos, G.C. Teskey, I.R. Winship, and R.J. Thompson. 2016. Metabotropic NMDA receptor signaling couples Src family kinases to pannexin-1 during excitotoxicity. *Nature Neuroscience*. 19:432-442.

Westfall, D.P., R.E. Stitzel, and J.N. Rowe. 1978. The postjunctional effects and neural release of purine compounds in the guinea-pig vas deferens. *European Journal of Pharmacology*. 50:27-38.

White, F.A., H. Jung, and R.J. Miller. 2007. Chemokines and the pathophysiology of neuropathic pain. *Proc Natl Acad Sci U S A*. 104:20151-20158.

Wilhelm, A., W. Volknandt, D. Langer, C. Nolte, H. Kettenmann, and H. Zimmermann. 2004. Localization of SNARE proteins and secretory organelle proteins in astrocytes in vitro and in situ. *Neuroscience Research*. 48:249-257.

Wilkin, G.P., D.R. Marriott, and A.J. Cholewinski. 1990. Astrocyte heterogeneity. *Trends in Neurosciences*. 13:43-46.

Windrem, M.S., S.J. Schanz, C. Morrow, J. Munir, D. Chandler-Militello, S. Wang, and S.A. Goldman. 2014. A competitive advantage by neonatally engrafted human glial progenitors yields mice whose brains are chimeric for human glia. *Journal of Neuroscience*. 34:16153-16161.

Wolf, S.A., H.W.G.M. Boddeke, and H. Kettenmann. 2017. Microglia in Physiology and Disease. *Annual Review of Physiology*. 79:619-643.

Woo, D.H., K.S. Han, J.W. Shim, B.E. Yoon, E. Kim, J.Y. Bae, S.J. Oh, E.M. Hwang, A.D. Marmorstein, Y.C. Bae, J.Y. Park, and C.J. Lee. 2012. TREK-1 and Best1 channels mediate fast and slow glutamate release in astrocytes upon GPCR activation. *Cell*. 151:25-40.

Woolf, C.J., and M.W. Salter. 2000. Neuronal plasticity: Increasing the gain in pain. *Science*. 288:1765-1769.

Xia, J., R. Pan, X. Gao, O. Meucci, and H. Hu. 2014. Native store-operated calcium channels are functionally expressed in mouse spinal cord dorsal horn neurons and regulate resting calcium homeostasis. *Journal of Physiology*. 592:3443-3461.

Xie, Y.F., S. Zhang, C.Y. Chiang, J.W. Hu, J.O. Dostrovsky, and B.J. Sessle. 2007. Involvement of glia in central sensitization in trigeminal subnucleus caudalis (medullary dorsal horn). *Brain, Behavior, and Immunity*. 21:634-641.

Xu, J. 2018. New insights into GFAP negative astrocytes in Calbindin D28k immunoreactive astrocytes. *Brain Sciences*. 8.

Xu, J., H. Peng, N. Kang, Z. Zhao, J.H.C. Lin, P.K. Stanton, and J. Kang. 2007. Glutamate-induced exocytosis of glutamate from astrocytes. *Journal of Biological Chemistry*. 282:24185-24197.

Yaksh, T.L., J.W. Pogrel, Y.W. Lee, and S.R. Chaplan. 1995. Reversal of nerve ligation-induced allodynia by spinal alpha-2 adrenoceptor agonists. *J Pharmacol Exp Ther*. 272:207-214.

Yaksh, T.L., and G.M. Tyce. 1981. Release of norepinephrine and serotonin in cat spinal cord: Direct in vivo evidence for the activation of descending monoamine pathways by somatic stimulation. *Journal de Physiologie*. 77:483-487.

Yasaka, T., G. Kato, H. Furue, M.H. Rashid, M. Sonohata, A. Tamae, Y. Murata, S. Masuko, and M. Yoshimura. 2007. Cell-type-specific excitatory and inhibitory circuits involving primary afferents in the substantia gelatinosa of the rat spinal dorsal horn in vitro. *Journal of Physiology*. 581:603-618.

Ye, Z.C., M.S. Wyeth, S. Baltan-Tekkok, and B.R. Ransom. 2003. Functional hemichannels in astrocytes: A novel mechanism of glutamate release. *Journal of Neuroscience*. 23:3588-3596.

Yeager, M., and B.J. Nicholson. 1996. Structure of gap junction intercellular channels. *Current Opinion in Structural Biology*. 6:183-192.

Yoon, B.E., and C.J. Lee. 2014. GABA as a rising gliotransmitter. *Front Neural Circuits*. 8:141.

Yoshihara, K., T. Matsuda, Y. Kohro, H. Tozaki-Saitoh, K. Inoue, and M. Tsuda. 2018. Astrocytic Ca^{2+} responses in the spinal dorsal horn by noxious stimuli to the skin. *Journal of Pharmacological Sciences*. 137:101-104.

Yoshimura, M., and T.M. Jessell. 1989. Primary afferent-evoked synaptic responses and slow potential generation in rat substantia gelatinosa neurons in vitro. *J Neurophysiol*. 62:96-108.

Yoshimura, M., and S. Nishi. 1992. Excitatory amino acid receptors involved in primary afferent-evoked polysynaptic EPSPs of substantia gelatinosa neurons in the adult rat spinal cord slice. *Neuroscience Letters*. 143:131-134.

Zhang, E.T., and A.D. Craig. 1997. Morphology and distribution of spinothalamic lamina I neurons in the monkey. *J Neurosci*. 17:3274-3284.

Zhang, H., S.Y. Yoon, H. Zhang, and P.M. Dougherty. 2012a. Evidence that spinal astrocytes but not microglia contribute to the pathogenesis of paclitaxel-induced painful neuropathy. *Journal of Pain*. 13:293-303.

Zhang, J., and Y. De Koninck. 2006. Spatial and temporal relationship between monocyte chemoattractant protein-1 expression and spinal glial activation following peripheral nerve injury. *Journal of Neurochemistry*. 97:772-783.

Zhang, M., N.A. Piskuric, C. Vollmer, and C.A. Nurse. 2012b. P2Y2 receptor activation opens pannexin-1 channels in rat carotid body type II cells: Potential role in amplifying the neurotransmitter ATP. *Journal of Physiology*. 590:4335-4350.

Zhang, Q., M. Fukuda, E. Van Bockstaele, O. Pascual, and P.G. Haydon. 2004a. Synaptotagmin IV regulates glial glutamate release. *Proceedings of the National Academy of Sciences of the United States of America*. 101:9441-9446.

Zhang, Q., T. Pangršič, M. Kreft, M. Kržan, N. Li, J.Y. Sul, M. Halassa, E. Van Bockstaele, R. Zorec, and P.G. Haydon. 2004b. Fusion-related Release of Glutamate from Astrocytes. *Journal of Biological Chemistry*. 279:12724-12733.

Zhang, Z., G. Chen, W. Zhou, A. Song, T. Xu, Q. Luo, W. Wang, X.S. Gu, and S. Duan. 2007. Regulated ATP release from astrocytes through lysosome exocytosis. *Nature Cell Biology*. 9:945-953.

Zubieta, J.K., and C.S. Stohler. 2009. Neurobiological mechanisms of placebo responses. *Annals of the New York Academy of Sciences*. 1156:198-210.

Zweifach, A., and R.S. Lewis. 1993. Mitogen-regulated Ca^{2+} current of T lymphocytes is activated by depletion of intracellular Ca^{2+} stores. *Proceedings of the National Academy of Sciences of the United States of America*. 90:6295-6299.

Varen EERSAPAH

DÉTECTION ET QUANTIFICATION DE LA LIBÉRATION D'ATP À PARTIR DES CELLULES GLIALES DE LA CORNE DORSALE DE MOELLE ÉPINIÈRE DE SOURIS : EFFET DE LA NORADRÉNALINE ET DES IMIDAZOLINES

Résum

Des cellules HEK293 exprimant de manière stable le récepteur P2X2 de rat ont été préincubées avec de la progestérone, un modulateur puissant de P2X2, puis utilisées pour détecter des concentrations nanomolaires d'ATP. Après chargement au Fura-2, ces cellules ont été déposées sur des cellules gliales DH pour quantifier la libération d'ATP. La phényléphrine ou une solution pauvre en K^+ ont induit une élévation réversible de $[Ca^{2+}]_i$, bloquée par le PPADS ou le BAPTA. La libération d'ATP induite par la phényléphrine a été inhibée par le GPN (perméabilisation des lysosomes sécrétoires) et par la bafilomycine A1 (inhibiteur de la pompe à protons). Nos résultats indiquent que l'ATP est libéré de manière calcium-dépendante à partir de deux pools vésiculaires distincts dans les cellules gliales DH, et que la noradrénaline cible spécifiquement les lysosomes sécrétoires

Mots clés :
Astrocyte; Exocytose; Libération non vésiculaire; Lysosome sécrétoire; Libération vésiculaire

Abstract

Human embryonic kidney 293 (HEK293) cells stably transfected with the rat P2X2 receptor were preincubated with progesterone, a potent modulator of P2X2 receptors, and used to detect low nanomolar concentrations of ATP. Fura-2-loaded HEK293-P2X2-PROG cells were acutely plated on top of cultured DH glial cells to quantify ATP release from single DH glial cells. Application of the α1 adrenoceptor agonist phenylephrine or of a low K^+ solution evoked reversible increases in the intracellular calcium concentration ($[Ca^{2+}]_i$) in the biosensor cells. All increases in $[Ca^{2+}]_i$ were blocked in the presence of PPADS or after preloading glial cells with BAPTA. ATP release induced by PHE was blocked by GPN that permeabilizes secretory lysosomes and bafilomycin A1, an inhibitor of the H^+-pump. Our results indicate that ATP is released in a calcium-dependent manner from two distinct vesicular pools coexisting in DH glial cells and that noradrenaline selectively target the secretory lysosome pool.

Keywords :
Astrocyte; Exocytosis; Non-vesicular release; Secretory lysosome; Vesicular release